International Doctoral Thesis / Tesis Doctoral Internacional

DEPARTAMENTO DE FISIOLOGÍA

INSTITUTO DE NUTRICIÓN Y TECNOLOGÍA DE LOS ALIMENTOS "JOSÉ MATAIX VERDÚ"

CENTRO DE INVESTIGACIÓN BIOMÉDICA

PROGRAMA DE DOCTORADO EN NUTRICIÓN Y CIENCIAS DE LOS ALIMENTOS

UNIVERSIDAD
DE GRANADA

Evaluation of the modulatory role of bioactive compounds obtained from products and by-products of olive grove origin on the pathogenesis of Alzheimer's disease in the experimental model *Caenorhabditis elegans*

Evaluación del papel modulador de los compuestos bioactivos obtenidos de productos y subproductos de origen oleícola sobre la patogénesis de la enfermedad de Alzheimer en el modelo experimental *Caenorhabditis elegans*

Doctorando: Jose Manuel Romero Márquez

Directores: José L. Quiles y Alfonso Varela López

Granada | 2023

Memoria que presenta el graduado en Nutrición Humana y Dietética

D. Jose Manuel Romero Márquez

Para aspirar al Grado de Doctor por la Universidad de Granada.

Fdo: Jose Manuel Romero Márquez

Aprobada por los directores de la Tesis Doctoral:

Fdo: **José Luís Quiles Morales** Fdo: **Alfonso Varela López**

Editor: Universidad de Granada. Tesis Doctorales
Autor: José Manuel Romero Márquez
ISBN: 978-84-1195-108-1
URI: https://hdl.handle.net/10481/85762

El doctorando / *The doctoral candidate* D. **Jose Manuel Romero Márquez** y los directores de la tesis / *and the thesis supervisors* Dr. D. **José Luis Quiles Morales** y Dr. D. **Alfonso Varela López**:

Garantizamos, al firmar esta tesis doctoral, que el trabajo ha sido realizado por el doctorando bajo la dirección de los directores de la tesis y, hasta donde nuestro conocimiento alcanza, en la realización del trabajo se han respetado los derechos de otros autores a ser citados, cuando se han utilizado sus resultados o publicaciones.

/

Guarantee, by signing this doctoral thesis, that the work has been done by the doctoral candidate under the direction of the thesis supervisors and, as far as our knowledge reaches, in the performance of the work, the rights of other authors to be cited (when their results or publications have been used) have been respected.

Granada, a 27 de septiembre de 2023.

Director de la tesis / *Thesis supervisor*	Director de la tesis / *Thesis supervisor*	Doctorando / *Doctoral candidate*
Fdo: José Luís Quiles Morales	Fdo: Alfonso Varela López	Fdo: Jose Manuel Romero Márquez

"Y preferí llegar al final con la conciencia tranquila, sabiendo que ya no podía hacer más"

- Antonio Mejías Martínez

Content

List of Tables

List of Figures

Figure 29. Effects of the three olive leaf extracts at 500 μg/ml on the paralysis phenotype and the influence of the different RNAi (DAF-16, SKN-1, SOD-2, SOD-3, and HSP-16.2) in the transgenic strain CL4176 at 34 h after the temperature upshift.

Figure 30. Effects of the three olive leaf extracts at 500 μg/ml on locomotive parameters in the transgenic strain BR5706.

Figure 31. Effects of the low-OL extract at 500 μg/ml on locomotive parameters in the transgenic strain BR5706 and the influence of the different RNAi (DAF-16, SKN-1, SOD-2, SOD-3, and HSP-16.2).

Figure 32. Effects of the high-OL extract at 500 μg/ml on locomotive parameters in the transgenic strain BR5706 and the influence of the different RNAi (DAF-16, SKN-1, SOD-2, SOD-3, and HSP-16.2).

Figure 33. Effects of the three olive leaf extracts at 500 μg/ml on OS3062/hsf-1::GFP and descriptive images of each group.

Figure 34. Effects of the three olive leaf extracts at 500 μg/ml on TJ375/hsp-16.2p::GFP strain and descriptive images of each group.

Figure 35. Effects of the three olive leaf extracts at 500 μg/ml on TJ356/daf-16p::GFP strain and descriptive images of each group.

Figure 36. Effects of the three olive leaf extracts at 500 μg/ml on LD1/skn-1::GFP strain and descriptive images of each group.

Figure 37. Effects of the three olive leaf extracts at 500 μg/ml on CF1553/sod-3p::GFP strain and descriptive images of each group.

Figure 38. Effects of the three olive leaf extracts at 500 μg/ml on CL2166/gst-4p::GFP strain and descriptive images of each group.

Figure 39. Intracellular reactive oxygen species (ROS) content of CL802 and CL4176 nematodes at 24 h after temperature up-shift and representative dot plots.

Figure 40. Mitochondrial reactive oxygen species (ROS) content of CL802 and CL4176 nematodes at 24 h after temperature up-shift and representative dot plots.

Summary

Alzheimer's disease (AD) is a multifactorial neurodegenerative disease of unknown etiology, first diagnosed by Alois Alzheimer in 1907. It is characterized by a progressive deterioration of cognitive function, memory, as well as language and orientation dysfunctions. The etiopathogenesis of AD is characterized by two histopathological events: the senile plaque aggregation formed by amyloid-β (Aβ) peptides in the central nervous system and the formation of neurofibrillary tangles (NFTs) associated to the accumulation of tau protein in the hippocampus, neocortical area, and amygdala. Although there is still no pharmacological therapy for its treatment, the preventive and/or therapeutic nutritional interventions against AD have been gaining prominence in recent years. It is known that 35% of dementias could be caused by modifiable risk factors associated with lifestyle, including the type of diet. In particular, the Mediterranean Diet (MD), characterized by a high consumption of legumes, vegetables, fruits, vitamins, and virgin olive oil, and a low consumption of red meat, has been shown to reduce the incidence of AD. MD presents a high contribution of bioactive substances such as phenolic compounds, which have been shown to exert a protective effect in AD. The leaves of the olive (OL) tree (*Olea europaea*) are the most abundant by-product in the olive grove industry. OLs have excellent medicinal properties thanks to the wide variety of bioactive compounds present in them. In particular, the intake of phytochemical compounds naturally present in foods, such as oleuropein, hydroxytyrosol, and luteolin are related to neuroprotective effects in AD through the modulation of mechanisms such as oxidative stress and neuroinflammation, besides reducing the deposition and toxicity of the misfolded proteins involved.

Building upon abovementioned aspects, the hypothesis of this study is that Alzheimer's Disease, along with related mechanisms such as cholinergic function, oxidative stress, and inflammatory processes, can be modulated by bioactive by-products obtained from the olive grove

industry. It's crucial to acknowledge that the redox and inflammatory state within cells play a pivotal role in the development of Alzheimer's Disease. In light of this, the use of olive leaf extracts could be an interesting approach to develop nutraceuticals as adjuvant therapy for Alzheimer's Disease. The main objective of this doctoral thesis was to evaluate the effect of olive leaf extracts to counteract the deleterious effects of Alzheimer's disease and its hallmarks. To reach this general objective, the following specific objectives were established:

1. Assessment of antioxidant capacity of fifty olive leaf samples from five different countries.
2. Phytochemical characterization of these extracts.
3. Evaluation of the cholinesterase, cyclooxygenase-2, and iron-oxidative inhibitory activity of these extracts.
4. Toxicological evaluation of the fifty olive leaf extracts in the *C. elegans* experimental model.
5. Selection of three samples (low, medium, and high activity) to be tested based on the aforementioned.
6. Assessment of the three OL extracts effects in markers related to redox biology and proteostasis network in different *C. elegans* strains.
7. Exploring the treatment effects on AD markers in both *in vitro* and *C. elegans* models, as well as investigating redox biology and delving into the associated molecular signaling pathways.

Results pointed out that the geographical origin considerably influenced the phytochemical profile, especially in relation to the content of secoiridoids, flavonoids, iridoids, hydroxycoumarins, and hydroxycinnamic acids. The antioxidant capacity was associated with the total content of phenolic compounds and flavonoids, which stood out in the samples from Spain and Italy. It was also shown that the inhibitory cholinesterase activity was influenced by several compounds present in the OL, with the Spanish, Italian, and Portuguese samples being the most interesting for this purpose. Despite the remarkable ability to inhibit

COX-2 activity exerted by the different OLs, no origin-related effect was observed for this marker among the investigated countries.

The large-scale assessment of the fifty olive leaf extracts demonstrated absence of lethal toxicity in the *C. elegans* Wild type, as demonstrated by lethality, growth and embryotoxicity test. Notwithstanding, minor toxic effects in terms of lower growth of the nematodes were detected in olive leaf extracts with elevated content in apigenin, eriodyctiol, esculin, or decaffeoylverbascoside. In the same way, OL extracts demonstrated significant anti-inflammatory, anti-cholinergic, and antioxidant activities. Compounds like luteolin-7-O-glucoside, isoharmnentin, and apigenin derivatives were identified as significant contributors to the AChE inhibitory activity. Among the rest of compounds, oleuropein derivatives, and hydroxytyrosol, showed noteworthy potential. Regarding COX-2 inhibitory activity, the enrichment of OL in secoiridoids seemed to be a significant determinant of the observed inhibitory effect. Oleuropein and its derivatives, along with ligstroside content, may exert an important role in the COX-2 inhibitory activity. Among the rest of compounds, luteolin 7-O-glucoside and verbascoside should be highlighted. In the same way, the diosmetin seems to be negatively associated with inhibitory effect of OL, probably attributed to the conversion of luteolin to diosmetin. Finally, authors demonstrated that both secoiridoids and flavonoids were found to contribute equally to the observed antioxidant effect. To cite, oleuropein and its derivatives, ligstroside and luteolin-7-O-glucoside content, may exert an important role in the ferric reducing antioxidant capacity. Among the rest of compounds, hydroxytyrosol, hydroxycoumarins, and verbascoside content must be highlighted.

Then, three olive leaf samples with different biomedical and phytochemical profiles were selected. For this purpose, three categories were generated: the low category, the medium category, and the high category based on AChE IA, COX-2 IA, FRAP, TPC, and TFC. The three olive leaf extracts demonstrated a moderate *in vitro* inhibitory capacity of the AChE, COX-2, and iron-reducing activity, being the high-OL extract the most effective.

According to AD experiments, the low and high-OL extract showed remarkable results against Aβ and tau proteotoxicity *in vivo*. Mid-OL exerts a slight improvement of amyloidogenic toxicity but did not affect to the locomotive behavior, which could be attributed to the apigenin derivatives content. The transcription factors SKN-1/NRF-2 and its downstream SOD-2 and SOD-3 has been demonstrated to be involved in the effects of low and high-OL extracts. HSP-16.2 has been shown to participate in mid-OL extracts benefits. In fact, the three olive leaf extracts were able to modulate redox biology through hormetic stress response but in a different way. All the extract were able to promote the nucleation of DAF-16/FOXO, whereas only low and high OL extract induced SKN-1/NRF-2. In presence of amyloidogenic pathology, all of them had great activity preventing an excess of intracellular ROS content, being the low-OL extract the most active. The protective effects exerted by low, mid, and high-OL extract effects on GSH metabolism may involve GST-4, HSP-16.2, and SOD-2, respectively. At mitochondrial level, only high-OL extract was able to reduce ROS content, through the involvement of SOD-2. In the hyperphosphorylated tau strain, both low and high OL extract reduced mitochondrial ROS content through the involvement of DAF-16/SKN-1 and its direct downstream SOD-2 and SOD-3.

Overall, these results open the door for the design and testing of nutraceuticals based on olive leaf extracts aimed at preventing or mitigating various aspects related to Alzheimer's disease.

Resumen

La enfermedad de Alzheimer (EA) es una patología neurodegenerativa multifactorial de etiología desconocida, diagnosticada por primera vez por Alois Alzheimer en 1907. Se caracteriza por un deterioro progresivo de la función cognitiva, la memoria, así como disfunciones del lenguaje y la orientación. La etiopatogenia de la EA se caracteriza por dos eventos histopatológicos: la agregación de placas seniles formadas por péptidos β-amiloide (Aβ) en el sistema nervioso central y la formación de ovillos neurofibrilares (NFT) asociados a la acumulación de proteína tau en el hipocampo, área neocortical y amígdala. Aunque todavía no existe una terapia farmacológica para su tratamiento, las intervenciones nutricionales preventivas y/o terapéuticas frente a la EA han ido ganando protagonismo en los últimos años. Se sabe que el 35% de las demencias podrían ser causadas por factores de riesgo modificables asociados al estilo de vida, incluido el tipo de dieta. En particular, se ha demostrado que la Dieta Mediterránea (DM), caracterizada por un alto consumo de legumbres, verduras, frutas, vitaminas y aceite de oliva virgen, y un bajo consumo de carne roja, reduce la incidencia de la EA. La DM presenta un alto aporte de sustancias bioactivas como los compuestos fenólicos, que han demostrado ejercer un efecto protector en la EA. Las hojas del olivo (OL) son el subproducto más abundante en la industria del olivar. Los OL tienen excelentes propiedades medicinales gracias a la amplia variedad de compuestos bioactivos presentes en ellas. En particular, la ingesta de compuestos fitoquímicos presentes naturalmente, como oleuropeína, hidroxitirosol y luteolina, se relaciona con efectos neuroprotectores en la EA a través de la modulación de mecanismos como el estrés oxidativo y la neuroinflamación, además de reducir el depósito y la toxicidad de las proteínas mal plegadas involucradas.

Partiendo de los aspectos mencionados anteriormente, la hipótesis de este estudio es que la enfermedad de Alzheimer, junto con mecanismos relacionados como la función colinérgica, el estrés oxidativo y los procesos inflamatorios, pueden ser modulados por subproductos obtenidos de la industria del olivar. Es crucial reconocer que el estado

inflamatorio y redox dentro de las células juega un papel fundamental en el desarrollo de la enfermedad de Alzheimer. En vista de esto, el uso de extractos de hoja de olivo podría ser un enfoque interesante para desarrollar nutracéuticos como terapia adyuvante para la enfermedad de Alzheimer. El principal objetivo de esta tesis doctoral fue evaluar el efecto de los extractos de hoja de olivo para contrarrestar los efectos deletéreos de la enfermedad de Alzheimer y sus características. Para alcanzar este objetivo general se establecieron los siguientes objetivos específicos:

1. Evaluar la capacidad antioxidante de cincuenta muestras de hojas de olivo procedentes de cinco países diferentes.
2. Caracterización fitoquímica de estos extractos.
3. Evaluación de la actividad inhibidora de la colinesterasa, la ciclooxigenasa-2 y la oxidación del hierro de estos extractos.
4. Evaluación toxicológica de los cincuenta extractos de hoja de olivo en el modelo experimental de *C. elegans*.
5. Selección de tres muestras (baja, media y alta actividad) a ensayar con base en lo antes mencionado.
6. Evaluación de los efectos de los tres extractos OL en marcadores relacionados con la biología redox y la red de proteostasis en diferentes cepas de *C. elegans*.
7. Explorar los efectos del tratamiento sobre los marcadores de EA en modelos tanto *in vitro* como de *C. elegans*, así como investigar la biología redox y profundizar en las vías de señalización molecular asociadas.

Los resultados señalaron que el origen geográfico influyó considerablemente en el perfil fitoquímico, especialmente en relación con el contenido de secoiridoides, flavonoides, iridoides, hidroxicumarinas y ácidos hidroxicinámicos. La capacidad antioxidante se asoció con el contenido total de compuestos fenólicos y flavonoides, que destacaron en las muestras de España e Italia. También se demostró que la actividad inhibidora de la colinesterasa estaba influenciada por varios compuestos presentes en la OL, siendo las muestras española, italiana y portuguesa las más interesantes para este propósito. A pesar de la notable capacidad para inhibir la actividad de la COX-2 ejercida por los diferentes OL, no se

observó ningún efecto relacionado con el origen de este marcador entre los países investigados.

La evaluación a gran escala de los cincuenta extractos de hoja de olivo demostró la ausencia de toxicidad letal en el *C. elegans*, como lo demostraron las pruebas de letalidad, crecimiento y embriotoxicidad. No obstante, se detectaron efectos tóxicos menores en términos de menor crecimiento de los nematodos en extractos de hoja de olivo con elevado contenido en apigenina, eriodyctiol, esculina o decaffeoilverbascósido.

De la misma manera, los extractos OL demostraron importantes actividades antiinflamatorias, anticolinérgicas y antioxidantes. Se identificaron compuestos como luteolina-7-O-glucósido, isoharmnentina y derivados de apigenina como contribuyentes importantes a la actividad inhibitoria de la AChE. Entre el resto de los compuestos, destacan los derivados de la oleuropeína y el hidroxitirosol. En cuanto a la actividad inhibidora de la COX-2, el enriquecimiento de OL en secoiridoides pareció ser un determinante significativo del efecto inhibidor observado. La oleuropeína y sus derivados, junto con el contenido de ligstrosido, pueden ejercer un papel importante en la actividad inhibidora de la COX-2. Entre el resto de los compuestos cabe destacar la luteolina 7-O-glucósido y el verbascósido. De la misma manera, la diosmetina parece estar asociada negativamente con el efecto inhibidor de la OL, probablemente atribuido a la conversión de luteolina en diosmetina. Finalmente, los autores demostraron que tanto los secoiridoides como los flavonoides contribuyen por igual al efecto antioxidante observado. Por ejemplo, la oleuropeína y sus derivados, el contenido de ligstrosido y luteolina-7-O-glucósido, pueden ejercer un papel importante en la capacidad antioxidante reductora del hierro. Entre el resto de los compuestos destaca el contenido en hidroxitirosol, hidroxicumarinas y verbascósidos.

Posteriormente se seleccionaron tres muestras de hoja de olivo con diferentes perfiles biomédicos y fitoquímicos. Para ello se generaron tres categorías: categoría low, categoría mid y categoría high en base a las puntuaciones obtenidas en las pruebas para AChE IA, COX-2 IA, FRAP, TPC y TFC. Los tres extractos de hoja de olivo han demostrado una

moderada capacidad inhibidora *in vitro* de la AChE, COX-2 y la actividad reductora de hierro, siendo el extracto high-OL el más eficaz.

Según los experimentos que evaluaron los marcadores de EA, los extractos low y high OL mostraron resultados notables contra la proteotoxicidad de Aβ y p-tau *in vivo*. Mid-OL ejerció una ligera mejora de la toxicidad amiloidogénica pero no afectó al comportamiento locomotor, lo que podría atribuirse al contenido de derivados de apigenina. Se ha demostrado que los factores de transcripción SKN-1/NRF-2 y sus dianas SOD-2 y SOD-3 están involucrados en los efectos de los extractos de low y high OL. Se ha demostrado que HSP-16.2 participó en los beneficios de los mid-OL. De hecho, los tres extractos de hoja de olivo pudieron modular la biología redox a través de la respuesta al estrés hormético, pero de una manera diferente. Todos los extractos fueron capaces de promover la nucleación de DAF-16/FOXO, mientras que solo los extractos de low y high OL bajo indujeron SKN-1/NRF-2. En presencia de patología amiloidogénica, todos tuvieron gran actividad previniendo un exceso de contenido de ROS intracelular, siendo el extracto de low OL el más activo. Los efectos protectores ejercidos por los efectos del extracto de OL bajo, medio y alto sobre el metabolismo del GSH pueden involucrar a GST-4, HSP-16.2 y SOD-2, respectivamente. A nivel mitocondrial, solo el extracto high OL fue capaz de reducir el contenido de ROS, mediante la participación de SOD-2. En la cepa tau hiperfosforilada, tanto el extracto de low OL como el high OL redujeron el contenido de ROS mitocondrial mediante la participación de DAF-16/SKN-1 y sus dianas SOD-2 y SOD-3.

En conjunto, estos resultados abren la puerta al diseño y ensayo de nutracéuticos basados en extractos de hoja de olivo destinados a prevenir o mitigar diversos aspectos relacionados con la enfermedad de Alzheimer.

Abbreviations

μg: microgram

μM: micromolar

20% H-OF: 20% hydroxytyrosol-rich extract from olive fruit

40% O-OL: olive leaf extract containing 40% of oleuropein

ABTS: 2,2'-azinobis [3-ethylbenzothiazoline-6-sulfonic acid]-diammonium salt

ACh: acetylcholine

AChE: acetylcholinesterase

AChE IA: AchE inhibitory activity

AChEI: AChE inhibitor

AD: Alzheimer's disease

ANOVA: analysis of variance

APP: amyloid precursor protein

ARE: antioxidant response element

Aβ: amyloid-β

BACE-1: β-secretase site-1

BChE: butyrylcholinesterase

BW: body weight

C. elegans: *Caenorhabditis elegans*

CAT: catalase

CAT: catechin equivalents

COX: cyclooxygenase

DAF: abnormal dauer formation

DMSO: dimethyl sulfoxide

DNA: deoxyribonucleic acid

DPPH: 2,2-Diphenyl-1-Picrylhydrazyl

EGF: endothelial growth factor

ESI: electrospray interface

ET: electron transfer

EU: European Union

FOXO: forkhead box transcription factor class O

FRAP: ferric reducing antioxidant power

g: gram

GA: gallic acid equivalent

GFP: green protein fluorescent

GSH: glutathione

GSH-Px: glutathione peroxidase

GSSG: glutathione disulfide

GST: glutathione S-transferase

h: hour

H_2DCFDA: 2′,7-dichlorodihydrofluorescein diacetate

HMGB1: high mobility group box protein 1

HPLC: high performance liquid chromatography

HSE: heat shock elements

HSF-1: heat shock factor-1

HSP-16.2: heat shock protein 16.2

HSR: heat shock response

IC50: half maximal inhibitory concentration

IGF-1: insulin/insulin-like growth factor-1

IKKβ: nuclear factor kappa-B kinase beta subunit inhibitor

IL: interleukin

iNOS: inducible nitric oxide synthase

ISS: IGF-1 signaling

kg: kilogram

LOX: lipoxidase

LPS: lipopolysaccharide

MAPK: mitogen-activated protein kinases

MCB: monoclorobimane

MD: mediterranean diet

mg: milligram

ml: milliliter

MnSOD: manganese SOD

NFTs: neurofibrillary tangles

NF-κB: nuclear factor kappa light chain enhancer of activated B cells

NGM: nematode growth medium

RNS: reactive nitrogen species

NRF-2: nuclear factor erythroid 2-related factor

OL: olive leaf

Pb: lead

PBMCs: peripheral blood mononuclear cell

PC: principal component

PCA: principal component analysis

PE2: prostaglandin E2

PKB: protein kinase B

PLS-DA: partial least squares-discriminant analysis

p-tau: hyperphosphorylated tau protein

RAGE: receptor for advanced glycated end products

redox: reduction oxidation

RNAi: ribonucleic acid interference

ROS: reactive oxygen species

SD: standard deviation

SKN-1: skinhead-1

SOD: superoxide dismutase

TAC: total antioxidant capacity

TFC: total flavonoid content

TNF-α: tumor necrosis factor α

TOF: time of flight

TPC: total phenolic content

UHD: Ultra High Definition

v: volume

VIP: variable of importance in projection

$\overline{X}_{1\text{-}50}$: population mean

SECTION I: INTRODUCTION

CHAPTER I. Olive leaf extracts as nutraceutical tool.

1.1. Introduction.

The leaves from the olive tree (*Olea europaea*) are one of the most abundant outgrowths in the olive grove industry. Olive leaves (OL) are long, hard, and lanceolate, measuring up to 8 cm in length and 2 cm in width. Their edges are rolled due to desiccation [1]. Leaves color ranges from green tones in the upper part to silver gray in the lower part of the tree [1]. These by-products are important players in the environmental impact of olive oil production, due to the high water and energy expenditure for their removal, as well as gas and trash generation. The European Union (EU) is the biggest producer of olive by-products worldwide. Spain, Greece, Italy, and Portugal generate nearly 99% of the EU production [2,3]. OL extract are mainly used for animal consumption, biomass production or incineration [4]. Nevertheless, they are rich in numerous bioactive compounds such as secoiridoids (i.e., oleuropein), phenolic alcohols (e.g., hydroxytyrosol and oleoside), flavones (e.g., luteolin and luteolin-7-O-glucoside), and phenolic acids (i.e, verbascoside) that might be used for other applications such as nutraceuticals development [5,6]. In particular, OL extract has demonstrated important biomedical properties such as antiviral, antimicrobial, anti-inflammatory, antioxidant, and anti-Alzheimer activities [5,7,8]. Therefore, the exploitation of OL extract to obtain value-added products enriched in phytochemicals might create new economic opportunities for the olive grove industry and reduce the environmental burden generated by these by-products.

Phenolic compounds are the main class of bioactive substances present in olive by-products, contributing to their health-promoting properties [5,7,8]. Recently, the profile and content of phytochemicals of OL extracts have been linked to their antioxidant capacity [4]. Therefore, the composition, concentration, and extraction yield of these compounds may affect the OL extract applications. Numerous factors have been

described as OL extract phytochemical profile modulators such as olive cultivar, climate, pruning season, drying conditions and the extraction solvent, among others [5].

1.2. Phytochemical characterization of olive leaves

OL extracts are consumed worldwide as a nutraceutical product due to its numerous and demonstrated health properties. In fact, considerable attention has been given to OL extract because of the remarkable content of polyphenols [1]. The most representative compounds of OL extract are those illustrated in **Figure 1**. Up to date, the best-known phenolic compounds in OL extract are secoiridoid derivatives, of which oleuropein is the most abundant. Additionally, the presence of phenolic alcohols (e.g., hydroxytyrosol, tyrosol and oleoside), flavones (e.g., luteolin and luteolin-7-O-glucoside) should be highlighted together with others.

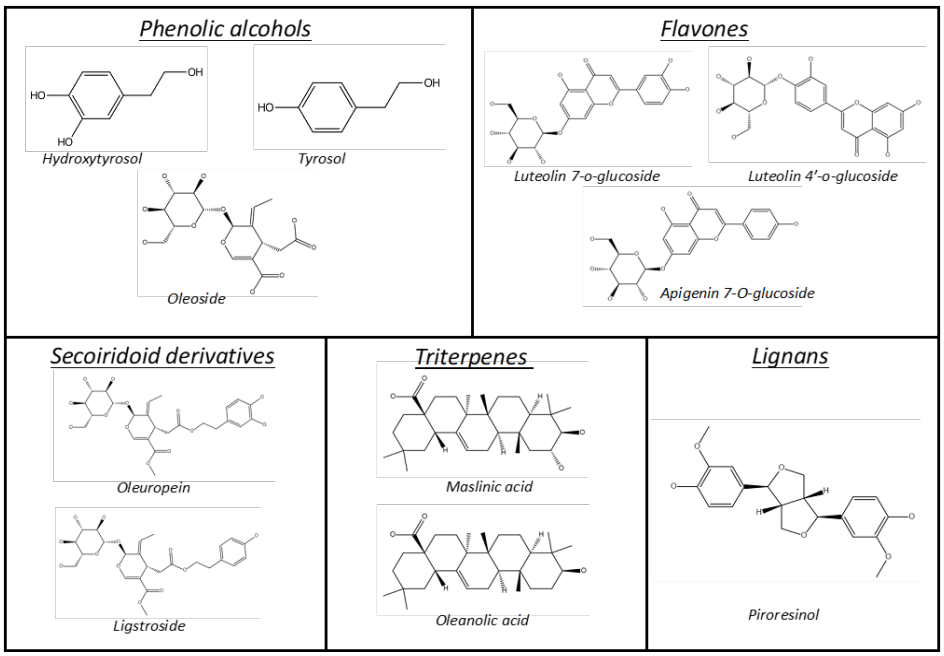

Figure 1. Most representative phytochemical compounds in olive leaves.

In the same way, other phenolic compounds, such as phenolic acids (e.g., verbascoside), flavanols (e.g., Epicatechin gallate), flavonols

(e.g., kaempferol-7-O-glucoside and rutin), among others, have also been described in OL extract (**Table 1**). The phytochemical profile of the OL extract can be affected by several factors, such as the olive tree's geographical location, cultivars, harvest season, drying temperature of leaves and the solvents used for extraction. In this regard, Kabbash *et al.* [9] demonstrated that olive leaves from Spain presented higher total flavonoid, phenolic and oleuropein content compared with olive leaves from Italy and Egypt. Similar results were obtained by Zhang *et al.* [10], which showed a higher total flavonoid, oleuropein and hydroxytyrosol content, among other phenolic compounds, in Spanish olive leaves compared with those harvested in China or Italy. These differences could also be attributed to the use of different cultivars. In this context, Nicoli *et al.* [11] found significant differences among 15 different olive tree cultivars from Italy regarding oleuropein, hydroxytyrosol, verbascoside, and flavones (luteolin and luteolin-7-O-glucoside) content. In the same way, Pasković *et al.* [12] reported several differences in oleuropein, verbascoside, rutin, catechin, phenolic alcohols (hydroxytyrosol and tyrosol) and flavones (luteolin and apigenin derivatives) content in 4 different olive tree cultivars from Croatia. On the other hand, the harvesting season has been demonstrated to influence the content of most of the phenolic compounds of OL extracts, even the same cultivar, with increases in olives harvested between March and April [9,12]. Additionally, it has been reported that the temperature of leaves drying after pruning can also affect the phenolic content. In this context, olive leaves dried using a freezing protocol (- 80ºC) presented higher amounts of phytochemicals compared with those dried using a hot air protocol (105 ºC), except for oleuropein, the content of which increased in hot air-dried olive leaves [10] Authors attributed these results to the fact that some molecules, such as flavonoids, easily break down into smaller compounds during dehydration, while the stability of secoiridoids, such as oleuropein, is relatively high. Finally, the method and solvent used for the extraction of olive leaf polyphenols has been reported to dramatically influence the final phenolic content. Most of the evaluated studies in this work used different proportions of methanol [12–16], ethanol [9–11] or

water [16,17] as solvent to obtain the olive leaf extract. However, only Kontogianni *et al.* [16] evaluated the direct influence of the solvent used in OL extract polyphenol extraction. Independently of the detection method (high performance liquid chromatography or nuclear magnetic resonance spectroscopy), the olive leaves extracted with methanol presented a higher content of oleuropein, hydroxytyrosol and luteolin and its derivatives compared with the aqueous OL extract. In fact, luteolin was not detected in the aqueous extract. For further studies, the phytochemical characterization of OL extract needs to be standardized to generate a homogeneous phenolic profile through the regulation of the previously mentioned factors.

Table 1. Phytochemical characterization of olive leaves

Compound	Formula	Content	Refs.
Secoiridoids			
Oleoside	$C_{16}H_{22}O_{11}$	nd-1.61	[18,19]
Oleoside 11-methyl ester	$C_{17}H_{24}O_{11}$	nd-1.03	[18,19]
Oleuropein	$C_{25}H_{32}O_{13}$	0.028-59.4	[9–16,18,20]
Ligstroside	$C_{25}H_{32}O_{12}$	0.17-0.86	[18,19]
Flavonoids			
Catechin	$C_{15}H_{14}O_6$	nd-0.0077	[12,15,17]
Epicatechin	$C_{15}H_{14}O_6$	nd-0.00022	[15,17,20]
Luteolin	$C_{15}H_{10}O_6$	nd-2.66	[10–13,15–17]
Luteolin-7-O-glu	$C_{21}H_{20}O_{11}$	0.30-39.78	[12,13,15,16]
Luteolin-4′-O-glu	$C_{21}H_{20}O_{11}$	0.040-3.30	[10,16]
Diosmetin	$C_{28}H_{32}O_{15}$	0.0021-0.013	[10]
Apigenin	$C_{15}H_{10}O_5$	nd-0.094	[10,12,15,17]
Apigenin-7-O-glu	$C_{21}H_{20}O_{10}$	0.079-2.15	[10,12,15,17,20]
Quercetin	$C_{15}H_{10}O_7$	nd-0.22	[10,13,17]
Rutin	$C_{27}H_{30}O_{16}$	0.0149-1.01	[10,12,13,15,20]
Taxifolin	$C_{15}H_{12}O_7$	0.003-0.274	[10,17]
Eriodictyol	$C_{15}H_{12}O_6$	nd-0.445	[10,15,17]
Hesperidin	$C_{28}H_{34}O_{15}$	nd-0.057	[15,17]
Phenolic alcohols			
Tyrosol	$C_8H_{10}O_2$	0.033-1.68	[12,15,20]
Hydroxytyrosol	$C_8H_{10}O_3$	0.067-10.93	[10,12,16,20]

Hydroxytyrosol glu	$C_{14}H_{20}O_8$	nd-0.677	[10,19]
Hydroxycoumarins			
Esculin	$C_{15}H_{16}O_9$	nd-0.061	[10,19]
Coumarin	$C_9H_6O_2$	0.004-0.020	[10]
Hydroxycinnamic acid			
Verbascoside	$C_{29}H_{36}O_{15}$	0.090-4.66	[11–13,15,17]
Phenolic acids			
Gallic acid	$C_7H_6O_5$	0.0017-1.40	[15,17,20]
p-Hydroxybenzoic acid	$C_7H_6O_3$	0.036-1.41	[13,15,17]
Vanillin	$C_8H_8O_3$	nd-0.001	[17,20]
Vanillic acid	$C_8H_8O_4$	0.003-2.74	[13,15,17]
p-coumaric acid	$C_9H_8O_3$	nd-0.044	[13,17,20]
Ferulic acid	$C_{10}H_{10}O_4$	nd-0.0096	[17,20]
Chlorogenic acid	$C_{16}H_{18}O_9$	nd-0.26	[10,13,15,17,20]
Caffeic acid	$C_9H_8O_4$	nd-0.202	[13,17,20]
Plantamajoside	$C_{29}H_{36}O_{16}$	nd-0.014	[10]
Triterpenes			
Maslinic acid	$C_{30}H_{48}O_4$	3.24-6.07	[10]
Oleanolic acid	$C_{30}H_{48}O_3$	7.58-10.48	[10]
Other compounds			
Pinoresinol	$C_{20}H_{22}O_6$	nd-0.016	[17,20]

Content is expressed as milligrams per gram of dry weight. Abbreviations: glu: glucoside; nd: no detectable.

1.3. Toxicological evaluation of olive leaves bioactive compounds

Olive leaves have been widely used as therapeutic tools throughout history [21]. In contrast to the classical belief that botanic related products are completely safe and lack toxicity, these products could cause several side effects since most of the chemical content remain uncharacterized. In addition, due to the easy access and low cost of these by-products as well as the possibility of self-medication without medical advice for many people around the world, the study of OL extract related toxicity is mandatory. Therefore, in this section, the evidence about toxicity related to the intake of olive leaves is discussed.

According to *in vitro* studies, the co-incubation of different concentrations (51.2, 128, 320, 800, 2000, and 5000 microgram [μg]/ milliliter [ml]) of OL extract did not reveal pro-mutagenic effect in different *Salmonella typhimurium* (TA98, TA100, TA1535, and TA1537) and *Escherichia coli* (WP2 uvrA) strains in Bacterial Reverse Mutation Test [22]. In the same way, coincubation with rising concentrations of OL extract (250, 500, 750, 1000, and 1250 μg/ml) did not affect the number of aberrant cells, polyploidy rates or endoreduplication metaphases in V79 male Chinese hamster lung cells in the Chromosomal Aberration Test [22]. Similarly, treatment with lower OL extract dosages (20, 40, 60, 70 or 80 μg/ml) has demonstrated not to reduce or even increase viability in different cell lines [23,24].

Acute toxicity of OL extract has also been evaluated in *in vivo* models. In this context, no adverse reactions, toxicity clinical signs or lethality were observed after 24-48 hours (h) of OL extract administration in *Caenorhabditis elegans* (0.1, 1, 10, 100, 1000 μg/ml, [*C. elegans*]), NMRI BR mice (500, 1000 and 2000 mg/kilogram [kg] of body weight [BW]) or Swiss albino mice (2000 mg/kg BW) [22,25,26]. In fact, no genotoxic activity of OL extract was observed in bone marrow from these NMRI BR mice consuming 500, 1000 or 2000 mg/ml for 48 h [22] or *Drosophila melanogaster* acutely exposed to 3.75 or 30 μg/ml of OL extract [27]. Additionally, no embryotoxicity were found after an acute exposure to 100 μg/ml of OL extract for 24 h in *C. elegans* Wild-type strain [26]. Regarding sub-chronic toxicity of OL, the intake of 100, 200, 400 or 2000 mg/kg BW of OL extract daily via gavage for 14 or 28 days did not produce mortality, signs of toxicity or behavioral and physical alterations in Wistar male and female rats. In addition, necropsy showed no abnormalities in the liver and kidney of treated rats [28]. Similar results were obtained in Wistar rats orally supplemented with 360, 600, or 1000 mg/kg BW of OL extract daily for three months [22]. Additionally, these authors found no alterations in organ weight (liver, adrenals, kidneys, thyroid/parathyroid, thymus, spleen, brain, heart, epididymites, testes, ovaries, fallopian tubes, and uterus) or pathological lesions in the most representative organs from

locomotor, digestive, lymphatic, integumentary, respiratory, cardiovascular, endocrine, excretory, reproductive as well as central and peripheral nervous systems [22]. Similarly, the consumption of 250 mg/day of OL extract in a double blind, randomized controlled trial for 12 months revealed absence of side effects in aged women [29]. In accordance with chronic toxicity, only one study evaluated the long-life effect of OL. In this context, lifelong administration of 100 μg/ml did not modify the survival rates in the *C. elegans* Wild-type strain [26].

Among the *in vivo* endpoint studies, some research has evaluated the influence of OL extract treatment in biochemical and hematological parameters. Interestingly, after an acute administration of 2000 mg/kg BW of OL, some hematological (hematocrit, hemoglobin, mean corpuscular volume, red blood cells and platelets) and biochemical parameters (cholesterol and creatinine levels) were reduced without producing abnormalities in liver or kidneys [28]. It should be noted that the solvent used in this work was a solution made with 51% of ethanol which could also interfere in hematological and biochemical studies and not be attributed to the treatment itself. In fact, when the same solvent was administered for 28 days, the effect on hematological and biochemical parameters disappeared, probably, due to an adaptation to alcohol consumption [28]. Similarly, the intake of 360, 600, or 1000 mg/kg BW of OL extract diluted in distilled water daily for three months did not alter most of the hematological parameters, electrolytes as well as renal and hepatic markers studied in rats [22]. According to hepatic markers, no adverse effects were noted related to aspartate and alanine aminotransferase, gamma glutamyl transferase and alkaline phosphatase levels in middle-aged people who consume 270 or 400 milligram (mg) of OL extract [30]. Similarly, no clinical changes were observed in classical biochemistry, hematological and electrolytes parameters as well as renal and liver function related parameters in a randomized controlled trial which administered 1000 mg/day of OL extract for 8 weeks [31].

1.4. Bioaccessibility and bioavailability of olive leaf polyphenols

A crucial point of drug administration is the capacity of the active principle to be absorbed, passed to the systemic circulation, and to exert its action on the specific sites. In the case of a multicomplex food matrix such as OL extract, it is necessary to evaluate the absorption and metabolism of numerous compounds present in it, and to evaluate the role of these compounds in the observed healthy effects. Some studies have investigated the pharmacokinetics of olive leaf phenolics by administering isolated compounds. However, in this work, the bioaccessibility and bioavailability of individual compounds were examined but after OL extract administration.

According with *in vitro* studies, gastric, intestinal as well as colonic digestion significantly reduced the bioaccessibility of numerous compounds naturally presents in OL extract, such as phenolic acids (e.g., verbascoside, chlorogenic, gallic and caffeic acid), phenolic alcohols (e.g., hydroxytyrosol and tyrosol), secoiridoid derivatives (e.g., oleuropein), flavones (e.g., luteolin 7-O-glucoside, apigenin 7-O-glucoside), flavanols (e.g., epicatechin) and flavonols (i.e. quercetin-3-O-rutinoside,quercetin-3-O-galactoside, Kaempferol and rutin) [18,20]. However, *in vitro* digestion also promoted the bioaccessibility and the potential bioavailability of some secoiridoid derivatives related to oleuropein hydrolysis such as oleoside and oleoside 11-methyl ester [18].

Up to date, only three investigations have explored the bioavailability of phenolic compounds from OL extract in humans. As can be observed in **Table 2**, numerous compounds such as secoiridoids derivatives, phenolic alcohols and flavonoids can be found in plasma or urine samples after OL extract ingestion. No significant influence of gender on the absorption of OL extract phenolic compounds was observed in middle-aged people after OL extract consumption (270 or 400 mg/d). Interestingly, the administration of OL extract through liquid glycerol preparation increased the plasma bioavailability of oleuropein

and reduced the time to peak of hydroxytyrosol derivatives compared with soft gel capsules administration [30].

Table 2. Olive leaf extracts metabolites found in plasma and urine samples in humans

Compounds	Formula	Plasma	Urine	Refs.
Phenolic alcohols				
Hydroxytyrosol	$C_8H_{10}O_3$	-	✓	[32]
Hydroxytyrosol sulfo glucuronide	$C_{14}H_{18}O_{12}$	✓	✓	[30,33]
Hydroxytyrosol glucuronide	$C_{14}H_{18}O_9$	✓	✓	[30,33]
Hydroxytyrosol sulfate	$C_8H_{10}O_6$	✓	✓	[30,33]
Hydroxytyrosol-acetate glucuronide	$C_{16}H_{20}O_{10}$	✓	✓	[33]
Tyrosol	$C_8H_{10}O_2$	-	✓	[32]
Tyrosol glucuronide	$C_{14}H_{18}O_8$	✓	✓	[33]
Homovanillic alcohol	$C_9H_{12}O_3$	-	✓	[32]
Homovanillic alcohol sulfate	$C_9H_{12}O_6S$	X	✓	[33]
Homovanillic alcohol glucuronide	$C_{15}H_{20}O_9$	✓	✓	[33]
Secoiridoid derivatives				
Oleuropein	$C_{25}H_{32}O_{13}$	✓	✓	[30]
Oleuropein aglycone	$C_{19}H_{22}O_8$	-	✓	[32]
Oleuropein aglycone dialdehyde	$C_{17}H_{20}O_6$	-	✓	[32]
Oleuropein aglycone derivative 1	$C_{25}H_{32}O_{15}$	✓	✓	[33]
Oleuropein aglycone derivative 2	$C_{25}H_{32}O_{14}$	✓	✓	[33]
Oleuropein aglycone glucuronide	$C_{25}H_{30}O_{14}$	✓	✓	[33]
Oleuropein sulfate	$C_{19}H_{22}O_{11}S$	✓	✓	[33]
Elenolic acid	$C_{11}H_{14}O_6$	X	✓	[33]
Elenolic acid glucuronide	$C_{17}H_{22}O_{12}$	X	✓	[33]
Flavonoids				
Luteolin	$C_{15}H_{10}O_6$	✓	X	[33]
Luteolin glucuronide	$C_{21}H_{18}O_{12}$	✓	X	[33]

Symbols: ✓: indicates presence of the compound in the sample; X: indicates the absence of the compound in the sample; -: indicates the absence of evidence about the specific metabolite in the sample.

According to the pharmacokinetics, the biological half-life of plasma oleuropein metabolites (1.33-2.01 h) was shorter than hydroxytyrosol derivatives (1.73-6.53 h), whereas the excretion peak rate in urine was 8-24 h for both metabolite classes [32,33]. The most abundant compounds found in urine were secoiridoids, hydroxytyrosol and its derivatives, probably, due to the rapid hydrolysis of oleuropein in the upper gastrointestinal tract [32,33]. It should be noted that the hydrolysis of oleuropein is not complete and numerous glucuronidated and sulfated derivatives from oleuropein can be found in plasma and urine, indicating that oleuropein is also conjugated by Phase II enzymes [33]. Curiously, in a study with pre- and post-menopausal women who were fed with 250 milligrams (mg) of OL extract revealed that OL extract related metabolites such as hydroxytyrosol glucuronide and sulfate, oleuropein aglycone glucuronide and aglycon derivative I, were present in higher concentrations in the plasma from post-menopausal women. Authors attributed these results to potential age-related changes such as alterations of hormonal status and a decrease in gastric emptying [33]. These results are extremely interesting due the existence of a potential increase of bioavailability of phenolic compounds from OL extract related, at least in part, to women's age, opening the door to their potential use in aging and age-related diseases.

CHAPTER II. Molecular mechanisms of the protective effects of olive leaf extracts against Alzheimer's disease

2.1. Alzheimer's disease

Alzheimer's disease (AD) is a multifactorial neurodegenerative disease of unknown etiology, first diagnosed by Alois Alzheimer in 1907. It is characterized by a progressive deterioration of cognitive function, memory, as well as language and orientation dysfunctions. AD is the cause of around 60-70% of global cases of dementia [34] and approximately 50 million people have been reported to suffer from this disease world-wide [35]. In fact, AD incidence rates double every 5 years from 60 years of age on [36] and it is estimated that dementia will affect 81.1 million people worldwide in 2040 [35,37].

2.1.1. Epidemiology of Alzheimer's disease

According to global statistics from the Global Burden Disease Study, AD has emerged as one of the fastest-growing diseases among the 50 leading causes of death from 1980 to 2016 [38]. In 1990, the prevalence of AD in Europe was 4.4% among individuals older than 65 years. With the ongoing aging of the world population, the number of people affected by AD follows a positive linear trend, estimated to reach approximately 106.8 million patients by 2050, with 16.51 million in Europe alone [39]. It's noteworthy that there are regional variations in the prevalence of AD in Europe, with higher prevalence in southern Europe (6.88%) compared to the north (4.31%). Additionally, females show a higher prevalence (7.13%) compared to males (3.31%). The prevalence also increases with age, from 0.97% in those aged 65 to 74 years to 22.53% in those aged over 85 years [39].

Regarding the incidence of AD in Europe, it currently stands at 10.8 per 1000 people/year. The incidence differs between the north (15.84 per 1000 people/year) and the south (8.97 per 1000 people/year). When considering sex, females have a higher incidence (13.25 per 1000

people/year) than males (7.02 per 1000 people/year). Furthermore, with advancing age, there is a notable increase in the incidence of AD, reaching 35.75 per 1000 people/year in individuals over 85 years of age [39]. Therefore, understanding the "natural history" of AD and its epidemiology is essential for developing early prevention strategies.

2.1.2. Classification

AD is classified based on the age of onset and whether there are hereditary factors associated with genetics. Following these criteria, it can be identifying two main types: early-onset AD, which typically appears before the age of 65 and accounts for only 1% of AD cases. This variant is the most dangerous and rapid form of the disease, with certain genes being affected, including the amyloid precursor protein (APP) gene, presenilin 1 gene, and presenilin 2 gene [40].

On the other hand, senile or late-onset AD, evolves slowly and presents with less aggressive symptoms. It usually appears after 65 years of age and constitutes 98% of AD cases. Although the exact cause remains unknown, it is believed to result from the interaction between genetic and environmental factors, with environmental factors being the major contributor to its development [41].

Lastly, there are rare cases known as atypical AD, where affected individuals are young. Often, these cases go unnoticed by primary care health personnel due to their non-specific signs and are sometimes misdiagnosed [40].

2.1.3. Etiopathogenesis and clinical signs of Alzheimer's disease

The etiopathogenesis of AD is characterized by two histopathological events: the senile plaque aggregation formed by amyloid-β (Aβ) peptides in the central nervous system and the formation of neurofibrillary tangles (NFTs) associated to the accumulation of tau protein in the hippocampus, neocortical area, and amygdala [37].

Senile plaques consist of a nucleus composed of extracellular deposits of Aβ, a peptide made up of 40-42 amino acids, which are two by-products of the amyloid precursor protein (APP). The APP can be processed following two different pathways: the non-amyloidogenic, when acting the alpha- and gamma-secretase enzymes leading to soluble polypeptides that can be broken down and recycled; or the amyloidogenic one, in which the beta- and gamma-secretases are involved producing the insoluble peptide Aβ that form extracellular aggregates [42]. The most abundant accumulation of aggregates in AD corresponds to $A\beta_{42}$, due to its insolubility and higher rate of fibrillation. On the other hand, NFTs are formed by intracellular insoluble aggregates of a hyperphosphorylated tau protein, which is typically associated with microtubules [43]. These protein deposits are surrounded by neuronal debris, apolipoproteins, activated microglia, and reactive astrocytes. This leads to the activation of microglia and astroglia, resulting in the release of inflammatory cytokines and generation of free oxygen radicals, promoting oxidative stress. The inflammatory mediators and oxidative stress cause neuronal injury and alter metal neuronal homeostasis, triggering hyperphosphorylation of the tau protein, the accumulation of $A\beta_{42}$, and the formation of NFTs and senile plaques [43].

In the same way, the accumulation of $A\beta_{42}$ oligomers and the formation of NFTs leads to neuronal dysfunction, resulting in a hyperactivity of acetylcholinesterase (AChE), favoring the degradation of acetylcholine (ACh), and promoting that AD patients develop severe ACh deficiency in the brain (**Figure 2**). This brain ACh deficit has been associated with memory loss and other cognitive symptoms related to AD [44].

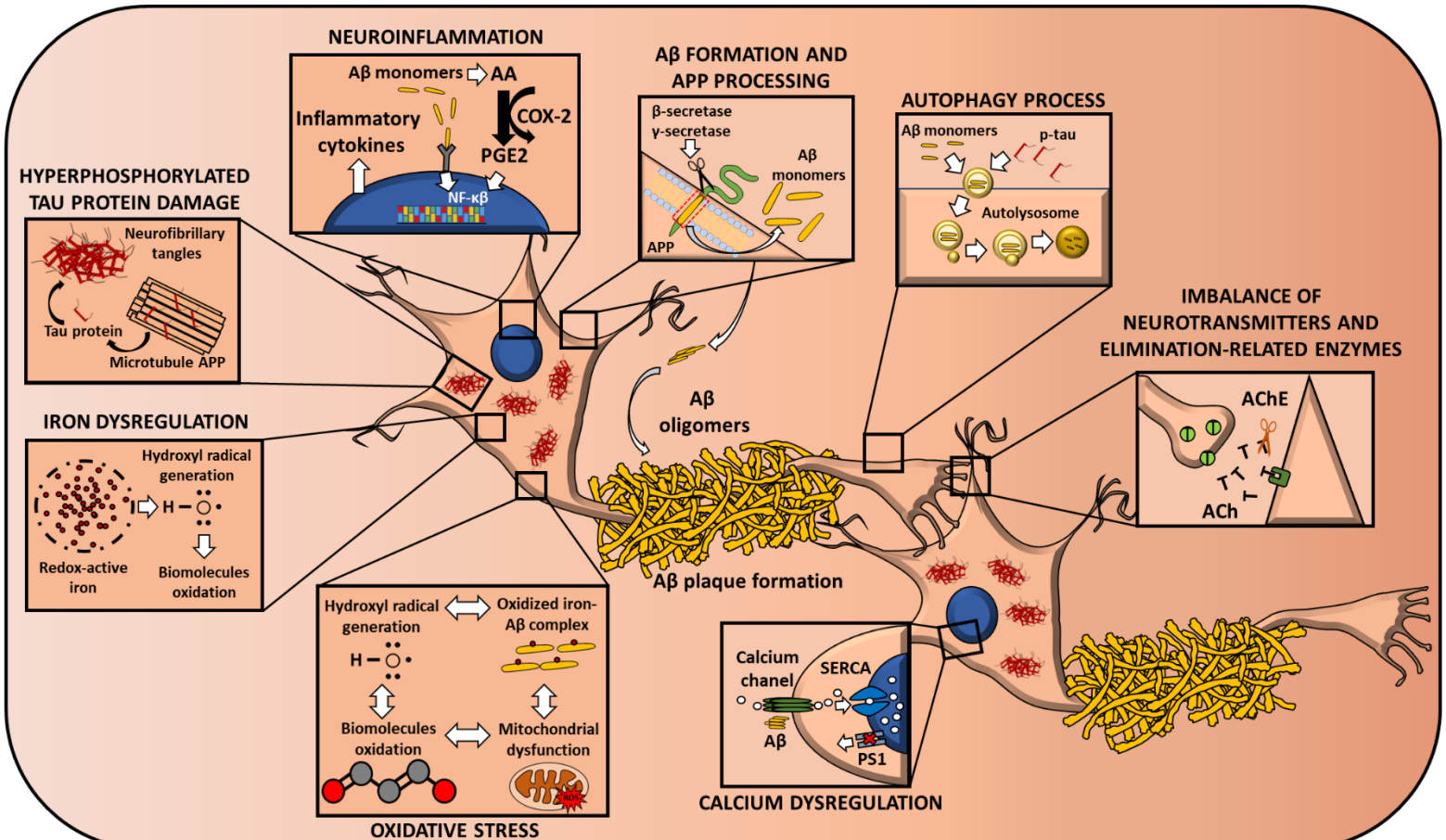

Figure 2. Summary of the main molecular mechanisms of the etiopathogenesis of Alzheimer's Disease. Abbreviations: AA: arachidonic acid; Aβ: amyloid β peptide; ACh: acetylcholine; AChE: acetylcholinesterase; APP: amyloid precursor protein; COX-2: cyclooxygenase-2; NF-kB: nuclear factor kappa-light-chain-enhancer of activated B cells; PGE2: prostaglandin E2.

Despite the etiopathogenesis of the different types of ADs sharing common factors, the symptoms and clinical manifestations are not entirely the same. The classic presentation of AD typically occurs in the elderly population and is characterized by amnestic mild cognitive impairment. This is due to an accumulation of tau and Aβ in the cortex of the medial temporal lobe, specifically the entorhinal cortex and hippocampus. As the disease progresses, more intense cognitive alterations appear, along with increased dependency, changes in behavior, memory deterioration, and other symptoms. Once senile AD is established, the life expectancy of patients is 8.5 years [45].

In contrast, the atypical AD variant exhibits different features. Memory is not affected as severely as in senile AD, particularly because the concentration of tau proteins is deposited mainly in the parieto-occipital lobes, leading to visual and motor alterations while relatively preserving memory. However, the life expectancy of patients with this variant of AD, once the symptoms have started, is 2.8 years [46].

2.1.4. Risk factors and treatment

AD is a multifactorial disease whose appearance and development are marked by the interaction between genetic predisposition and external factors throughout life [37]. Among the risk factors, aging, gender (higher incidence in women), alcohol and tobacco consumption, obesity, and metabolic disorders such as diabetes mellitus, as well as a low cultural level or family history have been highlighted [34]. Some of these risk factors including those related to physical activity, diet, smoking, obesity, and alcoholism could be modified to reduce the onset of the disease [37].

Once the AD is established, the pharmacological treatment is limited. As mentioned above, during AD, the patients develop severe ACh deficiency in the brain, which has been associated with the cognitive symptoms related to AD [44]. Therefore, the inhibition of this acetylcholinesterase (AChE) hyperactivity can extend the cholinergic

transmission time and increase the cholinergic signaling. In fact, AChE inhibitor (AChEI) drugs are the only pharmacological treatment approved for AD patients. Nowadays, the most widely used AChEI drugs are physostigmine, donepezil, rivastigmine, and galantamine, which exhibit some amelioration of AD symptoms, although they do not prevent the brain damage. However, due to the significant side effects, the use of these AChEI drugs is limited [47]. Similarly, other emerging pharmacological strategies have been proposed such as nonsteroidal anti-inflammatory drugs administration and iron chelation therapy for AD treatment with promising results [48,49]

Although there is still no effective pharmacological therapy for its treatment, the preventive and/or therapeutic nutritional interventions against AD have been gaining prominence in recent years [34]. It is known that 35% of dementias could be caused by modifiable risk factors associated with lifestyle, including the type of diet [34]. In particular, the Mediterranean Diet (MD), characterized by a high consumption of legumes, vegetables, fruits, vitamins and virgin olive oil, and a low consumption of red meat, has been shown to reduce the incidence of AD [34]. MD presents a high contribution of bioactive substances such as phenolic compounds, which have been shown to exert a protective effect in AD [50]. Particularly, the intake of phytochemical compounds naturally present in foods, such as oleuropein, hydroxytyrosol, luteolin or catechin are related to neuroprotective effects in AD through the modulation of mechanisms such as oxidative stress and neuroinflammation, besides reducing the deposition and toxicity of the misfolded proteins involved [51–56].

2.2. Effects of olive leaf bioactive compounds in the molecular mechanisms related to Alzheimer's disease

2.2.1. Aβ aggregation

As mentioned before, an abnormal extracellular accumulation and clearance of the Aβ in the brain is one of the main features of AD, which leads to neuron death and the typical symptoms of dementia [57]. In this regard, several studies have evidenced the protective role of OL extract and its bioactive molecules.

In vitro experiments indicated that individual compounds from OL extract were able to reduce both the aggregate size and occurrence of $A\beta_{42}$ fibrils [57]. In the human neuroblastoma SH-SY5Y cell line, treatment with an OL extract fraction enriched in phenolic compounds (oleuropein, hydroxytyrosol, verbascoside, luteolin, and quercetin) reversed the loss of viability induced by the neurotoxic agent $A\beta_{1-42}$. The lipid profile analysis performed using bioinformatic tools revealed that a great number of phosphatidylcholines and phosphatidylethanolamines significantly increased, whereas several triacylglycerols decreased in the treated neuroblastoma cells [58]. In the same model, treatment with the compounds and commercial preparation of OL extract exerted a stronger protection against $A\beta_{42}$, Cu-$A\beta_{42}$ or L-DOPA-$A\beta_{42}$ induced neurotoxicity, manifesting an increase on cell viability [57]. In accordance with a computational binding affinity test, the neurotoxicity reduction mentioned above might be attributed to the ability of oleuropein, hydroxytyrosol, luteolin, verbascoside and luteolin as well as its derivatives to strongly bind to the hairpin-turn of the $A\beta_{1-40}$ and $A\beta_{1-42}$ monomers and the subsequent reduction of Aβ fibrillization [59]. On the other hand, β-secretase site-1 (BACE-1) is involved in the generation of the Aβ aggregation since it participates in the amyloidogenic processing of the APP. *In vitro* assays have demonstrated that bioactive compounds present in olive tree-derived products, both non-flavonoid (e.g., hydroxytyrosol, verbascoside) and flavonoids (e.g., rutin, and quercetin)

have a remarkable inhibitory activity of the BACE-1 enzyme. The commercial olive biophenol extracts (olive leaf extract rich in oleuropein or hydroxytyrosol) also exerted a strong inhibitory activity, the latter being the most powerful. Although the action mechanism of extraction of olive biophenols is not clearly understood, the results showed a synergistic effect of the combination of flavonoid or non-flavonoid compounds in the extracts which are rich in biophenols [60].

Regarding the *in vivo* evidence, a transgenic strain of *C. elegans* expressing the human $A\beta_{1-42}$ peptide in muscle cells was used by Romero-Márquez *et al.* [26] for evaluating the anti-Aβ aggregation effect of an olive leaf extract containing 40% of OL (40% O-OL) extract. Results showed a delay in the amyloid-induced paralysis of worms and a reduction in the amount of Aβ deposits stained by Thioflavin T. The RNAi test showed the participation of abnormal dauer formation (DAF)-16, skinhead (SKN)-1, and heat shock protein (HSP)-16.2 pathways in those effects. This extract has been authorized to be used as an ingredient for nutritional supplements in human nutrition, so it could be a very promising approach for AD therapy. Similar results were found for a 20% hydroxytyrosol-rich extract from olive fruit (20% H-OF) [61].

Apart from cells and nematode models, the anti-amyloid effect of olive leaves has also been evaluated in rodents. The AD models 5xFAD and APPswe/PS1dE9 mice overproduce the Aβ peptide and develop progressive cerebral Aβ deposits and learning and memory impairment. Olive leaf extract enriched in oleuropein mixed with the powdered food was able to reduce the total Aβ deposits in the hippocampus and cortex in both 5xFAD [62] and APPswe/PS1dE9 [57] animals. The soluble $A\beta_{40}$ levels [62] and the size of Aβ plaques [57], respectively, were reduced as well. Furthermore, an increase in the expression of Aβ clearance proteins (P-gp and LRP1) was observed in the treated group. The induction of anti-amyloidogenic protein and enzyme expression (sAPPα and α-secretase) and the reduction of the amyloidogenic protein sAPPβ suggested that the olive leaf extract can modulate APP processing [62]. The effect of 40% O-

OL extract on Aβ production was also investigated in male white rabbits, although not in an AD model but in one of cervical myopathy. The increase of Aβ in spinal cord tissue neuron cells after receiving compression treatment was effectively reduced by the treatment [63]. These results could be attributed to the high content of oleuropein aglycone present in olive leaves, which was also demonstrated to reduce Aβ-induced neurotoxicity through the reduction of Aβ aggregates in rats cerebrally injected with $A\beta_{42}$ [64]. These results could be explained by Brogi *et al.* [65] using molecular docking. In this research, authors showed that oleuropein aglycone was able to move in depth within the Aβ fibrils targeting a key motif in Aβ peptide, promoting structural instability and Aβ fibril disaggregation.

2.2.2. NFTs formation

Together with Aβ aggregation, AD is characterized by the intracellular accumulation of hyperphosphorylated NFTs. The tau aggregation has been investigated using the experimental model *C. elegans*. In this case, a transgenic strain expressing the pro-aggregate human Tau protein in a constitutive pan-neuronal way was used. This strain manifests locomotion defects derived from tau deposition. Treatment with 40% O-OL extract improved several locomotive parameters related to tau neurotoxicity through the modulation of the DAF-16, SKN-1, and HSP16.2 pathways. Those transcription factors were also involved in the protective effect of the treatment against the Aβ proteotoxicity [26]. Likewise, in a rabbit model extracts with the same percentage of oleuropein decreased the high levels of p-tau in spinal cord tissue neuron cells after receiving compression treatment in the cervical myelopathy [63]. These results might be attributed to the high content of oleuropein and its derivatives and hydroxytyrosol, which have been shown to prevent tau fibrillization *in vitro* [66].

2.2.3. Neurotransmitters degradation enzymes

The action of specific enzymes on neurotransmitters or certain proteins can lead to the development and progression of neurodegenerative diseases such as AD. The cholinesterases, AChE and butyrylcholinesterase (BChE), are some of the enzymes associated with AD. AChE and BChE hydrolyze choline esters degrade the neurotransmitter acetylcholine. In fact, one of the hypotheses of AD is the cholinergic one. This system is severely affected in AD, and the over activation of the mentioned enzymes appear to promote amyloid Aβ fibril formation. The deficit in cerebral cholinergic transmitters ultimately results in memory loss with other cognitive symptoms that are characteristic of AD. In that sense, one enzyme involved is histone deacetylase, that is required for memory formation. Studies have shown the relation between defects in this enzyme and the development of neuropathology and tau neurofibrillary tangles formation [5].

On the other hand, AChE and BChE were effectively inhibited by the aforementioned commercial leaf extracts rich in hydroxytyrosol or oleuropein [60], but also by an ethanolic extract of olive leaves from different geographic origins [67]. In addition, different types of olive leaf extracts obtained by supercritical fluid extraction exerted that activity as well [68]. The best adsorbent was sea sand, that yielded extracts rich in triterpenes with moderate inhibitory activity of the enzyme [68]. In contrast, hydroxytyrosol [60], oleuropein [60] or maslinic acid [69] alone were not able to inhibit the enzymes, whereas oleanolic acid [70–72] and pinoresinol [73] had a very slight inhibitory activity. In the same way, some representative compounds present in OL extract such as tyrosol, luteolin 7-O-glucoside, and ligstroside showed a null correlation with both AChE and BchE inhibitory activity [74]. These results suggested that the enzyme inhibitory effect of OL extract might be caused, once again, by a synergism between different compounds present in the leaves.

2.2.4. Neuroinflammation

Inflammation is a common condition present in neurodegenerative diseases and is considered another pathological feature of AD. *In vitro* assays based on the ability of inhibiting the lipoxidase (LOX) demonstrated a modest anti-inflammatory potential of different types of OL extracts obtained by supercritical fluid extraction [68]. Positive results in that sense were found in cell cultures as well. Treatment with green olive leaves containing oleuropein 20% in N1 murine microglia cell culture decreased BSA-AGE-induced NO production [75]. The lipopolysaccharide (LPS)-induced increase of inflammatory markers was ameliorated by treatment with olive leaf extracts in human THP-1 monocytes [58] and in activated murine macrophages RAW 264.7 [76]. Concentrations of 20 and 40 μg/ml of an olive leaf fraction enriched in triterpenoid compounds reduced interleukin (IL)-6 and IL-1β secretion levels. Furthermore, the highest dose was able to reduce TNF-α levels in the monocyte cell line [58]. RAW 264.7 macrophages were treated with oleuropein-rich leaf extract in acute (50 μM extract with LPS for 24 h) or chronic exposure (50 μM extract pre-treatment for 24 h followed by LPS). Both acute and chronic treatment decreased NO production and strongly reduced the levels of Inducible nitric oxide synthase (NOS) and cyclooxygenase (COX)-2. Besides that, both types also decreased the mRNA expression of IL-1β and IL-6 whereas the acute one was able to reduce IL-1βR protein expression and mRNA expression for TGF-β [76].

In the same line, the potential anti-inflammatory activity of olive leaves was also demonstrated in rodents. The 5xFAD mice model accumulates high levels of Aβ along with astrogliosis and microgliosis. Animals treated with an OL extract spiked in refined olive oil and mixed with powdered food showed less astrocyte activation and GFAP levels, together with ameliorated astrocyte shape, compared with the control group fed only with the vehicle. Microglial activation in both hippocampus and cortex was reduced as were also the IL-1β levels. In

addition, the treatment also decreased NLRP3 in the brain, a finding which is associated with the significant reduction in pro-caspase-1 and pro-caspase-8. Components of the nuclear factor kappa light chain enhancer of activated B cells (NF-κB), a classical pathway involved in inflammation, were also modulated by the extract. OL extract consumption significantly reduced the expression of nuclear factor kappa-B kinase beta subunit inhibitor (p-IKKβ), an effect that was associated with increased levels of total IκBα and reduced p-IκBα [62]. In addition, authors studied the receptor for advanced glycated end products (RAGE), which is considered a major source of Aβ entry to the brain and is related with the increase of pro-inflammatory cytokines. The interaction of RAGE with high mobility group box protein 1 (HMGB1) and the upregulation of this last protein in AD are well known. Protein levels of RAGE and HMGB1 were downregulated by the treatment. Overall, the mechanisms involved in the anti-inflammatory activity of olive leaves were the reduction the NF-κB pathway, which regulates NLRP3 and RAGE/HGMB1 [62]. Likewise, the increase of tumor necrosis factor (TNF)-α, IL-1β and prostaglandin E2 (PE_2) levels caused by lead (Pb) neurotoxicity were reduced with olive leaf extract in the hippocampus of male Wistar rats. Pb is a well-known neurotoxic agent considered as a key mediator of inflammation and oxidative stress-induced neuropathological effects. The oral administration of the extract was able to reduce tissue Pb deposition and prevent the negative effects [77]. However, oral treatment with olive leaf extract to kainic acid-induced epilepsy Wistar rats did not exert a statistically significant decrease of the pro-inflammatory cytokine TNF-α, although other parameters related to oxidative stress were improved [78]. Additionally, treatment with OL extract containing 40% oleuropein resulted in a significant decrease of the inflammatory marker CD-68 (biomarker of activated microglia-macrophage) in a model of cervical myopathy in male white rabbits [63]. Inflammatory markers were also reduced in peripheral blood mononuclear cell (PBMCs) from male human patients treated for 8 weeks with 20 ml of liquid olive leaf extract, which provided 121.8 mg of oleuropein and 6.4 mg of hydroxytyrosol daily. A downregulation of

COX-2 and IL-8 gene expression was observed in PBMCs. Furthermore, authors found a downregulation of the transcription factor jun-B, which is related to macrophage activation, and the heparin binding endothelial growth factor (EGF)-like growth factor, both related to the NF-κB, in the treated group [79].

2.2.5. Oxidative stress

Oxidative stress and mitochondrial dysfunction are involved in the occurrence and progression of AD [80]. Aβ plaques and NFTs elevation are associated with increased levels of oxidation products from proteins, lipids and nucleic acids in the hippocampus and cortex [81]. In this context, OL extract supplementation was found to reduce deoxyribonucleic acid (DNA) damage and protein carbonyls in human PBMCs [82–84]. At the brain level, several *in vivo* studies demonstrated that OL extract consumption reduced DNA fragmentation, protein carbonyls, lipid peroxidation and peroxynitrite levels in different murine models of neurodegenerative diseases [77,78,85–88] or aging [89–91]. However, OL extract supplementation did not alter the urinary markers of oxidative status of healthy young adults, indicating a possible protective role of OL extract only in redox homeostasis impaired conditions such as aging or AD [92]. The antioxidant effects of OL extract might be explained through the capacity to reduce reactive oxygen species (ROS) or reactive nitrogen species (RNS) content, which leads to the reduction of oxidizing molecules such as DNA, protein, and lipids from different tissues. In this context, some authors have demonstrated the role of OL extract as ROS scavenger *in vitro* and *in vivo*. Among them, De Cicco *et al.* [93] observed that the preincubation with OL extract was able to reduce ROS content increase induced by sodium palmitate, a free radical generator, in RAW 264.7 cells. More recently, Romero-Márquez *et al.* [26] demonstrated that N2 Wild-type *C. elegans* strain supplemented with OL extract presented lower ROS content after an acute exposition to the prooxidant 2,2′-Azobis (2-methylpropionamidine) dihydrochloride. Additionally, OL extract supplementation has demonstrated protective

effects at neuron level. In this context, a combination of OL extract with *Hibiscus sabdariffa* leaves (13:2, w:w) was able to reduce ROS content in human SH-SY5Y neuroblastoma cells damaged by H2O2 [94].

Beyond free radical scavenger activity, OL extract supplementation has shown a modulatory activity over some inducible enzymes related to antioxidant response element (ARE) system. According to literature, plasma glutathione (GSH) levels and antioxidant enzymes activity such as glutathione peroxidase (GSH-Px), catalase (CAT), and superoxide dismutase (SOD), which contribute with the progression of the disease, significantly decreased in early AD [95]. Among the neurodegenerative-like murine model studies, OL extract supplementation has been found to increase the brain activity of numerous ARE such as SOD [85–89], CAT [86–89], GSH-Px [86,89], and glutathione S-transferase (GST) [77] as well as increase GSH [87,96] brain levels. Noteworthy, what these ARE have in common is that they are regulated, totally or partially, by the nuclear factor erythroid 2-related factor (NRF)-2 [97]. NRF-2 is a transcription factor involved in the protection against oxidative stress. Under oxidative stress conditions, NRF-2 translocate to the nucleus and promotes the genetic expression of a great number of ARE [98].

Clinically, the hippocampus from AD patients presents less nuclear NRF-2 compared to healthy controls although oxidative stress markers are higher [81]. This feature indicates that ARE cannot be activated as NRF-2 does not translocate from the cytoplasm into the nucleus in hippocampal neurons in patients with AD [99]. Therefore, NRF-2 activation has been proposed as a novel target in the treatment of AD. Interestingly, some treatments such as methylene blue have demonstrated that the reduction of tauopathy, oxidative stress, as well as locomotive and memory impairment induced by NFT formation, was mediated by NRF-2 activation in a mouse model of tauopathy [100]. In this context, some authors also described the capacity of OL extract to modulate NRF-2 *in vitro* [93] and *in vivo* [26,101]. Notwithstanding, only

one work researched the role of OL-induced NRF-2 nuclear translocation to fight AD *in vivo*. In this context, the authors focused on the role of OL extract in two different experimental *C. elegans* AD models. As mentioned in the previous sections, authors demonstrated that OL extract treatment was able to reduce the cytotoxic effect of Aβ through the reduction of Aβ plaque aggregation. In the same way, the authors described a reduction of the neurotoxic effect caused by tau aggregation in OL extract treated animals. The authors partially described the mechanism of action of OL extract using ribonucleic acid interference (RNAi) technology, indicating a key role of SKN-1, a *C. elegans* ortholog of the human NRF-2, in the progression of Aβ and tau protein cytotoxicity in *C. elegans* [26]. Therefore, the increase of NRF-2 translocation, and the subsequent activation of ARE, might be a possible mechanism of action underlying the protective anti-AD effect by olive leaf supplementation.

Another target with direct influence in oxidative stress is mitochondrial dysfunction. Mitochondrial dysfunction is one of the most predominant hallmarks of present in early stages of AD [80]. Despite the role of OL extract to counteract mitochondrial dysfunction during AD has not been directly assayed, some of its major compounds has been tested. Oleuropein has been shown to modulate mitochondrial superoxide anion production through an improvement of autophagy process in PC12 cells [102]. Similarly, the treatment with a mix of oleuropein and hydroxytyrosol prevented the reduction of functionality of these organelles induced by SH-SY5Y cell exposure to $A\beta_{1-42}$ aggregates [103]. On the other hand, treatment with oleuropein prevented, in a concentration-dependent manner, the loss in the mitochondrial membrane potential exerted by primary hippocampal neurons exposed to glucose plus $A\beta_{1-42}$ peptide [104].

2.2.7. Autophagy and proteostasis

Scientific evidence indicates that some AD hallmarks such as senile plaque formation are closely related to an alteration of the autophagic pathway and the incapacity to eliminate $A\beta_{1-42}$ aggregates

[105]. Indeed, alterations in autophagic-lysosomal degradation of proteins has been associated with AD, which were correlated with AD progression in both animal models and humans [105]. Recently, it has been demonstrated that the expression of mitogen-activated protein kinases (MAPK)/p38α protein is upregulated in the brain of APP-PS1 transgenic AD mouse whereas the knockdown of MAPK in the APP-PS1 mouse stimulates macroautophagy/autophagy, reducing amyloid pathology by increasing autophagic-lysosomal degradation of BACE-1 [106]. In the same way, high levels of phosphorylated protein kinase B (PKB) were associated clinically with the progression of NFT aggregation in AD patients [107]. These features seem to be consistent in a neurodegenerative rodent model induced by Pb. The exposure to Pb induced MAPK/p38 and PKB phosphorylation in the hippocampus of rats. Interestingly, OL extract supplementation was able to reduce both autophagy markers, which were associated with a reduction of Pb-induced neurotoxicity and an improvement of behavioral and locomotive tests [77].

Although there is limited data available about the modulatory effect of OL extract on autophagy markers during AD, Leri *et al.* [103] investigated the role of an oleuropein aglycone and hydroxytyrosol equal proportion mix in a cellular model of AD. In this context, the $A\beta_{1–42}$ oligomers exposure to human SH-SY5Y cells increased Beclin1, p62 and S6 expression as well as LC3II/I ratio. It seems that $A\beta_{1-42}$ promotes the expression and activation of autophagy regulation markers, indicating an accumulation of autophagosomes with disrupted degradative activity [108]. In addition, p62 is remarkably involved in AD due to autophagic degradation through the binding of the autophagy marker LC3 [109]. With this background, hydroxytyrosol mix treated cells presented a significant time-dependent reduction of p62 levels, which was reflected in lower $A\beta_{1–42}$ oligomers on the surface, suggesting that these aggregates were digested by autophagolysosomes. In the same way, the phosphorylation level of the ribosomal protein S6, a key downstream substrate of target of rapamycin, was reduced in cells treated with the

hydroxytyrosol mix, indicating an involvement of the AMP-activated protein kinase pathway in autophagy activation mediated by olive leaf phenols [103].

Similar to autophagy modulation, the role of proteostasis network modulation has been proposed as intervention for AD management. There is extremely limited information about this topic. As far as it is known, the only work which evaluated the direct role of OL extract on the proteostasis network component during AD was evaluated in *C. elegans*. In this research, OL extract treatment was able to reduce both Aβ and tau protein induced cytotoxicity whereas an overproduction of HSP-16.2 was reported in a green fluorescent protein (GFP)-reporter strain. HSP-16.2 is an important element of protein homeostasis which involves highly conserved stress responses that prevent protein mismanagement. In *C. elegans*, HSP-16.2 encodes HSP-16, which directly interacts with Aβ peptide and interferes with oligomerization pathways, leading to reduced formation of toxic species. To confirm the role of this protein in the protective effect shown by OL extract against AD, authors used RNAi technology to knock down HSP-16.2 in two different AD-like strains of *C. elegans*. Interestingly, the authors demonstrated that the protective effect of OL extract to fight both Aβ and tau protein induced cytotoxicity was mediated by HSP-16.2 overproduction. These results were confirmed by Thioflavin-T staining, which showed lower Aβ accumulation on OL extract treated worms, probably, due to an increase of Aβ clearance mediated by HSP-16.2 [26]. In conclusion, knowledge about the role of olive leaves to contrast AD via autophagy/proteostasis modulation is far from being complete to use it as AD prevention or therapy. Notwithstanding, the limited research available seems to indicate that the protective role of OL extract might be mediated by an enhancement of autophagy and proteostasis although more research is needed.

2.2.8. Essential metals dyshomeostasis

The homeostasis of essential metals is altered in AD patients [110,111]. This term refers to metals that are naturally present in the body

and play a role in the function of numerous proteins and enzymes or act as second messengers. Some studies have also demonstrated the association between essential metals (mainly calcium, iron, copper, and zinc) and AD pathological changes [110]. The evidence about the role of OL extracts to modulate metal metabolism in the AD context is limited. The only metal assayed directly in the context of AD was copper. In this context, two studies demonstrated that the treatment with OL extract was able to improve the survival rate in SH-SY5Y cells coincubated with $A\beta_{42}$ and copper [57,112]. Similarly, some of its major compounds have also been tested. Here, the treatment with oleuropein, hydroxytyrosol, verbascoside, and luteolin were able to improve the survival rate in SH-SY5Y cells damaged with $A\beta_{42}$ and copper [57,112]. In the same way, the treatment with oleuropein aglycone and hydroxytyrosol has been proven to reduce the intracellular free calcium pool in SH-SY5Y cells exposed to $A\beta_{1\text{-}42}$, which has been related to impaired AD pathology [103].

CHAPTER III. *C. elegans* as experimental model: toxicology, drug discovery, and Alzheimer Disease

3.1. Introduction

At the outset of the 20th century, the French librarian and biologist Emile Maupas bestowed the name *Rhabditis elegans* upon what we now recognize as *C. elegans*. His observations, recorded in 1900, recounted two instances of discovering this nematode near Algiers, Algeria [113]. In his detailed treatise on nematodes, Maupas expounded upon the C. anatomy of elegans, developmental processes, and modern experiments such as the induction of a response to starvation.

During the 1940s, Victor Nigon and Ellsworth Dougherty refined laboratory culture techniques for *C. elegans*, although it wasn't until the 1970s that *C. elegans* attained its status as a model organism, largely due to the pioneering efforts of Sydney Brenner. Brenner aimed to delve into developmental biology at the molecular level, unraveling genetic contributions through attributes such as its invariant developmental pattern, transparency, swift life cycle, and ease of cultivation [114]. Initially attracting geneticists and developmental biologists, *C. elegans* soon laid pivotal groundwork for the field of toxicology. Noteworthy achievements include the assessment of DNA damage and responses to stress at both phenotypic and genetic levels [113]. Phil Williams and his team were instrumental in establishing *C. elegans* as a toxicology model [115]. Following this, the study of responses to heavy metals, toxicogenomic analysis, and medium throughput toxicity testing was assessed. [116–118].

Similarly, Richard Nass advocated for the use of *C. elegans* in investigating neurodegeneration triggered by chemical substances [119]. Recent years have witnessed a significant rise in the number of research groups engaging in this field. Consequently, *C. elegans* has emerged as a firmly established model for studies in neurodegeneration.

3.2. Biological characteristics

C. elegans is a harmless free-living nematode, which sustains itself by consuming microorganisms. It is known for its cost-effectiveness and ease of maintenance in laboratory conditions. *C. elegans* has two sexes, a hermaphrodite, and a male. adult hermaphroditic are, self-fertilizing organisms measuring about 1 mm in length. They exhibit a reproductive cycle of 2.5-4 days at room temperature, with an average lifespan of roughly 18-20 days when cultured in solid media at 20°C [120].

Upon hatching, *C. elegans* can progress through four larval stages (L1-L4) or enter a dauer larval stage following the L2 stage, bypassing the L3 stage (**Figure 3**). The dauer larval stage is a suspended development phase used to survive unfavorable conditions. Upon the alleviation of adverse conditions, *C. elegans* can recover and transition into the L4 stage to resume normal development [121].

Figure 3. Graphic representation of the life cycle of the nematode.

3.3. Growth and maintaining

C. elegans can grow in both liquid and solid media, but the last one is the most common. In the laboratory, animals are typically grown on agar Petri dishes containing a lawn of Escherichia coli OP50, a non-pathogenic bacteria strain auxotroph for uracil. The nematodes live at temperatures that oscillate between 12 and 25 ºC, increasing growth twice for every increase of 10 ºC. The growth at temperatures above 25ºC is not

possible because the worms become sterile [120]. Animals can be age-synchronized by isolating eggs, which are resistant to the beaching solution due to the chitin shell that covers them. First stage larvae (L1-L2) survive cryopreservation in glycerol solution, allowing to freeze and preserve for a long period of time at -80 ºC.

3.4. *C. elegans* as toxicology model

A large part of the knowledge created in the food toxicology field is based on *in vivo* or *in vitro* experimentation. Both models present strengths and limitations depending on the type of information required. In this context, rodent and murine models present great similarities with humans (organs, molecular pathways, among others) being tagged as gold standard in toxicology [122]. However, these models are very expensive, and the time spent in experimentation procedures is large [123]. In addition, the current trend to reduce the use of experimental animals makes it necessary to search for alternative models that allow reducing the use of mammals in the field of food toxicology. In this case, the use of *in vitro* assays permits testing many compounds and observing alterations in toxicity pathways. Notwithstanding, has been described that the use *in vitro* models of toxicity such primary human cells and immortalized cells lines could report high rate of false-negative [124] as well as false-positives [125] when it tries to reflect the specific human metabolism [126]. An alternative option is the use of small invertebrate animals such as *C. elegans*, which has been described as an intermediate between *in vitro* and mammalian models. In fact, toxicity assays which evaluate endocrine, reproductory, neuromuscular and sensory systems performed in *C. elegans* consistently predicted toxicity scores in mammals [122]. Additionally, due to their great rate of homologous and concordant pathways as well as the rapid development, it is also used for new drugs discovery screening [127]. Therefore, the use of *C. elegans* in both biomedical areas permit to elucidate the effects of cell communications, tissue interactions as well as describe the mechanism of action of many given compounds in a short lapse time.

3.5. *C. elegans* as Alzheimer disease experimental model

The nervous system of *C. elegans* is small but complex. In the adult phase of *C. elegans*, the number of neurons varies based on the specific sex, with 383 neurons observed in males and 302 in hermaphrodites. These neurons are organized into distinct ganglia along the body, encompassing the head, ventral cord, and tail. Neuronal structures in *C. elegans* are typically uncomplicated, featuring a pair of neurites, except for mechanosensory neurons that exhibit branching structures. The neurites of these neurons primarily form synapses in key areas such as the nerve ring, ventral and dorsal nerve cords, and the tail. An intriguing aspect is that neurons in *C. elegans* can be fluorescently labeled *in vivo* through genetic modifications, rendering the nematode an exceptional model for investigating neurodegenerative disorders [128,129]. Remarkably, *C. elegans* employs a wide array of neurotransmitters found in the mammalian nervous system, including dopamine, γ-aminobutyric acid, serotonin, glutamate, and acetylcholine [128,129].

One striking advantage is the ability to generate transgenic nematodes expressing human proteins linked to neurodegeneration. This capability has facilitated studies that contribute to our understanding of human diseases (**Figure 4**) [130]. Transgenic strains expressing human Aβ and tau proteins, central players with neurotoxic effects associated with conditions like AD, have been devised [131,132]. Various *C. elegans* strains express Aβ peptide, placed either in skeletal muscle or neurons, and environmental factors like temperature can modulate this expression. The paralysis observed in muscle tissues in specific strains serves as a valuable phenotype for quantifying the impact of treatments on oligomer toxicity and validating potential AD therapies [133]. Notably, neuronal Aβ expression yields a distinct phenotype, marked by chemotaxis defects, impaired fluid movement, and deficits in odor preference, associated learning behavior, and experience-dependent learning [134].

The human tau protein, when expressed pan-neuronally, leads to uncoordinated movements and age-dependent neurodegeneration.

When expressed in tactile neurons, it results in mechanical and sensory impairments [131]. Other facets of AD pathology, including AChE activity and endoplasmic reticulum defects, have also been explored in the nematode [135]. Dysfunctions related to mitochondria and ROS production have been investigated also investigated [136,137]. Furthermore, genes linked to AD-associated mutations have homologs in *C. elegans*, including apl-1 (an APP-related gene), *ptl-1* (a tau homolog), and presenilin homologs like *sel-12* and *hop-1* [132].

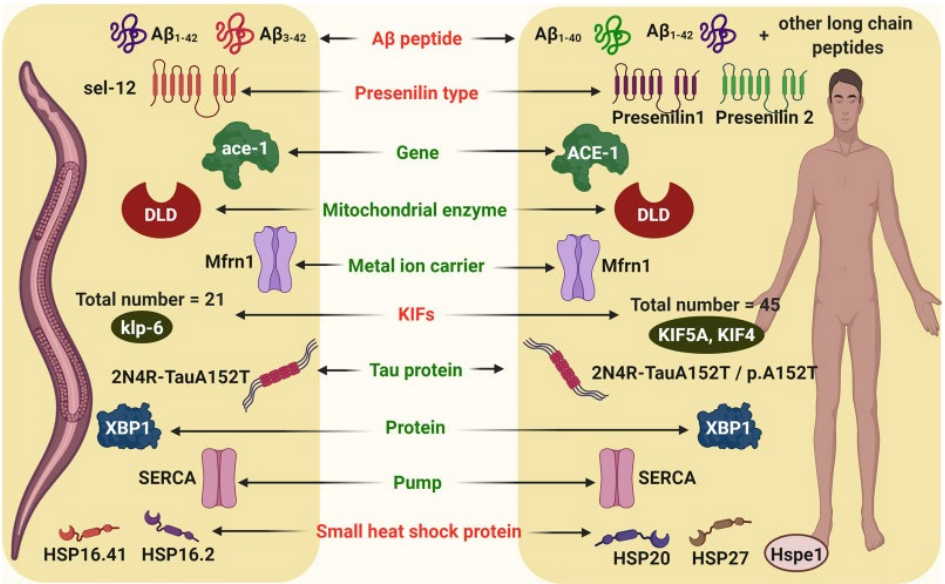

Figure 4. Comparison of protein/gene expression associated with Alzheimer's Disease in C. elegans vs Alzheimer's patient. Source: Paul et al., 2020.

3.6. *C. elegans* as experimental model: advantages and limitations

C. elegans possesses a range of attributes that position it as an experimental model. Its standout feature is an incredibly rapid three-day life cycle, maturing from egg to mature adult at 20ºC, while adaptability in growth temperatures allows developmental control [129]. Notably, self-fertilization expedites laboratory reproduction, with each hermaphroditic adult yielding 200 to 300 eggs [138]. Transparent physiology aids microscopic examination, revealing cellular details using

contrast or fluorescence techniques. Its sequenced genome and susceptibility to RNA interference offer insights into protective mechanisms [129]. *C. elegans* is an ideal model for studying neurological concerns owing to its accessible nervous system, clear characterization, and simplicity. It exhibits substantial biochemical conservation compared to humans, reflecting molecular and cellular similarities in neurons across nematodes and vertebrates [47,121]. The ease of genetic manipulation allows the creation of transgenic strains expressing human diseases, resulting in identifiable pathological behavioral patterns. These behaviors are closely tied to neuropathological issues, enabling observational experiments to effectively mirror pathological conditions. Overall, *C. elegans*' blend of neural accessibility, defined traits, and genetic flexibility, coupled with the absence of animal experimentation ethics committees, establishes it as a powerful tool for advancing neurological research [133,139].

Working with *C. elegans* for research presents remarkable advantages, yet also comes with notable drawbacks. Despite its benefits, the nematode's simple body structure lacks defined organs like a brain, blood, and internal systems. While its uncomplicated nervous system is advantageous for neurobiology study, it falls short in replicating the complexity of mammalian brains [139]. Therefore, findings in *C. elegans* must be verified through rodent experimentation. Additionally, the nematode's anatomy, including its cuticle, can impede the entry of certain compounds, potentially rendering them ineffective. The bacteria used as its food source can also alter compound composition, impacting absorption. These limitations highlight the need for careful consideration when interpreting results derived from this model [133].

SECTION II: HYPOTHESIS & OBJECTIVES

Hypothesis

Building upon the aspects outlined in the Introduction section, the hypothesis of this study is that Alzheimer's Disease, along with related mechanisms such as cholinergic function, oxidative stress, and inflammatory processes, can be modulated by bioactive by-products obtained from the olive grove industry. It's crucial to acknowledge that the redox and inflammatory state within cells play a pivotal role in the development of Alzheimer's Disease. In light of this, the use of olive leaf extracts could be an interesting approach to develop nutraceuticals as adjuvant therapy for Alzheimer's Disease.

Objectives

The main objective of this doctoral thesis was to evaluate the effect of olive leaf extracts to counteract the deleterious effects of Alzheimer's disease and its hallmarks. To reach this general objective, the following specific objectives were established:

1. Assessment of antioxidant capacity of fifty olive leaf samples from five different countries.
2. Phytochemical characterization of these extracts.
3. Evaluation of the cholinesterase, cyclooxygenase-2, and iron-oxidative inhibitory activity of these extracts.
4. Toxicological evaluation of the fifty olive leaf extracts in the *C. elegans* experimental model.
5. Selection of three samples (low, medium, and high activity) to be tested based on the aforementioned.
6. Assessment of the three OL extracts effects in markers related to redox biology and proteostasis network in different *C. elegans* strains.
7. Exploring the treatment effects on AD markers in both *in vitro* and *C. elegans* models, as well as investigating redox biology and delving into the associated molecular signaling pathways.

SECTION III: MATERIAL & METHODS

CHAPTER IV. Material

4.1. Chemicals and reagents

All reagents were of analytical grade and were purchased from Sigma-Aldrich (St. Louis, Missouri, USA), Thermo Fisher (Waltham, Massachusetts, USA), Extrasynthese (Genay Cedex, France), Agilent Technologies (Santa Clara, CA, USA), Roche (Basel, Switzerland), Panreac (Barcelona, Spain) or Merck (Darmstadt, Germany). Double distilled deionized water was obtained from a Milli-Q purification system from Millipore (Milford, MA, USA).

4.2. Equipment

- Incubators (VELP Scientifica FOC 120 E, Usmate, Italy).
- Motic dissecting microscope (Motic Inc., LTD., Hong Kong, China).
- Multi-Range Large Particle Flow Cytometer Biosorter (Union Biometrica, Massachusetts, USA).
- Wormlab Imaging System (MBF Bioscience, Williston, Vermont, USA).
- Nikon epi-fluorescence microscope (Eclipse Ni, Nikon, Tokyo, Japan) fitted with a Nikon DS-Ri2 camera (Tokyo, Japan).
- Synergy Neo2 microplate reader (Biotek, Winooski, Vermont, USA).
- High resolution SYNAPT G2 HDMS Q-TOF model (Waters, Mildford, USA).
- Waters ACQUITY I CLASS model chromatography instrument (Waters, Mississauga, ON, Canada) equipped with a mass spectrometer Waters XEVO.
- TQ-XS, with ionization performed by UniSpray (US).
- Agilent 1260 series liquid chromatograph equipped with a micro vacuum degasser, binary pump, thermostatted autosampler and column compartment, and diode array detector (Agilent Technologies, Santa Clara, CA, USA).

- Agilent 6540 Ultra High Definition (UHD) Accurate Mass Q-TOF detector equipped with a dual electrospray interface (ESI) Jet Stream interface (Agilent Technologies, Santa Clara, CA, USA).

4.3. Software

- FlowPilot software (Union Biometrica. Massachusetts, USA).
- Wormlab Imaging System Software (MBF Bioscience, Williston, Vermont, EE. UU).
- NIS-Elements BR (Nikon, Tokyo, Japan).
- SPSS 25.0 for Windows (IBM, Armonk, NY, USA).
- Masshunter workstation software version B.06.00 (Agilent Technologies, Santa Clara, CA, USA).
- MassLynx V4 software (Waters Laboratory Informatics, Mildford, USA).
- Metaboanalyst 5.0 (https://www.metaboanalyst.ca/).

CHAPTER V. Methods

5.1. Plant material characterization

5.1.1. Olive leaves obtention and extraction.

For this study, only OL from the so called "line of flight" were used, that is, the leaves that are collected along with the olives during the harvesting procedure. Leaves from the ground or leaves collected directly from the tree, were not included. Therefore, it is a true by-product derived from the olive harvesting, which inevitably reaches the mill, and for which it would be useful to find an application. Fifty olive leaves samples from four different countries were chosen for the present study (**Table 3**).

Table 3. Origin of the olive leaves from five different countries

Provider Institution	Region	Country	n
CRDOP Estepa	Seville	Spain	13
ACE	Jaen	Spain	7
IRTA	Barcelona	Spain	6
Pugliaolive	Bari	Italy	4
Parma University	Parma	Italy	2
NGC	Peloponnese	Greece	6
ACK	Kalamata	Greece	2
CEPAAL	Alentejo	Portugal	7
Esporão	Alentejo	Portugal	2
Alhouda cooperative	Ouezzan	Morrocco	1

Abbreviations: ACE: Almazara Cruz de Esteban; ACK: Agricultural Cooperative of Kalamata; CEPAAL: Centro de Estudos e Promoção do Azeite do Alentejo; CRDOP Estepa: Consejo Regulador Denominación de Origen Protegida Estepa; IRTA: Instituto de investigación y tecnología agroalimentarias; NGC: NILEAS Producers Group Company A.C. OL: olive leaves.

All samples were harvested between mid-November 2019 and mid-February 2020. Fresh OL were dried at room temperature, grinded by a blade mill, and passed through a mesh sieve (< 600 μm diameter) to obtain a fine powder. Then, plant material was stored in sealed bags at

−20 °C until extraction. The extraction procedure was performed according to the flowchart shown in **Figure 5**. One gram (g) (1.00 g ± 0.01 g) of dried OL powder was mixed with 20 ml of the extraction buffer (ethanol/Mili-Q water/formic acid, 80:20:0.1, volume (v):v:v) and stirred for 2 h in the dark at room temperature. Then, liquid OL mixture was centrifuged twice at 2400 x g for 15 minutes and the supernatants recovered. Supernatants were filtered using a 0.45 µm syringe filter (PBI International, Italy), aliquoted, evaporated by using an Speedvac SC110A (New York, USA), and stored at -80 °C until analyses [134].

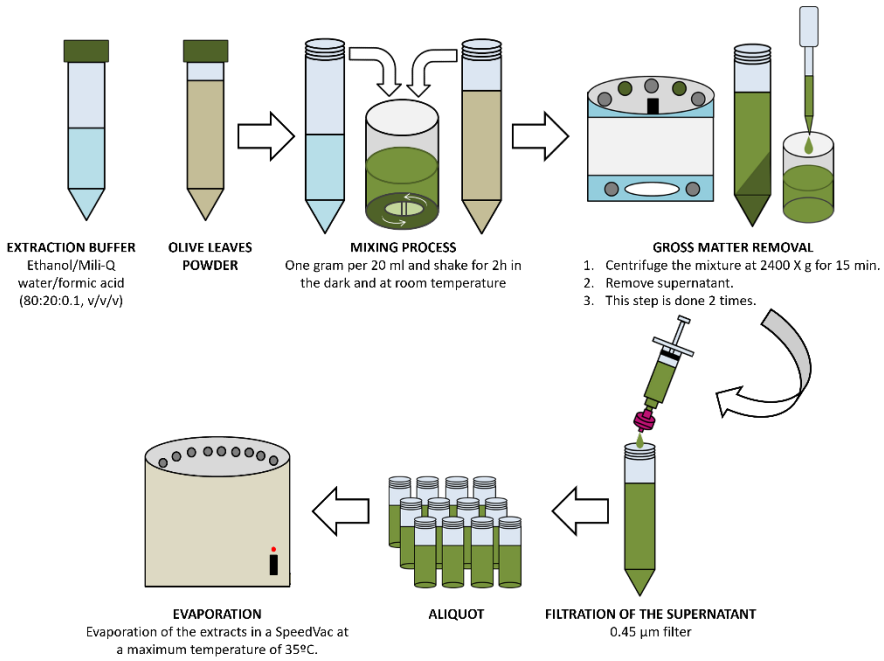

Figure 5. Schematic extraction process of the 50 olive leaf samples.

5.1.2. Identification and Quantification of the Phytochemical Compounds via HPLC-ESI-QTOF-MS/MS analysis

High performance liquid chromatography (HPLC) analyses were performed on an Agilent 1260 HPLC instrument (California, USA) equipped with a binary pump, an online degasser, an auto-sampler, a thermo-statically controlled column compartment, as well as a diode array detector. The samples were separated on an Agilent Zorbax Eclipse Plus C18 column (1.8 μm, 4.6 × 150 mm). The mobile phases consisted of water with 0.1% formic acid (A) and methanol with 0.1% formic acid (B) using a gradient elution according to the following profile: 0 min, 5% B; 5 min, 75% B; 10 min, 100% B; 18 min, 100% B; 25 min, 5% B. The initial conditions were maintained for 5 min. The flow rate was 0.8 ml/min, the column temperature was 30°C, and the injection volume was 5 μL. The compound concentrations of each OL extract were determined using the area of each individual compound and by interpolation in the corresponding calibration curve. Oleuropein, hydroxytyrosol, luteolin, luteolin-7-O-glucoside, and verbascoside were quantified by the calibration curves obtained from their respective commercial standards. The remaining compounds were tentatively quantified based on calibration curves from other compounds with structural similarities. Results are expressed as mean ± standard deviation (SD).

5.1.3. Total phenolic content

The total phenolic content (TPC) was carried out according to the Folin-Ciocalteu colorimetric method with some modifications performed by Romero-Márquez *et al.* [19]. Briefly, OL extracts and standards (gallic acid) were mixed with Folin-Ciocalteu reagent for 5 min in a 96-well plate. Then, sodium carbonate was pipette in each well, agitated, and incubated at room temperature for two hours in the dark. Finally, absorbance was recorded at 760 nm in a microplate reader Synergy Neo2 (Vermont, USA). Units were mg of gallic acid equivalent (GA) per gram (g) of dry weight (DW) extract. Results are expressed as mean ± SD.

5.1.4. Total flavonoid content

The total flavonoid content (TFC) was carried out agreeing to aluminum chloride colorimetric method with some modifications performed by Navarro-Hortal *et al.* [140]. Briefly, OL extracts and standards (catechin) were mixed with sodium nitrite for 6 min in a 96-well plate. Then, aluminum chloride was pipette, and incubated at room temperature for 5 min in the dark. Finally, sodium hydroxide was added in each well and the absorbance was recorded at 510 nm in a microplate reader Synergy Neo2 (Vermont, USA). Units were mg of catechin equivalents (CAT)/g of DW extract. Results are expressed as mean ± SD.

5.2 *In vitro* assays

5.2.1. Acetylcholinesterase inhibition assay

AChE inhibitory activity of OL extracts was performed using the colorimetric method proposed by Ellman with some modifications [141]. First, OL extracts (1000 μg/ml), and positive control (ethanol/Mili-Q water, 50:50, v/v) were incubated with AChE (10 mU/ml) and 5,5-dithiobis-(2-nitrobenzoic acid) (150 μM) in a 96-plate wells for 15 min at 30°C. Then, the acetylthiocholine iodide (substrate) was added, and the AChE activity was determined recording the changes in the absorbance at 405 nm in a Synergy 2 Biotek plate reader for 25 min at 30°C. The AChE inhibitory activities were expressed as the mean percentage inhibitory activity with respect the positive control ± standard error of the mean (SEM) and the concentration of the selected extracts causing 50 % inhibition of the AChE activity (IC50) was calculated using linear regression analysis.

5.2.2. Cyclooxygenase-2 inhibition assay

COX-2 inhibitory capacity of OL was performed via Biovision COX-2 Inhibitor Screening Kit (California, USA) following the manufactures instructions. First, OL ex-tracts (1 μg/ml) and positive

control (ethanol/Mili-Q water, 10:90, v/v) were incubated with arachidonic acid/sodium hydroxide solution and the Reaction Mix (COX-2 human recombinant enzyme, COX cofactor, COX probe and COX assay buffer) in a black 96-plate wells for at 37°C a Synergy 2 Biotek plate reader for 8 min. The fluorescent signal was recorded at 535 nm for extinction and 587 nm for emission. The COX-2 inhibitory activities were expressed as the mean percentage of inhibitory activity with respect the positive control ± SEM and the IC50 inhibitory COX-2 activity was calculated using linear regression analysis.

5.2.3. Total antioxidant capacity

The total antioxidant capacity of the studied OL was performed using three different methods based on electron transfer (ET). The ET-based methods analyze the ability of a specific antioxidant to reduce an oxidant, changing the color during this reaction. The color change magnitude is directly associated with the antioxidant concentration in the sample [142]. In this context, 2,2'-azinobis[3-ethylbenzothiazoline-6-sulfonic acid]-diammonium salt (ABTS), ferric reducing antioxidant power (FRAP, and 2,2-diphenyl-1-picrylhydrazyl (DPPH) methods were performed following the modified protocols described by Rivas-García *et al.* [134]. ABTS assay is based on the reduction of the free radical ABTS by the antioxidants present in samples. The absorbance values were measured at 734 nm. DPPH assay is based on the colorimetric measurement of the free radical DPPH reduction which is progressively lost when it is reduced by the antioxidant compounds of the samples. The absorbance was measured spectrophotometrically at 517 nm of wavelength. For the FRAP assay, this test evaluates the ability of the sample to reduce the ferric to ferrous ion. The absorbance when the iron, complexed with 2,4,6-tripyridyl-s-triazine, changes its color, was measured at 593 nm. A Synergy Neo2 microplate reader (Biotek, Winooski, Vermont, U.S.A.) was used to measure the absorbances. Every determination was performed at least three times. Units were μM of

Trolox/g of DW extract for the three methods. Results are expressed as mean ± SD.

5.3. *C. elegans* experiments

5.3.1. Maintenance and strains

All strains of *C. elegans* were obtained from the CGC (Minneapolis, MI, USA) and were housed at 20 °C on solid nematode growth medium (NGM) plates fed with *Escherichia coli* OP50 in an incubator (VELP Scientifica FOC 120 E, Usmate, Italy). The strains used were: N2-Wild type, LD1 *skn-1*::GFP (*ldIs7*); TJ356 *daf-16p*::GFP (*zIs356*); OS3062 *hsf-1*::GFP (*nsEx1730*); TJ375 *hsp-16.2p*::GFP (*gpIs1*); CF1553 *sod-3p*::GFP (*mu1s84*); and CL2166 *gst-4p*::GFP (*dvIs19*), BR5706 (*bkIs10*), CL802 (*smg-1*) and CL4176 (*dvIs27*). Only CL4176 and CL802 were housed at 16 °C. For experiments, a bleaching method was used to obtain age-matched embryos according with standards protocols [143]. Briefly, worms were washed and collected with M9 buffer and embryos were isolated using bleaching solution (sodium hypochlorite 4% and NaOH 0.5 N [20/80; v/v]). Then, embryos were washed three times and dispensed into the experimental plates.

5.3.2. Toxicological evaluation of the olive leaf extracts.

5.3.2.1. Lethality test

Short-term toxicity was assessed to analyze the potential lethal toxic effect of the different OL extracts and select no lethal concentrations for further experiments (**Figure 6A**). For this purpose, N2-embryos were grown in NGM plates for 48 h. Then, animals were moved to plates with rising concentrations of the specific OL extract (500, and 1000 μg/ml) or vehicle (dimethyl sulfoxide, DMSO) without food. After 24 h, nematodes were considered as alive or dead when there was no response to physical stimulus. Results are presented as percentage of fold change respect to the control of the average survival after 24 h of exposure. Three

independent experiments were conducted, each involving a minimum of 40 nematodes per treatment. For the rest of the tests, a non-toxic submaximal dose of 500 μg/ml was selected.

5.3.2.2. Embryotoxicity evaluation

The effect on embryonic development and viability of OL extracts was evaluated through the embryotoxicity test [144]. Briefly, N2-embryos were isolated and placed in NGM plates with *E. coli* OP50 and 500 μg/ml of the specific OL extract or vehicle (**Figure 6B**). After 24 h, larvae were scored using a microscope (Motic Inc., LTD. Hong Kong, China). Results are presented as percentage of fold change respect to the control of the mean of the relation between larvae found and the number of embryos dispensed. Three independent experiments were conducted, each involving a minimum of 50 nematodes per treatment.

5.3.2.3. Body length and width analysis

Body length and width analysis was done to evaluate the influence of OL extracts in nematodes growing according with Navarro-Hortal, *et al.* [145] with some modifications. Briefly, N2-Wild type embryos were placed in plates with 500 μg/ml of extracts or vehicle for 96 h. Then, worms were moved to slice and anesthetized with sodium azide (1 M). The WormLab Imaging System (MBF Bioscience, Williston, Vermont, EE. UU) was used to photograph and analyze the body length and size of the nematodes. Results are presented as percentage of fold change respect to the control of the average length and size of nematodes (**Figure 6C**). Three independent experiments were conducted, each involving a minimum of 20 nematodes per treatment.

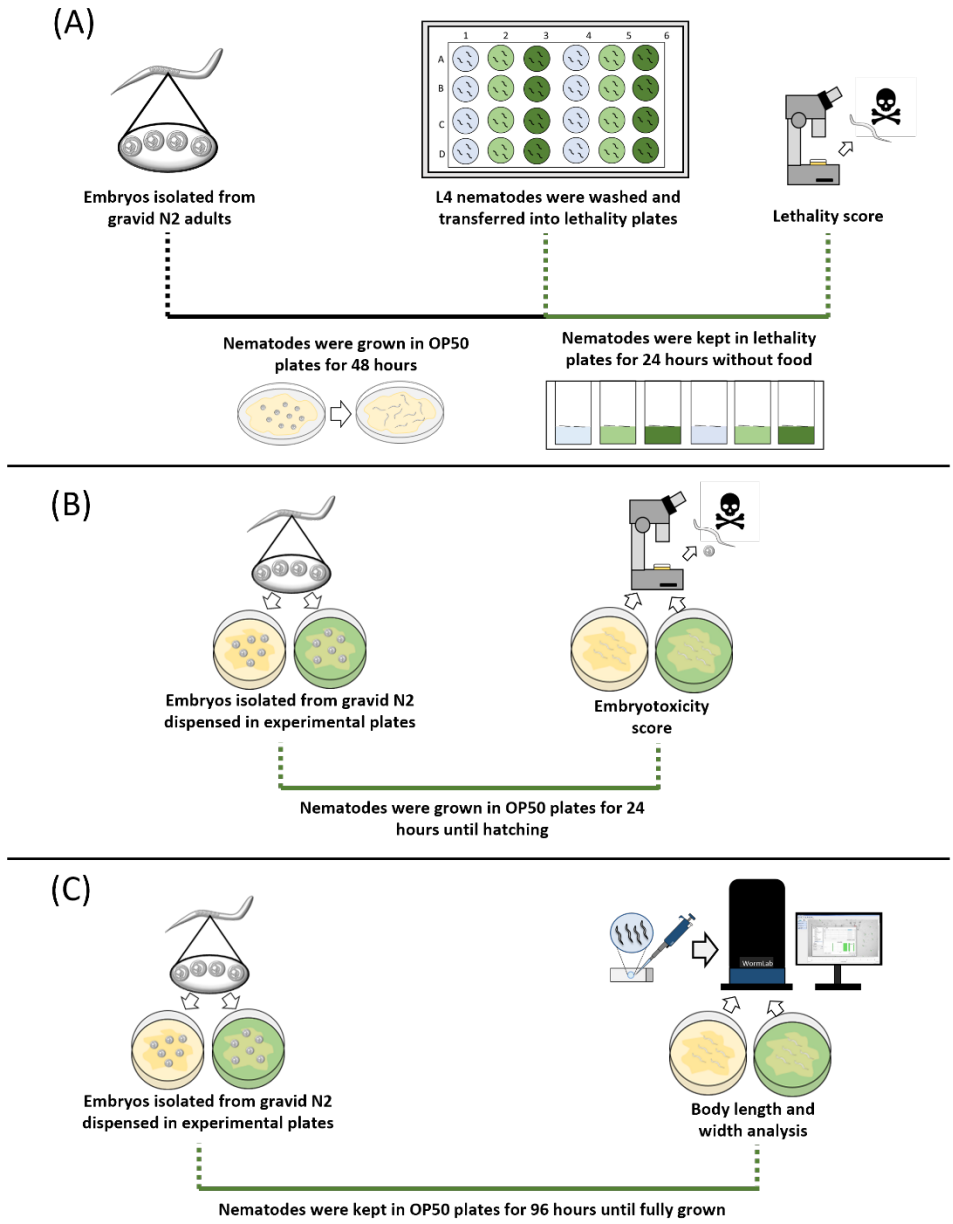

Figure 6. Schematic methodology of the toxicological experiments performed in the *C. elegans* strain N2-Wild type. (A) Lethality test; (B) Embryotoxicity test; (C) Body size analysis.

5.4. Alzheimer disease

5.4.1. Aβ-induced toxicity test

Aβ-induced toxicity tolerance test was done to determine the potential effect of OL extracts against amyloidogenic toxicity [61]. For this purpose, CL4176 was used. CL4176 is a sensitive temperature strain that expresses human amyloid β_{1-42} peptide in muscle cells which causes a progressive impairment of the movement until worms become paralyzed. CL802 was used as a negative control. Briefly, embryos from CL4176 Aβ (+) or CL802 Aβ (−) were placed in plates with 500 μg/ml of OL extracts or vehicle for 48 h at 16 °C. Next, nematodes were temperature-up-shifted to 25 °C for 22 h to induce endogenous Aβ production. Then, nematodes were counted every 2 h for 12 h (**Figure 7A**). Animals were classified as paralyzed when there was no feedback to physical stimulus but still being alive. Results are expressed as the percentage of non-paralyzed worms from three independent experiments with, at least, 100 worms per treatment.

5.4.2. Thioflavin T staining

Thioflavin T stain was used with the aim of visualizing Aβ aggregates in the CL4176 strain. Worms and plates were treated as for the paralysis assay. Synchronized CL4176 or CL802 eggs were placed on plates with the treatments and the control, seeded with *E. coli* OP50. After the incubation at 16 °C for 48 h, all the plates were moved to another incubator at 25 °C. Approximately at the time for 50% of paralysis of the non-treated group, the nematodes were collected by washes with M9 buffer and fixed with 4% paraformaldehyde (pH 7.4) at 4 °C for 24 h. After fixation, worms were permeabilized in 5% β-mercaptoethanol, 1% Triton X-100, and 125 mM Tris, pH 7.4 at 37 °C for 24 h. Next, two times washes with M9 buffer were performed to remove the permeabilization buffer. Then, samples were stained with 0.125% thioflavin T in 50% ethanol for 30 min and distained with sequential ethanol washes (50%, 75%, 90%, 75%, and 50% v/v), each one for 2 min [140]. Thioflavin T-stained worms

were observed under a Nikon epi-fluorescence microscope (Eclipse Ni, Nikon, Tokyo, Japan) and images were acquired at 40X magnification using the GFP filter with a Nikon DS-Ri2 camera (Tokyo, Japan). CL802 untreated worms were considered as negative control and the untreated CL4176 was the positive control, both incubated at 25 °C.

5.4.3. Hyperphosphorylated tau-induced neurotoxicity test

Tau-protein-induced toxicity test was done to evaluate the potential effect of OL extracts to front the neurotoxicity related to hyperphosphorylated tau protein (p-tau) aggregation [61]. For this purpose, BR5706 strain was used, which expresses a constitutive pro-aggregative human tau protein in neurons, reflecting in locomotion alterations. In this assay, embryos from BR5706 were placed in plates with 500 μg/ml of OL extracts or vehicle for 72 h at 20 °C. Then, worms were moved to a slide with M9 to stimulate animal locomotion. WormLab Imaging System (MBF Bioscience, Williston, Vermont, EE. UU) was used to document, track, and analyze worm movement (**Figure 7B**). Activity and swimming speed were selected as demonstrative parameters to evaluate mobility alterations. Results are expressed as percentage of fold change respect to the positive control of the average of activity and swimming speed. Three independent experiments were conducted, each involving a minimum of 80 nematodes per treatment.

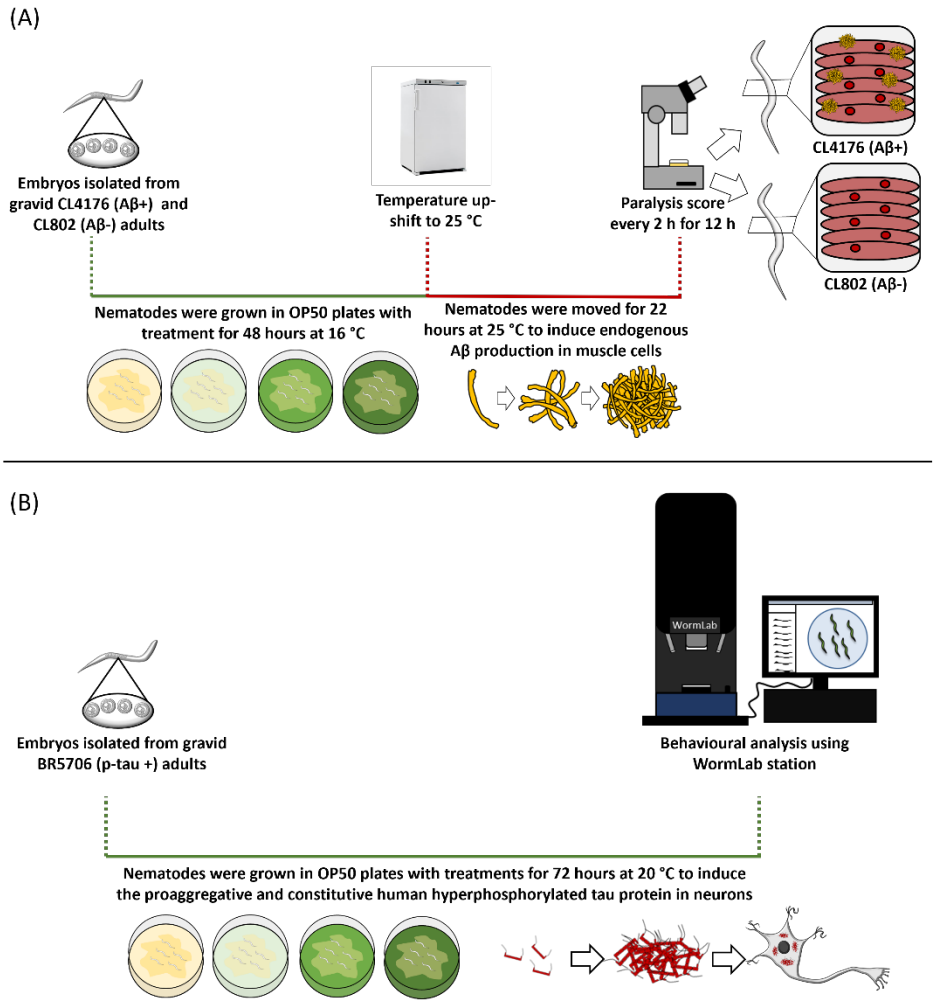

Figure 7. Schematic methodology of the Alzheimer's Disease experiments performed in *C. elegans*. (A) Amyloid-β induced toxicity test; (B) p-tau induced neurotoxicity test.

5.5. Redox biology

5.5.1. Analysis of antioxidant and proteostasis system components levels

Different worm strains containing transgenic genes coupled to the GFP reporter were used to observe the mechanisms under the protective role of OL extracts *in vivo* [145]. The transcription factors studied using different strains were SKN-1 (LD1), DAF-16 (TJ356), and heat shock transcription factor (HSF)-1 (OS3062). Among the downstream targets of the studied transcriptional factors, SOD-3 (CF1553), HSP-16.2 (TJ375), and GST-4 (CL2166) were studied. For this purpose, all strains were placed in plates with 500 μg/ml of OL extracts or vehicle for 48 h (**Figure 8**).

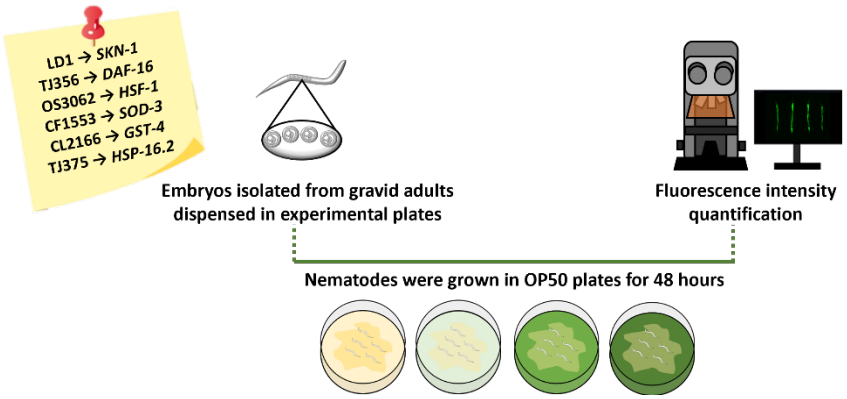

Figure 8. Schematic methodology of the green fluorescence protein (GFP) reporter test in *C. elegans*.

Then, nematodes were moved to a slide and anesthetized with sodium azide (15 μM). A Nikon DS-Ri2 camera was used to photograph the worms under the GFP filter (Tokyo, Japan) in the region of interest (**Table 4)**. Finally, to analyze the obtained images, the software NIS-Elements BR was used, and the background signal was removed from the analysis (Nikon, Tokyo, Japan). Results are presented as percentage of fold change respect to the control of the mean of the intensity of fluorescence levels of the specific strain analyzed. Three independent experiments were conducted, each involving a minimum of 90 nematodes per treatment. An exception was made for TJ356 results which are

presented as the percentage of fold change respect to the control of the average of a semi-quantitative scale (cytosolic "1", intermediate "2", or nuclear "3") of *daf-16*::GFP location.

Table 4. Specifications of the GFP reporter strains

Strain	Characteristics	Scale	ROI
LD1	The *skn-1* gene is fused to a GFP reporter and driven by the *skn-1* promoter.	10x	Whole worm
TJ356	The *daf-16a/b* gene is fused to a GFP reporter and driven by the *daf-16* promoter.	10x	Whole worm
OS3062	GFP expression of heat-shock proteins (*hsf-1*, *hsp-16.2*, and *hsp-16.41*).	40x	Worm's bulb
TJ375	The *hsp-16.2* gene is fused to a GFP reporter and driven by the *hsp-16.2* promoter.	40x	Worm's bulb
CF1553	The *sod-3* gene is fused to a GFP reporter and driven by the *sod-3* promoter.	10x	Whole worm
CL2166	The *gst-4* gene is fused to a GFP reporter and driven by the *gst-4* promoter.	10x	Whole worm

Abbreviations: GFP: Green fluorescent protein; ROI: Region of interest.

5.5.2. Intracellular ROS content

Intracellular ROS levels was conducted in both *C. elegans* AD model. Therefore, the current study employed the 2',7-dichlorodihydrofluorescein diacetate (H_2DCFDA) staining method to assess intracellular ROS levels. The nematodes from CL802 and CL4176 as well as BR5706 were growth in the same conditions as exposed for Aβ and p-tau toxicity test, respectively. For the amyloidogenic strain, the measurement of intracellular ROS content was made at the 24-h mark after the temperature upshift, while in the tauopathy strain, the analysis was conducted at 74 h post embryos bleaching (**Figure 9A**). For both cases, the dye was applied in the same form: nematodes were washed with M9 and exposed to 25 μM of H_2DCFDA for 2 h. Finally, yellow fluorescence intensity as well as the time of flight (TOF) signal were measured using a BioSorter® flow cytometer (Union Biometrica, Belgium, Europe). Results are expressed as percentage of fold change

respect to the positive control of the mean of yellow intensity of fluorescence normalized by TOF signal. Three independent experiments were conducted, each involving a minimum of 1000 nematodes per treatment.

5.5.3. Mitochondrial ROS content

Mitochondrial ROS content was conducted in both *C. elegans* AD model. Therefore, the current study employed the MitoTracker Red CM-H_2XRos staining method to assess mitochondrial ROS levels in the same conditions as intracellular ROS content. For dye application, the nematodes were washed with M9 and transferred to NGM plates containing 10 μM Mitotracker mixed with dead *E. coli* OP50 as a food source for 2 h (**Figure 9B**). Finally, red fluorescence intensity as well as the TOF signal were measured using a BioSorter® flow cytometer (Union Biometrica, Belgium, Europe). Results are expressed as percentage of fold change respect to the positive control of the mean of red intensity of fluorescence normalized by TOF signal. Three independent experiments were conducted, each involving a minimum of 1000 nematodes per treatment.

5.5.4. Glutathione content

GSH content was conducted in both *C. elegans* AD model. Then, the current study employed the monochloramine (MCB) staining method to determinate the total GSH content in the same conditions. For the dye application, the nematodes underwent a series of steps. Firstly, worms were washed with M9 buffer. Subsequently, the worms were exposed to a permeabilization buffer (M9 buffer with 1% Triton X). Following this, the nematodes were divided into two groups: the stained group, treated with 200 μM MCB, and the unstained group, treated with an equivalent amount of DMSO as a control. After an incubation period of 1 h in the dark, at a temperature of 20ºC, another wash step was performed using M9 buffer (**Figure 9C**). Following the washing, the samples were read using a Synergy Neo2 microplate reader (Biotek, Winooski, Vermont,

U.S.A.) operating in single reading mode. The measurements were taken at specific wavelengths: excitation at 380/20 nm and emission at 480/20 nm.

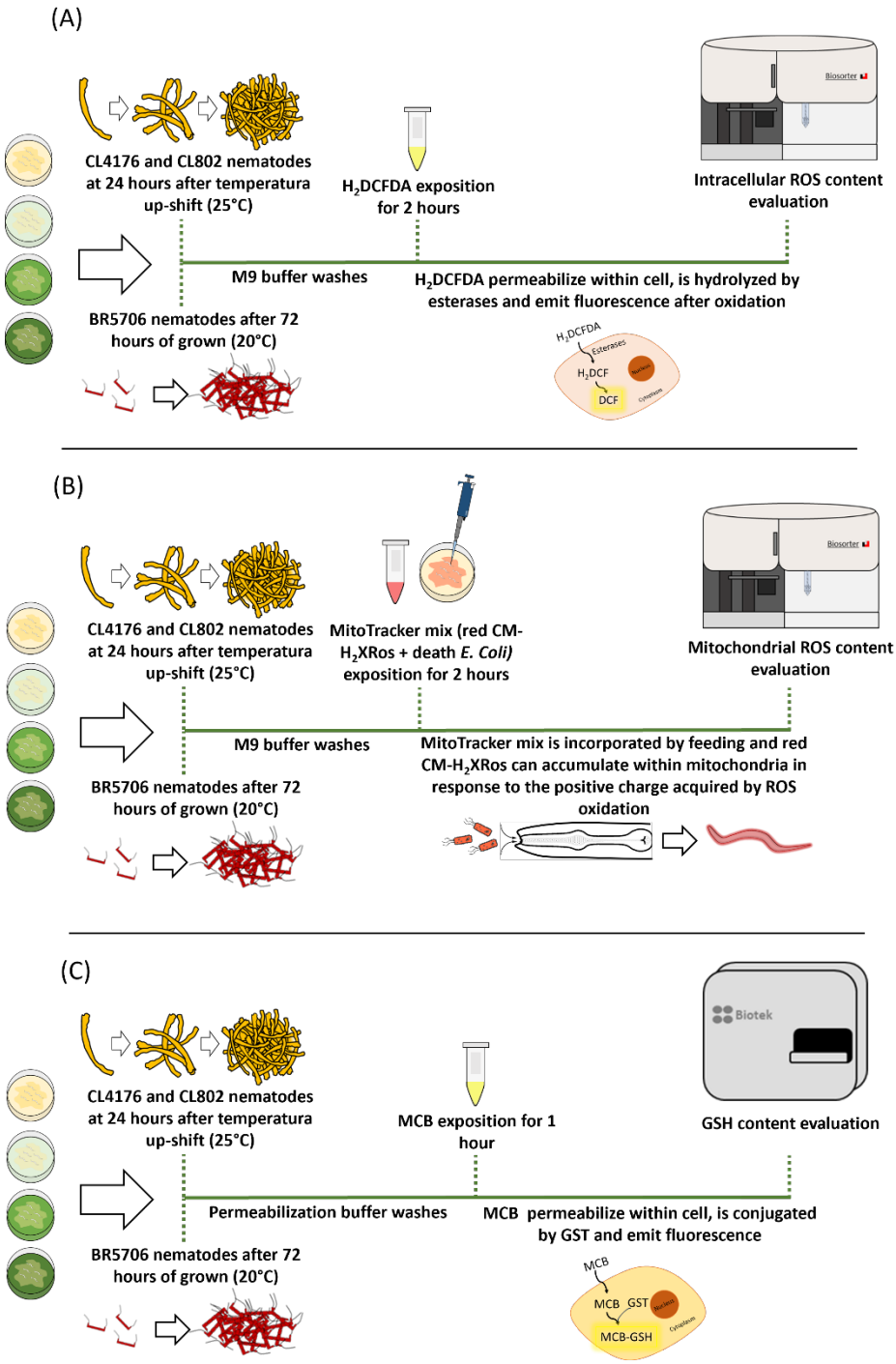

Figure 9. Schematic methodology of the redox biology experiments performed Alzheimer's Disease strains of *C. elegans*. (A) Intracellular ROS content test; (B) mitochondrial ROS content test; (C) GSH content evaluation.

5.6. RNAi experiments

The inhibition of the expression of target genes was performed using the RNAi technique. RNAi can be induced by feeding worms on bacteria expressing dsRNA. cDNA corresponding to the gene of interest is cloned into a bacterial expression vector between opposing phage T7 polymerase promoter sites. The feeding vector is then transformed into the *E. coli* HT115 strain carrying the DE3 lysogen, providing isopropyl β-D-1-thiogalactopyranoside (IPTG) inducible expression of the phage T7 RNA polymerase. HT115 (DE3) strain also lacks the Rnc gene, which encodes RNase.

The RNAi protocol was applied to two different experiments, namely the paralysis test, and the tau proteotoxicity evaluation test. *E. coli* HT115 expressing DAF-16/forkhead box transcription factor class O (FOXO), SOD-3 (Cultek SL, Madrid, Spain), SKN-1/NRF-2 and HSP-16.2 (Sources BioScience, Nottingham, UK) dsRNA were seeded on NGM plates containing 1 mM IPTG and 25 μg/mL carbenicillin. L3-L4 synchronized worms (F0), grown in standard conditions, were then moved to the RNAi plates. When the animals reached the fertile age, the eggs (F1) were isolated through the bleaching method.

For CL4176 and BR5706, used in the paralysis and movement test, respectively, those eggs were placed into the plates containing treatments with each RNAi and a plate without the RNAi. From this step, the experiments were carried out as explained above. A scheme of the process is represented in **Figure 10**.

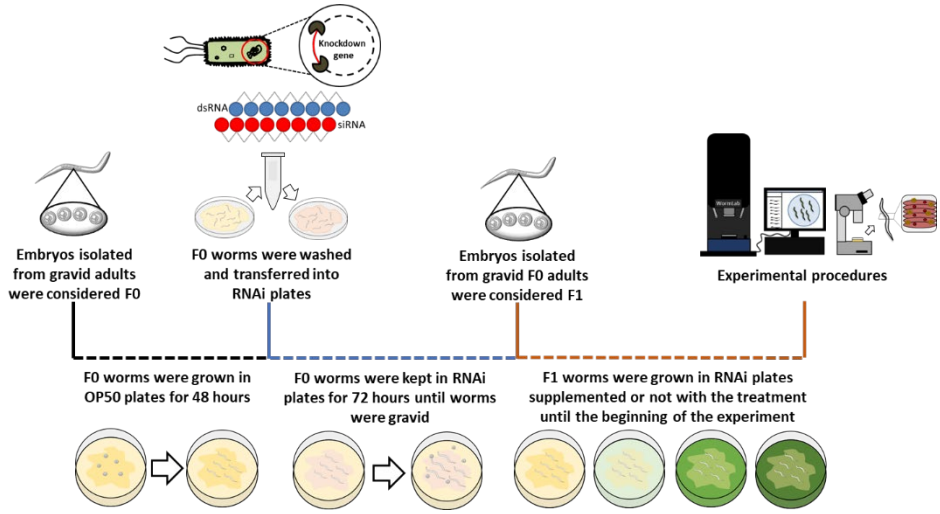

Figure 10. Scheme of the procedure for the gene silencing by RNAi technology.

5.7. Statistical Analysis

The experimental procedures were performed at least three times. The statistical software SPSS 24.0 was used for statistical analysis (IBM, Armonk, NY, USA) was used for the analysis of normality, variance homogeneity, analysis of variance (ANOVA) and Pearson's correlation analysis. ANOVA was carried out and *post hoc* Duncan's Multiple Range test was considered significant when $p < 0.05$. Principal component analysis (PCA) and partial least squares-discriminant analysis (PLS-DA) was applied using MetaboAnalyst V5.0 software. PCA and PLS-DA were used to analyze the normalized and auto-scaled mean values of the 42 compounds from 50 OL extracts analyzed by HPLC-ESI-QTOF-MS/MS and its relationship with cholinesterase, inflammatory, and iron-oxidative inhibitory activity, as well as nematodes body size. In the present PLS-DA, the selection criteria of the variable of importance in projection (VIP) score was values higher than 1, which correspond to $p < 0.05$. Results were presented as the mean ± SD for OL extracts characterization and as the mean ± SEM for *C. elegans* experiments.

SECTION IV: RESULTS & DISCUSSION

CHAPTER VI. Olive leaf extracts characterization

6.1. Individual characterization of olive leaf extracts

6.1.1. Total. phenolic compounds, total flavonoid compounds, and antioxidant capacity

Table 5 reveals the total content in phenols, flavonoids as well the total antioxidant capacity of the individual OL extracts and the population mean ($\overline{X}$1-50).

Table 5. TPC, TFC and TAC of fifty olive leaf extracts

	Origin	TPC	TFC	ABTS	DPPH
SU01	Spain	50.0 ± 8.17^{c}	38.1 ± 3.94^{c}	558 ± 93.5^{c}	215 ± 21.7^{b}
SU02	Spain	33.3 ± 9.38^{b}	14.2 ± 2.57^{a}	396 ± 33.6^{b}	159 ± 26.2^{b}
SU03	Italy	46.1 ± 2.21^{c}	38.1 ± 3.15^{c}	637 ± 61.3^{c}	224 ± 17.6^{b}
SU04	Portugal	47.6 ± 2.34^{c}	38.6 ± 2.8^{c}	638 ± 44.2^{c}	227 ± 15.2^{b}
SU05	Spain	37.9 ± 3.77^{c}	14.6 ± 1.5^{a}	431 ± 72.1^{b}	157 ± 52.2^{b}
SU06	Spain	38.5 ± 4.4^{c}	17.3 ± 2.33^{b}	478 ± 118^{b}	202 ± 58.8^{b}
SU07	Spain	33.3 ± 4.03^{b}	12.6 ± 1.17^{a}	372 ± 52.6^{b}	186 ± 24.6^{b}
SU08	Spain	34.4 ± 4.14^{b}	12.4 ± 1.71^{a}	517 ± 86.1^{c}	179 ± 40.1^{b}
SU09	Spain	31.3 ± 4.61^{b}	10.0 ± 2.00^{a}	382 ± 67.5^{b}	181 ± 50.1^{b}
SU10	Spain	30.2 ± 3.57^{b}	5.33 ± 1.65^{a}	465 ± 77.9^{b}	151 ± 35.3^{b}
SU11	Greece	30.7 ± 4.06^{b}	8.22 ± 1.39^{a}	304 ± 76.9^{a}	161 ± 56.5^{b}
SU12	Greece	29.1 ± 4.91^{b}	6.89 ± 3.27^{a}	342 ± 121^{b}	112 ± 44.5^{a}
SU13	Greece	32.6 ± 4.43^{b}	5.11 ± 3.95^{a}	286 ± 64^{a}	132 ± 30.2^{a}
SU14	Greece	31.8 ± 4.86^{b}	8.06 ± 2.71^{a}	352 ± 56.2^{b}	183 ± 30.9^{b}
SU15	Greece	34.2 ± 5.22^{b}	11.5 ± 1.5^{a}	419 ± 20.4^{b}	186 ± 26.4^{b}
SU16	Greece	34.0 ± 4.18^{b}	12.2 ± 2.67^{a}	462 ± 116^{b}	206 ± 51.2^{b}
SU17	Greece	32.4 ± 4.81^{b}	11.2 ± 3.84^{a}	396 ± 68.1^{b}	192 ± 63.5^{b}
SU18	Greece	28.7 ± 3.93^{b}	8.72 ± 0.950^{a}	411 ± 28.7^{b}	175 ± 38.1^{b}
SU19	Portugal	36.7 ± 5.09^{b}	11.0 ± 2.19^{a}	440 ± 87.8^{b}	164 ± 48.8^{b}
SU20	Portugal	36.0 ± 5.63^{b}	15.0 ± 1.73^{a}	430 ± 146^{b}	189 ± 45.4^{b}
SU21	Portugal	33.2 ± 4.89^{b}	8.56 ± 1.26^{a}	372 ± 90.1^{b}	170 ± 43.3^{b}
SU22	Portugal	36 ± 5.2^{b}	9.44 ± 1.17^{a}	466 ± 79.4^{b}	195 ± 54.9^{b}
SU23	Portugal	36.3 ± 4.9^{b}	12.6 ± 3.65^{a}	473 ± 64.1^{b}	187 ± 39.7^{b}
SU24	Portugal	34.5 ± 4.1^{b}	9.11 ± 1.71^{a}	502 ± 92.2^{c}	219 ± 72.3^{b}
SU25	Portugal	38.3 ± 3.09^{c}	18.6 ± 5.58^{b}	387 ± 15.4^{b}	297 ± 30.9^{b}

SU26	Portugal	35.3 ± 3.2^{b}	17.3 ± 3.04^{b}	426 ± 75.2^{b}	301 ± 41.0^{c}
SU27	Spain	31.6 ± 3.2^{b}	18.9 ± 4.22^{b}	437 ± 54.2^{b}	242 ± 36.0^{b}
SU28	Spain	27.2 ± 2.47^{a}	16 ± 4.27^{b}	362 ± 36.6^{b}	162 ± 54.0^{b}
SU29	Spain	37.4 ± 3.47^{b}	27.6 ± 4.43^{b}	518 ± 56.0^{c}	325 ± 13.0^{c}
SU30	Spain	38.6 ± 3.16^{c}	27.4 ± 3.64^{b}	606 ± 28.4^{c}	268 ± 55.7^{b}
SU31	Spain	49.7 ± 6.69^{c}	57.9 ± 7.61^{c}	720 ± 48.1^{c}	218 ± 66.3^{b}
SU32	Spain	51.9 ± 4.44^{c}	62.6 ± 6.9^{c}	760 ± 59.8^{c}	389 ± 41.3^{c}
SU33	Spain	33.8 ± 3.43^{b}	15 ± 4.5^{a}	452 ± 65.0^{b}	243 ± 65.4^{b}
SU34	Spain	32.9 ± 2.89^{b}	25.7 ± 5.67^{b}	451 ± 76.9^{b}	348 ± 6.20^{c}
SU35	Spain	31.6 ± 3.1^{b}	19.4 ± 5.25^{b}	440 ± 63.1^{b}	335 ± 11.9^{c}
SU36	Spain	36.3 ± 3.07^{b}	20.6 ± 5.22^{b}	496 ± 63.3^{c}	105 ± 41.0^{a}
SU37	Spain	39.9 ± 4.4^{c}	20.9 ± 4.17^{b}	530 ± 74.8^{c}	354 ± 31.1^{c}
SU38	Spain	52.8 ± 4.71^{c}	62.3 ± 9.24^{c}	713 ± 64.3^{c}	403 ± 24.6^{c}
SU39	Spain	36.8 ± 4.28^{b}	37.3 ± 6.48^{c}	465 ± 75.7^{b}	186 ± 42.5^{b}
SU40	Italy	42.8 ± 4.32^{c}	26.1 ± 6.61^{b}	610 ± 77.7^{c}	334 ± 41.6^{c}
SU41	Spain	37.2 ± 5.14^{b}	18 ± 5.6^{b}	531 ± 102^{c}	316 ± 11.7^{c}
SU42	Spain	35.8 ± 4.3^{b}	21.6 ± 2.79^{b}	575 ± 76.1^{c}	297 ± 38.3^{b}
SU43	Spain	43.0 ± 6.33^{c}	23.5 ± 5.69^{b}	647 ± 78.6^{c}	219 ± 39.9^{b}
SU44	Spain	37.0 ± 4.58^{b}	20.9 ± 5.49^{b}	550 ± 43.1^{c}	167 ± 32.3^{b}
SU45	Spain	40.2 ± 5.99^{c}	23.2 ± 2.94^{b}	603 ± 57.4^{c}	223 ± 44.4^{b}
SU46	Italy	34.6 ± 4.03^{b}	28.9 ± 5.17^{b}	486 ± 51.5^{c}	211 ± 22.7^{b}
SU47	Italy	34.8 ± 2.86^{c}	33.5 ± 5.05^{c}	575 ± 37.6^{c}	191 ± 59.7^{b}
SU48	Italy	43.6 ± 2.27^{b}	26.1 ± 2.50^{b}	655 ± 61.7^{c}	186 ± 25.5^{b}
SU49	Morocco	28.2 ± 1.17^{b}	12.3 ± 1.20^{a}	378 ± 25.0^{b}	196 ± 51.7^{b}
SU50	Italy	44.1 ± 3.48^{c}	18.6 ± 5.72^{b}	585 ± 78.7^{c}	213 ± 56.7^{b}
$\overline{X}$1-50	-	36.9 ± 6.15^{b}	20.8 ± 13.5^{b}	490 ± 110^{b}	221 ± 15.8^{b}

Results are expressed as mean ± SD. For each determination, "a" means that samples are below the $\overline{X}$1-50, "b" means that samples are not different from $\overline{X}$1-50, and "c" means that samples are above the $\overline{X}$1-50 ($p < 0.05$). Abbreviations: $\overline{X}$1-50; population mean; ABTS: 2.20-azinobis (3-ethylbenzothiazoline-6-sulfonic acid); CE: catechin equivalents; DPPH: 2.2-diphenyl-1-picryl-hydrazyl-hydrate; FRAP: ferric reducing antioxidant power; DW: dry weight; GAE: gallic acid equivalents. TFC: total flavonoids content. TPC: total phenolic compounds.

TPC and TFC evaluation is a rapid, sensitive, and robust method for assessing the quantitative composition of biologically active compounds. The determination of TFC and TPC in olive leaves was accomplished using the aluminum chloride colorimetric technique and

the Folin-Ciocalteu assay. The results revealed a uniform distribution of the OL extracts based on TPC. Over 60% of the extracts displayed similar levels, ranging from 27.2 ± 2.47 to 52.8 ± 4.71 mg GAE/g DW. The extracts with the highest TPC were SU38, SU32, SU31, and SU04, while the lowest TPC was observed in SU28, SU49, SU18, and SU12. On the contrary, the distribution of TFC exhibited a scattered pattern. More than 60% of the OL extracts displayed significant deviations from the reference value ($\overline{X}$1-50), with values spanning from 5.11 ± 3.95 to 62.6 ± 6.90 mg CE/g DW. Out of the total OL extracts, 44% exhibited lower TFC values, with particular emphasis on extracts SU13, SU10, SU12, and SU14. Conversely, only 16% of the extracts demonstrated higher TFC levels, including SU32, SU38, SU31, and SU04.

There are several *in vitro* assays to determinate total antioxidant capacity (TAC) of agri-food matrices and their by-products. Most of them are one-electron transfer-based methods, but their sensitivity depends on several factors such as pH, hydro/lipophilic affinity, etc. [142]. Therefore, it is strongly recommended to use at least two different methods for the determination of TAC, particularly when studying such phytochemically complex matrices as OL extracts. In the present work, TAC was assessed by three different methods, but only two will be discussed in this section. For the ABTS assay, the highest value was obtained by SU32, SU31, SU38, and SU48, while the lowest ABTS score was obtained by SU13, SU11, SU12, and SU14, exhibiting 46% of differences with the $\overline{X}$1-50. Contrarily, only 18% of the OL extracts presented variations from the $\overline{X}$1-50 for DPPH determination.

These results can be partially explained due to the content in phenolic compounds and, specifically, flavonoids, present in OL extracts, which were directly associated with their antioxidant capacity (**Figure 11**). According to the obtained data, a strong association was found between TPC and TFC with ABTS, whereas the association with DPPH was lower but still statistically significant. These results were also supported by Zhang *et al.* [4], who showed a strong association between

TFC with ABTS (r = 0.6236; $p < 0.001$), whereas DPPH was not significant in 32 OL samples from China.

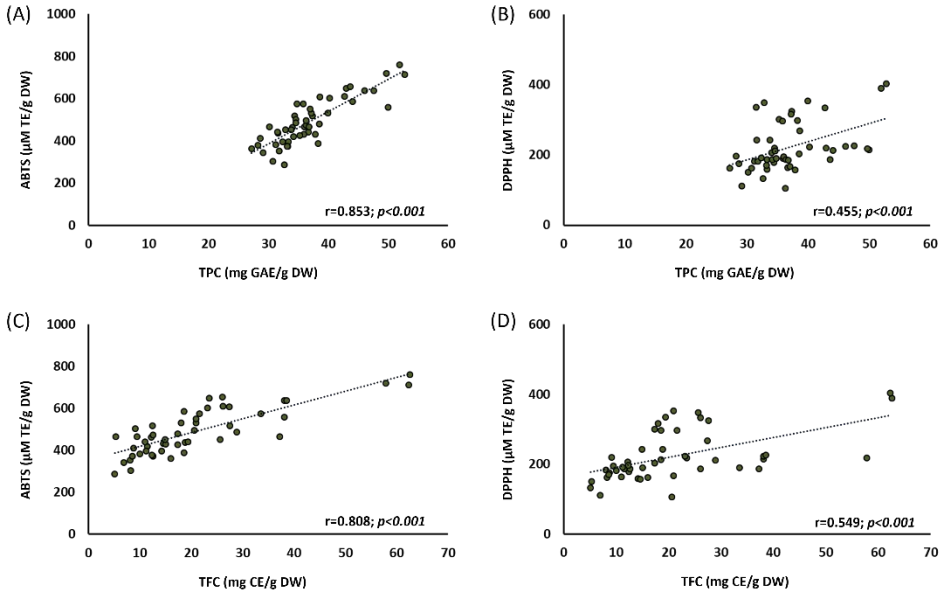

Figure 11. Pearson's correlation scatterplot of the relationships between (A) ABTS and TPC, (B) DPPH and TPC, (C) ABTS and TFC, (D) DPPH and TFC. Abbreviations: ABTS: 2.20-azinobis (3-ethylbenzothiazoline-6-sulfonic acid); CE: catechin equivalents; DPPH: 2.2-diphenyl-1-picryl-hydrazyl-hydrate; DW: dry weight; GAE: gallic acid equivalents.

These differences might also be explained by the different methods used to determine the antioxidant capacity. To mention, the application of DPPH method is limited due to the nitrogenous nature of the free radical, as the kinetic reaction is not linear between the free radical and the antioxidant compounds [142]. In addition, some antioxidants can react slowly or even be inert to the DPPH radical, and some reactions with phenolic compounds can be reversible in the DPPH assay [142,146,147]. Therefore, lower antioxidant capacity values can be obtained by this method, which might explain the absence of statistical differences in the literature [4,146]. In contrast, ABTS method, has shown to be more valid than DPPH assay for the evaluation of antioxidant activity [142,146].

6.1.2. Phytochemical compounds identification and quantification

Due to the great diversity of existing phenolic compounds, no commercial standards are available for all of them. Oleuropein, hydroxytyrosol, luteolin, luteolin-7-O-glucoside, and verbascoside were quantified by the calibration curves obtained from their respective commercial standards. The remaining compounds were tentatively quantified based on calibration curves from other compounds with structural similarities. The chromatograms were assessed, which led to identify a total of 42 compounds (**Figure 12**). **Table 6** shows a tentative identification of the compounds together with the molecular formula, the *m*/*z*, the determination error as well as the individual quantification for the $\overline{X}$1-50.

The phenolic profile of the examined OL extract is consistent with previous [148,149]. As can be seen, secoiridoids, a family that provides the bitter and pungent taste to olive oil, were the major type of phenolic compounds found in OL extracts [150]. Among the secoiridoids, the concentration of oleuropein was particularly noteworthy (26.7%). Its content exceeded that of the other derived compounds, indicating a prevalence of free oleuropein in contrast to what has been reported in the literature [18,20,151]. The remaining secoiridoids are found in a much lower concentration, as is the case for oleoside (4.53%). Additionally, other compounds with a significant presence in the studied OL extracts are flavonoids, with luteolin glucoside (17.3%) being the predominant type of phenolic compound within this family.

On the other hand, it should also be noted that there was a higher concentration of hydroxytyrosol in its glycosylated form (1.61%) than in its free form (0.595%), indicating that it must be hydrolyzed by intestinal enzymes or by the colonic microflora before absorption [152].

Table 6. Phytochemical identification and quantification of olive leaf extracts

	Formula	m/z	Error	$\overline{X}$1-50
Secoiridoids				
1-β-D-Glu-ACD EA I1	$C_{17}H_{28}O_{11}$	4.071.562	-0.420	0.307 ± 0.203
1-β-D-Glu-ACD EA I2	$C_{17}H_{28}O_{11}$	4.071.561	-0.230	0.637 ± 0.560
A-DM EA	$C_{10}H_{16}O_5$	2.150.929	-1.69	0.180 ± 0.278
D-OH EA I2	$C_{10}H_{14}O_5$	2.130.768	0.110	0.020 ± 0.101
H-DA-DM EA	$C_9H_{14}O_5$	2.010.772	-1.63	0.044 ± 0.103
Hy-DA-DM EA I1	$C_{10}H_{14}O_5$	2.130.769	0.090	0.104 ± 0.119
Hy-DA-DM EA I2	$C_9H_{12}O_5$	1.990.615	-1.21	0.198 ± 0.346
Hydroxyoleuropein	$C_{25}H_{32}O_{14}$	5.551.712	1.45	0.235 ± 0.448
Ligstroside	$C_{25}H_{32}O_{12}$	5.231.815	1.36	0.115 ± 0.292
Oleoside	$C_{16}H_{22}O_{11}$	389.109	-0.050	0.997 ± 1.85
Oleoside methyl ester	$C_{17}H_{24}O_{11}$	4.031.243	0.940	0.772 ± 1.28
Oleuropein	$C_{25}H_{32}O_{13}$	539.177	0.200	5.85 ± 14.0
Oleuropein diglu	$C_{31}H_{42}O_{18}$	7.012.288	1.85	0.060 ± 0.173
Oleuropein I	$C_{25}H_{32}O_{13}$	5.391.767	0.780	0.555 ± 1.44
Flavonoids				
(+)-Eriodictyol	$C_{15}H_{12}O_6$	2.870.565	-1.05	0.082 ± 0.109
Apigenin	$C_{15}H_{10}O_5$	269.046	-1.49	0.181 ± 0.223
Apigenin-7-O-glu	$C_{21}H_{20}O_{10}$	4.310.981	0.870	0.279 ± 0.210
Apigenin-7-O-rut	$C_{27}H_{30}O_{14}$	5.771.559	0.700	0.400 ± 0.222
Azelaic acid	$C_9H_{16}O_4$	1.870.979	-1.55	0.574 ± 0.775
Chrysoeriol-7-O-glu	$C_{22}H_{22}O_{11}$	4.611.086	0.860	0.547 ± 0.251
Diosmetin	$C_{16}H_{12}O_6$	2.990.562	-0.320	0.226 ± 0.160
I-3-O-β-D-glu	$C_{31}H_{28}O_{14}$	6.231.395	1.94	0.028 ± 0.050
Luteolin	$C_{15}H_{10}O_6$	2.850.412	-2.43	0.291 ± 0.203
Luteolin 7-O-glu	$C_{21}H_{20}O_{11}$	4.470.934	0.120	1.09 ± 1.10
Luteolin glu	$C_{21}H_{20}O_{11}$	4.470.934	0.060	3.81 ± 2.20
Luteolin rut I1	$C_{27}H_{30}O_{15}$	5.931.502	1.79	0.001 ± 0.006
Luteolin rut I2	$C_{27}H_{30}O_{15}$	5.931.505	1.39	0.018 ± 0.042
Luteolin-7,4-O-diglu	$C_{27}H_{30}O_{16}$	6.091.451	1.84	0.084 ± 0.077
Oxidized quercetin	$C_{15}H_8O_7$	299.0196	300	0.000 ± 0.002
Taxifolin	$C_{15}H_{12}O_7$	3.030.509	0.520	0.002 ± 0.012
Phenolic alcohols				
Hydroxytyrosol	$C_8H_{10}O_3$	1.530.556	-0.840	0.131 ± 0.13
Hydroxytyrosol glu	$C_{14}H_{20}O_8$	3.151.086	-0.080	0.355 ± 0.515
4-Ethylguaiacol	$C_9H_{12}O_2$	1.510.764	0.360	0.094 ± 0.071
Iridoids				
Loganic acid	$C_{16}H_{24}O_{10}$	3.751.297	0.150	0.223 ± 0.101
7-Epiloganin	$C_{17}H_{26}O_{10}$	3.891.457	-0.580	0.667 ± 0.298
Lamiol	$C_{16}H_{26}O_{10}$	377.146	-1.34	0.778 ± 0.459

Hydroxycoumarins				
Esculetin	$C_9H_6O_4$	1.770.198	-2.32	0.179 ± 0.205
Esculin	$C_{15}H_{16}O_9$	3.390.721	0.230	0.054 ± 0.049
Hydroxycinnamic acid				
Verbascoside	$C_{29}H_{36}O_{15}$	6.231.974	1.41	0.307 ± 0.408
Decaffeoylverbascoside	$C_{20}H_{30}O_{12}$	4.611.665	0.190	1.17 ± 0.842
Phenolic acids				
p-Hydroxybenzoic acid	$C_7H_6O_3$	1.370.247	-1.67	0.037 ± 0.059
Other compounds				
Lauroside B	$C_{19}H_{32}O_9$	4.031.972	0.480	0.343 ± 0.329

Results are expressed as milligram of compound (mean ± SD) per gram of dry weight. Error is expressed in parts per million. Abbreviations: $\overline{X}$1-50: population mean; 1-β-D-Glu-ACD elenolic acid I1: 1-β-D-Glucopyranosyl acyclodihydroelenolic acid isomer 1; 1-β-D-Glu-ACD elenolic acid I2: 1-β-D-Glucopyranosyl acyclodihydroelenolic acid isomer 2; A-DM elenolic acid: aldehydic form of decarboxymethyl elenolic acid; D-OH elenolic acid I2: decarboxylated form of hydroxy elenolic acid isomer 2; EA: elenolic acid; glu: glucoside; H-DA-DM elenolic acid: hydrated product of the dialdehydic form of decarboxymethyl elenolic acid; Hy-DA-DM elenolic acid I1: hydroxylated product of the dialdehydic form of decarboxymethyl elenolic acid isomer 1; Hy-DA-DM elenolic acid I2: hydroxylated product of the dialdehydic form of decarboxymethyl elenolic acid isomer 2; m/z: mass to charge ratio; OL: olive leaves; I: isomer; rut: rutinoside.

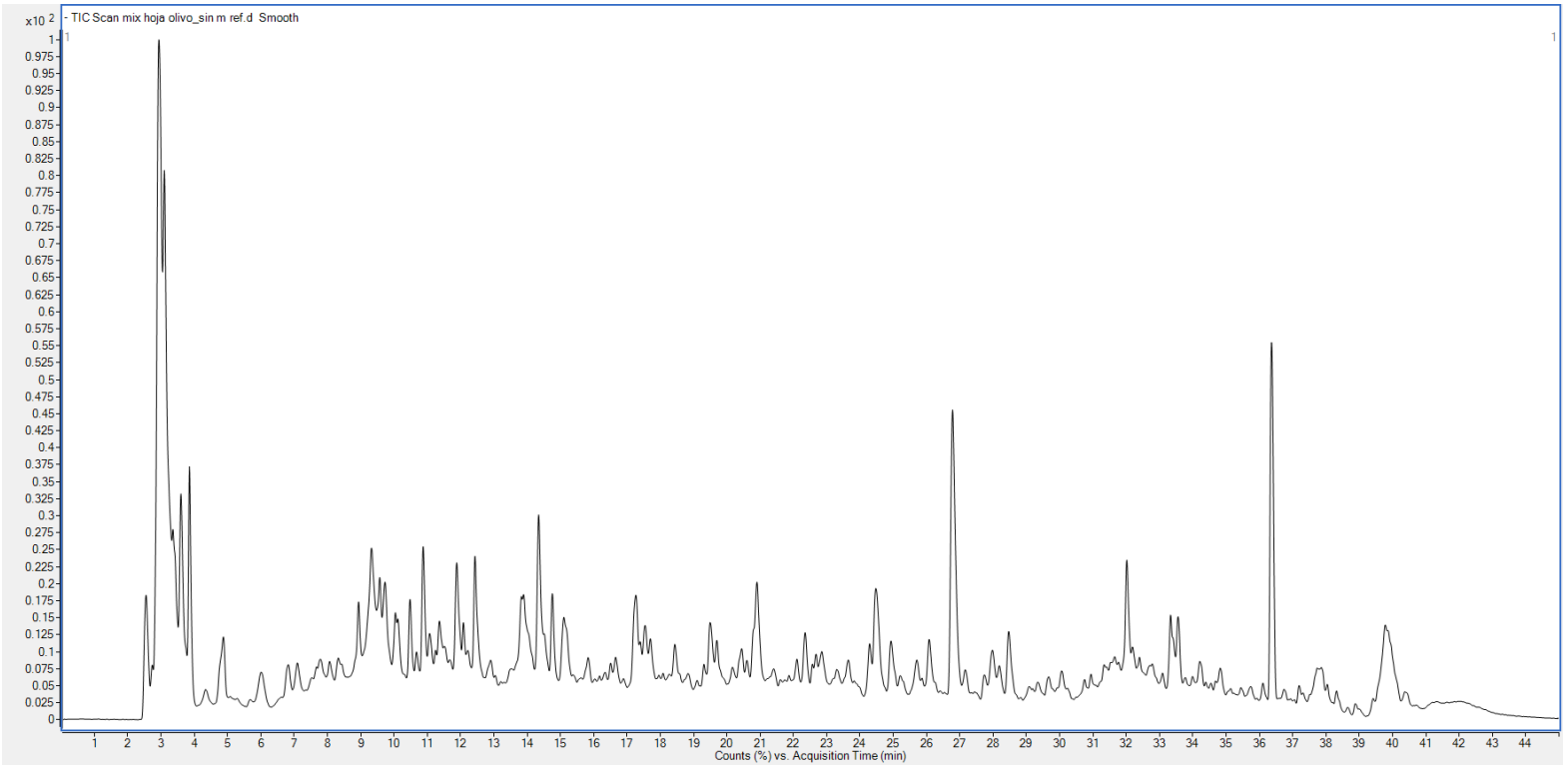

Figure 12. Quantitative characterization of olive leaves extracts by HPLC-ESI-QTOF-MS/MSTIC of pool sample at a concentration of 10 mg/ml.

6.2. Impact of olive leaf extract origin in TPC, TFC and antioxidant capacity

6.2.1. TPC, TFC and antioxidant capacity

The total content of phenolic compounds and flavonoids clustered by countries can be observed in **Table 7**. An exception was made for the Moroccan sample, which was excluded from this analysis due to not meeting the statistical sample threshold (almost 3) for country clustering. In this context, the Italian OL presented the highest values of TPC and TFC (41.0 ± 5.01 mg GA/g DW and 28.7 ± 6.75 mg CAT/g DW, respectively), followed by the Portuguese samples (37.1 ± 4.20 mg GA/g DW and 15.6 ± 9.30 mg CAT/g DW, respectively) and the Greek OL (31.7 ± 2.05 mg GA/g DW and 8.99 ± 2.47 mg CAT/g DW, respectively).

Table 7. TPC, TFC and TAC of OL extracts from four countries

Determination	Spain	Italy	Greece	Portugal
TPC (mg GA/g DW)	37.8 ± 6.80^{ab}	41.0 ± 5.00^{b}	31.7 ± 2.0^{a}	37.1 ± 4.20^{ab}
TFC (mg CAT/g DW)	24.7 ± 15.2^{b}	28.6 ± 6.70^{b}	9.0 ± 2.50^{a}	15.6 ± 9.30^{ab}
ABTS (μM Trolox/g DW)	517 ± 108^{bc}	591 ± 60.0^{c}	372 ± 61.0^{a}	459 ± 78.0^{ab}
DPPH (μM Trolox/g DW)	240 ± 82.0	226 ± 55.0	168 ± 32.0	217 ± 51.1

Results are expressed as mean ± SD. For each determination, different letters indicate statistically significant differences between countries ($p < 0.05$). Abbreviations: ABTS: 2.20-azinobis (3-ethylbenzothiazoline-6-sulfonic acid); CE: catechin equivalents; DPPH: 2.2-diphenyl-1-picryl-hydrazyl-hydrate; FRAP: ferric reducing antioxidant power; DW: dry weight; GAE: gallic acid equivalents. OL: olive leaves. TFC: total flavonoids content. TPC: total phenolic compounds. TAC: total antioxidant capacity.

When comparing with the existing evidence, the TPC of the Spanish and Italian samples were similar, or even higher, than those found in the literature [7,10], whereas TFC were lower [7,9,10]. Similarly, the TPC and TFC for Greek samples were in accordance with those obtained by Petridis *et al.* [153] and Papoti *et al.* [154] in OL samples from Greek varieties. However, there are no specific data available to compare the TPC and TFC obtained in the Portuguese OL samples, since the single found study expressed the values in fresh weight [155]. The phenolic and

flavonoid content in OL extracts can be modified by numerous factors such as the olive leaves harvesting season, drying conditions and the extraction solvent, which can affect the determinations in order to compare between countries [5]. According to literature, harvesting season has been shown to modulate the TPC and TFC, showing higher values the leaves cultivated between March and April [9,12]. Similarly, the drying method and the solvent used for OL extraction have been related with changes into the phenolic and flavonoid content [10,16]. Therefore, these procedures were standardized for the 49 samples, with all samples collected between November and February. Likewise, for all samples, room temperature and ethanol/water mixture were selected as drying and extraction methods, respectively, to reduce the influence of these factors on the determinations.

In the present work, the antioxidant capacity was assessed by two different methods. For the ABTS assay, the highest value was obtained by the Italian and Spanish OL samples, followed by the Portuguese OL. In contrast, the lowest ABTS score was obtained by the Greek samples. No statistical differences were obtained for DPPH assay among samples from different origins. As mentioned before, these differences might also be explained by the different methods used to determine the antioxidant capacity. The application of DPPH method is limited due to the nitrogenous nature of the free radical, as the kinetic reaction is not linear between the free radical and the antioxidant compounds [142]. In contrast, ABTS method, has shown to be more valid than DPPH assay for the evaluation of antioxidant activity [142,146].

6.2.2. Phytochemical profile

Table 8 shows the phytochemical profile of OL according to the geographical origin, where 42 compounds were quantified and divided into eight groups.

Table 8. Phytochemical profile of olive leaf extracts from four different countries

	Spain	Italy	Greece	Portugal
Secoiridoids				
1-β-D-Glu-ACD EA I1	0.370 ± 0.170	0.320 ± 0.130	0.400 ± 0.220	0.330 ± 0.190
1-β-D-Glu-ACD EA I2	0.670± 0.370^{a}	0.180 ± 0.070^{a}	0.670 ± 0.450^{ab}	1.21 ± 0.760^{b}
A-DM EA	0.240 ± 0.190	0.130 ± 0.120	0.510 ± 0.520	0.070 ± 0.010
D-OH EA I2	-	-	0.5 ± 0.12	-
H-DA-DM EA	0.150 ± 0.170	0.110 ± 0.070	0.320 ± 0.140	-
Hy-DA-DM EA I1	0.190 ± 0.100^{a}	-	0.180 ± 0.030^{b}	0.160 ± 0.090^{a}
Hy-DA-DM EA I2	0.280 ± 0.140	0.330 ± 0.170	0.670 ± 0.800	0.420 ± 0.330
Hydroxyoleuropein	0.480 ± 0.580	0.520 ± 0.260	-	0.540 ± 0.560
Ligstroside	0.860 ± 0.120	-	-	-
Oleoside	1.61 ± 1.13	-	-	0.930 ± 1.03
Oleoside methyl ester	1.03 ± 1.18	0.460 ± 0.600	-	0.700 ± 0.720
Oleuropein	10.27 ± 18.69	4.72 ± 9.04	0.110 ± 0.060	2.69 ± 6.61
Oleuropein diglu	0.310 ± 0.120	-	-	-
Oleuropein isomer	3.15 ± 2.27	1.19 ± 1.67	-	-
Flavonoids				
(+)-Eriodictyol	0.190 ± 0.090^{b}	-	-	0.080 ± 0.080^{a}
Apigenin	0.140 ± 0.080^{a}	0.730 ± 0.270^{b}	0.180 ± 0.160^{a}	0.120 ± 0.080^{a}
Apigenin-7-O-glu	0.290 ± 0.160	0.500 ± 0.360	0.090 ± 0.040	0.380 ± 0.130
Apigenin-7-O-rut	0.520 ± 0.220^{b}	0.180 ± 0.050^{a}	0.320 ± 0.110^{a}	0.340 ± 0.080^{ab}
Azelaic acid	0.500 ± 0.360^{a}	2.02 ± 1.47^{b}	0.130 ± 0.050^{a}	0.270 ± 0.100^{a}
Chrysoeriol-7-O-glu	0.620 ± 0.160^{b}	0.530 ± 0.350^{ab}	0.270 ± 0.150^{a}	0.670 ± 0.160^{ab}
Diosmetin	0.190 ± 0.090^{a}	0.510 ± 0.130^{c}	0.320 ± 0.160^{b}	0.160 ± 0.070^{a}
I-3-O-β-D-glu	0.030 ± 0.020	0.100 ± 0.120	0.040 ± 0.050	0.080 ± 0.080
Luteolin	0.270 ± 0.190	0.380 ± 0.180	0.430 ± 0.300	0.190 ± 0.080
Luteolin 7-O-glu	1.14 ± 0.670	1.74 ± 2.37	0.620 ± 0.530	1.10 ± 1.22
Luteolin glu	4.96 ± 2.06^{b}	2.90 ± 2.06^{ab}	1.28 ± 0.930^{a}	3.43 ± 1.19^{ab}
Luteolin rutinoside I1	-	0.030 ± 0.020	-	-
Luteolin rutinoside I2	0.100 ± 0.050	-	0.070 ± 0.050	-
Luteolin-7,4-O-diglu	0.150 ± 0.050	-	-	0.070 ± 0.050
Oxidized quercetin	0.014 ± 0.001	-	-	-
Taxifolin	0.040 ± 0.040	-	-	-
Phenolic alcohols				
Hydroxytyrosol	0.120 ± 0.090^{a}	0.350 ± 0.130^{b}	0.050 ± 0.010^{a}	0.120 ± 0.130^{a}
Hydroxytyrosol glu	0.360 ± 0.460	0.500 ± 1.00	0.360 ± 0.380	0.330 ± 0.450
4-Ethylguaiacol	0.100 ± 0.060	0.090 ± 0.020	0.150 ± 0.110	0.080 ± 0.030
Iridoids				

Loganic acid	0.260 ± 0.060^{b}	0.110 ± 0.110^{a}	0.130 ± 0.090^{a}	0.260 ± 0.100^{b}
7-Epiloganin	0.700 ± 0.210^{ab}	0.980 ± 0.350^{b}	0.540 ± 0.430^{a}	0.510 ± 0.220^{a}
Lamiol	0.930 ± 0.340^{b}	0.100 ± 0.060^{a}	0.740 ± 0.660^{b}	0.790 ± 0.290^{b}
Hydroxycoumarins				
Esculetin	0.140 ± 0.060^{b}	0.680 ± 0.190^{c}	0.050 ± 0.020^{a}	0.100 ± 0.040^{ab}
Esculin	0.080 ± 0.050	0.040 ± 0.030	-	0.040 ± 0.020
Hydroxycinnamic acid				
Verbascoside	0.410 ± 0.520	0.380 ± 0.250	0.080 ± 0.040	0.180 ± 0.140
Decaffeoylverbascoside	1.33 ± 0.860	0.600 ± 0.640	0.960 ± 0.930	1.04 ± 0.360
Phenolic acids				
p-Hydroxybenzoic acid	-	0.050 ± 0.040	-	0.090 ± 0.140
Other compounds				
Lauroside B	0.280 ± 0.160^{a}	0.300 ± 0.290^{ab}	0.370 ± 0.290^{ab}	0.710 ± 0.390^{b}

Results are expressed as milligram of compound (mean ± SD) per gram of dry weight. For each compound, different letters between countries indicate statistically significant differences ($p < 0.05$). the symbol (-) was added when the specific compound was no detected. Abbreviatures: 1-β-D-Glu-ACD elenolic acid I1: 1-β-D-Glucopyranosyl acyclodihydroelenolic acid isomer 1; 1-β-D-Glu-ACD elenolic acid I2: 1-β-D-Glucopyranosyl acyclodihydroelenolic acid isomer 2; A-DM elenolic acid: aldehydic form of decarboxymethyl elenolic acid; D-OH elenolic acid I2: decarboxylated form of hydroxy elenolic acid isomer 2; EA: elenolic acid; glu: glucoside; H-DA-DM elenolic acid: hydrated product of the dialdehydic form of decarboxymethyl elenolic acid; Hy-DA-DM elenolic acid I1: hydroxylated product of the dialdehydic form of decarboxymethyl elenolic acid isomer 1; Hy-DA-DM elenolic acid I2: hydroxylated product of the dialdehydic form of decarboxymethyl elenolic acid isomer 2; OL: olive leaves; I: isomer; rut: rutinoside.

In this case, the Spanish and the Italian samples presented the highest flavonoid content, standing out the content in luteolin and its derivatives (luteolin glucoside and luteolin-7-O-glucoside), as well as apigenin and its derivatives (apigenin-7-O-glucoside and apigenin-7-O-rutinoside). The Italian samples, but not the Spanish ones, showed the highest content of hydroxytyrosol (**Table 3**). In the same way, other phenolic compounds, such as iridoids (e.g., 7-epiloganin), and hydroxycoumarins (e.g., esculetin) were spotlighted in the Spanish and Italian samples while lamiol and lauroside B were abundant in the Greek and Portuguese OL. Taken together, the most representative phytochemical compounds in the OL studied in this work, including phenolic alcohols (hydroxytyrosol), flavonoids (luteolin-7-O-glucoside, luteolin-4-O-glucoside, and apigenin-7-O-glucoside), as well as secoiridoids and its derivatives (oleoside, and ligstroside) were lower

compared to the OL extracts previously reviewed by Romero-Márquez *et al.* from Spain, China, Italy, and Turkey. An exception was observed in the oleuropein content, reaching levels compatible with the literature in the Spanish, Italian and Portuguese OL samples [5].

Although it has been suggested that the olive variety may contribute to the differences in terms of phytochemical composition [12,156], some authors have shown that despite the differences between cultivars, Spanish OL have a higher content of flavonoids and secoiridoids than Italians, indicating a similar effect of geographical origin beyond the variety of OL used [9]. In fact, the pruning season has been demonstrated to be the major influence on the phytochemical profile, even in the same cultivar [9,12]. In the same way, regular annual precipitation and warms summers temperatures, as well as limited pluvial floods, have been associated with an improvement in the phytochemical content in olive threes [157,158]. Therefore, in the context of climate change, there is a strong northwest-southeast gradient in these features in Europe. In particular, the Eastern Mediterranean countries such as Greece have reported a reduction in the annual precipitation, an increase in summer hot-dry weather, and winter floods conditions [159]. In contrast, south-west Mediterranean countries such as Spain or Italy, seems to conserve similar bioclimatic conditions [160]. These results might explain the differences reported in the phytochemical profile regarding to Spain, Italy, Portugal, and Greece. Therefore, in the present work, it has been demonstrated that the geographical origin dramatically influences the content of some compounds such as secoiridoids, flavonoids, iridoids, hydroxycoumarins, and hydroxycinnamic acids in olive leaves.

6.2.3. Principal component analysis

PCA has been extensively used as an unsupervised exploratory method to decrease the dimensionality of datasets. It has been widely used in several research fields, such as microbiome studies, population genetics, epidemiology, and agricultural sciences [4]. In the present work, it was applied considering the large volume of data/variables analyzed, with the intention of better interpreting the obtained results and visualizing possible relationships among them. In that sense, the PCA was performed by the MetaboAnalyst V5.0 using the information obtained from the 49 samples, including: TPC, TFC, TAC (ABTS, and DPPH), and the 42 compounds quantified by HPLC-ESI-QTOF-MS/MS.

The first two principal components (PCs) described 37.8% of total variance (PC1 23.1%, and PC2 14.7%) and were used to visualize the relationship between countries. The distribution of the four evaluated countries is shown in **Figure 13**. As shown in the score plots, PC1 was able to separate the Italian samples from the Greek ones, whereas the PC2 was able to separate the Italian samples from the Portuguese OL. Nevertheless, the Spanish OL could not be differentiated as a group due to their high variability and were randomly distributed in **Figure 13**. Most of the samples from Spain, Greece and Portugal are distributed in the right part of PC1 and the upper part of PC2, whereas the Italian samples were in the opposite quadrant. An interesting feature was observed concerning the distribution of 7 samples from Spain in a similar way as the Italian OL. The Spanish samples situated in the bottom-left quadrant have in common that they are from Andalusia, the south of Spain. This might be explained due to the similarities between the Italian and the Andalusian climate, exerting similar threshold temperatures, which has been associated with bioclimatic requirements for olive development [160].

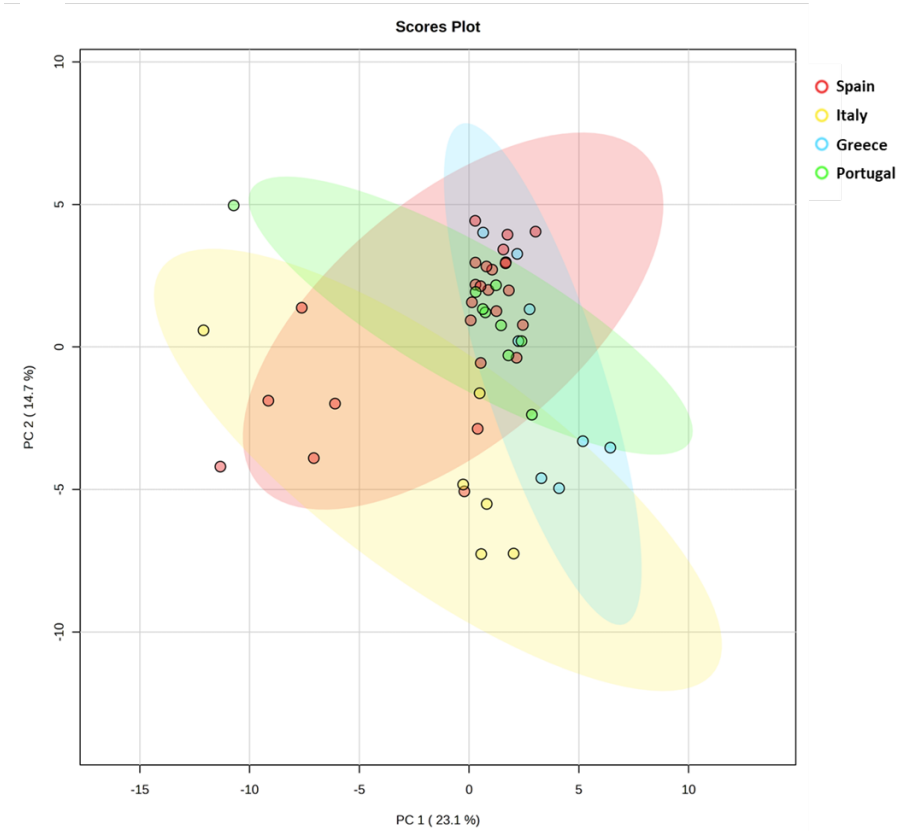

Figure 13. PCA score plot for the OL extracts from Spain, Italy, Greece, and Portugal. PCA shows the results obtained from the mean values of the four colorimetric determinations (TPC, TFC, ABTS, and DPPH) and the 42 phytochemical compounds present in the OL from

CHAPTER VII. Preliminary evaluation of the anti-Alzheimer's disease properties of olive leaf extracts: an approach of the cholinesterase, inflammatory, and iron-oxidative inhibitory activity *in vitro*

The pathophysiology of AD is well known to involve two histopathological hallmarks: the aggregation of Aβ and the hyperphosphorylation of tau protein, which leads to the formation of Aβ-plaques and NFTs in brain [161]. However, the reason for the deposition and aggregation remains unclear. Some authors demonstrated the role of oxidative stress and neuroinflammation in the AD progression through the regulation of Aβ and tau hyperphosphorylation deposition [162,163]. Concerning neuroinflammation, it has been found that COX-2 expression was increased in the brain of AD patients [163–166]. This COX-2 elevation has been epidemiologically correlated with the severity of AD pathology in humans [163,164]. In the same way, animal studies exposed that COX-2 has an important role in spreading Aβ deposits as well as increases the tau-pathology [161]. In this context, numerous authors have shown that drugs which could selectively inhibit COX-2 might reduce the clinical aspects of AD [167–169]. Nonetheless, the posology of these drugs has been associated with different side effects [170]. In the same way, oxidative stress and redox-active iron accumulation have been detected as an early mark in AD pathophysiology, which has been described as key factor on the formation of Aβ-plaque cores [162]. During AD, iron reactive species can react with numerous biomolecules through hydroxyl radicals generation, producing oxidizing species, which leads to contribute oxidative stress [171]. Hydroxyl radicals can origin lipid peroxidation in brain, resulting in successive liberation of redox-active iron into the cytosol. This leads to increased concentration of labile iron pool that may cause cell damage and result in ferroptosis reported on this neurodegenerative process.

Beyond the amyloid and tau propagation hypotheses, various other hypotheses regarding the progression of Alzheimer's disease exist. Notably, in 1976, Davies and Maloney introduced the cholinergic hypothesis of AD [172]. The cholinergic hypothesis suggests that there exits an alteration of ACh concentration in neurons during the pathogenesis of AD. In this context, part of the hypothesis indicates that there exists a hyperactivity of AChE, favoring the degradation of ACh, and promoting that AD patients develop severe ACh deficiency in the brain. This brain ACh deficit has been associated with memory loss and other cognitive symptoms related to AD [44]. Therefore, the AChE inhibition can extend the cholinergic transmission time and increase the cholinergic signaling. In fact, AChEI drugs are the only pharmacological treatment approved for AD patients. Nowadays, the most widely used AChEI drugs are physostigmine, donepezil, rivastigmine, and galantamine, which exhibit an amelioration of AD symptoms, without preventing the brain damage. However, due to the significant side effects, the use of these AChEI drugs is limited [47]. Hence, the use of natural by-products with antioxidant activity and nutraceutical potential concerning to AChE and COX-2 inhibitory activity, might be an interesting approach for adjuvant therapy of AD.

7.1. Individual inhibitory AChE and COX-2 activities and FRAP values of olive leaf extracts

Table 9 reveals the inhibitory cholinergic and inflammatory activity of the individual OL extracts and the mean value for the fifty samples ($\overline{X}$1-50). In the same way, the capacity to reduce iron is also exposed. Concerning AChE IA, only 16% of samples exhibited higher AChEI activity than the $\overline{X}$1-50. Among these, 75% of these samples were from Spain and 12.5% each were from Italy and Portugal. Conversely, 24% of the samples showed lower AChEI activity than the $\overline{X}$1-50, with approximately 42% of them originating from Greece, 25% from Portugal, 16.4% from Spain, and 8.3% from Italy and Morocco.

Table 9. AChE and COX-2 inhibitory activity, as well as FRAP of fifty olive leaf extracts

	Origin	AChE IA	COX-2 IA	FRAP
SU01	Spain	100 ± 2.08^{c}	41.2 ± 1.03^{c}	443 ± 115^{c}
SU02	Spain	83.9 ± 3.74^{c}	18.4 ± 1.27^{b}	236 ± 42.0^{a}
SU03	Italy	67.4 ± 1.24^{c}	33.1 ± 0.790^{b}	730 ± 103^{c}
SU04	Portugal	100 ± 0.940^{c}	39.5 ± 2.78^{c}	751 ± 103^{c}
SU05	Spain	35.1 ± 0.600^{b}	24.8 ± 6.56^{b}	338 ± 36.9^{b}
SU06	Spain	44.7 ± 1.50^{c}	17.0 ± 0.080^{b}	370 ± 33.7^{b}
SU07	Spain	38.2 ± 0.910^{b}	27.1 ± 8.15^{b}	283 ± 66.2^{b}
SU08	Spain	57.1 ± 1.43^{c}	28.2 ± 6.65^{b}	356 ± 34.0^{b}
SU09	Spain	39.33 ± 1.58^{b}	19.6 ± 2.25^{b}	292 ± 32.3^{b}
SU10	Spain	38.48 ± 1.79^{b}	20.2 ± 0.550^{b}	275 ± 19.1^{a}
SU11	Greece	3.49 ± 2.88^{a}	30.9 ± 1.46^{b}	216 ± 22.4^{a}
SU12	Greece	14.2 ± 1.57^{a}	28.3 ± 2.49^{b}	229 ± 9.30^{a}
SU13	Greece	5.64 ± 1.38^{a}	19.7 ± 0.240^{b}	202 ± 30.2^{a}
SU14	Greece	10.2 ± 2.08^{a}	28.5 ± 1.30^{b}	230 ± 10.9^{a}
SU15	Greece	11.2 ± 0.950^{a}	34.8 ± 7.41^{b}	326 ± 43.3^{b}
SU16	Greece	35.97 ± 2.00^{b}	25.2 ± 3.93^{b}	372 ± 42.8^{b}
SU17	Greece	32.8 ± 0.380^{b}	30.1 ± 3.99^{b}	298 ± 53.6^{b}
SU18	Greece	29.0 ± 0.750^{b}	27.4 ± 3.59^{b}	254 ± 25.2^{a}
SU19	Portugal	17.0 ± 0.170^{a}	24.4 ± 6.08^{b}	344 ± 43.2^{b}
SU20	Portugal	17.4 ± 1.04^{a}	29.1 ± 5.90^{b}	334 ± 26.0^{b}
SU21	Portugal	28.2 ± 2.53^{b}	35.6 ± 2.32^{c}	247 ± 20.0^{a}
SU22	Portugal	33.88 ± 0.870^{b}	23.0 ± 7.91^{b}	301 ± 38.2^{b}
SU23	Portugal	26.0 ± 4.79^{b}	21.5 ± 3.90^{b}	334 ± 18.0^{b}
SU24	Portugal	29.8 ± 1.86^{b}	12.0 ± 2.06^{a}	345 ± 67.5^{b}
SU25	Portugal	10.7 ± 3.27^{a}	13.8 ± 4.46^{a}	249 ± 65.7^{a}
SU26	Portugal	26.2 ± 1.2^{b}	16.4 ± 4.73^{b}	354 ± 64.6^{b}
SU27	Spain	36.9 ± 2.11^{b}	26.5 ± 7.33^{b}	309 ± 51.5^{b}
SU28	Spain	33.2 ± 1.16^{b}	16.5 ± 4.23^{b}	238 ± 56.6^{a}
SU29	Spain	42.1 ± 0.680^{b}	28.42 ± 8.80^{b}	382 ± 59.1^{b}
SU30	Spain	31.4 ± 0.780^{b}	18.8 ± 4.62^{b}	389 ± 68.0^{b}
SU31	Spain	45.4 ± 2.05^{c}	34.5 ± 1.57^{b}	800 ± 118^{c}
SU32	Spain	27.2 ± 2.53^{b}	36.6 ± 1.42^{c}	851 ± 112^{c}
SU33	Spain	25.0 ± 2.84^{b}	13.8 ± 3.71^{a}	279 ± 59.9^{b}

SU34	Spain	11.3 ± 2.42[a]	24.9 ± 6.23[b]	362 ± 51.5[b]
SU35	Spain	14.8 ± 1.40[a]	34.9 ± 6.30[b]	335 ± 55.3[b]
SU36	Spain	29.6 ± 0.450[b]	27.5 ± 4.74[b]	344 ± 46.7[b]
SU37	Spain	28.5 ± 1.85[b]	20.9 ± 0.600[b]	366 ± 66.3[b]
SU38	Spain	56.0 ± 2.77[c]	29.1 ± 4.83[b]	851 ± 94.1[c]
SU39	Spain	32.3 ± 6.44[b]	36.0 ± 13.54[c]	459 ± 87.2[c]
SU40	Italy	38.4 ± 1.41[b]	16.9 ± 0.380[b]	473 ± 72.2[c]
SU41	Spain	23.7 ± 2.37[b]	19.7 ± 3.99[b]	366 ± 61.1[b]
SU42	Spain	29.7 ± 1.48[b]	30.2 ± 0.790[b]	342 ± 47.3[b]
SU43	Spain	26.5 ± 2.39[b]	26.8 ± 1.90[b]	408 ± 84.6[c]
SU44	Spain	34.7 ± 1.94[b]	27.7 ± 4.55[b]	321 ± 62.0[b]
SU45	Spain	35.2 ± 1.86[b]	32.1 ± 0.190[b]	370 ± 49.3[b]
SU46	Italy	29.9 ± 0.960[b]	23.7 ± 1.93[b]	365 ± 37.4[b]
SU47	Italy	26.7 ± 2.36[b]	26.0 ± 3.29[b]	488 ± 45.7[c]
SU48	Italy	37.3 ± 2.99[b]	29.5 ± 6.83[b]	538 ± 36.6[c]
SU49	Morocco	14.6 ± 0.510[a]	10.6 ± 1.46[a]	312 ± 13.5[b]
SU50	Italy	20.1 ± 1.29[a]	19.0 ± 5.60[b]	439 ± 43.0[c]
$\overline{X}$1-50	-	33.3 ± 2.87[b]	25.6 ± 1.08[b]	382 ± 158[b]

Results are expressed as mean ± EEM. For each determination, "a" means that samples are below the $\overline{X}$1-50, "b" means that samples are not different from $\overline{X}$1-50, and "c" means that samples are above the $\overline{X}$1-50 ($p < 0.05$). Abbreviations: AChE IA: acetylcholinesterase inhibitory activity; COX-2 IA: Cycloxygenase-2 inhibitory activity; FRAP: ferric reducing antioxidant power; $\overline{X}$1-50: population mean.

Regarding COX-2 IA, the 82% of OL extracts demonstrated a similar modulatory COX-2 activity than $\overline{X}$1-50. In fact, only 10% of samples exhibited higher COX-2 activity than the $\overline{X}$1-50. Of these, 60% of these samples were from Spain and 40% were from Portugal. In contrast, 8% of the samples demonstrated lower COX-2 activity than the $\overline{X}$1-50, indicating a consistent modulatory effect of OL extracts on this parameter. Among these, 50% originated from Portugal, while 25% each were from Spain and Morocco.

Concerning FRAP, 24% of samples exhibited higher FRAP values than the $\overline{X}$1-50. Among these, 58.3% of these samples were from Spain

and 33.3% were from Italy, and 8.3% were originated from Portugal. Conversely, 25% of the samples showed lower FRAP values than the $\overline{X}$1-50, with 50% of them originating from Greece, 30% from Spain, and 20% from Portugal.

7.2. Unraveling the phytochemical contribution behind the observed effect in cholinesterase, inflammatory, and iron-oxidative inhibitory activity of olive leaf extracts

In the present section, an in-depth phytochemical characterization was conducted, focusing on the anti-cholinergic, anti-inflammatory, and anti-oxidative effects of OL. Moreover, the individual contributions of each compound were proposed and examined to better understand their impact.

7.2.1. Phytochemical profile of olive leaf extracts based on the AChE inhibitory activity

The cholinergic hypothesis suggests that there exits an alteration of ACh concentration in neurons during the pathogenesis of AD. In this context, part of the hypothesis indicates that there exists a hyperactivity of AChE, favoring the degradation of ACh, and promoting that AD patients develop severe ACh deficiency in the brain. This brain ACh deficit has been associated with memory loss and other cognitive symptoms related to AD [44]. Therefore, the AChE inhibition can extend the cholinergic transmission time and increase the cholinergic signaling. In fact, AChEI drugs are the only pharmacological treatment approved for AD patients. However, due to the significant side effects, the use of these AChEI drugs is limited [47]. Therefore, the formulation of cholinergic-based strategies using natural by-products with proven low side effects has been proposed for nutraceutical development for AD treatment. For this purpose, OL extracts were divided into four subpopulations based on quartiles distribution concerning their AChE

inhibitory activity into high (A1), medium-high (A2), medium-low (A3), and low (A4) subpopulations (**Figure 14**).

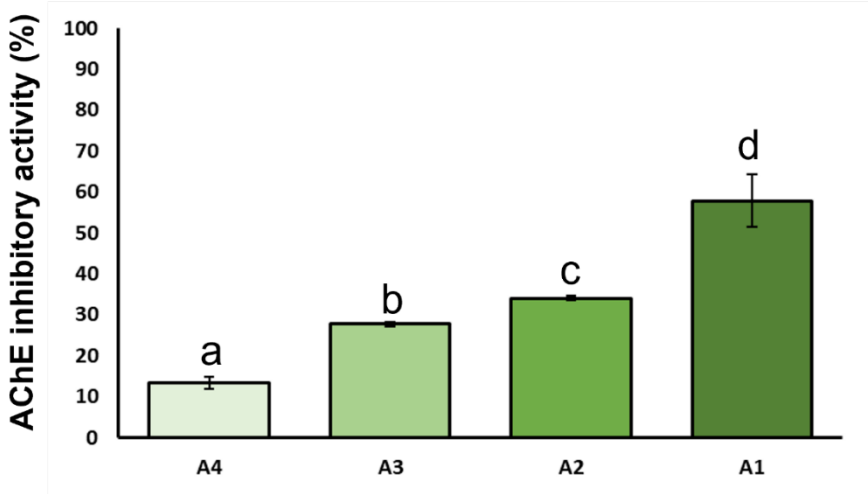

Figure 14. Acetylcholinesterase inhibitory activity of olive leaf extracts subpopulations. For each parameter, columns with different letters indicate statistically significant differences between subpopulations ($p < 0.05$). Abreviattions: A1: high AChE inhibitory activity; A2: medium-high AChE inhibitory activity; A3: medium-low AChE inhibitory activity; A4: low AChE inhibitory activity.

In the same way, to generate a phytochemical profile of the protective effect observed, the 42 individual compounds of OL extracts were clustered in base of aforementioned classification (**Table 10**). The content of secoiridoids seems to influence the modulatory activity of the AChEI exhibited by OL since more than 70% of the studied secoiridoids were different between A1 and A4 subpopulations. In this context, the OL extracts from A1 presented higher content in oleuropein and its derivatives (oleuropein diglucoside, oleuropein isomer, and hydroxyoleuropein), oleoside methyl ester, and ligstroside content compared to OL extracts from A4 subgroup. In fact, oleuropein and its derivatives (oleuropein diglucoside, oleuropein isomer) as well as ligstroside content were different between A1 and A2 subpopulations, indicating that these secoiridoids might contribute substantially to AChEI activity.

Table 10. Phytochemical profile of the olive leaf extracts based on AChE inhibitory activity

	A4	A3	A2	A1
Secoiridoids				
1-β-D-Glu-ACD EA I1	0.286 ± 0.265	0.298 ± 0.152	0.390 ± 0.193	0.261 ± 0.180
1-β-D-Glu-ACD EA I2	0.512 ± 0.698	0.777 ± 0.622	0.789 ± 0.54	0.493 ± 0.301
A-DM EA	0.345 ± 0.462^{b}	0.126 ± 0.126^{ab}	0.177 ± 0.181^{ab}	0.069 ± 0.106^{a}
D-OH EA I2	0.078 ± 0.193	-	-	-
H-DA-DM EA	0.108 ± 0.176^{b}	0.026 ± 0.043^{ab}	0.031 ± 0.055^{ab}	0.010 ± 0.035^{a}
Hy-DA-DM EA I1	0.074 ± 0.121	0.132 ± 0.087	0.127 ± 0.115	0.086 ± 0.145
Hy-DA-DM EA I2	0.431 ± 0.545^{b}	0.161 ± 0.248^{ab}	0.140 ± 0.164^{ab}	0.053 ± 0.154^{a}
Hydroxyoleuropein	0.044 ± 0.096^{a}	0.193 ± 0.377^{ab}	0.167 ± 0.276^{ab}	0.526 ± 0.688^{b}
Ligstroside	-	0.059 ± 0.203^{a}	0.070 ± 0.241^{a}	0.323 ± 0.438^{b}
Oleoside	0.470 ± 0.973	0.906 ± 1.38	0.654 ± 1.90	1.92 ± 2.59
Oleoside methyl ester	0.230 ± 0.367^{a}	0.748 ± 0.810^{ab}	0.710 ± 1.71^{ab}	1.39 ± 1.59^{b}
Oleuropein	1.04 ± 2.19^{a}	3.29 ± 9.25^{a}	3.76 ± 10.9^{a}	15.0 ± 22.0^{b}
Oleuropein diglu	-	0.017 ± 0.058^{a}	0.024 ± 0.083^{a}	0.192 ± 0.296^{b}
Oleuropein I	0.060 ± 0.195^{a}	0.266 ± 0.922^{a}	0.350 ± 1.21^{a}	1.50 ± 2.22^{b}
Flavonoids				
(+)-Eriodictyol	0.051 ± 0.079	0.129 ± 0.116	0.108 ± 0.134	0.045 ± 0.089
Apigenin	0.194 ± 0.148	0.169 ± 0.14	0.239 ± 0.321	0.125 ± 0.247
Apigenin-7-O-glu	0.202 ± 0.214	0.311 ± 0.143	0.278 ± 0.191	0.327 ± 0.268
Apigenin-7-O-rut	0.273 ± 0.164	0.436 ± 0.194	0.446 ± 0.259	0.453 ± 0.232
Azelaic acid	0.337 ± 0.321	0.649 ± 0.776	0.884 ± 1.23	0.460 ± 0.490
Chrysoeriol-7-O-glu	0.364 ± 0.288^{a}	0.577 ± 0.202^{b}	0.545 ± 0.212^{b}	0.703 ± 0.175^{b}
Diosmetin	0.257 ± 0.172	0.192 ± 0.092	0.253 ± 0.160	0.201 ± 0.199
I-3-O-β-D-glu	0.012 ± 0.029^{a}	0.014 ± 0.017^{a}	0.018 ± 0.022^{a}	0.066 ± 0.082^{b}
Luteolin	0.240 ± 0.173	0.222 ± 0.143	0.334 ± 0.231	0.367 ± 0.234
Luteolin 7-O-glu	0.474 ± 0.346^{a}	0.882 ± 0.491^{a}	0.964 ± 0.394^{a}	2.00 ± 1.76^{b}
Luteolin glu	2.21 ± 1.74^{a}	4.12 ± 2.04^{b}	3.94 ± 2.24^{b}	5.01 ± 1.98^{b}
Luteolin rut I1	-	-	0.001 ± 0.003	0.003 ± 0.012
Luteolin rut I2	0.002 ± 0.007^{a}	0.005 ± 0.018^{a}	0.019 ± 0.040^{ab}	0.044 ± 0.064^{b}
Luteolin-7,4-O-diglu	0.028 ± 0.048^{a}	0.093 ± 0.071^{b}	0.087 ± 0.085^{b}	0.127 ± 0.071^{b}
Oxidized quercetin	-	-	-	0.001 ± 0.004
Taxifolin	0.001 ± 0.004	-	0.001 ± 0.003	0.006 ± 0.023
Phenolic alcohols				
Hydroxytyrosol	0.078 ± 0.071^{a}	0.113 ± 0.115^{ab}	0.128 ± 0.093^{ab}	0.203 ± 0.186^{b}
Hydroxytyrosol glu	0.151 ± 0.184^{a}	0.176 ± 0.139^{a}	0.408 ± 0.579^{ab}	0.677 ± 0.730^{b}
4-Ethylguaiacol	0.138 ± 0.114^{b}	0.090 ± 0.023^{ab}	0.084 ± 0.022^{ab}	0.061 ± 0.057^{a}
Iridoids				
Loganic acid	0.165 ± 0.112^{a}	0.228 ± 0.087^{ab}	0.220 ± 0.094^{ab}	0.278 ± 0.084^{b}
7-Epiloganin	0.569 ± 0.351	0.636 ± 0.263	0.754 ± 0.293	0.715 ± 0.275
Lamiol	0.613 ± 0.464	0.821 ± 0.321	0.906 ± 0.539	0.787 ± 0.484
Hydroxycoumarins				
Esculetin	0.134 ± 0.199	0.177 ± 0.199	0.189 ± 0.164	0.219 ± 0.257
Esculin	0.036 ± 0.049	0.061 ± 0.037	0.060 ± 0.045	0.058 ± 0.063

Hydroxycinnamic acid				
Verbascoside	0.153 ± 0.117[a]	0.274 ± 0.404[ab]	0.283 ± 0.345[ab]	0.512 ± 0.578[b]
Decaffeoylverbascoside	0.800 ± 0.880[a]	0.986 ± 0.424[ab]	1.24 ± 0.856[ab]	1.63 ± 0.936[b]
Phenolic acids				
p-Hydroxybenzoic acid	0.023 ± 0.019	0.031 ± 0.010	0.032 ± 0.011	0.062 ± 0.113
Other compounds				
Lauroside B	0.366 ± 0.516	0.308 ± 0.248	0.304 ± 0.240	0.387 ± 0.250

Subpopulations (A1 to A4) were made based on quartiles distribution concerning their AChE inhibitory activity. Results are expressed as mean ± SD. For each parameter, columns with different letters indicate statistically significant differences between subpopulations ($p < 0.05$). Abbreviations: 1-β-D-Glu-ACD elenolic acid I1: 1-β-D-Glucopyranosyl acyclodihydroelenolic acid isomer 1; 1-β-D-Glu-ACD elenolic acid I2: 1-β-D-Glucopyranosyl acyclodihydroelenolic acid isomer 2; A-DM elenolic acid: aldehydic form of decarboxymethyl elenolic acid; D-OH elenolic acid I2: decarboxylated form of hydroxy elenolic acid isomer 2; EA: elenolic acid; glu: glucoside; H-DA-DM elenolic acid: hydrated product of the dialdehydic form of decarboxymethyl elenolic acid; Hy-DA-DM elenolic acid I1: hydroxylated product of the dialdehydic form of decarboxymethyl elenolic acid isomer 1; Hy-DA-DM elenolic acid I2: hydroxylated product of the dialdehydic form of decarboxymethyl elenolic acid isomer 2; OL: olive leaves; I: isomer; rut: rutinoside.

Concerning flavonoid contents, a substantial difference was also found between A1 and A4 subpopulations, with nearly 50% of the individual flavonoid contents showing variations. Specifically, OL extracts from A1 presented higher content in luteolin derivatives (luteolin 7-O-glucoside, luteolin-7,4-O-diglucoside, luteolin glucoside, and luteolin rutinoside isomer 1 and 2), chrysoeriol-7-O-glucoside, and isorhamnetin 3-O-β-D-(6-p-coumaroyl) glucoside compared with those OL from A4 subpopulation. Among the flavonoids, the content in luteolin-7-O-glucoside and isorhamnetin 3-O-β-D-(6-p-coumaroyl) glucoside might also contribute to the AChEI activity since its content was two and three times, respectively, higher than the observed in A2 subpopulation. On the other hand, the phenolic alcohol (hydroxytyrosol and hydroxytyrosol glucoside), hydroxycinnamic acid (verbascoside and decaffeoylverbascoside), and iridoid (loganic acid) content were higher in those OL from the A1 compared with those from A4 but not with A2 subpopulations. Surprisingly, and in contrast to the results, over 25% of the examined secoiridoids corresponded to elenolic acid derivatives,

which were found to be more abundant in the OL extracts from A4 subpopulations. Similarly, was observed with phenolic alcohols such as 4-Ethylguaiacol in A4 subpopulations, indicating a possible negative relation between these compounds and the AChEI activity.

7.2.2. Phytochemical profile of olive leaf extracts based on the COX-2 inhibitory activity

Some authors demonstrated the role of neuroinflammation in the AD process, found that COX-2 expression was increased in the brain of AD patients [163–166]. In this context, numerous authors have shown that drugs which could selectively inhibit COX-2 might reduce the clinical aspects of AD [167–169]. Nonetheless, the posology of these drugs has been associated with numerous side effects [170]. Hence, the formulation of COX-2 inhibitors based on natural by-products with proven low side effects has been proposed for nutraceutical development for the treatment of inflammation and its consequences related with AD [173]. For this purpose, OL extracts were divided into four subpopulations based on quartiles distribution concerning their COX-2 inhibitory activity into high (C1), medium-high (C2), medium-low (C3), and low (C4) subpopulations (**Figure 15**).

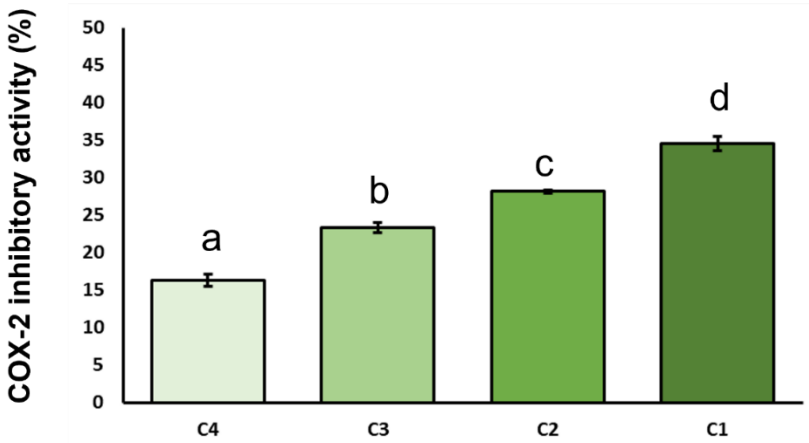

Figure 15. Cyclooxygenase-2 inhibitory activity of olive leaf extracts subpopulations. Results are expressed as mean ± SEM. For each parameter, columns with different letters indicate statistically significant differences between subpopulations ($p < 0.05$). Abbreviations: C1: high COX-2 inhibitory activity; C2: medium-high COX-2 inhibitory activity; C3: medium-low COX-2 inhibitory activity; C4: low COX-2 inhibitory activity.

In the same way, to generate a phytochemical profile of the protective effect observed, the 42 individual compounds of OL extracts were clustered in base of aforementioned classification (**Table 11**). The content of secoiridoids seems to influence the modulatory activity of the COX-2 exhibited by OL since over 55% of the studied secoiridoids were different between C1 and C4 subpopulations. In this context, the OL extracts from C1 presented higher content in oleuropein and its derivatives (oleuropein diglucoside, oleuropein isomer, and hydroxyoleuropein), oleoside and its derivatives (oleoside methyl ester), and ligstroside in comparison with those OL extracts from A4 subgroup. In effect, oleuropein derivatives (oleuropein diglucoside and hydroxyoleuropein), oleoside and its derivatives as well as ligstroside content seem to exhibit an important anti-inflammatory role since C1 and C2 subpopulations were different in these compounds. Similarly, C1 and C3 subpopulations were different in all the secoiridoids, indicating that these compounds might contribute to a dose-response manner to COX-2 inhibitory activity.

Table 11. Phytochemical profile of the olive leaf extracts based on COX-2 inhibitory activity

	C4	C3	C2	C1
Secoiridoids				
1-β-D-Glu-ACD EA I1	0.340 ± 0.186	0.293 ± 0.160	0.327 ± 0.253	0.270 ± 0.219
1-β-D-Glu-ACD EA I2	0.557 ± 0.554	0.789 ± 0.604	0.500 ± 0.517	0.704 ± 0.585
A-DM EA	0.091 ± 0.129^{a}	0.147 ± 0.209^{ab}	0.333 ± 0.443^{b}	0.159 ± 0.212^{ab}
D-OH EA I2	-	-	0.084 ± 0.200	-
H-DA-DM EA	0.024 ± 0.047	0.050 ± 0.102	0.060 ± 0.13	0.045 ± 0.123
Hy-DA-DM EA I1	0.164 ± 0.140^{b}	0.079 ± 0.099^{ab}	0.114 ± 0.128^{a}	0.056 ± 0.082^{a}
Hy-DA-DM EA I2	0.138 ± 0.261^{ab}	0.197 ± 0.186^{ab}	0.395 ± 0.584^{b}	0.077 ± 0.129^{a}
Hydroxyoleuropein	0.033 ± 0.063^{a}	0.059 ± 0.099^{a}	0.214 ± 0.294^{a}	0.618 ± 0.703^{b}
Ligstroside	-	-	0.082 ± 0.285^{a}	0.365 ± 0.422^{b}
Oleoside	0.137 ± 0.146^{a}	0.455 ± 0.952^{a}	0.676 ± 1.80^{a}	2.65 ± 2.46^{b}
Oleoside methyl ester	0.287 ± 0.315^{a}	0.356 ± 0.708^{a}	0.520 ± 0.938^{a}	1.87 ± 1.87^{b}
Oleuropein	0.571 ± 0.558^{a}	0.985 ± 2.23^{a}	6.47 ± 19.7^{ab}	15.0 ± 17.3^{b}
Oleuropein diglu	-	-	0.040 ± 0.137^{a}	0.193 ± 0.280^{b}
Oleuropein I	0.001 ± 0.003^{a}	0.059 ± 0.203^{a}	0.569 ± 1.97^{ab}	1.55 ± 1.79^{b}
Flavonoids				
(+)-Eriodictyol	0.093 ± 0.123	0.044 ± 0.058	0.119 ± 0.144	0.072 ± 0.091
Apigenin	0.230 ± 0.230	0.192 ± 0.219	0.231 ± 0.300	0.075 ± 0.074
Apigenin-7-O-glu	0.292 ± 0.140	0.203 ± 0.183	0.288 ± 0.229	0.327 ± 0.270
Apigenin-7-O-rut	0.457 ± 0.190	0.350 ± 0.269	0.464 ± 0.221	0.331 ± 0.195
Azelaic acid	0.453 ± 0.447	0.732 ± 1075	0.638 ± 1.03	0.490 ± 0.413
Chrysoeriol-7-O-glu	0.634 ± 0.107	0.495 ± 0.283	0.490 ± 0.282	0.559 ± 0.290
Diosmetin	0.297 ± 0.141^{b}	0.242 ± 0.150^{b}	0.251 ± 0.190^{b}	0.117 ± 0.106^{a}
I-3-O-β-D-glu	0.010 ± 0.014^{a}	0.022 ± 0.030^{ab}	0.026 ± 0.027^{ab}	0.054 ± 0.087^{b}
Luteolin	0.297 ± 0.196	0.327 ± 0.211	0.310 ± 0.226	0.235 ± 0.192
Luteolin 7-O-glu	0.684 ± 0.192^{a}	0.749 ± 0.371^{a}	0.949 ± 0.535^{a}	1.93 ± 1.86^{b}
Luteolin glu	4.08 ± 1.56	3.55 ± 2.61	3.91 ± 2.58	3.69 ± 2.21
Luteolin rut I1	0.003 ± 0.012	-	0.001 ± 0.003	-
Luteolin rut I2	0.011 ± 0.040	0.016 ± 0.040	0.017 ± 0.042	0.027 ± 0.047
Luteolin-7,4-O-diglu	0.086 ± 0.058	0.082 ± 0.088	0.096 ± 0.096	0.072 ± 0.070
Oxidized quercetin	-	-	0.001 ± 0.004	-
Taxifolin	-	-	0.007 ± 0.023	0.002 ± 0.005
Phenolic alcohols				
Hydroxytyrosol	0.098 ± 0.081	0.131 ± 0.107	0.097 ± 0.092	0.195 ± 0.192
Hydroxytyrosol glu	0.213 ± 0.304	0.419 ± 0.581	0.229 ± 0.312	0.557 ± 0.712
4-Ethylguaiacol	0.064 ± 0.040	0.104 ± 0.055	0.111 ± 0.105	0.098 ± 0.068
Iridoids				
Loganic acid	0.221 ± 0.077	0.207 ± 0.123	0.189 ± 0.077	0.269 ± 0.112
7-Epiloganin	0.668 ± 0.265	0.645 ± 0.311	0.742 ± 0.383	0.618 ± 0.247
Lamiol	0.778 ± 0.495	0.674 ± 0.524	0.777 ± 0.456	0.876 ± 0.387
Hydroxycoumarins				
Esculetin	0.190 ± 0.220	0.193 ± 0.217	0.150 ± 0.160	0.183 ± 0.234
Esculin	0.042 ± 0.033	0.040 ± 0.031	0.055 ± 0.063	0.076 ± 0.059

Hydroxycinnamic acid				
Verbascoside	0.126 ± 0.063[a]	0.212 ± 0.159[a]	0.224 ± 0.370[a]	0.651 ± 0.588[b]
Decaffeoylverbascoside	1.37 ± 0.920	1.17 ± 0.976	1.16 ± 0.894	0.958 ± 0.601
Phenolic acids				
p-Hydroxybenzoic acid	0.026 ± 0.015	0.026 ± 0.016	0.030 ± 0.015	0.064 ± 0.112
Other compounds				
Lauroside B	0.370 ± 0.347	0.369 ± 0.378	0.285 ± 0.349	0.344 ± 0.274

Subpopulations (C1 to C4) were made based on quartiles distribution concerning their COX-2 inhibitory activity. Results are expressed as mean ± SD. For each parameter, columns with different letters indicate statistically significant differences between subpopulations ($p < 0.05$). Abbreviations: Abbreviations: 1-β-D-Glu-ACD elenolic acid I1: 1-β-D-Glucopyranosyl acyclodihydroelenolic acid isomer 1; 1-β-D-Glu-ACD elenolic acid I2: 1-β-D-Glucopyranosyl acyclodihydroelenolic acid isomer 2; A-DM elenolic acid: aldehydic form of decarboxymethyl elenolic acid; D-OH elenolic acid I2: decarboxylated form of hydroxy elenolic acid isomer 2; EA: elenolic acid; glu: glucoside; H-DA-DM elenolic acid: hydrated product of the dialdehydic form of decarboxymethyl elenolic acid; Hy-DA-DM elenolic acid I1: hydroxylated product of the dialdehydic form of decarboxymethyl elenolic acid isomer 1; Hy-DA-DM elenolic acid I2: hydroxylated product of the dialdehydic form of decarboxymethyl elenolic acid isomer 2; OL: olive leaves; I: isomer; rut: rutinoside.

Concerning flavonoid contents, COX-2 modulatory activity seems to be less influenced by flavonoid contents in comparison with AChEI activity. In this case, only the 19% of the flavonoids studied were statistically different between C1 and C4 subpopulations, while about 50% of the flavonoids studied were different in A1 and A4 subpopulations (AChEI activity subgroups). In this context, OL extracts from C1 presented the highest content in luteolin 7-O-glucoside over the rest, indicating a possible modulatory effect of this compound on neuroinflammation. Similarly, the isorhamnetin 3-O-β-D-(6-p-coumaroyl) glucoside content was also higher, but only compared with those OL extracts from C4 subgroup. Likewise, as luteolin-7-O-glucoside, the verbascoside content was also distinguished on C1 over the rest. In contrast to the results, but in the same line with the results obtained in the previous section, the content of elenolic acid derivatives such as hydroxylated product of the dialdehydic form of decarboxymethyl elenolic acid isomer 1 as well as the flavonoid diosmetin were found to be more abundant in the OL extracts from C4 subpopulations, indicating a

possible negative relation between these compounds and the COX-2 inhibitory activity.

7.2.3. Phytochemical profile of olive leaf extracts based on FRAP

Redox-active iron accumulation and oxidative stress have been detected as an early mark in AD pathophysiology, which has been described as key factor on the formation of Aβ-plaque cores [162]. During AD, iron reactive species can react with numerous biomolecules through hydroxyl radicals generation, producing oxidizing species, which leads to contribute oxidative stress [171]. Hydroxyl radicals can origin lipid peroxidation in brain, resulting in successive liberation of redox-active iron into the cytosol [174–176]. Numerous authors targeted the use of ROS scavengers as emerging strategies to fight the hydroxyl radical productions during oxidative stress caused by iron species in AD [171,177]. Therefore, the antioxidant assay FRAP was selected to evaluate the iron-reductive capacity of OL samples. For this purpose, OL extracts were divided into four subpopulations based on quartiles distribution concerning their ferric reducing antioxidant power activity into high (F1), medium-high (F2), medium-low (F3), and low (F4) subpopulations (**Figure 16**).

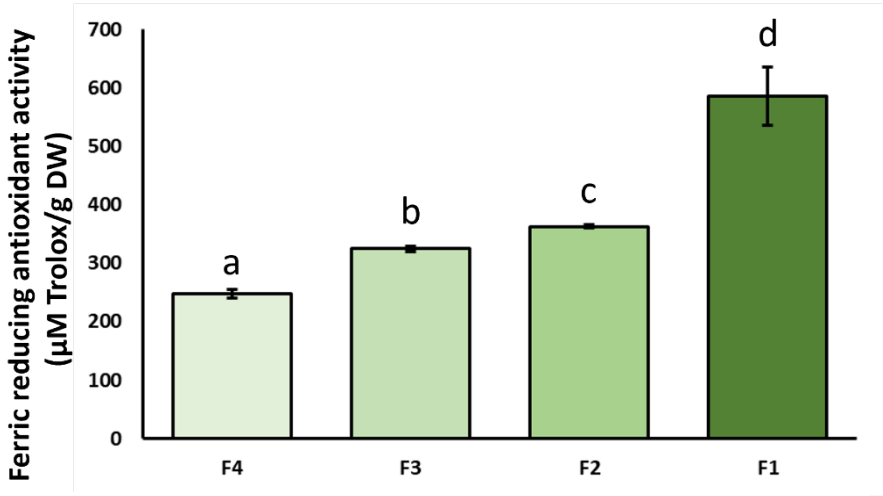

Figure 16. Iron-reducing capacity of olive leaf extracts subpopulations. Results are expressed as mean ± SEM. For each parameter, columns with different letters indicate statistically significant differences between subpopulations ($p < 0.05$). Abbreviations: F1: high FRAP activity; A2: medium-high FRAP activity; A3: medium-low FRAP activity; A4: low FRAP activity; FRAP: ferric reducing antioxidant power.

To generate a phytochemical profile of the protective effect observed, the 42 individual compounds of OL extracts were clustered in base of aforementioned classification (**Table 12**). The content of secoiridoids seems to strongly influence the ferric reducing antioxidant power exhibited by OL since the 50% of the studied secoiridoids were found to be more abundant in the OL extracts from F1 subpopulation. Specifically, the OL extracts from F1 presented the highest content in oleuropein and its derivatives (oleuropein diglucoside, oleuropein isomer, and hydroxyoleuropein), oleoside and its derivatives (oleoside methyl ester), and ligstroside over the rest.

Table 12. Phytochemical profile of the olive leaf extracts based on FRAP

	F4	F3	F2	F1
Secoiridoids				
1-β-D-Glu-ACD EA I1	0.326 ± 0.254	0.364 ± 0.222	0.295 ± 0.132	0.248 ± 0.187
1-β-D-Glu-ACD EA I2	0.385 ± 0.397[a]	0.860 ± 0.533[b]	0.856 ± 0.629[b]	0.482 ± 0.555[a]
A-DM EA	0.320 ± 0.442	0.203 ± 0.256	0.104 ± 0.124	0.089 ± 0.095
D-OH EA I2	0.078 ± 0.193	-	-	-
H-DA-DM EA	0.054 ± 0.126	0.040 ± 0.128	0.057 ± 0.102	0.027 ± 0.044
Hy-DA-DM EA I1	0.100 ± 0.128	0.133 ± 0.110	0.123 ± 0.112	0.062 ± 0.123
Hy-DA-DM EA I2	0.298 ± 0.560	0.194 ± 0.251	0.208 ± 0.267	0.092 ± 0.168
Hydroxyoleuropein	0.013 ± 0.028[a]	0.097 ± 0.114[a]	0.104 ± 0.165[a]	0.704 ± 0.674[b]
Ligstroside	-	-	-	0.441 ± 0.439
Oleoside	0.230 ± 0.482[a]	0.689 ± 1.20[a]	0.224 ± 0.447[a]	2.76 ± 2.76[b]
Oleoside methyl ester	0.268 ± 0.472[a]	0.500 ± 0.706[a]	0.260 ± 0.304[a]	2.00 ± 1.92[b]
Oleuropein	0.159 ± 0.232[a]	0.912 ± 0.824[a]	1.29 ± 2.31[a]	20.3 ± 22.2[b]
Oleuropein diglu	-	-	-	0.229 ± 0.284
Oleuropein I	-	0.007 ± 0.023[a]	0.059 ± 0.203[a]	2.07 ± 2.25[b]
Flavonoids				
(+)-Eriodictyol	0.045 ± 0.095	0.123 ± 0.128	0.077 ± 0.100	0.085 ± 0.109
Apigenin	0.181 ± 0.142	0.115 ± 0.085	0.157 ± 0.176	0.263 ± 0.368
Apigenin-7-O-glu	0.149 ± 0.146[a]	0.323 ± 0.196[b]	0.246 ± 0.166[ab]	0.398 ± 0.248[b]
Apigenin-7-O-rut	0.399 ± 0.219[ab]	0.496 ± 0.207[b]	0.449 ± 0.241[b]	0.269 ± 0.174[a]
Azelaic acid	0.210 ± 0.119[a]	0.323 ± 0.306[a]	0.615 ± 0.792[ab]	1.13 ± 1.11[b]
Chrysoeriol-7-O-glu	0.399 ± 0.297[a]	0.612 ± 0.176[b]	0.573 ± 0.219[ab]	0.609 ± 0.250[b]
Diosmetin	0.288 ± 0.140	0.190 ± 0.095	0.227 ± 0.125	0.196 ± 0.235
I-3-O-β-D-glu	0.007 ± 0.013[a]	0.015 ± 0.021[a]	0.032 ± 0.032[ab]	0.058 ± 0.085[b]
Luteolin	0.291 ± 0.173	0.250 ± 0.205	0.379 ± 0.264	0.248 ± 0.155
Luteolin 7-O-glu	0.485 ± 0.370[a]	0.819 ± 0.229[a]	0.877 ± 0.295[a]	2.13 ± 1.73[b]
Luteolin glu	2.66 ± 2.07	4.33 ± 2.35	4.50 ± 2.34	3.85 ± 1.80
Luteolin rut I1	-	-	-	0.004 ± 0.012
Luteolin rut I2	0.011 ± 0.038	0.006 ± 0.016	0.028 ± 0.054	0.026 ± 0.048
Luteolin-7,4-O-diglu	0.073 ± 0.079	0.103 ± 0.081	0.101 ± 0.081	0.062 ± 0.067
Oxidized quercetin	-	-	0.001 ± 0.004	-
Taxifolin	-	0.001 ± 0.004	-	0.007 ± 0.023
Phenolic alcohols				
Hydroxytyrosol	0.053 ± 0.041[a]	0.080 ± 0.050[a]	0.092 ± 0.060[a]	0.291 ± 0.151[b]
Hydroxytyrosol glu	0.160 ± 0.220	0.380 ± 0.534	0.293 ± 0.359	0.586 ± 0.743
4-Ethylguaiacol	0.111 ± 0.103	0.088 ± 0.064	0.097 ± 0.063	0.079 ± 0.045
Iridoids				
Loganic acid	0.179 ± 0.113[a]	0.269 ± 0.074[b]	0.226 ± 0.079[ab]	0.219 ± 0.117[ab]
7-Epiloganin	0.607 ± 0.373	0.671 ± 0.252	0.606 ± 0.249	0.780 ± 0.295
Lamiol	0.641 ± 0.540	0.996 ± 0.248	0.858 ± 0.451	0.640 ± 0.479
Hydroxycoumarins				
Esculetin	0.065 ± 0.046[a]	0.115 ± 0.061[a]	0.149 ± 0.107[a]	0.382 ± 0.302[b]
Esculin	0.022 ± 0.031[a]	0.056 ± 0.047[ab]	0.045 ± 0.032[a]	0.090 ± 0.058[b]
Hydroxycinnamic acid				

Verbascoside	0.100 ± 0.042[a]	0.13 ± 0.055[a]	0.227 ± 0.199[a]	0.750 ± 0.585[b]
Decaffeoylverbascoside	1.11 ± 0.948[ab]	1.52 ± 0.839[b]	1.35 ± 0.900[ab]	0.722 ± 0.484[a]
Phenolic acids				
p-Hydroxybenzoic acid	0.028 ± 0.017	0.026 ± 0.016	0.022 ± 0.017	0.069 ± 0.109
Other compounds				
Lauroside B	0.218 ± 0.251[a]	0.524 ± 0.387[b]	0.406 ± 0.341[ab]	0.243 ± 0.268[a]

Subpopulations (F1 to F4) were made based on quartiles distribution concerning their ferric iron reducing activity. Results are expressed as mean ± SD. For each parameter, columns with different letters indicate statistically significant differences between subpopulations ($p < 0.05$). Abbreviations: Abbreviations: 1-β-D-Glu-ACD elenolic acid I1: 1-β-D-Glucopyranosyl acyclodihydroelenolic acid isomer 1; 1-β-D-Glu-ACD elenolic acid I2: 1-β-D-Glucopyranosyl acyclodihydroelenolic acid isomer 2; A-DM elenolic acid: aldehydic form of decarboxymethyl elenolic acid; D-OH elenolic acid I2: decarboxylated form of hydroxy elenolic acid isomer 2; EA: elenolic acid; glu: glucoside; H-DA-DM elenolic acid: hydrated product of the dialdehydic form of decarboxymethyl elenolic acid; Hy-DA-DM elenolic acid I1: hydroxylated product of the dialdehydic form of decarboxymethyl elenolic acid isomer 1; Hy-DA-DM elenolic acid I2: hydroxylated product of the dialdehydic form of decarboxymethyl elenolic acid isomer 2; OL: olive leaves; I: isomer; rut: rutinoside.

Concerning flavonoid contents, FRAP seems to be more influenced by flavonoid contents in comparison with COX inhibitory activity. In this case, the 25% of the flavonoids studied were statistically different between F1 and F4 subpopulations, while about 19% and 50% of the flavonoids studied were different in COX-2 and AChE on their specific subpopulations. Precisely, OL extracts from F1 presented the highest content in luteolin 7-O-glucoside over the rest. Similarly, the isorhamnetin 3-O-β-D-(6-p-coumaroyl) glucoside, apigenin-7-O-glucoside, azelaic acid, and chrysoeriol-7-O-glucoside content were also higher, but only compared with those OL extracts from F4 subgroup. Likewise, as luteolin-7-O-glucoside, the hydroxycoumarins (esculin and esculetin), hydroxytyrosol, as well as verbascoside content were also distinguished on F1 over the rest, indicating a possible modulatory effect of these compounds on ferric reducing antioxidant capacity. In contrast to the results, but in the same line with the results obtained in the previous section, a strong but not significative tendence was found between the aldehydic form of decarboxymethyl elenolic acid content and FRAP,

indicating a possible negative relation between these compounds and the ferric reducing antioxidant capacity.

7.2.4. Partial least squares-discriminant analysis and correlation analysis

Partial least squares-discriminant analysis (PLS-DA) is a useful algorithm that can be used for predictive and descriptive modelling as well as for discriminative variable selection. PLS-DA has demonstrated great success in modelling high-dimensional datasets for diverse purposes such as metabolomics and food analysis [178]. In the present study, MetaboAnalyst V5.0 software was used to analyze the normalized and auto-scaled mean values of the 42 compounds analyzed by HPLC-ESI-QTOF-MS/MS its relationship with cholinesterase, inflammatory, and iron-oxidative inhibitory activity. Important features were identified by VIP scores in the present PLS-DA. A VIP score is a measure of a variable's importance in the PLS-DA model. It summarizes the contribution a variable makes to the model. The VIP score of a variable is calculated as a weighted sum of the squared correlations between the PLS-DA components and the original variable. The weights correspond to the percentage variation explained by the PLS-DA component in the model. The number of terms in the sum depends on the number of PLS-DA components found to be significant in distinguishing the classes. The X axis indicates the VIP scores corresponding to each variable on the Y-axis. The most contributory variables in class discrimination in the PLS-DA model were selected using VIP score values higher than 1, that correspond to $P < 0.05$ and was delimited with a discontinued line in **Figures 17B**, **18B**, and **19B**. In the same way, Pearsons's correlation analysis was employed to corroborate the results obtained in VIP score.

Figure 17A, provides the PLS-DA analysis based on AChEI activity subpopulations, which shows a different distribution between subgroup 1 and 4 (high vs low AChEI activity). The PLS-DA analysis reveals an interesting trend in the spatial distribution towards the top-

right part of the plot, indicating an increase in AChEI activity. The VIP score for AChEI activity shows that over 40% of the studied compounds might exert a modulatory effect on cholinergic function. Among the compounds of interest, over the 35% correspond to flavonoids. To mention, luteolin-7-O-glucoside content received the greatest VIP score and Pearson's correlation value in the inhibition of AChE activity exerted by OL extracts (**Figure 17B**). This result is in accordance with those *in vitro* studies that reported a remarkably potent inhibitory activity of luteolin-7-O-glucoside even at lower doses than those present in the A1 subpopulation [179,180]. Similarly, luteolin and its derivatives (luteolin rutinoside) and isoharmnentin derivatives also exhibited a moderate AChEI activity in Ellman *in vitro* assay [181–183]. In the same way, apigenin derivatives also showed a potential AChEI activity in a molecular docking study [173]. Those molecules content was also positively associated with AChEI activity in Pearson's correlation analysis **Table 13**.

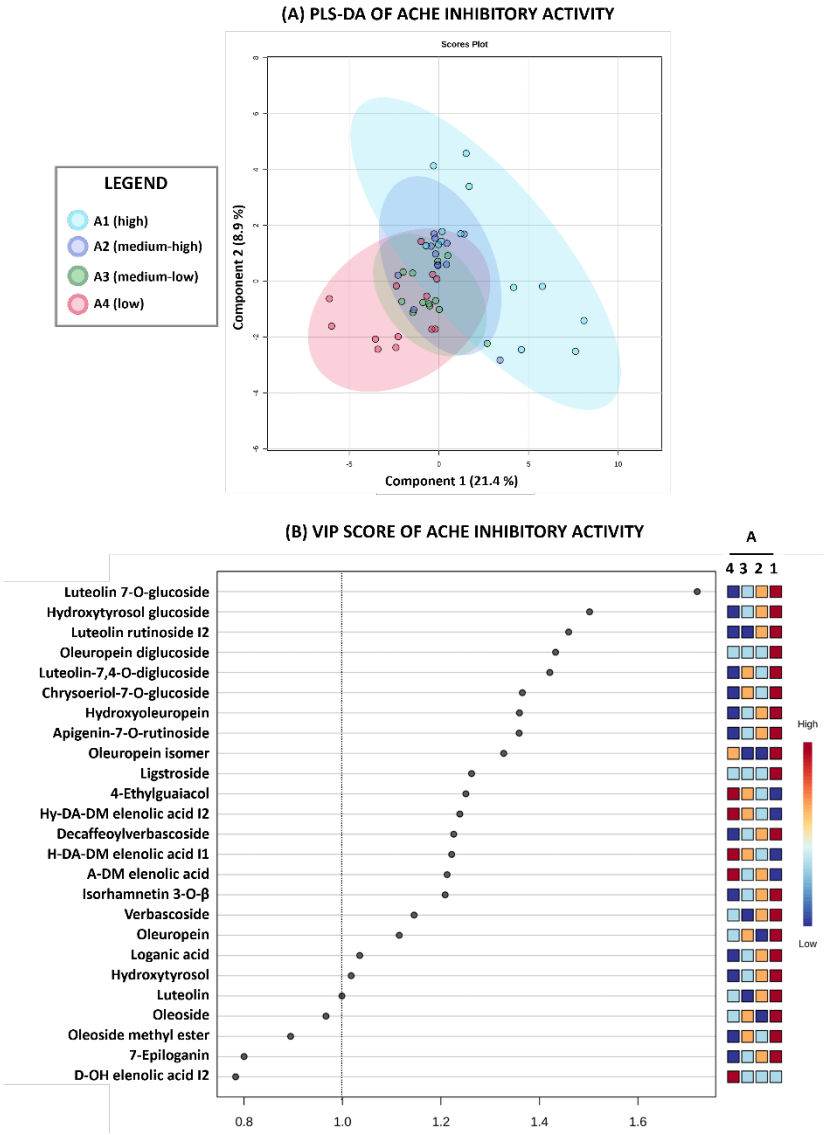

Figure 17. Multivariate data analysis of OL extracts based on AChE inhibitory activity. (A) Partial least squares discriminant analyses (PLS-DA) scores plot obtained from the mean values of the 42 phytochemical compounds present in the OL from the different subpopulations of inhibitory activity of AChE. (B) Variable importance in projection (VIP) score plots for the top 25 most important phytochemical compounds by PLS-DA. The heatmap indicates the relative concentration of the specific compound in the different subpopulations and the dashed line means statistically significant at $p < 0.05$. Abbreviations: A-DM elenolic acid: aldehydic form of decarboxymethyl elenolic acid; D-OH elenolic acid I2: decarboxylated form of hydroxy elenolic acid isomer 2; H-DA-DM elenolic acid: hydrated product of the dialdehydic form of decarboxymethyl elenolic acid; Hy-DA-DM elenolic acid I2: hydroxylated product of the dialdehydic form of decarboxymethyl elenolic acid isomer 2; I: isomer.

On the other hand, the VIP score shows that over 40% of the compounds of interest are secoiridoids, that might indicate that this family is involved in the cholinergic modulatory activity exerted by OL extracts. In this context, oleuropein and its derivatives (oleuropein isomer, oleuropein diglucoside, and hydroxyoleuropein) were the compounds with more contribution in the A1 subpopulation. Despite the results obtained in VIP score and the moderate association value, *in vitro* studies demonstrated that isolated oleuropein presents a very low AChEI activity in Ellman test [182]. However, oleuropein supplementation has shown to improve ACh content in brains from rodent models of cerebral stroke, which correlated with an improve of cognitive impairment [184]. This incongruence between *in vitro* and *in vivo* experiments might explain due the rapid and partial hydrolysis of oleuropein in the upper gastrointestinal tract to hydroxytyrosol and its derivatives [5]. Literature review indicates that phenolic compounds with multiple hydroxyl groups are believed to enhance the AChEI activity due the stronger binding capacity [185]. However, the role of hydroxyoleuropein in AChEI activity has not been explored and there is not data available to compare. Nonetheless, the phenolic alcohol, hydroxytyrosol received a significative VIP score, with demonstrated inhibitory activity of AChE *in vitro* [186,187]. Other compounds detected by VIP score with null effect in AChEI activity were loganic acid and verbascoside [182,188]. Another plausible explanation could be that, although each compound has an individual contribution, the synergistic effect of the phytochemical combination in OL extracts, at the presented doses, could be the reason behind the inhibitory effect on AChE [5,189]. Nonetheless, the enrichment of OL with individual compounds may increase the inhibitory activity. This feature is evident when compare AChEI activity using whole OL extracts enriched in oleuropein or hydroxytyrosol. In this context, an OL extract with a lower oleuropein content than A1 but similar with A2 subgroup exerted a remarkable inhibitory activity of AChE but was 2.7 times lower than OL extract 25% enriched in hydroxytyrosol [182]. Similarly, just as the enrichment of certain compounds may enhance the inhibitory activity, the current evidence indicates that some compounds

might diminish the AChEI activity of olive leaves. In the present research, A4 subgroup contained the highest elenolic acid derivatives (A-DM elenolic acid, H-DA-DM elenolic acid and Hy-DA-DM elenolic acid I2) content over the rest. The VIP score for these compounds oscillate between 1.2 and 1.4, indicating a potential role of these compounds in the AChEI activity. Pearsons's correlation analysis demonstrated a moderate and negative association between these compounds and the AChEI activity of OL extracts **Table 10**. This inverse tendence with AChEI activity has been previously reported in olive leaves samples from a Greece. In this context, this OL samples exhibited a very low AChEI activity and were strongly and negatively correlated with the content of the hydrated product of the dialdehydic form of decarboxymethyl elenolic acid [19]. This feature was also observed in a study evaluating the AChEI activity of two different varieties of extra-virgin olive oil (EVOO). Authors demonstrated that the EVOO with the lowest AChEI activity was three times richer in elenolic derivatives [190]. These results might be explained due to the fact that these compounds, are linked to oleuropein, hydroxytyrosol, and ligstroside structures, and an excess of these free elenolic acid derivatives might indicate an excessive degradation of oleuropein, hydroxytyrosol, and ligstroside, which may reduce the AChEI properties of OL extracts [191].

Concerning COX-2 inhibitory activity, the PLS-DA analysis shows that the distribution of the different subpopulations seems to follow the same trend as AChEI but is less clear between subgroup 1 and 4 (high *vs.* low COX-2 inhibitory activity), probably due to the smaller therapeutic range exerted by OL samples in comparison with AChEI activity (**Figure 18A**). In the presented PLS-DA analysis, no discernible differences in spatial distribution were observed between groups 2 and 3, and even group 4, indicating similarities among these groups. The VIP score for COX-2 inhibitory activity shows that almost 30% of the studied compounds might exert a modulatory effect on inflammatory function. Among the compounds of interest, less of the 20% correspond to flavonoids (**Figure 18B**). To mention, luteolin-7-O-glucoside content

received the greatest VIP score and Pearson's correlation value in the flavonoid family regarding to COX-2 inhibitory activity. This result is in accordance with a study that reported a remarkably potent COX-2 inhibitory activity of luteolin-7-O-glucoside in an hepatitis-induced ICR mice [192]. Similarly, Isorhamnetin 3-O-β-D-(6-p-coumaroyl) glucoside also exhibited a moderate positive correlation, but the research about the inhibitory COX-2 activity is null. In contrast, diosmetin were found to be more abundant in the OL extracts from C4 subpopulations and exhibited a negative association with COX-2 inhibitory activity (**Table 11**). From a biosynthetic point of view, flavonoids are derived from a limited number of flavanone intermediates. The production of diosmetin can occur through two enzymatic pathways: firstly, via the enzyme flavone O-methyltransferase using luteolin as a substrate, and secondly, through the enzyme flavanone 3'-hydroxylase using apigenin as a substrate [193]. Luteolin is a substrate necessary to the formation of luteolin-7-O-glucoside, a flavonoid with a remarkable anti-inflammatory effect. Therefore, the formation of diosmetin might compromise the formation of luteolin-7-O-glucoside. Consequently, this process might potentially lead to a reduction in the COX-2 inhibitory activity due a reduction in luteolin-7-O-glucoside.

On the other hand, the VIP score shows that 50% of the compounds of interest are secoiridoids, that might indicate that this family is strongly involved in the anti-inflammatory activity exerted by OL extracts. In this context, oleoside content received the greatest VIP score and one of the higher Pearson's correlation values in the secoiridoid family regarding to COX-2 inhibitory activity (**Figure 18B**). However, there is no evidence of the modulatory effect of this compound or its derivatives on COX-2 activity, but it opens the field for further research to test the anti-inflammatory capacity of oleoside. Despite the limitation mentioned above, PLS-DA assigned to oleuropein and its derivatives (oleuropein isomer, oleuropein diglucoside, and hydroxyoleuropein) a significantly high VIP score and these findings were further supported by Pearson's correlation analysis (**Table 13**). The anti-inflammatory activity

of these compounds is well described. To mention, oleuropein consumption in rodents has been related to reduce COX-2 protein levels or gene expression under pro-inflammatory conditions such as renal injury, atopic dermatitis, and ulcerative colitis [194–198]. In fact, the inhibitory capacity of COX-2 mediated by oleuropein in ulcerative colitis was also probed in human with promising results [199]. Other secoiridoid detected by VIP score with high positive correlation values were ligstroside and A-DM elenolic acid. Verbascoside was proven their selective COX inhibition using molecular docking [200,201] whereas the role of A-DM elenolic acid has not been explored. In the present research, A4 subgroup contained the highest Hy-DA-DM elenolic acid I2 content over the rest and was negatively correlated with COX-2 inhibitory activity (**Table 13**). This association might be explained since these compounds, are mainly linked to oleuropein, hydroxytyrosol, and ligstroside structures. Therefore, as mentioned before, an increase of elenolic acid derivatives might suggest an excessive degradation of these compounds, which may reduce their biomedical properties [191].

Among hydroxycinnamic acids studied, verbascoside was pointed out by PLS-DA and Pearson's analysis. In the present research, C1 subpopulation presented the highest verbascoside content over the rest (**Table 11**). In fact, verbascoside has shown to reduce both, expression and activity of COX-2 *in vitro* [202] and *in vivo* [203].

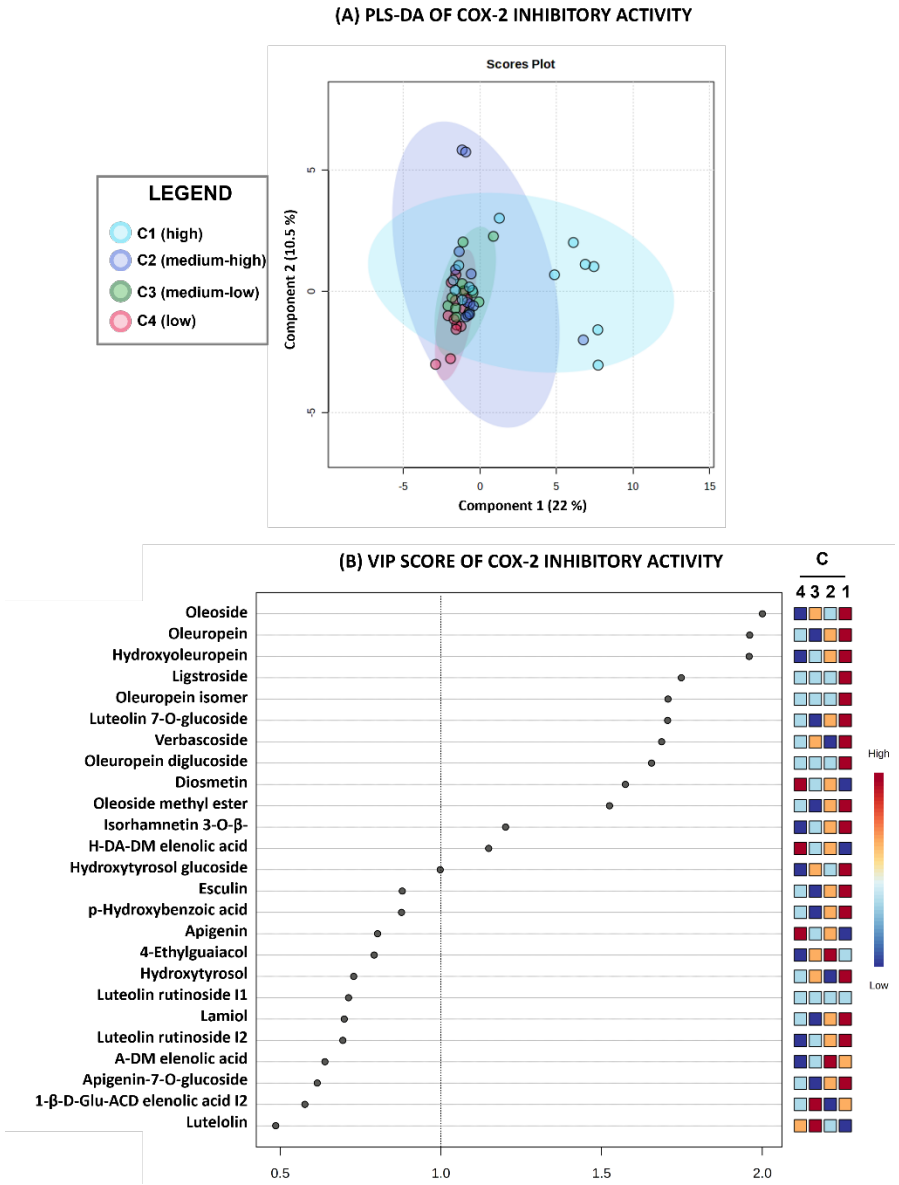

Figure 18. Multivariate data analysis of OL extracts based on COX-2 inhibitory activity. (A) Partial least squares discriminant analyses (PLS-DA) scores plot obtained from the mean values of the 42 phytochemical compounds present in the OL from the different subpopulations of inhibitory activity of COX-2. (B) Variable importance in projection (VIP) score plots for the top 25 most important phytochemical compounds by PLS-DA. The heatmap indicates the relative concentration of the specific compound in the different subpopulations and the dashed line means statistically significant at $p < 0.05$. Abbreviations: 1-β-D-Glu-ACD elenolic acid I1: 1-β-D-Glucopyranosyl acyclodihydroelenolic acid isomer 1; A-DM elenolic acid: aldehydic form of decarboxymethyl elenolic acid; H-DA-DM elenolic acid: hydrated product of the dialdehydic form of decarboxymethyl elenolic acid; I: isomer.

Finally, regarding the ferric reducing antioxidant capacity, the PLS-DA analysis reveals a distinct distribution between groups 1 and 4 (high *vs.* low FRAP) as depicted in **Figure 19A**. The PLS-DA analysis revealed a clear overlap in spatial distribution of the subpopulation F2 and F3, while group 1 exhibits significant differentiation, likely attributed to its remarkable antioxidant capacity. The VIP score for FRAP shows that among 40% of the studied compounds might exert a modulatory effect on antioxidant capacity. In this context, the phenolic alcohol, hydroxytyrosol received the greatest VIP score and Pearson's correlation value over the rest. The antioxidant contribution of hydroxytyrosol, and its derivatives with OL has been widely described using FRAP test *in vitro* [204–206]. In addition, hydroxytyrosol supplementation has been shown to increase the ferric reducing antioxidant capacity of plasma in a mouse model of systemic inflammation [207].

On the other hand, the VIP score shows that 35% of the compounds of interest are secoiridoids, that might indicate that this family is strongly involved in the antioxidant activity exerted by OL extracts. In this context, oleuropein, and its derivatives (oleuropein isomer and hydroxyoleuropein) received one of the higher VIP score and Pearson's correlation values. F1 subpopulation presented the highest content in oleuropein and its derivatives over the rest. *In vitro* studies demonstrated that the ferric reducing antioxidant capacity of OL increases with the content of oleuropein [208,209]. In fact, a 40% oleuropein-rich OL extract exerted a very high FRAP while reducing the β-amyloid and tau proteotoxicity in *C. elegans*. Authors attributed these features to the regulation of oxidative stress exhibited by oleuropein rich OL during AD [26]. PLS-DA assigned significantly high VIP score to oleoside and its derivatives as well as ligstroside content, and these findings were further supported by Pearson's correlation analysis (**Table 13**). These results align with those obtained in different *in vitro* studies, which demonstrated that the ferric reducing antioxidant capacity of OL increases with the content of oleoside and ligstroside. [209]. In contrast with the results, a secoiridoid namely A-DM elenolic acid was negatively

correlated with FRAP (**Table 13**). This feature can be explained in a similar manner to what was mentioned earlier in the context of AChE and COX-2 inhibitory activities for elenolic acid derivatives [191].

Among the compounds of interest, less than 25% corresponded to flavonoids (**Figure 19**B). To mention, the luteolin-7-O-glucoside content received the greatest VIP score and Pearson's correlation value in the flavonoid family about antioxidant activity. This result is in accordance with a study that reported a remarkably potent ferric reducing antioxidant capacity of luteolin-7-O-glucoside which was able to reduce DNA oxidative markers in RAW264.7 cells [179]. Similarly, azelaic acid also exhibited a moderate positive correlation, with promising results against paraquat-induced oxidative stress in *C. elegans* [210]. PLS-DA assigned apigenin-7-glucoside a significantly high VIP score and these findings were further supported by a study that demonstrated that the FRAP of OL increases with the content of apigenin-7-glucoside [209].

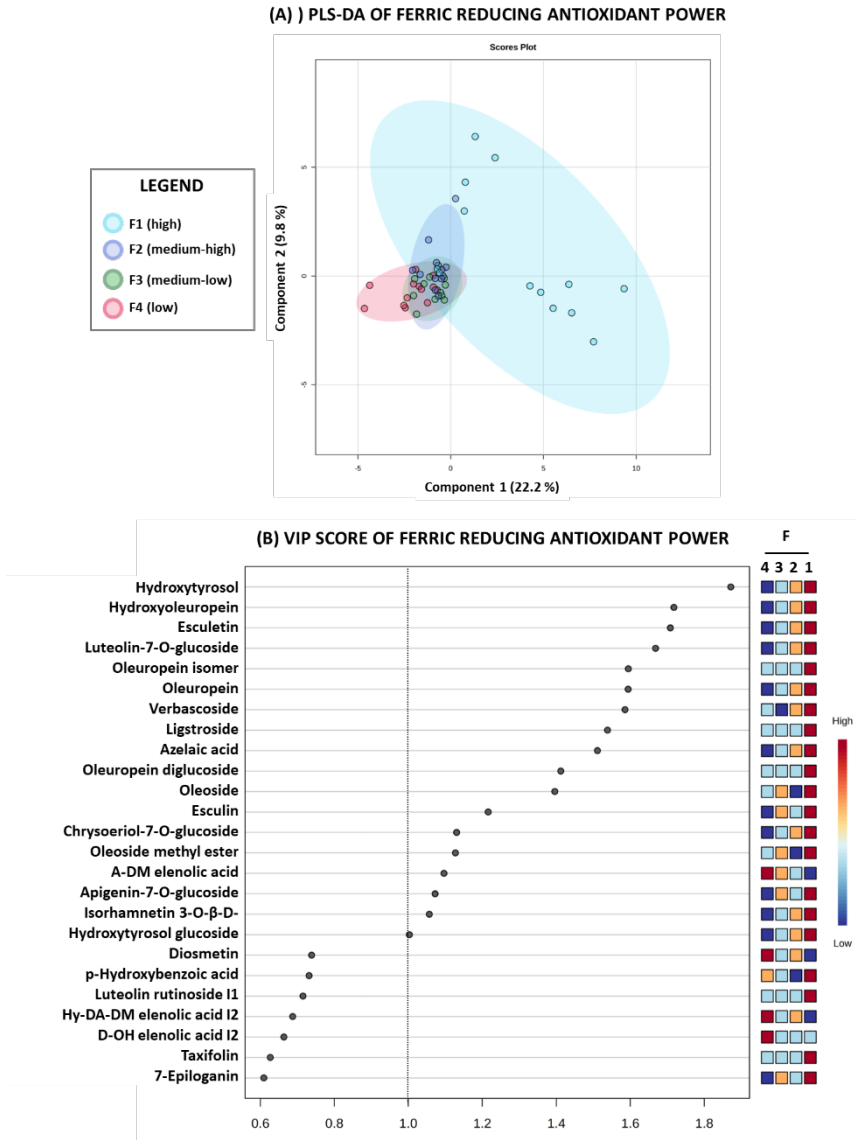

Figure 19. Multivariate data analysis of OL extracts based on FRAP. (A) Partial least squares discriminant analyses (PLS-DA) scores plot obtained from the mean values of the 42 phytochemical compounds present in the OL from the different subpopulations of inhibitory activity of FRAP. (B) Variable importance in projection (VIP) score plots for the top 25 most important phytochemical compounds by PLS-DA. The heatmap indicates the relative concentration of the specific compound in the different subpopulations and the dashed line means statistically significant at $p < 0.05$. Abbreviations: A-DM elenolic acid: aldehydic form of decarboxymethyl elenolic acid; D-OH elenolic acid I2: decarboxylated form of hydroxy elenolic acid isomer 2; Hy-DA-DM elenolic acid I2: hydroxylated product of the dialdehydic form of decarboxymethyl elenolic acid isomer 2; I: isomer.

Other hydroxycompounds pointed out by VIP score and corroborated with Pearsons's correlation analysis were hydroxycoumarins (esculetin and esculin) as well as verbascoside content. These compounds were mainly present in F1 subpopulation, indicating a strong contribution to the antioxidant activity exerted by OL extracts. These results are consistent with those reported in the literature, as esculetin, esculin, and verbascoside have been identified as potent ferric reducing antioxidant agents [209,211–213].

Table 13. Pearson's correlation analysis of AChE and COX-2 inhibitory activity, as well as FRAP with phytochemical compounds.

	AChE IA		**COX-2 IA**		**FRAP**	
	r value	Sig	*r* value	Sig	*r* value	Sig
Secoiridoids						
A-DM elenolic acid	-0.325	0.021	0.489	0.000	-0.326	0.021
H-DA-DM elenolic acid	-0.326	0.021	-	-	-	-
Hy-DA-DM elenolic acid I1	-	-	-0.287	0.043	-	-
Hy-DA-DM elenolic acid I2	-0.386	0.006	-	-	-	-
Hydroxyoleuropein	0.366	0.009	0.410	0.003	0.537	0.000
Ligstroside	0.387	0.005	0.489	0.000	0.524	0.000
Oleoside	-	-	0.483	0.000	0.446	0.001
Oleoside methyl ester	0.312	0.027	0.443	0.001	0.449	0.001
Oleuropein	0.348	0.013	0.399	0.004	0.501	0.000
Oleuropein diglucoside	0.388	0.005	0.412	0.003	0.458	0.001
Oleuropein isomer	0.354	0.012	0.463	0.001	0.503	0.000
Flavonoids						
Apigenin-7-O-rutinoside	0.288	0.043	-	-	0.371	0.008
Azelaic acid	-	-	-	-	0.452	0.001
Chrysoeriol-7-O-glucoside	0.456	0.001	-	-	-	-
Diosmetin	-	-	-0.384	0.006	-	-
Isorhamnetin 3-O-β-D-glu	0.379	0.007	0.312	0.027	0.389	0.005
Luteolin 7-O-glucoside	0.489	0.000	0.411	0.003	0.523	0.000
Luteolin glucoside	0.432	0.002	-	-	-	-
Luteolin rutinoside I2	0.387	0.006	-	-	-	-
Luteolin-7,4-O-diglucoside	0.437	0.002	-	-	-	-
Phenolic alcohols						
Hydroxytyrosol	0.347	0.014	-	-	0.648	0.000
Hydroxytyrosol glucoside	0.402	0.004	-	-	-	-
4-Ethylguaiacol	-0.383	0.006	-	-	-	-
Iridoids						
Loganic acid	0.381	0.006	-	-	-	-
Hydroxycoumarins						
Esculetin	-	-	-	-	0.555	0.000

Esculin	-	-	-	-	0.459	0.001
Hydroxycinnamic acid						
Verbascoside	0.307	0.030	0.450	0.001	0.578	0.000
Decaffeoylverbascoside	0.371	0.008	-	-	-	-

Abbreviations: A-DM elenolic acid: aldehydic form of decarboxymethyl elenolic acid; H-DA-DM elenolic acid: hydrated product of the dialdehydic form of decarboxymethyl elenolic acid; Hy-DA-DM elenolic acid I1: hydroxylated product of the dialdehydic form of decarboxymethyl elenolic acid isomer 1; Hy-DA-DM elenolic acid I2: hydroxylated product of the dialdehydic form of decarboxymethyl elenolic acid isomer 2.

A summary of the protective effects of OL extracts and its components against *in vitro* parameters of AD is found in **Figure 20**.

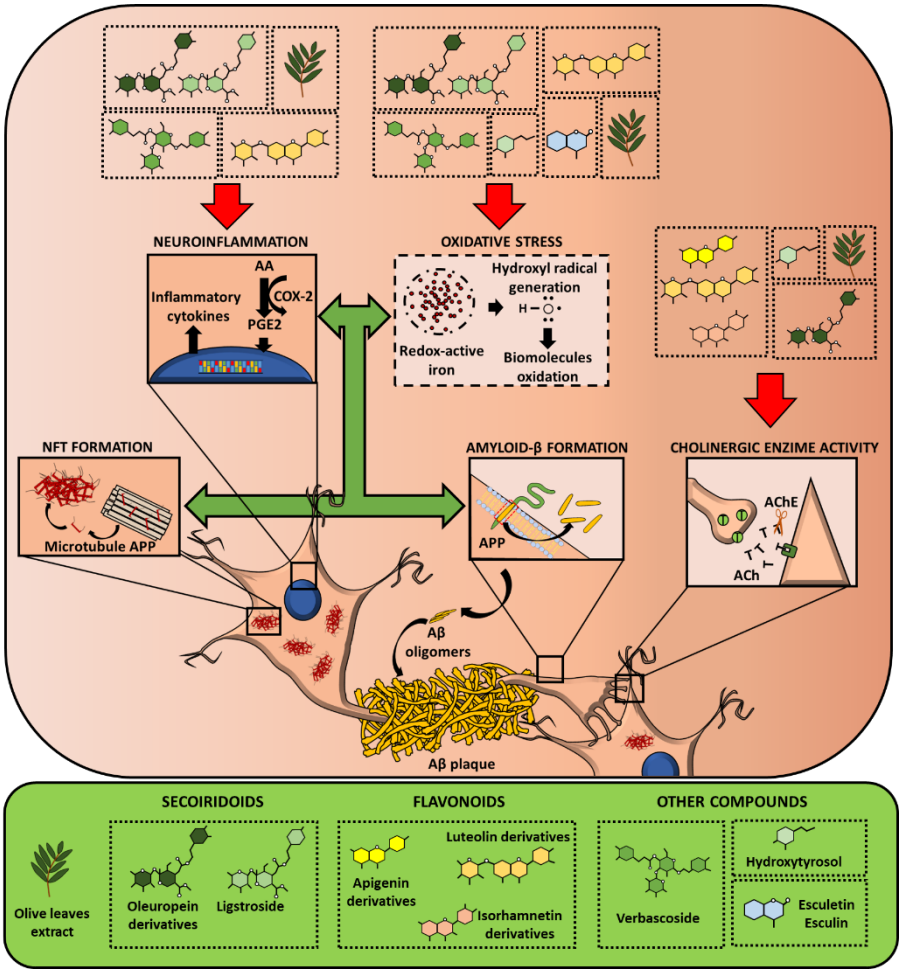

Figure 20. Modulatory effect of olive leaf extracts and it's phytochemicals on Alzheimer's disease physiopathology *in vitro*. Green arrows represent promotion of the process, whereas red arrows represent reduction in the process. Abbreviatures: AA: araquidonic acid; AChE: acetylcholinesterase; APP: amyloid precursor protein; Aβ: amyloid beta; COX-: cyclooxygenase-2; NFT: neurofibrillary tangles; PGE2: prostaglandin E2.

7.3. Impact of the origin of olive leaves in the cholinesterase, inflammatory, and iron-oxidative inhibitory activity.

As it can be observed in **Figure 21**, the highest inhibitory AChE activity percentage was exhibited by the Spanish (38.5 ± 3.72) and the Italian (36.6 ± 6.76) samples. In contrast, the lowest AChE inhibitory activity percentage was observed by the Greek OL (17.8 ± 4.53). These variations might be attributed to differences in the phytochemical profile.

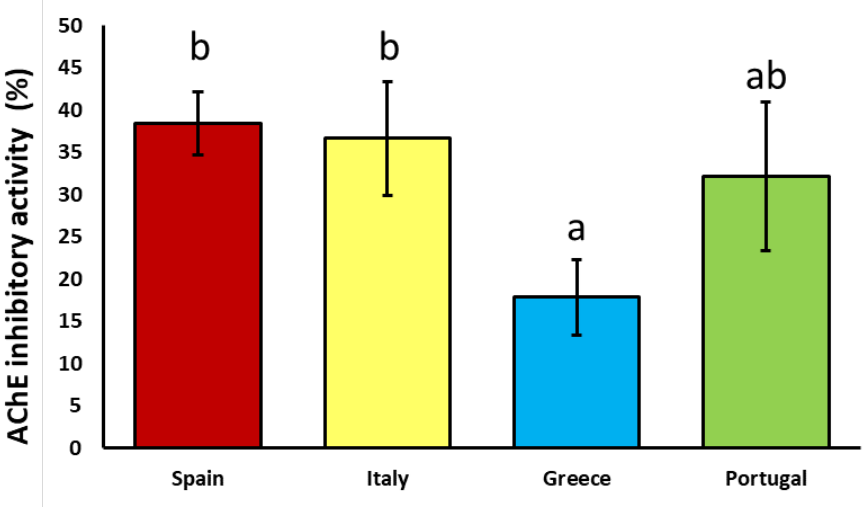

Figure 21. Acetylcholinesterase (AChE) inhibitory activity exerted by OL extracts from Spain, Italy, Greece, and Portugal. Results are expressed as mean ± standard error of the mean. For each of the parameters, bars with different letters indicate statistically significant differences between countries ($p < 0.05$). OL: olive leaves.

Pearsons's correlation and VIP score analysis showed that AChE inhibitory activity may be influenced by numerous compounds in the OL. As depicted in **Figure 17B**, the observed AChE inhibitory activity percentage of the Spanish samples appears to be linked mainly to their elevated levels of secoiridoids (oleuropein, hydroxyoleuropein, oleuropein isomer, ligstroside, and oleoside), followed by the flavonoids (luteolin-7,4-O-diglucoside, luteolin glucoside, luteolin rutinoside, Chrysoeriol-7-O-glucoside, and apigenin-7-O-rutinoside), and

hydroxycinnamic acids (verbascoside and decaffeoylverbascoside) contents. These compounds possess inhibitory properties, as mentioned earlier, which could account for their impact on the AChE inhibitory activity observed in the Spanish samples (**Figure 21**). Likewise, the anti-cholinesterase activity exhibited by the Italian samples appears to be distinct, likely due to their specific phytochemical profile. In this case, flavonoids (luteolin rutinoside, luteolin-7-O-glucoside, and isorhamnetin 3-O-β-D-(6-p-coumaroyl) glucoside) seem to exert a significant influence on this parameter. Furthermore, other compounds with modulatory activity were present in substantial levels, including secoiridoids (oleuropein diglucoside), phenolic alcohols (hydroxytyrosol and hydroxytyrosol glucoside), and hydroxycinnamic acids (verbascoside and decaffeoylverbascoside). In contrast, the Italian samples were found to present significative levels of H-DA-DM elenolic acid, which was associated with lower AChE IA. These compounds likely contribute to the observed anti-cholinesterase effects observed in the Italian samples (**Figure 21**).

The anti-cholinergic activity of the Portuguese samples might be associated with oleoside methyl ester and chrysoeriol-7-O-glucoside content in a similar way to the Spanish samples, indicating a possible influence of the geographical region on the anticholinergic activity promoted by these compounds (**Figures 17A** and **17B**). In the same way, the lower flavonoid (isorhamnetin 3-O-β-D-(6-p-coumaroyl) glucoside, apigenin-7-O-rutinoside, and luteolin 7-O-glucoside) content and the high presence of elenolic acid derivatives might elucidate the non-statistical downward trend observed in AChEI activity (AChE IA) in comparison with the Spanish and Italian samples. Nevertheless, despite the different correlations with specific compounds, no statistical differences were found between the anti-AChE activity of the Spanish, Italian and Portuguese samples. This effect might be attributed to the fact that the total phenolic content is similar among samples. Therefore, the specific individual phytochemical compound contribution to the anti-cholinergic activity might be masked due a synergist activity with the rest

of compounds, as previously described [5]. Finally, the Greek samples exhibited the lowest anti-cholinergic activity over the rest. In this case, an interesting result concerning the neuroprotective effect was found. As mentioned before, the high content in elenolic acid derivatives has been associated with low AChE IA (**Figure 17B**). This association and the low phenolic content might explain, at least in part, the low AChE inhibitory activity exerted by the Greek samples.

Despite the remarkable anti-inflammatory activity exerted by the different OL, no origin-related effect was observed (**Figure 22**). Pearson's correlations and VIP score indicate that the major contribution to the anti-inflammatory activity exerted by OL was attributed to oleoside and its derivatives, oleuropein and its derivatives, ligstroside, luteolin-7-O-glucoside, and verbascoside content (**Figure 18B**). These results are in accordance with the literature, which showed that OL [214,215], and numerous isolated compounds such as oleuropein and its derivatives [199,215], verbascoside [202], and luteolin-7-O-glucoside [216] were able to reduce COX-2 activity. However, there are not available information about the anti-inflammatory effect of oleosides and its derivatives in the current literature, and this work provides the opportunity for further research to evaluate the potential biomedical properties of these compounds.

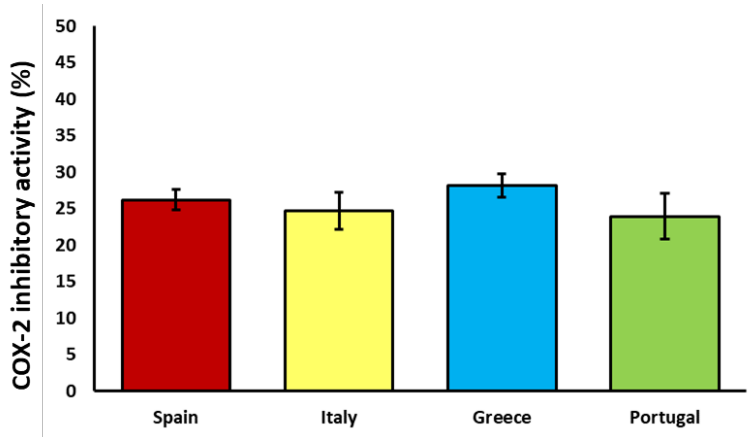

Figure 22. Cyclooxygenase (COX)-2 inhibitory activity exerted by OL extracts from Spain, Italy, Greece, and Portugal. Results are expressed as mean ± standard error of the mean. For each of the parameters, bars with different letters indicate statistically significant differences between countries ($p < 0.05$). OL: olive leaves.

The iron-reductive capacity also appears to be influenced by the origin of the plant material. In this context, the Italian samples exhibited the highest FRAP value, followed by the Spanish and Portuguese samples (**Figure 23**). Conversely, the Greek samples displayed the lowest FRAP value once again. Regarding **Table 8**, it was observed that the Italian samples were the primary source of hydroxytyrosol and esculetin, which received some of the highest VIP and correlation values among all the compounds in relation to FRAP (**Table 13** and **Figure 19B**). Similarly, the Spanish samples contained significant levels of secoiridoids (such as oleuropein and its derivatives, oleoside and its derivatives, and ligstroside), which were also associated with a strong modulatory effect on FRAP. In contrast, the Portuguese samples contained moderate levels of flavonoids (luteolin and its derivatives, apigenin and its derivatives, and isorhamnetin 3-O-β-D-(6-p-coumaroyl) glucoside), which might contribute to the FRAP value obtained for these samples.

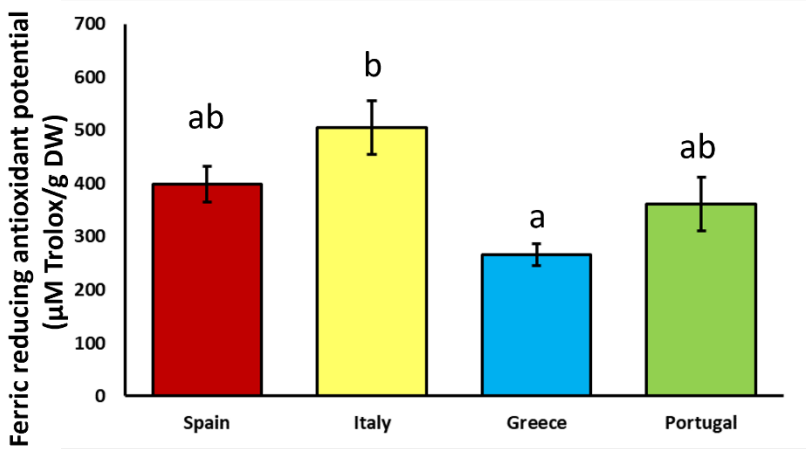

Figure 23. Ferric iron reducing potential (FRAP) exerted by OL extracts from Spain, Italy, Greece, and Portugal. Results are expressed as mean ± EEM. For each of the parameters, bars with different letters indicate statistically significant differences between countries ($p < 0.05$). OL: olive leaves.

Lastly, the Greek samples displayed the lowest FRAP values. In these samples, the aldehydic form of decarboxymethyl elenolic acid was found to be abundant and negatively correlated with the antioxidant

function. Additionally, the low phytochemical profile of the Greek samples could also partially explain the results obtained in the present study. Taken together, these findings suggest that the varying phytochemical compositions in the different samples produced by the geographical origin may account for the differences in their iron-reductive capacity effects.

CHAPTER VIII. Toxicological assessment of the olive leaf extracts in *C. elegans*

Olive leaves have been widely used as therapeutic tools throughout history [21]. In contrast to the classical belief that botanic related products are completely safe and lack toxicity, these products could cause several side effects and many of the chemical content remain uncharacterized. In addition, due to the easy access and low cost of these byproducts as well as the possibility of self-medication without medical advice for many people around the world, the study of OL related toxicity is mandatory. Therefore, in this section, the toxicity related to OL exposition was evaluated in *C. elegans*.

C. elegans has been described as an intermediate between *in vitro* and mammalian models. In fact, toxicity assays which evaluate endocrine, reproductory, neuromuscular and sensory systems performed in *C. elegans* consistently predicted toxicity scores in mammals [122]. Therefore, the use of *C. elegans* in toxicological area permit to generate a massive screening of many given compounds in a short lapse time.

8.1. Large-scale toxicological evaluation of olive leaf extracts

As a first approach to the *in vivo* effects of the OL extracts, different tests were used to evaluate the toxicity in *C. elegans*. First, short-term toxicity was evaluated by the 24h-lethality test. This test was made with three different concentrations (0, 500, and 1000 μg/ml) of OL extracts directly diluted in NGM. After 24 h of exposition, all the tested doses were found to be non-lethal for the exposed worms, with a survival percentage close to 100% at every dosage level (**Table 14**, 1000 μg/ml was not represented). These results align with those obtained by several authors who demonstrated the absence of lethality in OL extracts at similar doses proposed in this work [26,204]. Based on these results, a non-lethal submaximal concentration (500 μg/ml) for all OL extracts was selected for further experiments.

Table 14. Toxicological characterization of olive leaf extracts

	Origin	Lethality	Viability	Length	Width
Control	-	100 ± 0.164	100 ± 2.24	100 ± 0.74[b]	100 ± 3.23
SU01	Spain	101 ± 0.000	97.6 ± 4.9	110 ± 1.78[b]	105 ± 1.78
SU02	Spain	101 ± 0.000	116 ± 5.62	105 ± 2.02[b]	99.1 ± 1.53
SU03	Italy	101 ± 0.000	95.1 ± 7.56	103 ± 2.56[b]	105 ± 1.48
SU04	Portugal	101 ± 0.000	110 ± 6.03	99.2 ± 1.4[b]	98.5 ± 1.33
SU05	Spain	99.5 ± 1.12	111 ± 9.3	102 ± 1.11[b]	102 ± 1.12
SU06	Spain	99.2 ± 1.4	115 ± 10.8	106 ± 1.59[b]	104 ± 1.35
SU07	Spain	101 ± 0.000	116 ± 8.25	110 ± 1.36[c]	105 ± 1.58
SU08	Spain	101 ± 0.000	118 ± 8.31	114 ± 1.49[c]	101 ± 1.25
SU09	Spain	101 ± 0.000	124 ± 12	108 ± 1.94[c]	105 ± 1.77
SU10	Spain	99.5 ± 1.12	115 ± 7.49	108 ± 1.24[c]	97.8 ± 1.38
SU11	Greece	101 ± 0.000	109 ± 9.05	105 ± 0.91[b]	105 ± 1.37
SU12	Greece	101 ± 0.000	108 ± 5.73	103 ± 1.17[b]	108 ± 0.940
SU13	Greece	101 ± 0.000	103 ± 6.4	98.1 ± 1.58[b]	106 ± 1.11
SU14	Greece	99.9 ± 0.745	108 ± 5.42	99.3 ± 1.25[b]	107 ± 1.25
SU15	Greece	101 ± 0.000	115 ± 4.95	96.9 ± 2.94[b]	107 ± 1.20
SU16	Greece	101 ± 0.000	112 ± 5.99	95.7 ± 1.84[b]	109 ± 1.45
SU17	Greece	98.3 ± 1.32	110 ± 4.48	100 ± 2.75[b]	111 ± 1.60
SU18	Greece	100 ± 0.658	100 ± 4.45	99.4 ± 2.22[b]	112 ± 1.34
SU19	Portugal	101 ± 0.000	113 ± 4.84	95.3 ± 2.17[b]	112 ± 1.42
SU20	Portugal	101 ± 0.000	105 ± 7.09	91.2 ± 2.42[a]	109 ± 1.02
SU21	Portugal	98.8 ± 1.86	109 ± 6.28	77.7 ± 1.74[a]	110 ± 2.72
SU22	Portugal	101 ± 0.000	118 ± 6.66	81.2 ± 1.67[a]	108 ± 1.26
SU23	Portugal	101 ± 0.000	98.2 ± 8.03	85.8 ± 3.43[a]	109 ± 1.59
SU24	Portugal	98.9 ± 1.282	113 ± 9.29	88.0 ± 1.94[a]	110 ± 1.24
SU25	Portugal	98.3 ± 1.68	107 ± 4.7	80.7 ± 2.07[a]	109 ± 1.39
SU26	Portugal	98.8 ± 1.36	105 ± 9.26	90.0 ± 3.15[a]	116 ± 2.29
SU27	Spain	99.5 ± 1.12	112 ± 2.51	75.8 ± 2.22[a]	106 ± 2.07
SU28	Spain	101 ± 0.000	101 ± 9.09	84.5 ± 2.27[a]	114 ± 1.98
SU29	Spain	98.3 ± 1.68	104 ± 9.32	82.2 ± 2.78[a]	111 ± 1.77
SU30	Spain	96.6 ± 2.18	95.8 ± 4.26	85.8 ± 2.12[a]	106 ± 1.47
SU31	Spain	99.7 ± 0.972	99.1 ± 3.6	86.8 ± 3.14[a]	110 ± 14.5
SU32	Spain	97.3 ± 1.82	107 ± 4.95	87.6 ± 3.03[a]	101 ± 13.2
SU33	Spain	97.5 ± 2.23	105 ± 3.93	85.4 ± 2.08[a]	104 ± 13.8
SU34	Spain	98.4 ± 1.48	94.5 ± 8.14	85.9 ± 2.57[a]	107 ± 12.7
SU35	Spain	96 ± 1.99	102 ± 7.11	101 ± 2.33[b]	87.7 ± 2.18
SU36	Spain	97.5 ± 2.23	115 ± 2.82	73.3 ± 1.92[a]	93.4 ± 2.34
SU37	Spain	99.4 ± 0.828	100 ± 5.35	75.3 ± 2.14[a]	90.8 ± 2.96
SU38	Spain	96.1 ± 1.67	90 ± 13.1	85.6 ± 2.16[a]	89.1 ± 2.90
SU39	Spain	97.8 ± 1.25	110 ± 6.4	82.4 ± 2.95[a]	91.4 ± 2.60

SU40	Italy	101 ± 0.000	100 ± 8.56	95.9 ± 1.68[b]	94.4 ± 2.59
SU41	Spain	99.9 ± 0.745	103 ± 12.1	80.6 ± 2.13[a]	97 ± 1.15
SU42	Spain	101 ± 0.000	104 ± 8.52	93.3 ± 2.97[b]	98 ± 1.65
SU43	Spain	101 ± 0.000	126 ± 18.8	82.7 ± 2.87[a]	96.8 ± 2.30
SU44	Spain	101 ± 0.000	111 ± 7.88	75.9 ± 2.79[a]	91.1 ± 1.44
SU45	Spain	101 ± 0.000	110 ± 9.50	71.5 ± 2.79[a]	95.7 ± 1.17
SU46	Italy	101 ± 0.000	95.7 ± 9.43	87.4 ± 2.13[a]	98.9 ± 1.16
SU47	Italy	101 ± 0.000	93.1 ± 4.06	87.1 ± 2.89[a]	92.8 ± 2.08
SU48	Italy	100 ± 0.349	106 ± 8.99	94.1 ± 1.43[b]	101 ± 0.890
SU49	Morocco	101 ± 0.000	106 ± 5.51	76.7 ± 2.01[a]	92.9 ± 1.58
SU50	Italy	99.1 ± 1.08	113 ± 13.5	74.5 ± 2.52[a]	92.9 ± 1.67

Toxicological characterization of olive leaf extracts in the *C. elegans* N2-Wild type strain. All tests exposed were performed using 500 μg/ml. Results are mean ± SEM. For each parameter, different lowercase letters mean statistically significant differences ($p < 0.05$).

Then, the influence of OL extracts on the development and viability of embryos was also assessed. As shown in **Table 14**, OL extracts did not exert embryotoxicity at the assayed dose, showing that 500 μg/ml was a suitable dose for subsequent experiments. These results align with previous studies that found no embryotoxicity or even increased viability when using OL extracts at lower doses (100 and 400 μg/ml) as proposed in this work [26,144]. The influence of OL extracts on body size of *C. elegans* was also evaluated. In this context, 56% of the assayed extracts led to lower body length than control in the worms. Among them, 60.7% were from Spain, 25% from Portugal, 10.7% from Italy, and 3.6% from Morrocco. In contrast, only 8% of the extracts shown a higher body length of the nematodes when compared with control, and all these extracts were from Spain. These results are in contrast with those obtained by Romero-Márquez *et al.* [26], which showed that 100 μg/ml of OL extract enriched to 40% oleuropein did not alter the growth in worms. In the same line, Feng *et al.* [217] demonstrated that oleuropein might not be implicated in the reduction of body size observed, as pure oleuropein extract, in higher doses (0, 21.6, 97.2, 237.6 μg/ml) did not alter the body length.

8.2. Variable importance in projection score for body length

To evaluate the modulatory effect on growth of the individual phytochemical compounds present in OL extracts, a VIP score from PLS-DA was used. For this purpose, worms treated with OL extracts were separated into three groups: lower length, normal length, and higher length, concerning the effect obtained in the body length analysis. Next, the phytochemical compounds were matched with the specific growth effect, and PLS-DA was applied.

In this context, the VIP score suggests that luteolin (0.287 μg/ml) and oxidized quercetin (1.74×10^{-6} μg/ml) contents in the OL extracts may be the major factors responsible for the higher body size in this subpopulation. This finding aligns with a study by Xiao *et al.* [218] and Li *et al.* [219], which demonstrated that isolated luteolin (5.73 μg/ml) and oxidized quercetin (0.080 μg/ml) promotes the induction of DAF-2/DAF-16 insulin-like signaling pathway in *C. elegans*. DAF-16 serves as a central modulator of the insulin/insulin-like growth factor(IGF)-1 signaling (IIS) pathway, which is a conserved phosphorylation cascade that controls growth in *C. elegans* [220]. In contrast, OL extracts with low luteolin (0.102 μg/ml) and oxidized quercetin (0 μg/ml) contents led to worms with a lower body size, once again indicating the role of these compounds in modulating the observed effects on worm development (**Figure 24**). In the same way, apigenin derivative content seems to be responsible for a lower nematode growth through DAF-16 modulation [221]. Despite the results obtained in the VIP score, which associate numerous compounds such as decaffeoylverbascoside, and esculin content, among others, as potential growth modulators, no current evidence is available for comparison.

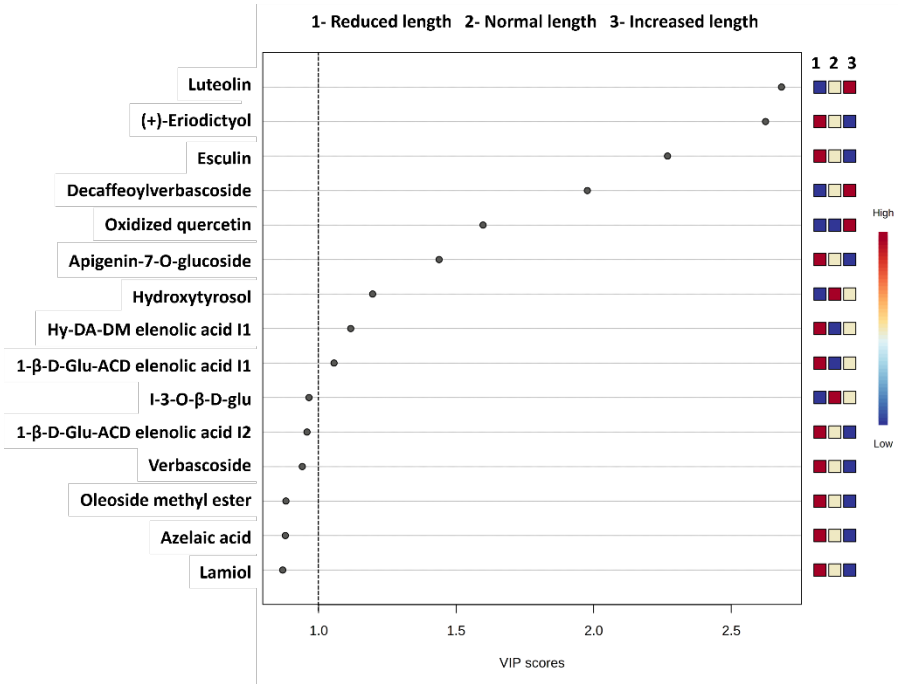

Figure 24. Variable importance in projection (VIP) score plots for the top 15 most important phytochemical compounds concerning body lenght by PLS-DA. The heatmap indicates the relative concentration of the specific compound in the different subpopulations and the dashed line means statistically significant at $p < 0.05$. Abbreviations: 1-β-D-Glu-ACD elenolic acid: 1-β-D-Glucopyranosyl acyclodihydroelenolic acid; Hy-DA-DM elenolic acid: hydroxylated product of the dialdehydic form of decarboxymethyl elenolic acid; I-3-O-β-D-glu: isorhamnetin 3-O-β-D-(6-p-coumaroyl) glucoside; I: isomer

Finally, no differences were observed in the width of worms exposed to 500 μg/ml of OL extracts. Overall, the absence of evident toxicity in the olive leaf extracts evaluated in the present study is of great interest concerning the potential biomedical applications of the extracts.

CHAPTER IX. Olive leaf extracts selection and phytochemical profile

9.1. Olive leaf extracts selection

Scientific literature explains that the numerous health effects of olive leaves such as anti-cancer [222], anti-viral [223], anti-inflammatory [224,225], and antioxidant [226] are associated with the phytochemical content. However, the role of olive leaves on AD is unclear. Therefore, the goal of this section was to select three olive leaf samples with different biomedical and phytochemical profiles. For this purpose, three categories were generated: the low category, the medium category, and the high category. The low category contained the samples that obtained the lowest scores for AChE IA, COX-2 IA, FRAP, TPC, and TFC. In the same way, the medium category contained the samples closest to the median of the population for each parameter, whereas the high category contained the samples with the highest activities in the tests. The flowchart of the protocol applied to select the OL extracts is represented in **Figure 25.** The first screening was conducted with the *in vitro* parameters of AD (AChE IA, COX-2 IA, and FRAP), with only the 10% of the samples selected for each category from the 50 samples. Then, duplicates were removed from the population, and a total of 34 samples (64%) were selected for the next step, comprising 10 (20%), 13 (26%), and 11 (22%) samples in the high, medium, and low categories, respectively. Subsequently, the samples selected were ordered concerning their phenolic and flavonoid contents, with only the top five samples selected from the highest and lowest values for each parameter in the high and low categories. Similarly, the five samples closest to the median of the population for TPC and TFC were selected. Again, duplicates were removed from the population, and 24 samples (46%) remaining, consisting of 6 (12%), 9 (18%), and 8 (16%) samples in the high, medium, and low categories, respectively (**Figure 25**). Given the absence of evidence toxicity in the OL extracts *in vivo*, these samples were selected for further analysis in the sample selection process.

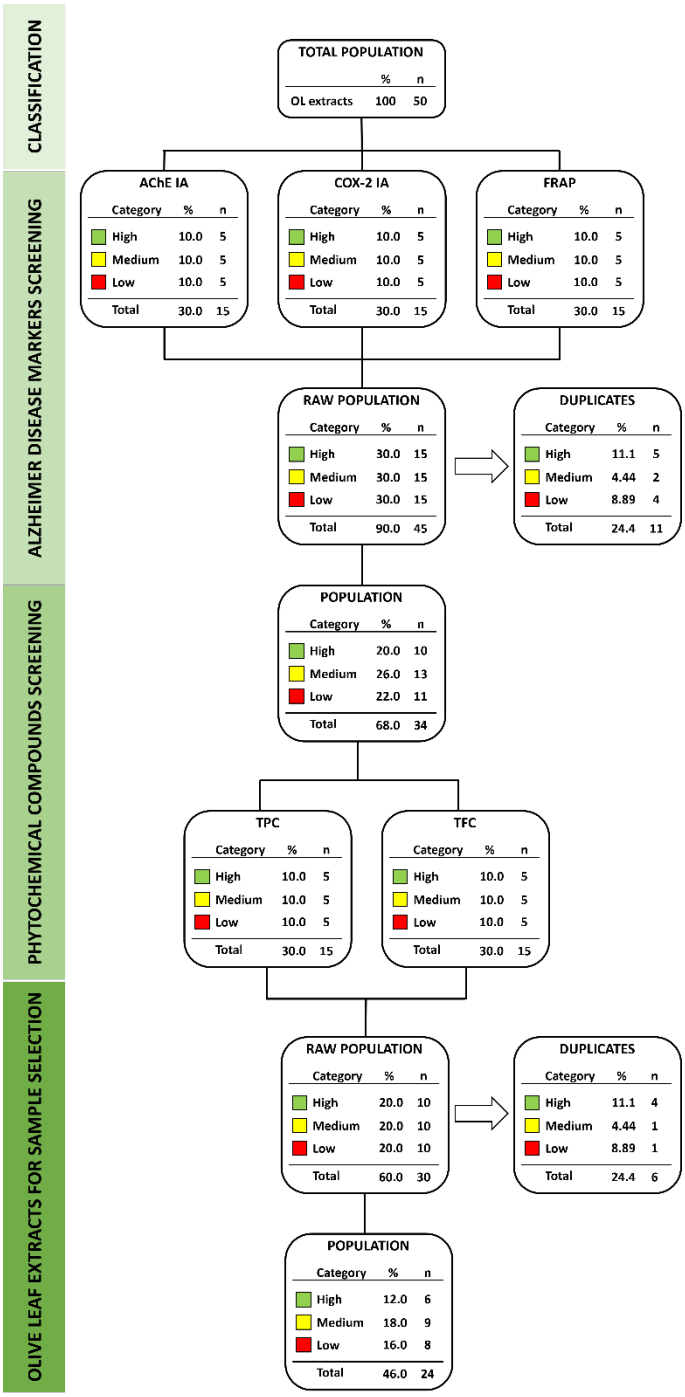

Figure 25. Flow chart for olive leaf extract selection for further analysis.

After sample screening, 24 OL extracts were identified for further analysis. Among these, 6 samples were selected from the high category, while 9 and 8 samples were chosen from the medium and low categories, respectively. The sample selection analysis involved ordering the OL extracts based on specific parameters (AChEI, COX-2, FRAP, TPC, and TFC) within each category. For the high category, the samples were ranked from high to low values, and numerical values from ten to the end of the category were assigned, starting with the highest. Conversely, the low category was ordered from low to high, and the ten score was assigned to the lowest. Lastly, the medium category was ordered, and the sample closest to the $\overline{X}$1-50 received a score of ten, while lower scores were assigned to samples farther from the median. Then, the values obtained in each parameter were summed and the average of this data was made for each sample to obtain the sample selection score in each category. Finally, one sample for each category was selected for further analysis. As can be seen in **Figure 26A**, the sample SU11, from Greece, was classified as the OL extract with the lowest biomedical activity and phytochemical content *in vitro*. In the same way, the sample SU42, from Spain, was considered as the OL extract with the biomedical activity and phytochemical content closer to the $\overline{X}$1-50 (**Figure 26B**). Finally, the SU04, from Portugal, was classified as the OL extract with the highest biomedical activity and phytochemical content *in vitro* (**Figure 26C**). Therefore, these three OL extracts, each with different phytochemical and biomedical properties *in vitro*, were selected to deep in the *in vitro* markers of AD and to evaluate their potential modulatory activity on numerous AD hallmarks in the experimental model *C. elegans*.

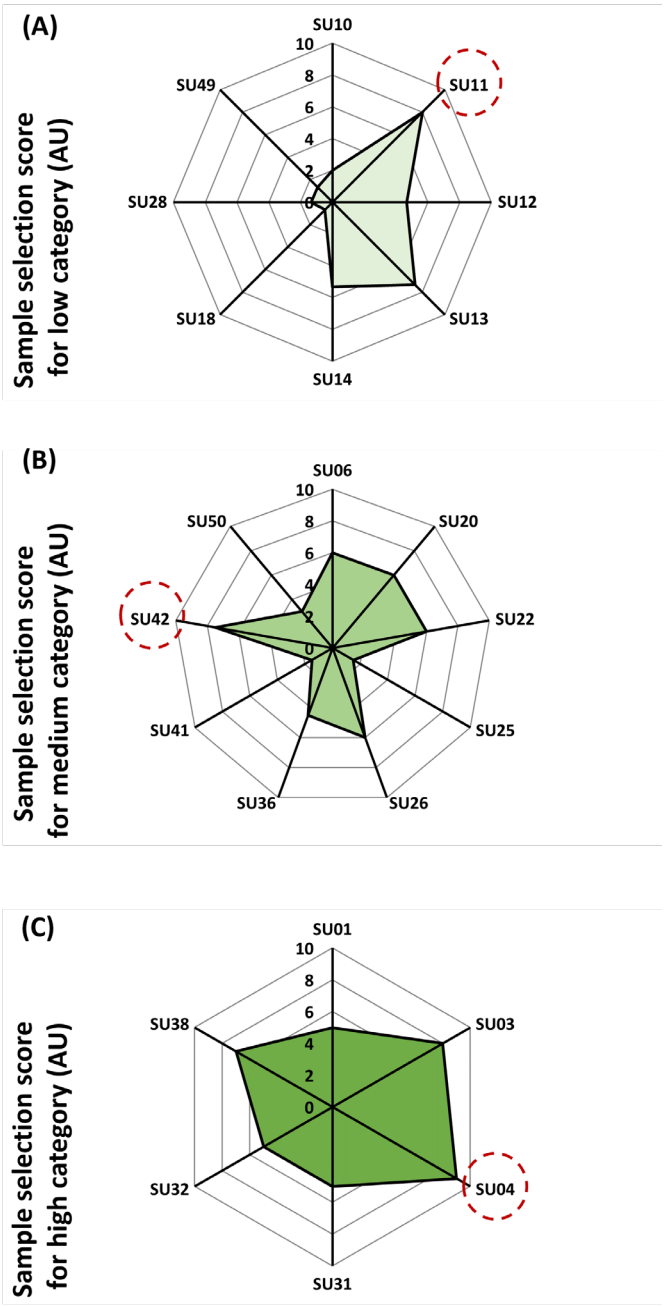

Figure 26. Radar chart for olive leaf extract selection in the low, mid, and high categories. (A) Olive leaf sample score in low category; (B) olive leaf sample score in medium category; (C) olive leaf sample score in high category.

9.2. Biomedical and phytochemical characterization of the three-olive leaf extracts

The effectiveness of the sample selection is evident in **Table 15**. Across the various tests conducted, the three OL extracts exhibited notable differences. High-OL extract displayed higher values in 85.7% of the applied tests compared to the $\overline{X}$1-50. Similarly, mid-OL extract showed similarities in 85.7% of cases with the $\overline{X}$1-50, while the low-OL extract yielded lower values in 57.1% of the tests conducted.

Table 15. *In vitro* characteristic of the three olive leaf extracts

	$\overline{X}$1-50	Low-OL	Mid-OL	High-OL
TPC	36.9 ± 6.15^{b}	30.7 ± 4.06^{b}	35.8 ± 4.3^{b}	47.6 ± 2.34^{c}
TFC	20.8 ± 13.5^{b}	8.22 ± 1.39^{a}	21.6 ± 2.79^{b}	38.6 ± 2.8^{c}
ABTS	490 ± 110^{b}	304 ± 76.9^{a}	575 ± 76.1^{c}	638 ± 44.2^{c}
DPPH	221 ± 15.8^{b}	161 ± 56.5^{b}	297 ± 38.3^{b}	227 ± 15.2^{b}
FRAP	382 ± 158^{b}	216 ± 22.4^{a}	342 ± 47.3^{b}	751 ± 103^{c}
AChE IA	33.3 ± 2.87^{b}	3.49 ± 2.88^{a}	29.7 ± 1.48^{b}	100 ± 0.940^{c}
COX-2 IA	25.6 ± 1.08^{b}	30.9 ± 1.46^{b}	30.2 ± 0.790^{b}	39.5 ± 2.78^{c}

Results are expressed as mean ± SD, except for AChE and COX-2 IA, which is expressed as mean ± EEM. For each determination, "a" means that samples are below the $\overline{X}$1-50, "b" means that samples are not different from $\overline{X}$1-50, and "c" means that samples are above the $\overline{X}$1-50 ($p < 0.05$). Abbreviatures: ABTS: 2,2'-azinobis [3-ethylbenzothiazoline-6-sulfonic acid]-diammonium salt; AChE IA: acetylcholinesterase inhibitory activity; COX-2 IA: cyclooxygenase-2 inhibitory activity; DPPH: 2,2-Diphenyl-1-Picrylhydrazyl; FRAP: ferric reducing antioxidant power; TFC: total flavonoid content; TPC: total phenolic content.

After OL extract selection process, the individual phytochemical characterization is presented in **Table 16.** As shown in **Table 16**, the low-OL extract contained only 7.1% of the secoiridoids studied, whereas the mid and high-OL extracts contained the 57.1% of the studied secoiridoids. Among the studied secoiridoids, the high-OL sample was source of oleuropein and oleoside and its derivatives, as well as ligstroside whereas the mid-OL extract had a secoiridoids content was mostly similar to that of $\overline{X}$1-50.

Table 16. Phytochemical compounds quantification of the three OL extracts

	$\overline{X}$1-50	Low-OL	Mid-OL	High-OL
Secoiridoids				
1-β-D-Glu-ACD EA I1	0.307 ± 0.203^{b}	-	0.621 ± 0.02^{c}	-
1-β-D-Glu-ACD EA I2	0.637 ± 0.560^{b}	-	0.197 ± 0.002^{a}	0.239 ± 0.007^{a}
A-DM EA	0.180 ± 0.278^{b}	-	0.374 ± 0.008^{c}	-
Hy-DA-DM EA I1	0.104 ± 0.119^{b}	-	0.153 ± 0.02^{c}	-
Hy-DA-DM EA I2	0.198 ± 0.346^{b}	0.05 ± 0.007^{a}	-	-
Hydroxyoleuropein	0.235 ± 0.448^{b}	-	0.220 ± 0.016^{b}	0.937 ± 0.05^{c}
Ligstroside	0.115 ± 0.292^{b}	-	-	0.910 ± 0.027^{c}
Oleoside	0.997 ± 1.85^{b}	-	0.187 ± 0.003^{a}	2.96 ± 0.088^{c}
Oleoside methyl ester	0.772 ± 1.28^{b}	-	0.597 ± 0.041^{b}	4.35 ± 0.125^{c}
Oleuropein	5.85 ± 14.0^{b}	-	1.80 ± 0.021^{a}	19.0 ± 0.891^{c}
Oleuropein diglu	0.060 ± 0.173^{b}	-	-	0.936 ± 0.08^{c}
Oleuropein I	0.555 ± 1.44^{b}	-	-	3.30 ± 0.082^{c}
Flavonoids				
(+)-Eriodictyol	0.082 ± 0.109^{b}	-	0.285 ± 0.007^{c}	0.011 ± 0.002^{a}
Apigenin	0.181 ± 0.223^{b}	0.024 ± 0.004^{a}	0.252 ± 0.001^{b}	-
Apigenin-7-O-glu	0.279 ± 0.210^{b}	-	0.431 ± 0.008^{c}	0.566 ± 0.001^{c}
Apigenin-7-O-rut	0.400 ± 0.222^{b}	-	0.733 ± 0.006^{c}	0.365 ± 0.014^{b}
Azelaic acid	0.574 ± 0.775^{b}	0.045 ± 0.001^{a}	1.156 ± 0.01^{c}	0.325 ± 0.003^{b}
Chrysoeriol-7-O-glu	0.547 ± 0.251^{b}	-	0.596 ± 0.01^{b}	0.956 ± 0.009^{c}
Diosmetin	0.226 ± 0.160^{b}	0.104 ± 0.002^{a}	0.257 ± 0.001^{b}	-
I-3-O-β-D-glu	0.028 ± 0.050^{b}	-	-	0.238 ± 0.012^{c}
Luteolin	0.291 ± 0.203^{b}	0.068 ± 0.001^{a}	0.12 ± 0.002^{a}	0.156 ± 0.008^{a}
Luteolin 7-O-glu	1.09 ± 1.10^{b}	-	0.657 ± 0.016^{a}	4.332 ± 0.107^{c}
Luteolin glu	3.81 ± 2.20^{b}	0.163 ± 0.001^{a}	6.99 ± 0.16^{c}	6.723 ± 0.076^{c}
Luteolin rut I2	0.018 ± 0.042^{b}	-	-	0.039 ± 0.008^{c}
Luteolin-7,4-O-diglu	0.084 ± 0.077^{b}	-	0.143 ± 0.00^{c}	0.171 ± 0.00^{c}
Phenolic alcohols				
Hydroxytyrosol	0.131 ± 0.13^{b}	-	0.056 ± 0.001^{a}	0.471 ± 0.031^{c}
Hydroxytyrosol glu	0.355 ± 0.515^{b}	-	0.058 ± 0.001^{a}	1.52 ± 0.007^{c}
4-Ethylguaiacol	0.094 ± 0.071^{b}	0.084 ± 0.005^{a}	0.073 ± 0^{a}	-
Iridoids				
Loganic acid	0.223 ± 0.101^{b}	0.017 ± 0.000^{a}	0.227 ± 0.005^{b}	0.411 ± 0.003^{c}
7-Epiloganin	0.667 ± 0.298^{b}	0.122 ± 0.005^{a}	0.944 ± 0.005^{c}	0.995 ± 0.006^{c}
Lamiol	0.778 ± 0.459^{b}	0.089 ± 0.000^{a}	1.12 ± 0.002^{c}	0.819 ± 0.017^{b}
Hydroxycoumarins				
Esculetin	0.179 ± 0.205^{b}	0.012 ± 0.001^{a}	0.148 ± 0.001^{b}	0.115 ± 0.002^{b}
Esculin	0.054 ± 0.049^{b}	-	0.091 ± 0.001^{c}	0.052 ± 0.001^{b}
Hydroxycinnamic acid				
Verbascoside	0.307 ± 0.408^{b}	0.043 ± 0.001^{a}	0.083 ± 0.002^{a}	0.545 ± 0.006^{c}
Decaffeoylverbascoside	1.17 ± 0.842^{b}	0.090 ± 0.004^{a}	1.21 ± 0.049^{b}	1.33 ± 0.018^{b}
Phenolic acids				
p-Hydroxybenzoic acid	0.037 ± 0.059^{b}	-	0.03 ± 0.001^{b}	0.415 ± 0.001^{c}
Other compounds				
Lauroside B	0.343 ± 0.329^{b}	-	0.418 ± 0.003^{b}	0.928 ± 0.025^{c}

Results are expressed as milligram of compound (mean ± SD) per gram of dry weight. Error is expressed in parts per million. For each compound, different letters between countries indicate statistically significant differences ($p < 0.05$). the symbol (-) was added when the specific compound was no detected. m/z: mass to charge ratio. Abbreviations: 1-β-D-Glu-ACD elenolic acid I1: 1-β-D-Glucopyranosyl acyclodihydroelenolic acid isomer 1; 1-β-D-Glu-ACD elenolic acid I2: 1-β-D-Glucopyranosyl acyclodihydroelenolic acid isomer 2; A-DM elenolic acid: aldehydic form of decarboxymethyl elenolic acid; D-OH elenolic acid I2: decarboxylated form of hydroxy elenolic acid isomer 2; glu: glucoside; H-DA-DM elenolic acid: hydrated product of the dialdehydic form of decarboxymethyl elenolic acid; Hy-DA-DM elenolic acid I1: hydroxylated product of the dialdehydic form of decarboxymethyl elenolic acid isomer 1; Hy-DA-DM elenolic acid I2: hydroxylated product of the dialdehydic form of decarboxymethyl elenolic acid isomer 2; OL: olive leaves; I: isomer; rut: rutinoside.

Concerning flavonoid contents, the low-OL extract contained only 31.3% of the flavonoids studied, whereas the mid and high-OL extracts contained the 68.8% of the studied flavonoids. It should be highlighted the differences between mid and high-OL extracts. Mid-OL extract was mostly source of apigenin derivatives whereas high OL-extract was mostly source of luteolin derivatives.

Among the other compounds with modulatory proved effects, the hydroxytyrosol, hydroxytyrosol glucoside, and verbascoside content were found to be higher than the $\overline{X}$1-50 in the high-OL extract. In contrast, these compounds were found to be lower than in the $\overline{X}$1-50 or even not detected in the mid and low-OL extracts.

Beyond the agronomical factors mentioned earlier that could account for the differences between extracts, it is important to highlight that the selection of these extracts was deliberate, aimed at achieving these phytochemical variations.

CHAPTER XI. Evaluation of Alzheimer's disease parameters

AD is a multifactorial neurodegenerative disease characterized by two histopathological events: the senile plaque aggregation formed by Aβ in the central nervous system and the formation of NFTs associated to the accumulation of tau protein in the hippocampus, neocortical area, and amygdale. These events are associated with an increase in cholinergic and mitochondrial dysfunction, oxidative stress, neuroinflammation and disturbances in the proteostasis network, which favor the appearance of senile plaques and NFTs, generating atrophy and neuron death characteristic of AD.

10.1. Cholinesterase and inflammatory half maximal inhibitory concentration of the three-olive leaf extracts *in vitro*

Part of the cholinergic hypothesis indicates that there exists a hyperactivity of AChE, favoring the degradation of ACh, and promoting that AD patients develop memory loss and other cognitive symptoms related to AD. As expected, and regarding OL samples, the lowest IC50 value was obtained by high-OL extract, indicating that it was the most effective extract to inhibit cholinesterase activity (**Table 17**). In contrast, the highest IC50 of cholinesterase inhibitory activity was obtained by the low-OL extract.

Table 17. IC50 for AChE inhibitory activity assay for olive leaf extracts

	IC50 (μg/ml)	R^2	Linear regression formula
Oleuropein	225	0.971	y = 3.7771x + 36.555
Hydroxytyrosol	50.6	0.986	y = 1.1012x – 4.4927
Luteolin-7-O-glu	50.7	0.949	y = 0.6644x + 17.497
Low-OL	6331	0.990	y = 135.6x – 448.66
Mid-OL	1444	0.994	y = 43.311x – 721.92
High-OL	1350	0.982	y = 35.49x – 424.69

Abbreviatures: glu: glucoside; IC50: half maximal inhibitory concentration; OL: olive leaves.

Taking into account the results obtained in VIP score regarding AChEI activity, some isolated compounds such as oleuropein, hydroxytyrosol, and luteolin-7-O-glucoside were also evaluated. In this context, isolated hydroxytyrosol and luteolin-7-O-glucoside demonstrated IC50 values 26.6 times lower than the high-OL extract, indicating a strong AChE inhibitory activity *in vitro*. These results are in accordance with the presented VIP score and with studies that evaluated the AChE inhibitory activity using isolated hydroxytyrosol or luteolin-7-O-glucoside [179,180,186,187]. On the other hand, oleuropein achieved a significant but low VIP score in the section 7.2.1. Similarly, a study indicated that oleuropein exerts a very low AChE IA *in vitro* [96]. This result was confirmed in the *in vitro* AChE IA test, with an IC50 only 6 times lower than that of the high-OL extract. These results could potentially account for the strong modulatory effect observed in the high-OL extract, considering it is the primary source of these compounds.

Concerning neuroinflammation, it has been found that COX-2 expression was increased in the brain of AD patients, which has been epidemiologically correlated with the severity of AD pathology in humans. As expected, the lowest IC50 value was obtained by high-OL extract, even lower than hydroxytyrosol alone, indicating that was the most effective extract to inhibit COX-2 activity (**Table 18**). Suppressively, the highest IC50 of cholinesterase inhibitory activity was obtained by the mid-OL extract.

Table 18. IC50 for COX-2 inhibitory activity assay for olive leaf extracts

	IC50 (μg/ml)	**R^2**	**Linear regression formula**
Oleuropein	8.38	0.938	y = 0.1843x + 0.837
Hydroxytyrosol	1.87	0.970	y = 0.0592x – 1.0586
Low-OL	2.32	0.986	y = 0.0549x - 0.4273
Mid-OL	2.81	0.960	y = 0.0666x - 0.5215
High-OL	1.72	0.981	y = 0.0562x - 1.0903

Abbreviatures: COX-2: cyclooxygenase-2; IC50: half maximal inhibitory concentration; OL: olive leaves.

In contrast to the presented VIP score (**Figure 17**), hydroxytyrosol exhibited a very low IC50 value for COX-2, indicating that this compound exerts robust COX-2 inhibitory activity *in vitro*, whereas the VIP score assigned no significant effect. Notwithstanding, the modulatory effect of COX-2 exerted by hydroxytyrosol is well described in cell lines [227,228] and rodents [207,229]. Similarly, the isolated oleuropein exhibited a higher IC50 value than the less effective OL, indicating that this compound exerts a low COX-2 inhibitory activity *in vitro*. However, the anti-inflammatory activity through COX-2 modulation of this compound is well described in rodents [194–198] and even in humans [199]. These data highlight a limitation of the present work. First, the multivariable analysis can predict variables of importance for further sample selection, but it cannot generate causal associations. However, the analysis permits the generation of a conceptual framework of the therapeutic effect of olive leaves. Similarly, despite the usefulness of *in vitro* tests to evaluate the anti-inflammatory properties of many samples, they avoid biological interactions and complexity within physiological systems. Therefore, studying the potential modulatory effect of the three extracts *in vivo* is mandatory.

10.2. Effect of the three-olive leaf extract in amyloid-β metabolism *in C. elegans*

The Aβ cascade hypothesis postulates that the abnormal deposition of $A\beta_{42}$ peptide in form of senile plaques in the central nervous system initiates the sequence of events that lead to classic symptoms of AD [230,231]. Therefore, alleviating Aβ accumulation has been considered one of the most promising therapeutic approaches for AD [232]. Hence, the potential modulatory effect of the three OL extracts was evaluated in *C. elegans* AD models.

Initially, the Aβ-induced toxicity tolerance test was done to determine the potential effect of the three OL extracts in counteracting the deleterious effect of the amyloidogenic pathology. For this purpose, the transgenic strains CL4176 and CL802 were employed. CL4176 is a temperature-sensitive strain that expresses the human amyloid $A\beta_{1-42}$ peptide in muscle cells. This expression and aggregation of the $A\beta_{1-42}$ peptide lead to a gradual impairment of movement in the worms, eventually resulting in paralysis [140]. Similarly, CL802 was used as a negative control (Aβ-) because it is genetically similar but does not express the human amyloid peptide. On the other hand, untreated CL4176 served as the positive control (Aβ+). As shown in **Figure 27**, the positive control (Aβ+) became paralyzed over time, while the negative control (Aβ-) remained unaffected.

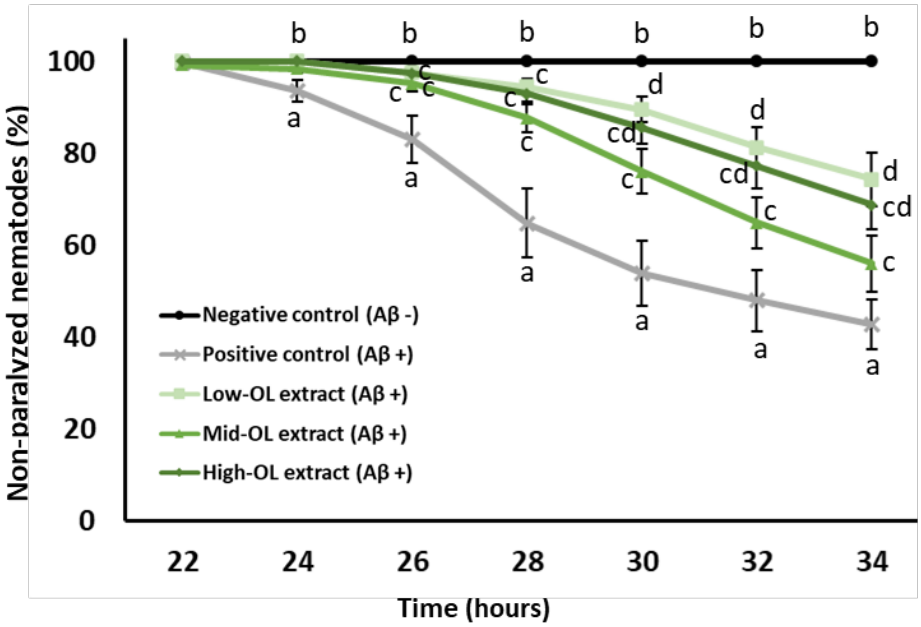

Figure 27. Effects of the three OL extracts at 500 μg/ml on the paralysis phenotype. Results are expressed as mean ± SEM. Abbreviatures: Aβ: amyloid-β; OL: olive leaves.

An interesting feature was observed concerning OL extracts: all the assayed samples demonstrated their effectiveness in delaying the amyloidogenic toxicity. However, an interesting, "inverted U-shape" tendence effect was observed in the modulatory activity exerted by the

OL extracts. The administration of 500 μg/ml of low-OL and high OL-extracts exerted a similar modulatory activity against Aβ toxicity, whereas the mid-OL extract exhibited the lowest protective effect. These results were supported by Thioflavin T staining. Thioflavin T staining can bind Aβ aggregates in form of fluorescent green shiny dots. As shown **Figure 28**, the negative control presented total absence of green dots. Conversely, the positive control contained numerous Aβ aggregates in consequence of amyloidogenic pathology progression. As mentioned, the "inverted U-shape" tendence effect was also corroborated in the staining. The Aβ aggregates were more relatable in the mid-OL extract, whereas the two extremes presented the lowest or even absence of accumulation. These results indicate that the anti-amyloidogenic toxicity activity exerted by the OL extracts was mediated through the reduction of Aβ aggregation in the treated nematodes. These results are in accordance with those authors who demonstrated that numerous olive by-products are able to reduce amyloidogenic-induced toxicity through Aβ aggregation in *C. elegans* [26,204]. As expected, the lowest Aβ aggregation was observed in the high-OL extract. This effect might be attributed to elevated oleuropein content in high-OL extract, which is shown to reduce, Aβ aggregation *in vitro* and in *C. elegans* [64,233,234].

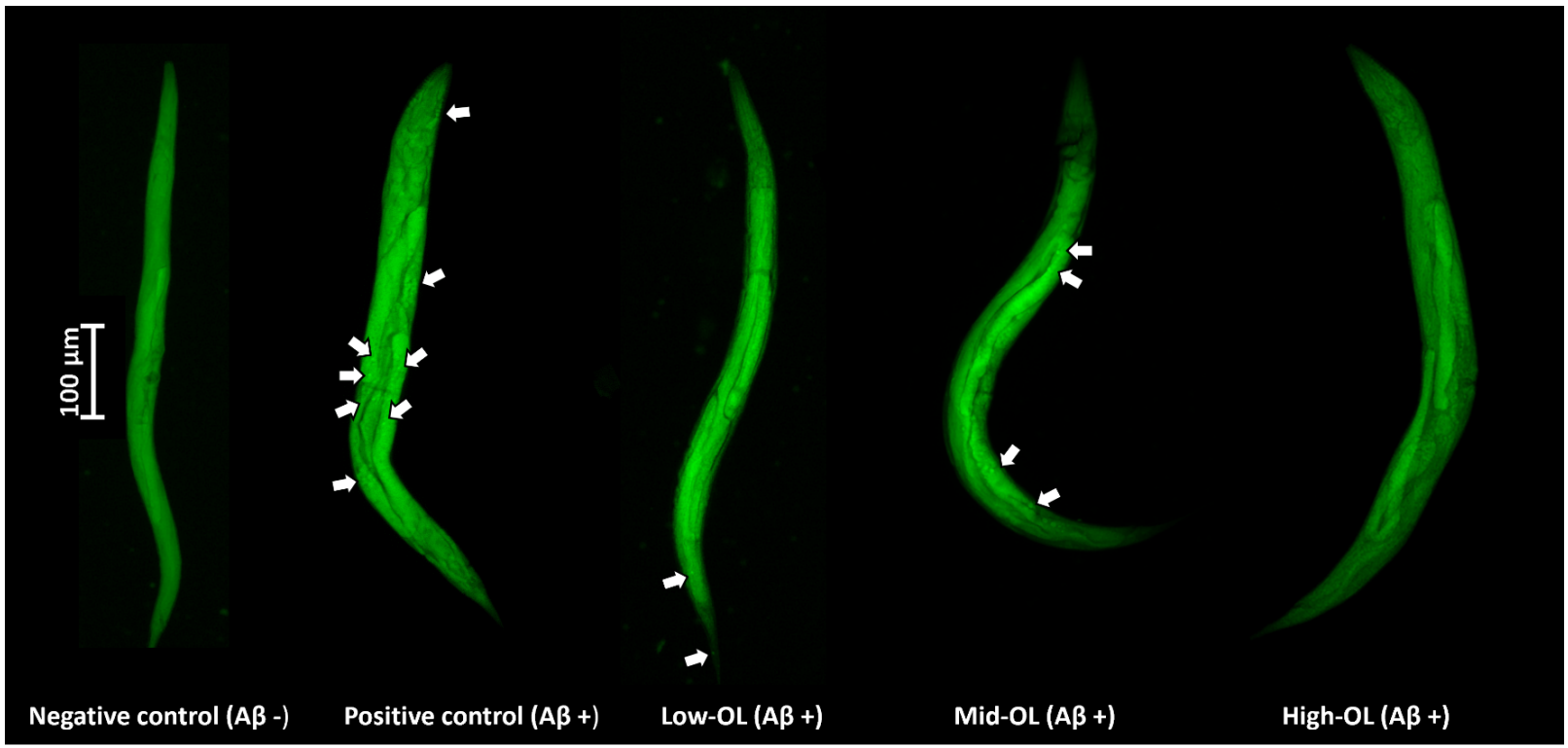

Figure 28. Representative images of the thioflavin T staining in CL4176 and CL802 nematodes collected 28 h after the temperature upshift. Pictures were taken at 10X magnification. White arrow shows the Aβ aggregated. Abbreviations: Aβ: amyloid-β; OL: olive leaves.

Despite the relatively low content of phytochemicals in the low-OL extract, the values of TPC and TFC suggest the presence of compounds that could not be identified or quantified using the HPLC-ESI-QTOF-MS/MSTIC method. In fact, the total quantified phytochemicals amounted only to 0.911 mg/g, whereas TFC (8.22 mg/g of DW) and TPC (30.7 mg/g of DW) were approximately eight- and thirty-fold higher, respectively.

A plausible hypothesis is that the modulatory effect exerted by OL extracts might be attributed, at least in part, to the overall phytochemical content. In this scenario, once the OL extract attains a therapeutical phytochemical content, the individual contributions could take a secondary role in the general effect. It becomes plausible that olive biophenols synergistically collaborate to combat amyloidogenic toxicity *in vivo,* as previously demonstrated both *in vitro* and *in vivo* [235]. Building upon this foundation, it has been observed that as the total amount of phytochemical compounds increases in the extracts, the effectiveness against amyloid-induced toxicity of the treatments did not increase. Different epidemiological studies demonstrated that once an optimal therapeutic phytochemical intake is achieved, no further benefits are observed at histological levels [236–239]. Indeed, when the intake of phytochemical rich plant-based food is adjusted in the regression analysis, amyloid imaging biomarkers have been shown to be modulated in this manner [240].

According to the literature, the entirety of studies that evaluated the effectiveness of olive by-products in AD employed a single dose of the same sample [26,204,241]. Notably, two studies evaluated the protective role of 40% O-OL and 20% H-OF extracts in a *C. elegans* model of AD [26,204]. In both studies, the same dose of extracts was applied (100 μg/ml), revealing a similar strong modulatory effect of these olive by-products against amyloidogenic toxicity in *C. elegans*. Interestingly, despite the individual phytochemical content was different, the TPC in the experimental medium for 40% O-OL (21 μg) and 20% H-OF (20 μg)

extracts exhibited similarity. These results strongly support the hypothesis that one of the major contributors to avoid the amyloidogenic toxicity in *C. elegans* is the total phytochemical content, probably, due a synergic effect between compounds. Notwithstanding, this hypothesis does not explain completely the decrease in effectiveness in the therapeutic effect of mid-OL extract compared with low OL extract.

Another potential explanation could involve the hormetic effect. Numerous authors have proposed that olive biophenols might manifest their health benefits through mild-induced stress [242–245]. Hormesis pertains to the advantageous stimulation at low doses by an environmental agent or exposure to an external stressor that is harmful at higher doses [246]. The three OL extracts might trigger their therapeutic effects via mild stress-induced hormesis. This hypothesis finds support in numerous studies which poses that the gerontoprotective effect of olive by-products or its biophenols might be linked to the hormetic response in different *C. elegans* models [26,144,204,217,244]. The theoretical graph depicting the hormesis response is often described as a perfect "U-shape" or "inverted U-shape" in terms of dose-response effects. However, numerous biological models have shown that the hormetic response can manifest as peaks and dips before reaching the maximum hormetic effect, ultimately forming a "U" or "inverted U-shape", as proposed in this study [247]. Thus, the combination of both mentioned hypotheses could indicate that the phenolic content may be sufficient to induce mild hormetic stress, while the individual phytochemical content may play a role in influencing the molecular pathways involved in the observed variations in this specific *C. elegans* strain at the tested doses.

To elucidate putative mechanisms underlying the effects of three OL extracts concerning the inhibition of the Aβ peptide formation, RNAi technology was applied. The role of DAF-16, which is the homolog of the mammalian FOXO in *C. elegans* was investigated. In mammalian cells, FOXOs' functions include cell cycle regulation at various key checkpoints, apoptosis, repair of damaged DNA, and the regulation of glucose

metabolism. In particular, DAF-16/FOXO acts through the canonical transcriptional target of IIS with an important performance in the regulation of Aβ aggregation [220,248]. In the same way, the role of SKN-1, which is the homolog of the mammalian NRF-2 in *C. elegans* was investigated. The NRF-2 is a transcription factor responsible for the regulation of cellular redox balance and protective antioxidant and phase II detoxification responses in mammals. Also, SKN-1/NRF-2 is involved in xenobiotic and oxidative stress responses which is critical in early pathogenic processes in AD [249]. Among the downstream targets, some genes were also evaluated due to involvement in the antioxidant system (SOD-2 and SOD-3) and the important role in the degradation of misfolded proteins (HSP-16.2) [220]. In this context, CL4176 worms treated with OL extracts were exposed to RNAi clones for DAF-16/FOXO, SKN-1/NRF-2, SOD-2, SOD-3 and HSP-16.2 under the same experimental conditions as mentioned in the paralysis assay.

Concerning low-OL extract, the nematodes knocked out of SOD-3 gene revealed the influence of this gene in the therapeutic effect exerted by the extract (**Figure 29A**). SOD-3 encodes auxiliary and inducible manganese SOD (MnSOD) mitochondrial isoforms, which have been related to a reduction in Aβ plaque deposition [250]. In fact, some researchers have proved that SOD-3 overexpression is involved in the mild stress response in *C. elegans* [144,204,251,252].

On the other hand, the nematodes knocked out of HSP-16.2 gene revealed the influence of this gene in the therapeutic effect exerted by the extract mid-OL extract (**Figure 29B**). HSP-16.2 has been shown to interfere directly with Aβ oligomerization pathways which leads a reduction in Aβ toxic species formation in *C. elegans* [26,204,253,254]. Some researchers have proved that overexpression of HSP-16.2 are involved in the mild-stress response in *C. elegans* [251,252,255,256]. In fact, the plausible hormetic effect of an olive pulp enriched in hydroxytyrosol (6%) has been previously proposed by Di Rosa *et al.* [245] in a *C. elegans* model of Parkinson's disease.

The most intriguing outcomes emerged from the high-OL extract treatment. Here, the SKN-1/NRF-2 pathway was involved in the protective effect of the high-OL extract (**Figure 29C**). This can be associated with SKN-1/NRF-2 activation, which has been shown to decrease Aβ aggregation levels and toxicity [98]. Curiously, when their direct downstream, SOD-2 and SOD-3 genes were knocked out, an increase of the effectiveness of high-OL extract was observed. These results might be attributed to an overcompensation of the SOD network mediated by the high-OL extract modulation of SKN-1/NRF-2. In this context, SKN-1/NRF-2 encode both SOD-2 and SOD-3 gene expression. SOD-2 encodes the major MnSOD mitochondrial isoforms whereas SOD-3 encodes auxiliary and inducible ones in *C. elegans*. When SOD-2 is knocked out, there exists an overcompensation of SOD-3 production and *vice versa* [257]. This heightened production of SOD enzymes contributes to the improvement of the therapeutic effect induced by the high-OL extract, which has been related to a reduction of AD markers in rodents [258,259] and in *C. elegans* [26]. Interestingly, this effect may suggest a mitohormetic effect, as the mild stress induced by the high-OL extract could potentially prime the ARE system for SOD overcompensation when MnSODs were knocked out. In the same way, when HSP-16.2 was knocked down, the effectiveness of high-OL was enhanced. This effect might be attributed to the intimal interaction between HSP-16.2 and ARE system in stress situations [255,256]. To mention, the treatment with *Ginko biloba* reduced the intracellular ROS content and increased the survival rate under oxidative stress condition, through the downregulation of HSP-16.2 expression, probably, due an enhancement of the ARE system [255,256]. These results might explain the relation between the observed effect in the RNAi experiments concerning high-OL extract.

As observed in the results, the low-OL extract showed dependency of SOD-3 while high-OL extract relied on the SKN-1/NRF-2 pathway, respectively. These results are particularly interesting due indicates that the low-OL and high-OL extracts promotes protective

effects against amyloidogenic toxicity through ARE system modulation but at different levels. In low-OL extract, the individual inhibition of DAF-16/FOXO and SKN-1/NRF-2 did not alter the effectiveness of the extract, this may be attributed due both MnSOD target enzymes present shared encoding with both transcription factors. In contrast, the inhibition of SKN-1/NRF-2 generated the total abolishment of the effectiveness of high-OL extract. Conversely, the individual inhibition of both MnSODs seems to enhance the effect of high-OL extract, which suggests that its action is predominantly mediated through the modulation of the ARE system, particularly at the mitochondrial level, as elucidated by the RNAi experiments. This effect might be attributed to the high content of secoiridoids present in the extract. These compounds have been shown to induce mitohormetic effects by upregulating the SKN-1/NRF-2 signaling pathway and modulating mitochondrial function in *C. elegans* [244,260]. These results hold significant interest as mitohormesis has been proposed as promising strategy to fight neurodegenerative diseases [261].

On the other hand, the mid-OL extract exhibited a protective effect through the modulation of the proteostasis network. This may be attributed also to their specific composition. Notably, the mid-OL extract, with its high content of apigenin derivatives, has been shown to enhance DAF-16/FOXO translocation and subsequently induce HSP-16.2 in *C. elegans* [262]. Interestingly, the abolishment of DAF-16/FOXO by RNAi did not alter the effectiveness of the extract through HSP-16.2 downregulation. This is attributed due HSP-16.2 present a shared encoding with heat shock factor (HSF)-1 [263]. Curiously, the induction of DAF-16/FOXO and HSP-16.2 by the mid-OL extract, along with their subsequent protective effects, could be attributed to a potential side effect. This could be related to the fact that high concentrations of isolated apigenin derivatives have been shown to exhibit non-lethal toxic effects through DAF-16/FOXO/HSP-16.2 modulation on *C. elegans* [221]. These results are in accordance with those obtained in the VIP score of toxicological assessment concerning the body size analysis in the section 8.2. Thus, the exposition of low doses of apigenin present in mid-OL

extract may promote the activation of proteostasis network and exert its amyloid-induced toxicity inhibitory activity through the response to mild-induced stress. Although the differences in the composition of each extract, these results hold significant interest as they may confirm the potential hormetic effect exerted by the OL extracts in delaying the progression of amyloidogenic pathology the assayed.

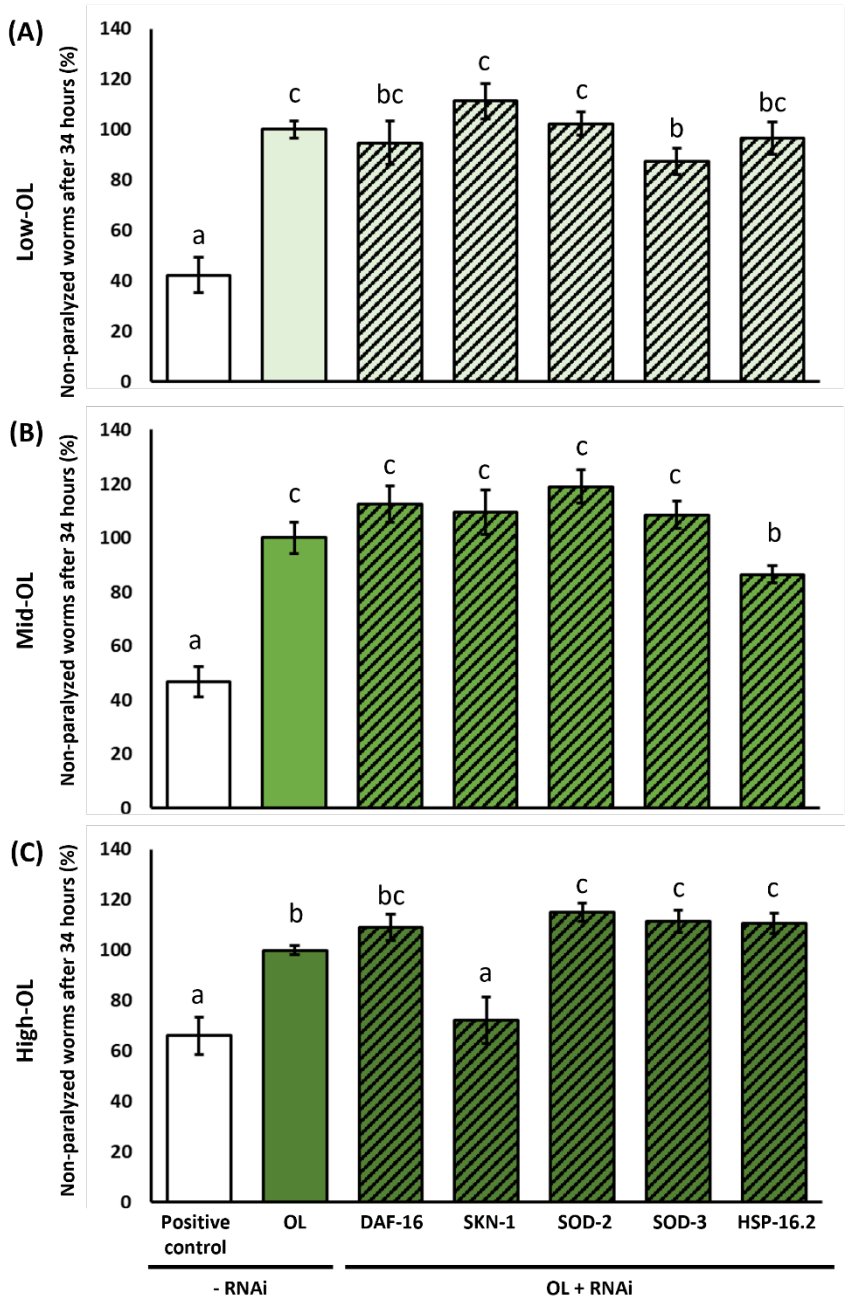

Figure 29. Effects of the three OL extracts at 500 μg/ml on the paralysis phenotype and the influence of the different RNAi (DAF-16, SKN-1, SOD-2, SOD-3, and HSP-16.2) in the transgenic strain CL4176 at 34 h after the temperature upshift. (A) Low-OL extract; (B) mid-OL extract; (C) high-OL extract. Different letters mean statistically significant differences ($p < 0.05$). Results are expressed as mean ± SEM. Abbreviatures: OL: olive leaves.

10.3. Effect of the three-olive leaf extract in hyperphosphorylated tau protein metabolism

In AD brain tau is three to four-fold more hyperphosphorylated than the normal adult brain tau. The cytosolic abnormally hyperphosphorylated tau in AD brain is distinguished by its ability to disrupt microtubules and forming NFTs. Therefore, the inhibition of abnormal hyperphosphorylation of tau offers a promising therapeutic target for AD and related tauopathies [264].

For this purpose, the *C. elegans* strain BR5706 was used. BR5706 present a constitutive pan-neuronal expression of pro-aggregative human tau protein which results in locomotion defects. Depending on the growth media, *C. elegans* can crawl, burrow, and swim [265]. Here, animals were forced to swim to stimulate the movement and the effects of the three OL extracts on tau-induced neurotoxicity impairment were evaluated. The activity index and swimming speed were chosen as representative parameters. According to the Wormlab software used in this study, activity represents the brush stroke normalized by the time taken to perform the two strokes, whereas swimming speed refers to the distance covered by the worm along its central axis over a two-stroke interval.

As illustrated in **Figure 30A** and **30B**, both the low and high OL-extracts exhibited the ability to mitigate the neurotoxicity associated with hyperphosphorylated tau protein aggregation, as indicated by the two studied parameters, in a similar manner. In contrast, mid-OL extract did not alter the activity rate. The similar therapeutic effects of the low and high-OL extracts, strongly supports the aforementioned hypothesis suggesting that the modulatory effect of OL extracts could be attributed partially to the overall phytochemical content.

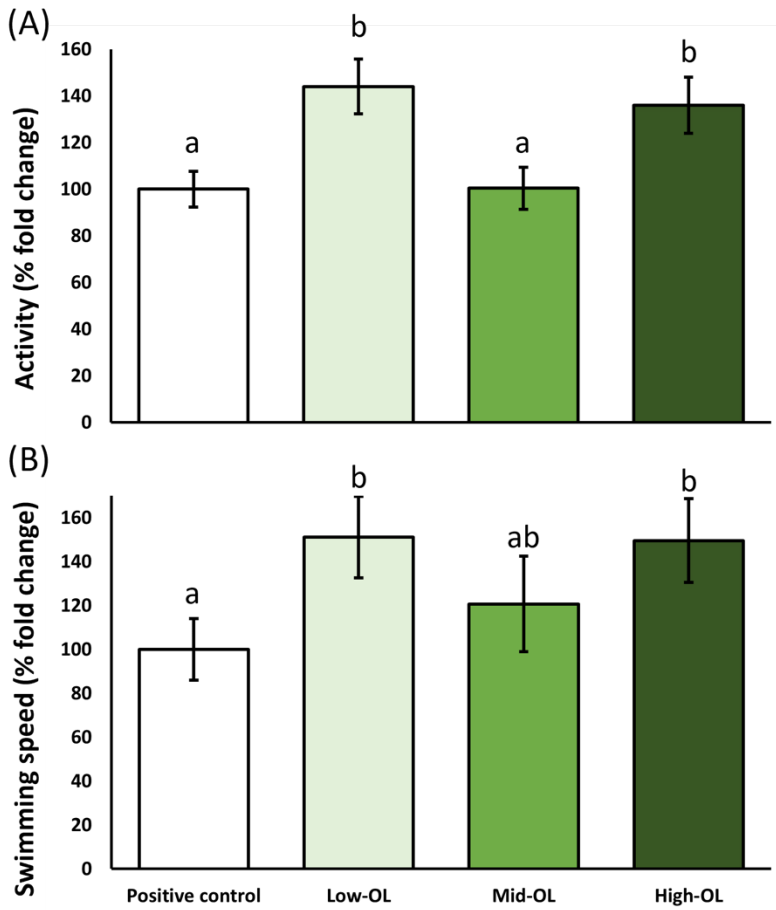

Figure 30. Effects of the three OL extract at 500 μg/ml on locomotive parameters in the transgenic strain BR5706. (A) Activity index; (B) swimming speed. Different letters mean statistically significant differences ($p < 0.05$). Results are expressed as mean ± SEM. Abbreviatures: OL: olive leaves.

However, the results obtained from mid-OL extract treated worms introduce discrepancies about this hypothesis in this specific strain. It should be noted that BR5706 is recognized for its heightened sensitivity to environmental variations, including NGM enrichment in treatments, in contrast to other strains like the Wild-type N2 or even CL4176 [145,266]. In this strain, treatment with mid-OL extract induced a slight toxicity, leading to a reduction in the growth of the exposed nematodes (**Figure Annex 1**). It's noteworthy that mid-OL extract is source of eriodictyol, esculin, and apigenin-7-O-glucoside, which were associated with reduced growth according to the VIP score in the toxicological assessment in section 8.2. As mentioned before, higher concentrations of apigenin resulted in a stress response in *C. elegans*, leading to the inhibition of larval growth [221]. In the same way, Tiwari *et al.* [267] demonstrated that growth impairment is also associated with locomotive alterations in *C. elegans*. Consequently, the potential modulatory effect of this extract might be obscured by the heightened sensitivity of this strain to the stress-induced by apigenin content, as it has been reported previously in other matrices with their specific components [145,266]. In fact, a slight tendence to improve the swimming speed was observed in the mid-OL extract worms, although it was not significative.

On the other hand, the plausible hormetic response of some compounds, including OL extract, has been also described through the regulation of SKN-/NRF-2/ARE [26,100,268] and small chaperones [26,269] in tauopathies. Therefore, to elucidate the mechanisms underlying the effects of two effective OL extracts, RNAi technology was applied.

As shown in Figure **31A** and **31B**, the nematodes treated with the low-OL extract and exposed to bacteria containing DAF-16/FOXO, SKN-1/NRF-2, and HSP-16.2 RNAi exhibited a complete abolition of the therapeutic effect of the extract, bringing the effects back to the levels observed in the positive control. DAF-16/FOXO and SKN-1/NRF-2 are

well-known transcription factors involved in the antioxidant, xenobiotic, and stress response, so inhibiting those master regulators could also block some downstream target genes such as SOD or HPS-16.2 that have an important role in tauopathies in *C. elegans* [249]. Therefore, the results presented in this section are in accordance with those studies who proposed the hormetic effect of OL in the treatment of tauopathies through the ARE system and chaperones modulation. Curiously, the role of SOD-2, the major mitochondrial isoform in *C. elegans*, in the therapeutic effect of low-OL extract is less clear.

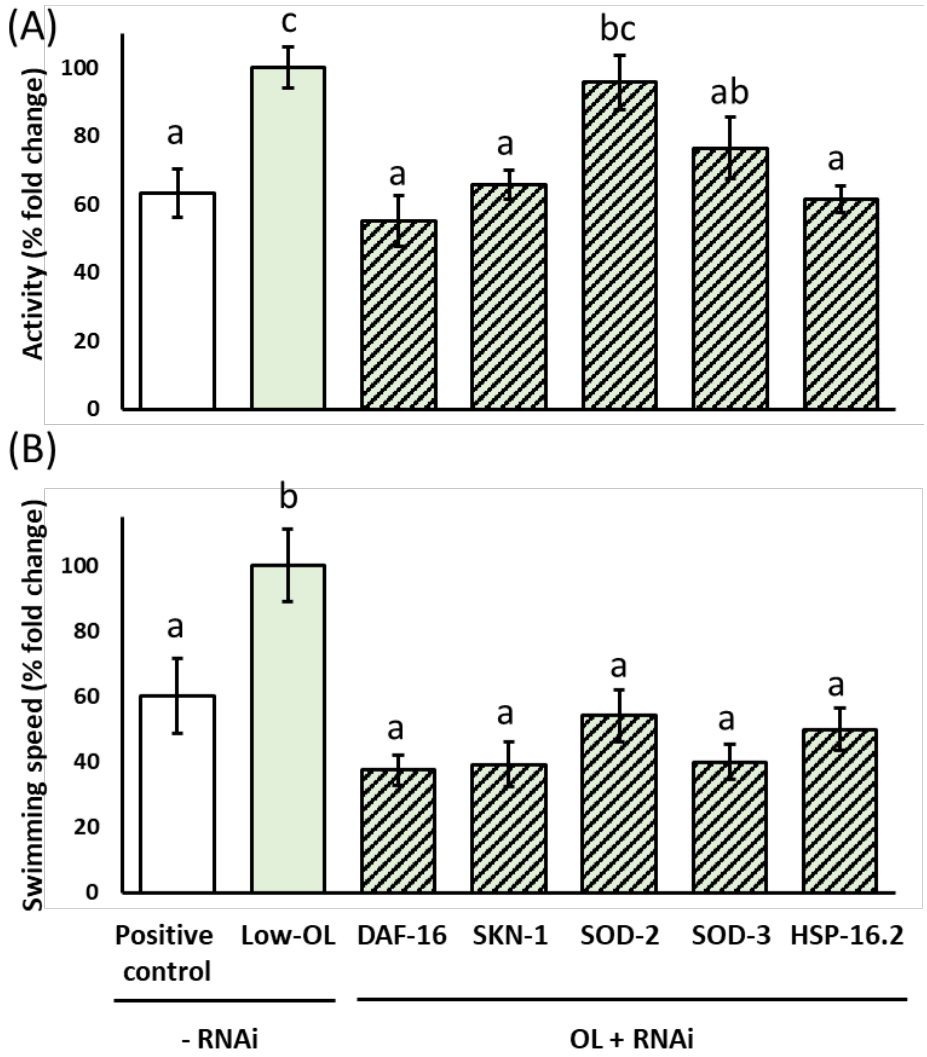

Figure 31. Effects of the low-OL extract at 500 μg/ml on locomotive parameters in the transgenic strain BR5706 and the influence of the different RNAi (DAF-16, SKN-1, SOD-2, SOD-3, and HSP-16.2). (A) Activity index; (B) swimming speed. Different letters mean statistically significant differences ($p < 0.05$). Results are expressed as mean ± SEM. Abbreviatures: OL: olive leaves.

On the other hand, the nematodes treated with the high-OL extract and exposed to bacteria containing the RNAi for DAF-16/FOXO and SKN-1/NRF-2 genes not only exhibited a complete abolition of the therapeutic effect of the extract, even received lower activity and swimming speed than the positive control (**Figure 32A** and **32B**). These findings are highly intriguing as they reveal that the high-OL extract may also induce a hormetic response in this particular strain. Prolonged exposure to hormetic substances stimulates the enhancement of defense mechanisms. When the promoter genes are knocked out, the capacity to respond diminishes entirely, as evident in the cases of DAF-16/FOXO and SKN-1/NRF-2. Similarly, the significance of SOD-2 becomes more pronounced in relation to the low-OL extract, owing to the heightened importance of the ARE system. Interestingly, in contrast to the results obtained in the amyloidogenic strain, the inhibition of both SOD genes did not enhance the effectiveness of the treatment. This observation could be attributed to the fact that DAF-16/FOXO and SKN-1/NRF-2 encode numerous genes associated with the ARE system, which collectively contribute to antioxidant defense or, maybe, directly through the free radical scavenging activity of the extract in this strain. Notably, as the phenolic content increases, the role of chaperones becomes less clear, underscoring the involvement of the ARE system in the effect of high-OL extract.

The evidence regarding the role of olive by-products in counteracting the effects of tauopathy diseases is limited. Notably, two studies assessed the protective role of 40% O-OL and 20% H-OF extracts in a *C. elegans* model of tauopathy [26,204]. In both studies, the same dose of extracts (100 μg/ml) was administered, revealing a similar therapeutic effect of these olive by-products, as measured by the swimming speed in the same *C. elegans* strain. However, only the 40% O-OL extract studied the mechanisms beyond the therapeutic effects. In this work, authors demonstrated that protective effect of 40% O-OL extract was strongly modulated by DAF-16/FOXO, SKN-1/NRF-2, and HSP-16.2. Interestingly, the authors proposed that the mitochondrial modulation exerted by the

SOD-2 enzyme played a key role in the effectiveness of the extract [26]. Both 40% O-OL and high-OL extracts have in common the high content in secoiridoids and phenolic acids, which have been shown to have mitohormetic effects by upregulating the SKN-1/NRF-2 signaling pathway and modulating mitochondrial function in *C. elegans* [26,244,260]. In particular, the content of some individual compounds present in high-OL extract such as oleuropein derivatives (12 μg/ml) and hydroxytyrosol derivatives (1 μg/ml) content has shown to interfere *in vitro* with tau fibrillization and aggregation at a very low dosage (5.4 and 3.1 μg/ml, respectively) resulting in a reduction of tau toxicity [66]. These results hold a significant interest as mitohormesis has been proposed as promising strategy to counteract neurodegeneration [261].

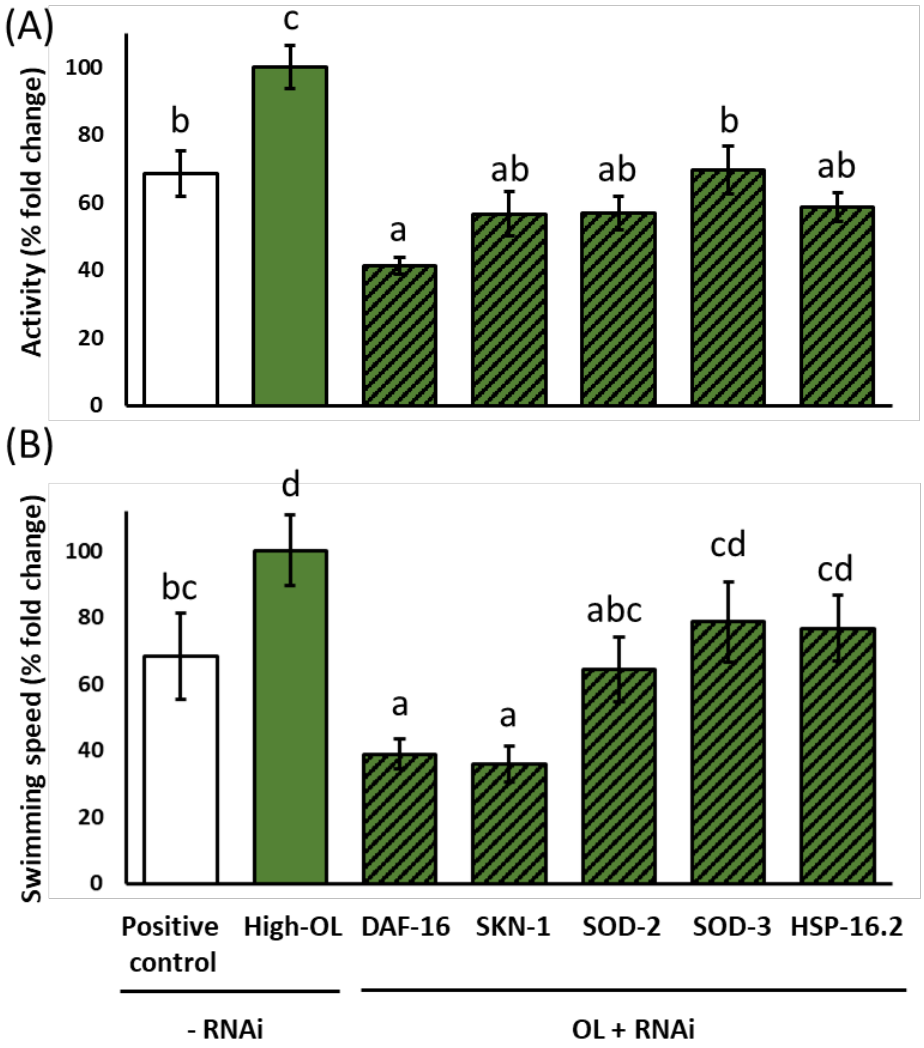

Figure 32. Effects of the high-OL extract at 500 μg/ml on locomotive parameters in the transgenic strain BR5706 and the influence of the different RNAi (DAF-16, SKN-1, SOD-2, SOD-3, and HSP-16.2). (A) Activity index; (B) swimming speed. Different letters mean statistically significant differences ($p < 0.05$). Results are expressed as mean ± SEM. Abbreviatures: OL: olive leaves.

CHAPTER XI. Effect of the three-olive leaf extracts on redox biology and proteostasis network in *C. elegans*

The reduction oxidation (redox) biology depends on the balance between prooxidants and antioxidants. Numerous prooxidant agents has been identified such as ROS, RNS, and oxidized biomolecules, among others. The highest intracellular generator of ROS is the mitochondrial electron transport chain [270]. To offset the ROS elevation, numerous enzymatic (SOD, CAT, GSH-PXs, GSH reductases, thioredoxines, peroxiredoxines, and glutharedoxines) and non-enzymatic (GSH, α tocopherol, ascorbate, coenzyme Q, and carotenoids) antioxidants form part in the antioxidant defense. These systems rely on the presence of cellular redox pairs (such as $NADP^+$/NADPH, NAD^+/NADH, and GSH/GSSG) that play a pivotal role in cellular electron transfer, facilitating the neutralization of ROS [271]. Nevertheless, an excessive accumulation of ROS leads to oxidative stress. Oxidative stress is characterized for the excessive production of free radicals and/or the failure of the endogenous antioxidant defense system to control them. Free radicals, are atoms or molecules (chemical species) possessing one or more unpaired electrons in their outer orbit or valence shell, rendering them exceedingly reactive. Due to its high reactivity, the altered production of ROS or RNS can lead to cumulative oxidative damage in macromolecules such as nucleic acids, proteins and lipids that can alter the cell signaling and cause anormal function or its death [272].

On the other hand, the proteostasis network serves to ensure that correctly folded proteins are generated at the right time and cellular location. Additionally, it prevents proteins from misfolding and aggregating. Beyond regulation of folding, the proteostasis network also ensures that superfluous and misfolded protein species are removed, either by autophagy or by degradation mediated by the proteasome. Together, these mechanisms avoid the accumulation of protein aggregates, which are potentially toxic. Proteostasis can be disturbed by

numerous pathological conditions related to aging such as neurodegenerative diseases, inflammation, and oxidative stress [273].

11.1. Effect of the three-olive leaf extracts on components of the antioxidant and proteostasis network in *C. elegans*

11.1.1. Effect on proteostasis network: effect on HSF-1 and HSP-16.2

Organisms have evolved intricate stress-response pathways to counteract endogenous stressors and uphold cellular homeostasis. In the face of various neurodegenerative diseases, the conserved transcription factor HSF-1 binds to heat shock elements (HSEs) in the promoters of heat-inducible genes, triggering the expression of HSPs such as HSP-16.2 and HSP70. These proteins are adept at identifying and re-folding unfolded or misfolded proteins, averting their accumulation in a process known as the heat shock response (HSR) [274]. Heat shock factor (HSF)-1 plays a vital role in sustaining proteostasis and can suppress protein toxicity and aggregation across various organisms [275]. Notably, a decline in proteostasis networks, including the HSR, accompanies an increase in proteotoxicity in *C. elegans* [275]. However, this repression of the HSR can be counteracted by HSF-1, which mitigates the proteotoxicity of several aggregation proteins into adulthood. Beyond bolstering proteostasis, HSF-1 also enhances stress resistance in *C. elegans*.

In this context, to elucidate the role of OL extracts on HSF-1 pathway, the transgenic strain OS3062 was used. As mentioned before, OS3062 present GFP gene fused to *hsf-1*. In this context, the treatment with low and high-OL extracts did not alter the basal levels of HSF-1 in nematodes. Contrarily, the treatment with mid-OL, led to slightly lower levels of this transcription factor in the exposed nematodes (**Figure 33**). The studies about the role of OL extract, or any of the studied compounds in the present work, in the HSF-1 pathway is extremely limited. To cite, the study performed by Feng *et al.* [217], which showed that the treatment with pure isolated oleuropein (237.6 μg/ml) was able to increase mRNA

levels of HSF-1 in *C. elegans*. However, this concentration is far to obtain using realistic doses of OL extract.

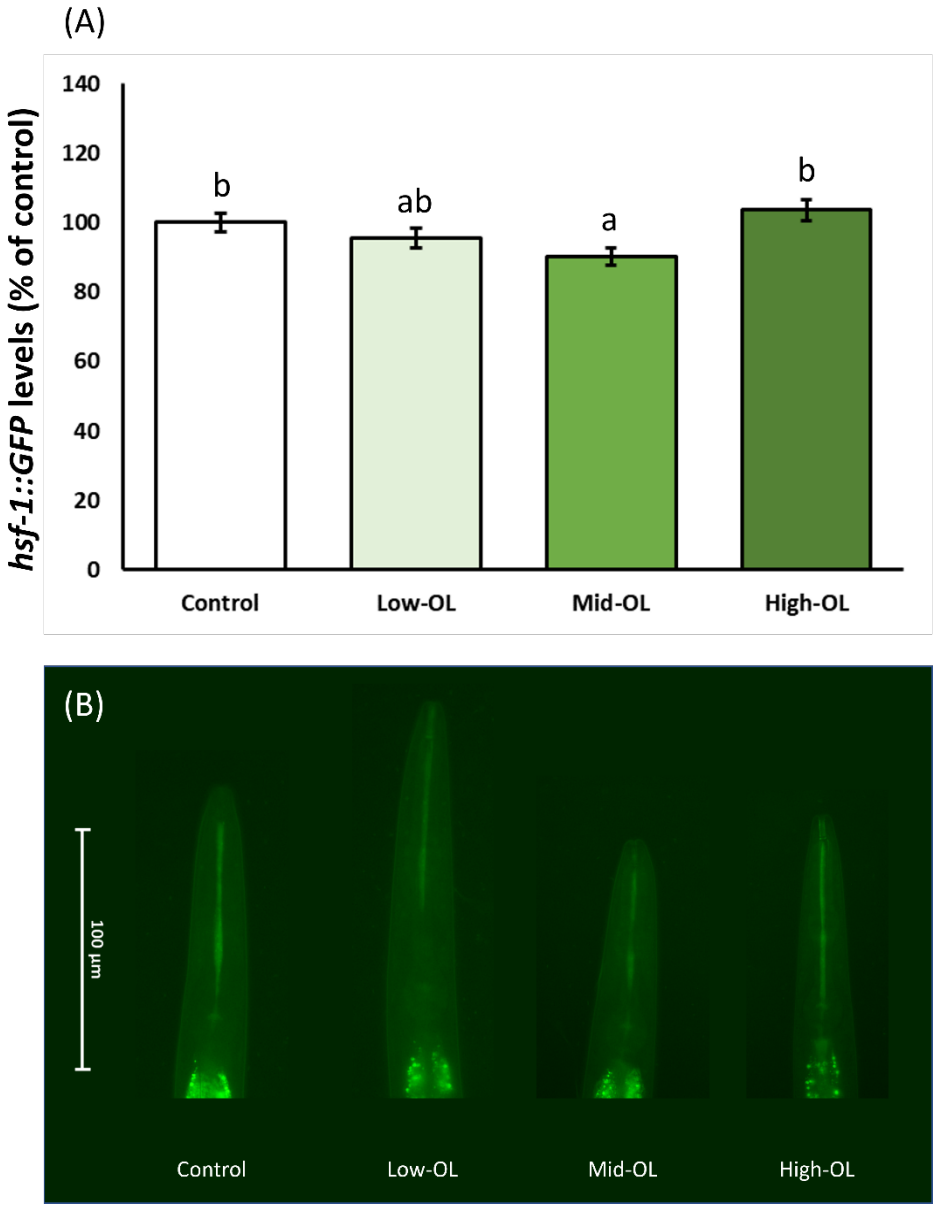

Figure 33. Effects of the three OL extract at 500 µg/ml on OS3062/*hsf-1*::GFP and descriptive images of each group. (A) Quantification of the GFP expression. (B) OS3062/*hsf-1*::GFP strain (40X magnification). Different letters mean statistically significant differences ($p < 0.05$). Results are expressed as mean ± SEM. Abbreviatures: OL: olive leaves.

Similarly with the results obtained in OS3062 strain, the treatment with 500 μg/ml of low and high-OL extracts did not alter the basal levels of HSP-16.2 in TJ375 strain. Contrarily, the treatment with mid-OL extract shown higher levels of HSP-16.2 (**Figure 34**). These results can be explained due the nature of the regulation of HSF-1. HSF-1 is negatively regulated by its own HSPs production, such as HSP70. In basal and mild-stress conditions, HSP70 and HSP-16.2 are produced in a similar way [275,276]. Therefore, the elevated levels of HSP-16.2 can be assumed as indirect marker of HSF-1 negative feedback regulator in this analysis. Then, the higher HSP-16.2 production induced by mid-OL might prevent high HSF-1 levels by negative feedback.

Similar to HSR, hormetic stress can amplify stress resistance. While it has been proposed that hormesis operates through the activation of stress-response pathways like HSR/HSF-1 and the IGF-1/IIS signaling pathway, the role of HSPs as the sole effector molecules of hormesis remains uncertain [245,251,277,278]. In this context, three studies evaluated the role of olive by-products such as methanolic OL, 20% H-OF, and 40% O-OL extracts in HSP-16.2 levels using the TJ375 strain. In this context, the totality of the treatments increased the fluorescence in this strain [26,144,204]. Authors attributed the induction to a hormetic mechanism related to the high content in hydroxytyrosol and oleuropein, respectively [26,204]. However, it is unlikely that the effect of the mid-OL extract could be attributed to these compounds since the presence of these phytochemicals is over 40 times lower. In contrast, the effect might be attributed to the apigenin derivatives content. As mentioned before, the administration of isolated apigenin has been shown to induce non-lethal toxic effects, which increased HSP-16 levels in *C. elegans* [221]. Interestingly, the induction promoted by mid-OL extract of HSP-16.2 could be attributed to a stress response to a mild-low dose of apigenin on *C. elegans*. These results strongly support that the mid-OL extract induces hormetic stress and promotes protective effects through the modulation

of HSP-16.2, as evidenced in the RNAi analysis for the amyloid and hyperphosphorylated tau-induced proteotoxicity test.

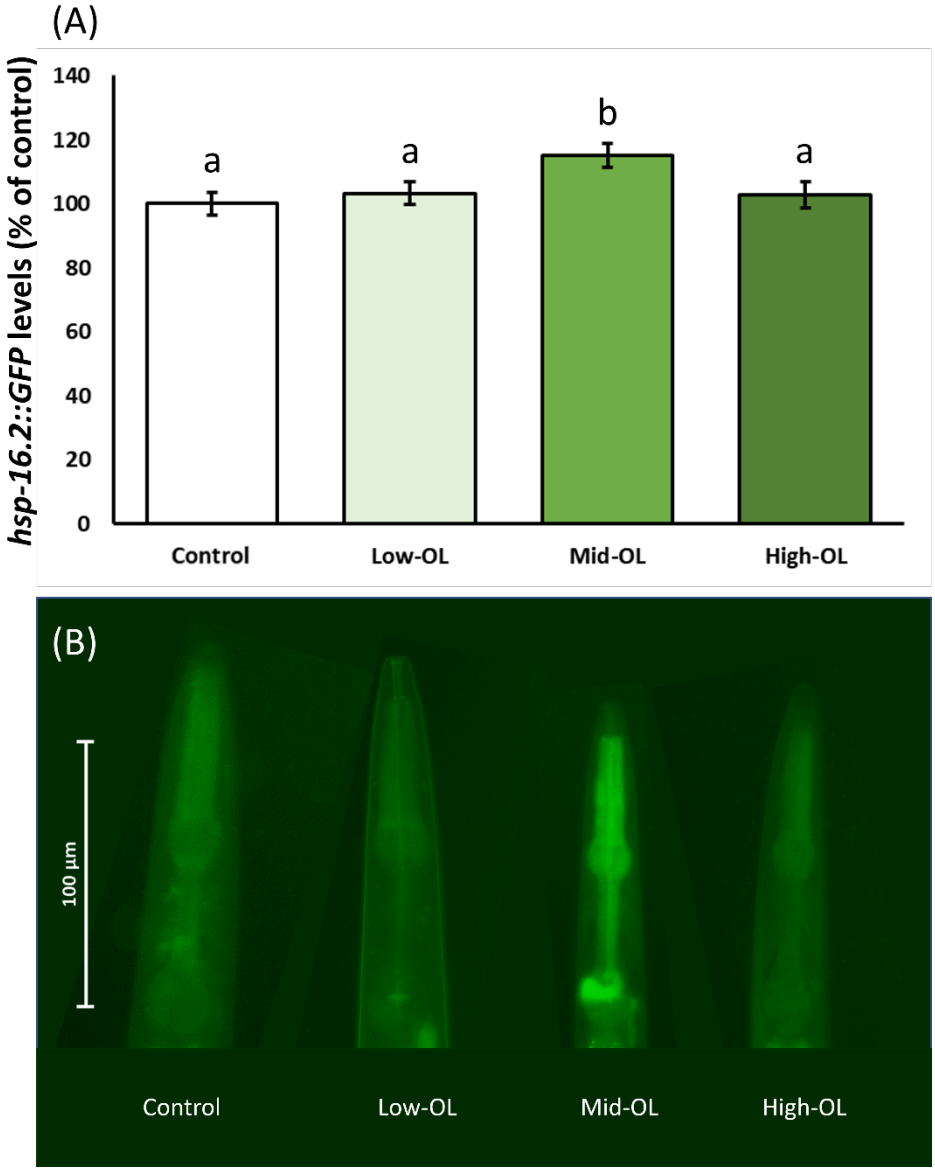

Figure 34. Effects of the three OL extract at 500 µg/ml on TJ375/*hsp-16.2p*::GFP strain and descriptive images of each group. (A) Quantification of the GFP expression. (B) TJ375/*hsp-16.2p*::GFP strain (40X magnification). Different letters mean statistically significant differences ($p < 0.05$). Results are expressed as mean ± SEM. Abbreviatures: OL: olive leaves.

11.1.2. Effect on antioxidant system components: DAF-16/FOXO, SKN-1/NRF-2, SOD-3, and GST-4

DAF-16/FOXO is a transcription factor that encodes numerous genes related to the ARE system and proteostasis network such as SOD-3 and HSP-16.2 [255,279]. To elucidate the role of OL extracts on DAF-16/FOXO pathway, the transgenic strain TJ356 was used. As mentioned before, TJ356 present a GFP gene fused to daf-*16a/b* and *daf-16p*, which migrates to the nucleus when it is activated where modulate gene expression. For the analysis of TJ356, a semi-quantitative scale was applied according to cytosolic, intermediate, and nuclear location of DAF-16/FOXO was adopted. In this context, the treatment with 500 μg/ml of all OL extracts led to higher values for nucleation of DAF-16/FOXO in the treated nematodes compared to control (**Figure 35**). This may indicate that the dose used was enough to induce DAF-16/FOXO in all treatments. These results are in accordance with the obtained by Luo *et al.* [144], which demonstrated an enhancement of nuclear distribution of DAF-16/FOXO in TJ356 nematodes treated with 400 μg/ml of methanolic OL extract. However, a distinct modulatory activity was observed among the extracts. The mid-OL extract exhibited the highest induction of DAF-16/FOXO. This outcome could be attributed to the fact that DAF-16/FOXO also regulates the expression of *hsp-16.2*, which was also found to be in a higher proportion in nematodes treated with mid-OL extract in the TJ375 strain. This correlation suggests that, despite the induction of DAF-16/FOXO by all three OL extracts, the influence of DAF-16/FOXO on the ARE system or the proteostasis network might vary based on the phenolic content of the extract. Notably, the mid-OL extract, with its high content of apigenin derivatives, has been shown to enhance DAF-16/FOXO translocation and subsequently induce HSP-16.2 in *C. elegans* [262]. Interestingly, the induction of DAF-16/FOXO and HSP-16.2 by the mid-OL extract, along with their subsequent protective effects, could be attributed to a potential side effect. This could be related to the fact that high concentrations of isolated apigenin derivatives have been shown to exhibit non-lethal toxic effects through DAF-16/FOXO/HSP-16.2

modulation on *C. elegans* [221]. These results are in accordance with those obtained in the VIP score of toxicological assessment and the growth impairment observed in the BR5706 strain mediated by mid-OL extract. These results hold significant interest as they may indicate a mild-induced stress effect exerted by the OL extracts in the different AD strains.

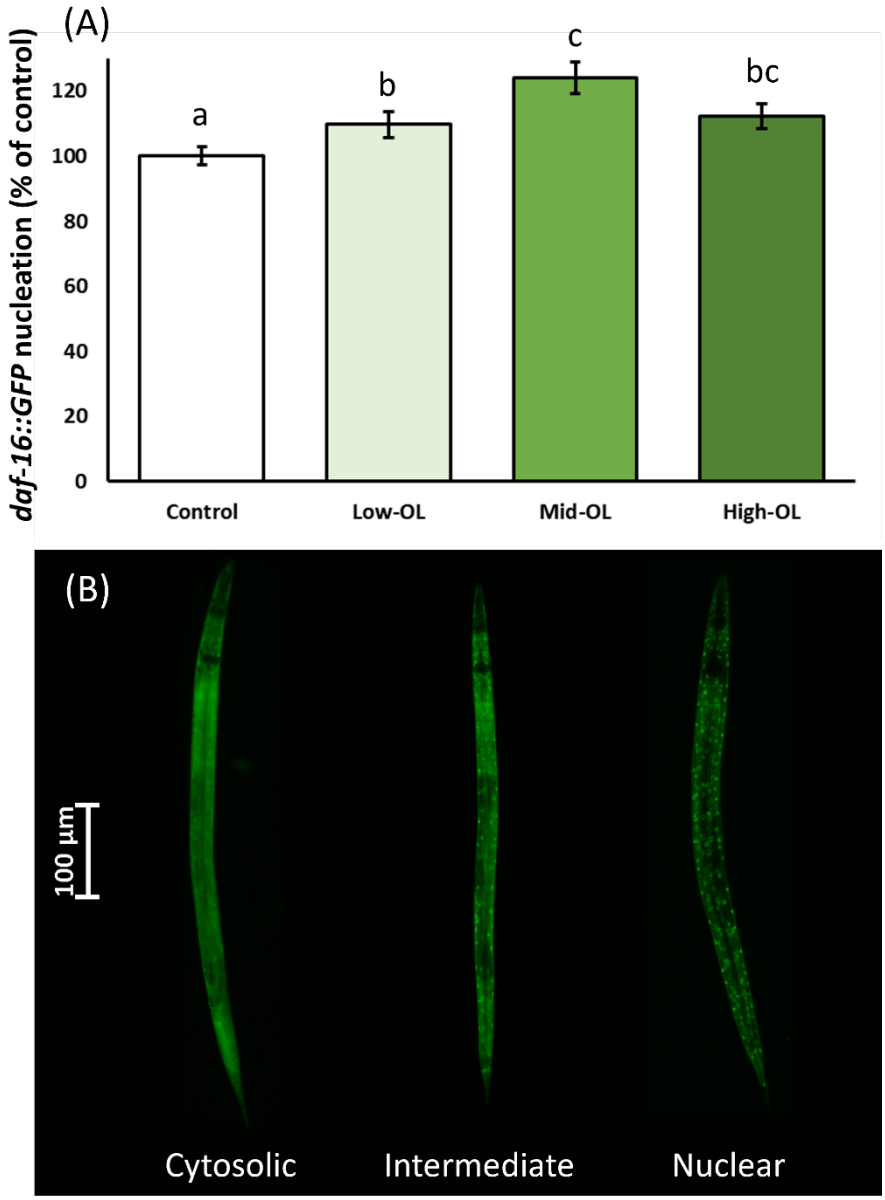

Figure 35. Effects of the three OL extract at 500 µg/ml on TJ356/*daf-16p*::GFP strain and descriptive images of each group. (A) Quantification of the GFP expression. (B) Representative pictures of the semi-quantitative distribution of *daf-16p*::GFP status (10X magnification). Different letters mean statistically significant differences ($p < 0.05$). Results are expressed as mean ± SEM. Abbreviatures: OL: olive leaves.

SKN-1/NRF-2 is a transcription factor involved in xenobiotic and oxidative stress responses [260]. Numerus ARE system genes are downstream of SKN-1/NRF-2 such as the SOD-3 and GST-4 [280]. In addition, SKN-1/NRF-2 is also involved in proteostasis maintenance, immunity, metabolism, and mitochondrial function [260]. To elucidate the role of OL extracts on SKN-1/NRF-2 pathway, the transgenic strain LD1 was used. In this context, the treatment with 500 μg/ml of low and high-OL extracts led to a higher expression of SKN-1/NRF-2 (**Figure 36**). Contrarily, the administration of mid-OL extract did not alter the levels of SKN-1/NRF-2. These results are in accordance with those obtained in the amyloid and p-tau assays, which poses that the modulatory activity of mid-OL extract is mainly attributed to the proteostasis network modulation mediated by DAF-16/FOXO and HSF-1. In fact, a recent study proposed that *skn-1* is foremost important in proteostasis maintenance from day 1 of adulthood in a constitutive Aβ-aggregation strain of *C. elegans* [281]. It's noteworthy that the GFP expression tests were conducted in the L4 stage, whereas the experiments involving amyloid, and p-tau were also carried out in the L4 stage or early stages of young adulthood. This highlights the clear absence of the effect from the mid-OL extract on proteostasis modulation mediated by SKN-1/NRF-2.

In contrast, the role of SKN-1/NRF-2 in the promotion of lifespan and stress response is crucial since early larvae development in the Wild type N2 strain [281]. This might help explain why both low and high-OL extracts were responsible for higher SKN-1/NRF-2 levels, whereas mid-OL extract did not exhibit the same effect at the same doses.

Interestingly, the high-OL extract induced the highest SKN-1/NRF-2 levels (23%). This effect might be attributed to the high content of secoiridoids present in the extract. These compounds have been shown to induce mitohormetic effects by upregulating the SKN-1/NRF-2 signaling pathway and modulating mitochondrial function in *C. elegans* [244,260]. These findings are consistent with the results obtained from the experiments involving amyloid and p-tau, which emphasized the pivotal

role of SKN-1/NRF-2 and the major mitochondrial MnSOD, SOD-2, in the health benefits conferred by the high-OL extract.

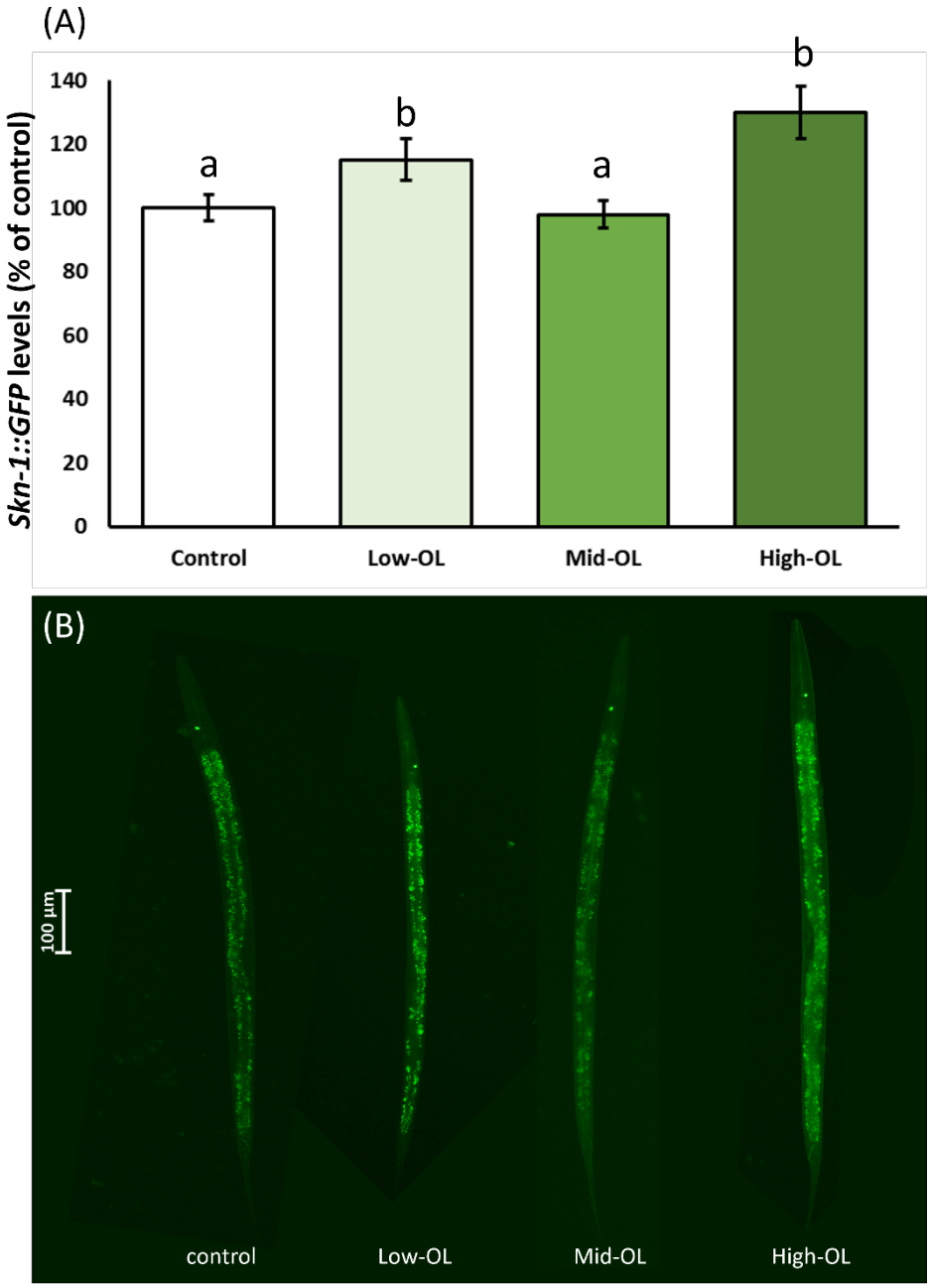

Figure 36. Effects of the three OL extract at 500 µg/ml on LD1/*skn-1*::GFP strain and descriptive images of each group. (A) Quantification of the GFP expression. (B) LD1/*skn-1*::GFP strain (10X magnification). Different letters mean statistically significant differences ($p < 0.05$). Results are expressed as mean ± SEM. Abbreviatures: OL: olive leaves.

The antioxidant defense system can be categorized based on its nature, either endogenous or exogenous. SOD-3 and GST-4 serve as examples of endogenous enzymatic antioxidants [282]. MnSOD enzyme family fulfills its protective role at the mitochondrial level by converting the superoxide molecules into molecular oxygen and hydrogen peroxide. This is achieved through cyclic redox reactions featuring a manganese metal center at its active site [282]. In fact, SOD-3 encodes auxiliary and inducible MnSOD mitochondrial isoforms, which has been related to modulate numerous health effects related to aging such as mitochondrial function and lifespan (although this last effect is nowadays controversial) [257,283–287]. Because the expression of these enzymes can be influenced by xenobiotics, they are becoming valuable molecular targets for drug-based interventions [288].

To assess the role of OL extracts on SOD-3 levels, the transgenic strain CF1553 was used. Among the OL extracts studied, only the treatment with 500 μg/ml of low-OL extract was able to induce the basal levels of SOD-3 in CF1553 strain (**Figure 37**). These results are consistent with studies that assessed the enhancement of SOD-3 levels mediated by olive by-products with lower doses in CF1553 strain [26,204]. Similarly, these findings are aligned with the obtained in the amyloid and p-tau induced toxicity experiments, which revealed the involvement of SOD-3 in the therapeutic effect exerted by low-OL.

In contrast, the influence of mid and high-OL extracts on SOD-3 was null. As mentioned before, these findings suggest that the mid-OL extract exerts its protective effect mainly through proteostasis modulation, beyond the antioxidant activity. In contrast, the high-OL extract is deeply involved in the ARE system modulation. However, the nematodes exposed to the extract did not show higher basal levels of SOD-3. As observed in the amyloidogenic and p-tau induced toxicity test, the role of the high-OL extract may be mediated through SOD-2 modulation rather than by SOD-3. Increasing evidence indicates that SOD-2 is the most active mitochondrial enzyme in *C. elegans* [289,290],

being the potential target for the mitohormesis proposed by secoiridoid contents [244,260]. These results are highly intriguing as they suggest an isoform-specific effect of the treatment based on the phytochemical composition.

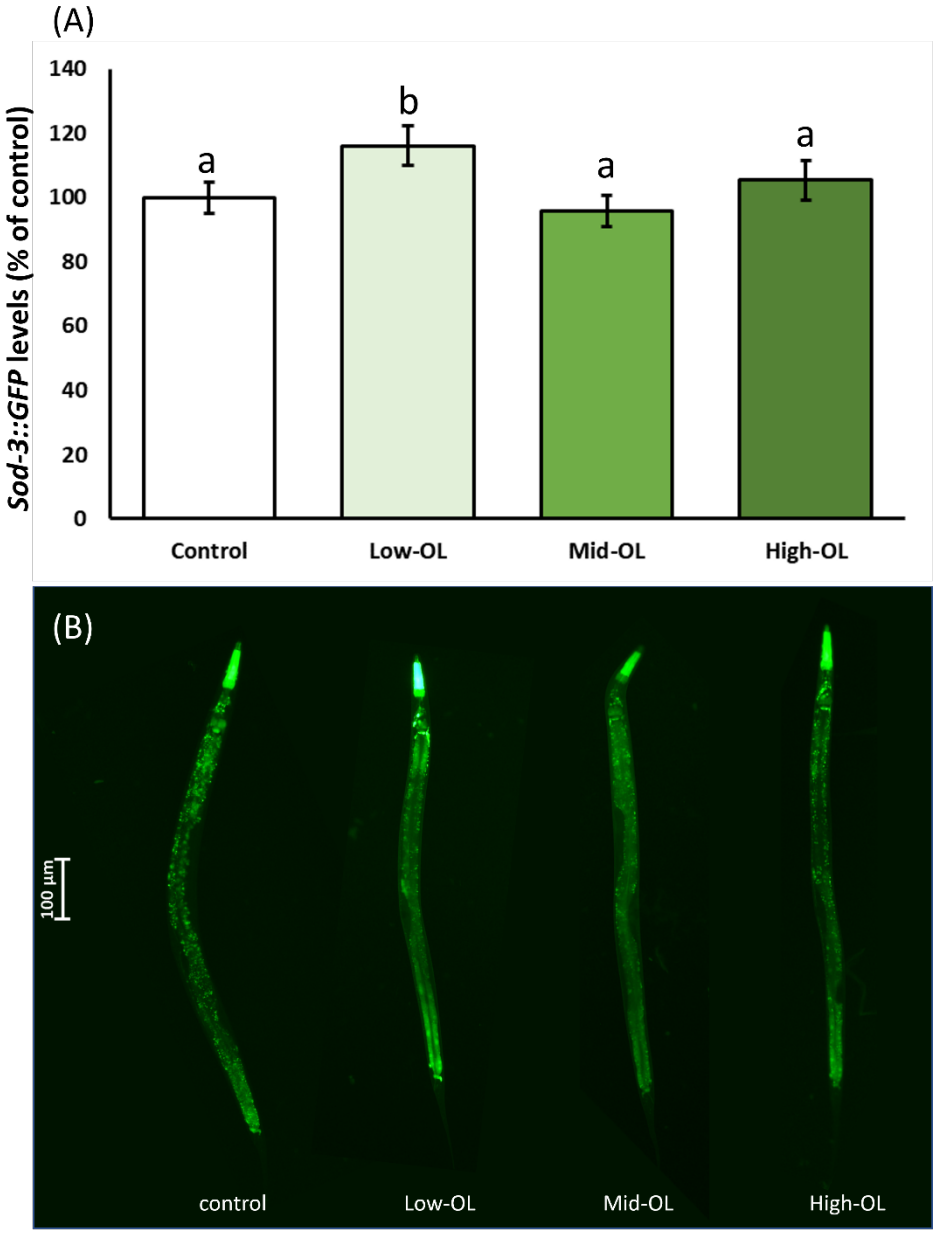

Figure 37. Effects of the three OL extract at 500 µg/ml on CF1553/*sod-3p*::GFP strain and descriptive images of each group. (A) Quantification of the GFP expression. (B) CF1553/*sod-3p*::GFP (10X magnification). Different letters mean statistically significant differences ($p < 0.05$). Results are expressed as mean ± SEM. Abbreviatures: OL: olive leaves.

Similarly, the effect of OL extracts was also assessed on GST-4 levels. GSTs are enzymes with diverse functions that utilize GSH in conjugation reactions. GST-4 is a well-studied cytosolic enzyme of the sigma subfamily, which plays a role in phase II detoxification in *C. elegans* [291,292]. Numerous substances that enhance the intensity of the GST-4 fluorescence reporter have been documented to elevate stress resistance and counteract oxidative stress in *C. elegans* [204,291,293,294].

To assess the role of OL extracts on GST-4 expression levels, the transgenic strain CL2166 was used. Among the OL extracts studied, only the treatment with 500 μg/ml of low and mid-OL extracts were able to show higher expression levels of GST-4 in CL2166 strain (**Figure 38**). However, the greatest value was found for low-OL (25%). These differences can be attributed to the transcription factor activated as a consequence of treatment with each extract. Both extracts induced DAF-16/FOXO translocation to the nucleus, achieving the highest induction in the mid-OL treated nematodes. In contrast, only the low-OL extract was able to promote the expression of SKN-1/NRF-2 in the nematodes exposed. DAF-16/FOXO encodes for HSP-16.2, and it has been demonstrated that one of the primary targets of HSP-16.2 are enzyme systems responsible for regulating cellular GSH levels [255]. Consequently, an elevation in GSH levels could potentially contribute to an increase in the activity of GSH-related enzymes [255,256,295,296]. In contrast, although GST-4 levels is not exclusively regulated by SKN-1/NRF-2, there is a direct effect of SKN-1/NRF-2 in the regulation of phase II enzymes [297]. Notwithstanding, the treatment with the high-OL extract did not increase the basal levels of GST-4 (**Figure 38**). Indeed, an OL extract 3.4 times richer in oleuropein and its derivatives reduced the GST-4 levels in the same *C. elegans* strain [26]. This result could be attributed to the strong antioxidant activity of the extract, particularly as a free radical scavenger, mainly attributed to the elevated content of oleuropein and its derivatives. *In vitro* studies have demonstrated that numerous ROS scavengers are able to reduce the expression or the activity of different inducible antioxidant enzymes such as GST [298]. The

proof of such a feature has been demonstrated in different randomized double-blind trials, which reported that the intake of oleuropein-rich EVOO enhanced plasma GSH as well as reduced the activity of GSH-Px [299,300].

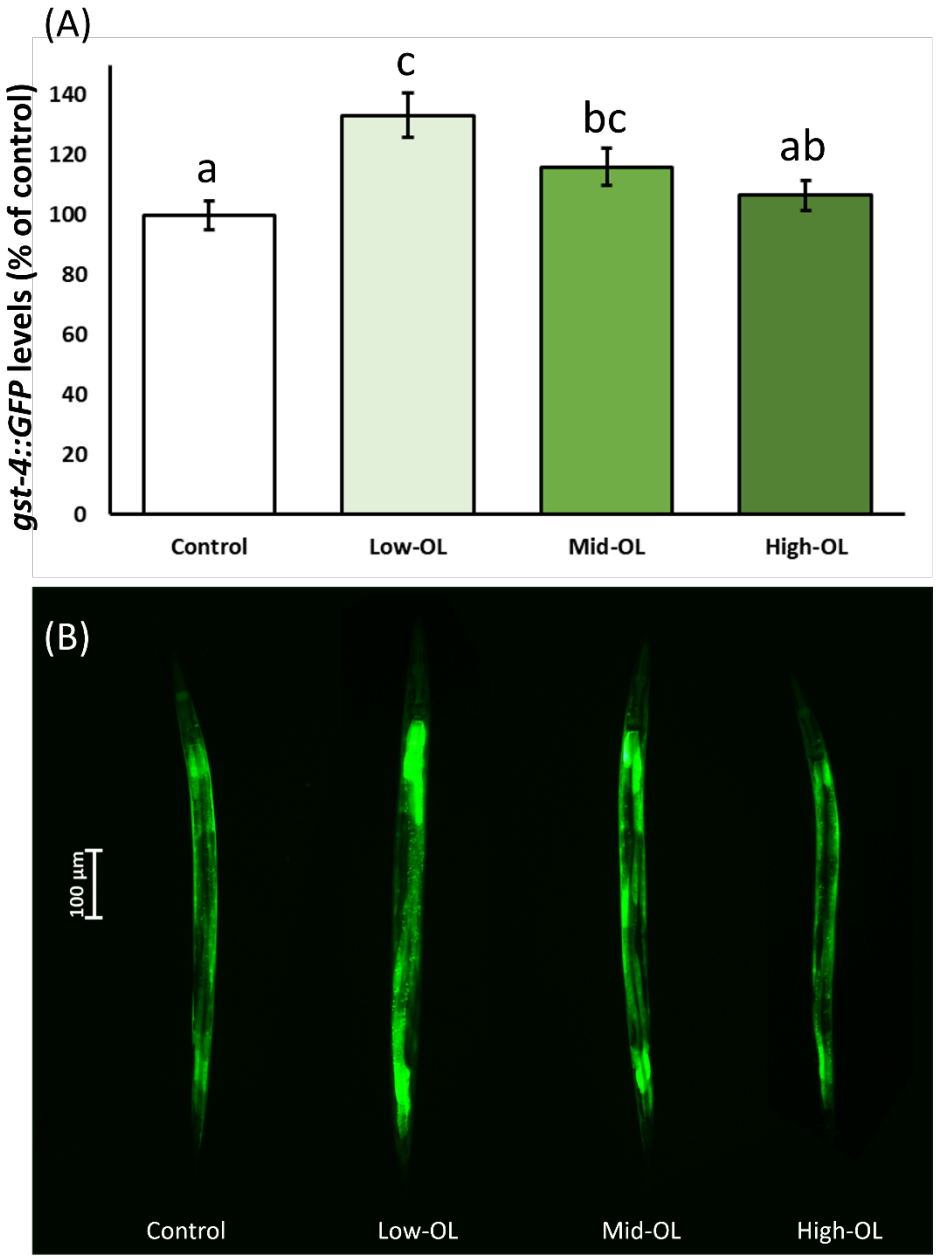

Figure 38. Effects of the three OL extract at 500 µg/ml on CL2166/*gst-4p*::GFP strain and descriptive images of each group. (A) Quantification of the GFP expression. (B) CL2166/*gst-4p*::GFP strain (10X magnification). Different letters mean statistically significant differences ($p < 0.05$). Results are expressed as mean ± SEM. Abbreviatures: OL: olive leaves.

11.2. Effect of the three-olive leaf extracts on redox biology during Alzheimer's disease

11.2.1. Redox biology during amyloidogenic pathology

11.2.1.1. Intracellular ROS content

The accumulation of $A\beta_{1-42}$ has been recognized as an important factor in the progression of neurodegeneration in AD patients due its disruptive effects can be also exerted via oxidative stress induction [137,301]. Senile depositions in form of Aβ plaques has been associated with increased markers of lipid peroxidation [302] as well as low levels of enzymatic and non-enzymatic antioxidants have been found in AD patients [303,304]. Interestingly, oxidative stress has been identified as an early feature in the AD physiopathology in both human and animal models [137,305–308].

Hence, to examine the impact of the three OL extracts in preventing Aβ-induced oxidative stress, the measurement of intracellular ROS levels was conducted in the amyloidogenic *C. elegans* model. A study by Drake *et al.* [137] demonstrated that the CL4176 strain could reproduce oxidative damage in specific tissues prior to the occurrence of Aβ plaque deposition, although ROS levels were not quantified. The authors established that a temperature upshift led to an increase in protein carbonylation, starting 24 h post temperature induction. Therefore, the current study employed the H_2DCFDA dye method to assess intracellular ROS levels at the 24-h mark after the temperature upshift, replicating the conditions observed in the early stages of AD. For this purpose, the nematodes were growth in the same conditions as exposed for Aβ-induced toxicity test. In the same way, untreated CL802 was used as negative control (Aβ-), while untreated CL4176 was used as positive control (Aβ+). As depicted in **Figure 39**, the production of $A\beta_{1-42}$ in the positive control resulted in an exacerbation of intracellular ROS content compared to the negative control. This observation aligns with existing literature, which suggests an escalation of oxidative damage preceding

Aβ aggregation during the initial stages of AD [137,305–308]. This finding underscores the validity of the experimental model in assessing oxidative stress in AD.

As described in **Figure 39**, all the treatments were able to partially prevent intracellular ROS formation in the CL4176 nematodes. Interestingly, the greatest preventive effect was achieved by the low-OL extract (∇123%) compared with the positive control. This result may be attributed to the induction of GST-4 manifested in the GFP-reporter strain. Here, the treatment with 500 μg/ml of low-OL extract led to a higher GST-4 expression level by 25%. As mentioned, GST-4 can catalyze the conjugation of the reduced form of GSH to xenobiotic substrates for detoxification purposes. GSH is often referred to as the major antioxidant of the cell, although other functions have been described [291]. Hence, it is unsurprising that with a pronounced engagement of GST-4, there is an increased utilization of GSH and a consequent reduction in intracellular ROS content [291]. Seddik *et al.* [77], demonstrated that the supplementation with OL extract increased the GST activity in the brains of Pb-induced neurotoxicity rats, which was associated with lower oxidative markers and Pb deposition in brain. Despite the levels of SOD-3 were also up-regulated (Δ14%) in low-OL treated nematodes, its relative contribution to fight oxidative stress in *C. elegans* is very small to explain the differences with the rest of OL extracts [309].

In the case of mid-OL extract, the intracellular ROS was a 73% lower than in control. A pattern can also be noticed with GST-4 levels: the nematodes treated with mid-OL extract presented a 1.8 times lower levels of GST-4 than that in low-OL treated worms. Interestingly, this trend was also evident in the determination of intracellular ROS content, with the reduction exerted by mid-OL extract being 1.7 times lower than that in low-OL treated nematodes. This correlation provides additional insight into the role of GST-4 in the observed lower intracellular ROS content in nematodes treated with mid-OL extract. As mentioned before, the induction of GST-4 levels in the mid-OL extract treated nematodes may

be involved the hormetic stress of mid-OL extract in HSP-16.2 overproduction (Δ13%). These results highlighted the role of this chaperone in the regulation of the activity of GSH-related enzymes, indicating that the role of HSP-16.2 is not exclusively in the degradation of misfolded proteins [255,256,295,296].

Finally, the nematodes treated with high-OL extract exhibited a 77% lower ROS levels compared to control, even though GST-4 was not modulated. A possible explanation is the influence of the high-OL extract on SOD-2. Although SOD-2 expression or levels were not directly evaluated, the RNAi experiments illustrated a strong modulatory activity of this mitochondrial MnSOD in the amyloidogenic model. SOD-2 has been demonstrated to be the major and most active MnSOD isoform in *C. elegans*, which may significantly contribute to the amelioration of oxidative stress in presence of amyloid pathology [257–259,309]. Another possible explanation can be attributed to the potent free radical scavenging activity of the high-OL extract. Various preclinical assays demonstrated that treatment with OL extract can effectively reduce ROS content after induction with free radical generators while reduce the expression of inducible antioxidant enzymes such as GST in cell lines and in *C. elegans* [26,93,94]. Many authors have attributed the high antioxidant activity of OL extract to its content in secoiridoids [310,311]. The proof of such a feature has been demonstrated in different randomized double-blind trials, which reported that the intake of oleuropein-rich EVOO enhanced plasma total antioxidant capacity and GSH content, while reduced the activity of GSH-Px, indicating a direct radical scavenger activity of the olive by-product [299,300]. These results are in accordance with those obtained in the preliminary assessment of the influence of phytochemical compounds on the antioxidant activity of the extracts in section 7.2. In this case, as depicted by the VIP score for the FRAP assay, the highest contribution to iron-reducing antioxidant capacity was exerted by the secoiridoids content. However, it should be noted that the potential involvement of other antioxidant enzymes, which were not investigated in the current study, cannot be disregarded.

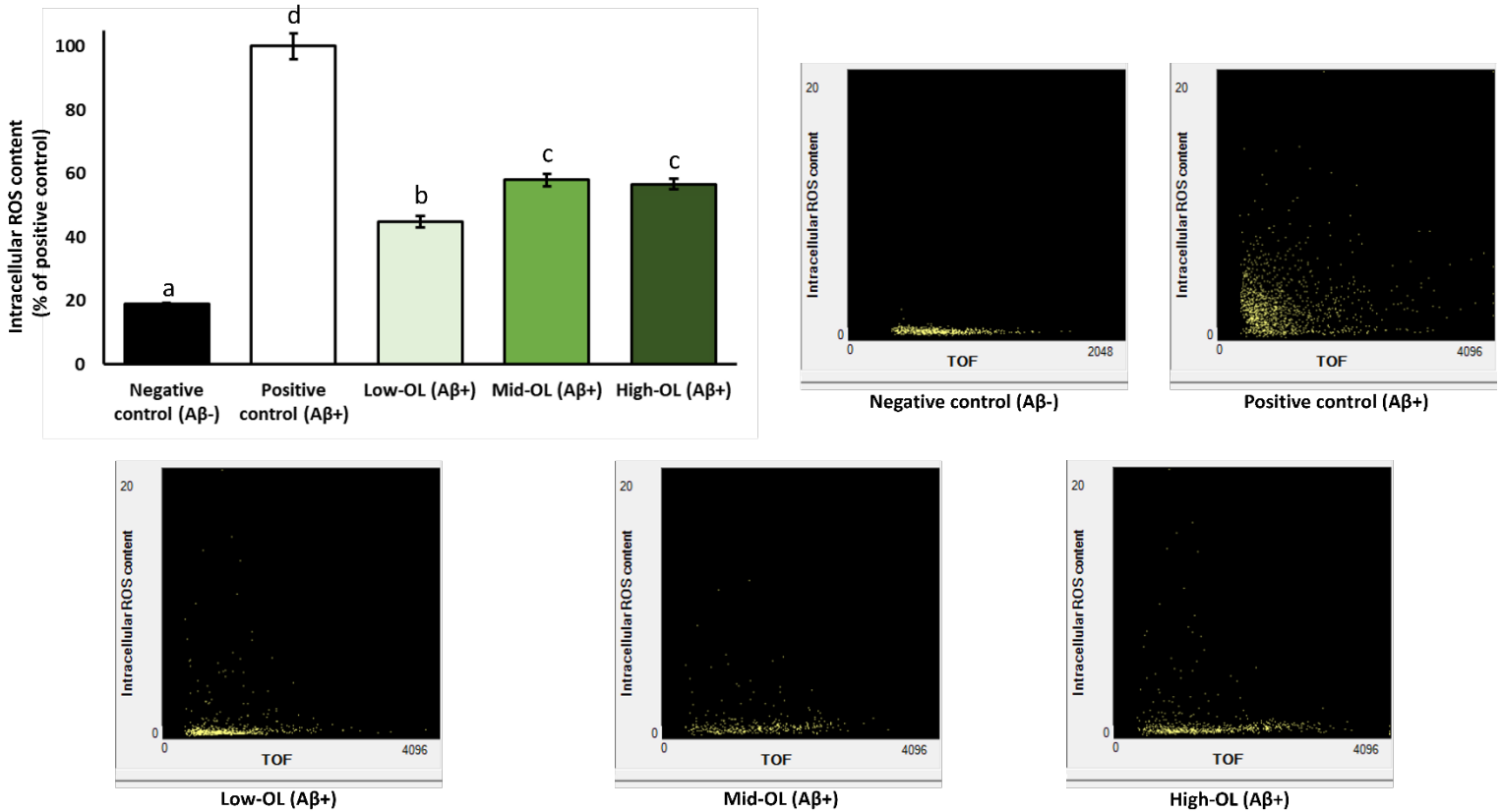

Figure 39. Intracellular reactive oxygen species (ROS) content of CL802 and CL4176 nematodes at 24 h after temperature up-shift and representative dot plots. Nematodes from CL802 and CL4176 treated with or without 500 µg/ml of low, mid, or high-OL extracts. Dot plot of intracellular ROS content *vs.* TOF (time of flight; worm size) representative panels for each experimental group of red fluorescence intensity extracted from flow cytometer software are presented. Different letters mean statistically significant differences ($p < 0.05$). Results are expressed as mean ± SEM. Abbreviatures: OL: olive leaves.

11.2.1.2. Mitochondrial ROS content

Under physiological conditions, ROS can be derived from complexes I and III in the mitochondrial electron transport chain, where electrons can be directly donated to molecular oxygen to form a superoxide anion [250]. Numerous enzymes present in mitochondria, such as SOD, GSH-Px, and cytochrome c oxidase have been found to be significantly decreased in AD patients [312–315]. In contrast, redox-active compounds such as oxidized iron and biomolecules were increased in the brains of AD patients, leading to an increase in oxidative stress within mitochondria [312–315]. Furthermore, Aβ oligomers can bind to oxidized iron and accumulate within the mitochondrial membrane, leading to the disruption of the electron transport chain complexes [316,317]. This disruption can subsequently result in an increased production of ROS beyond the capacity of the mitochondrial defense mechanisms [318,319]. This cascade of events, characterized by Aβ-induced mitochondrial dysfunction, contributes to the generation of significant levels of ROS within the intracellular compartment, and exacerbates the production of Aβ oligomers [318,319]. This process establishes a vicious cycle that further accelerates the progression of AD pathology.

Hence, to examine the impact of the three OL extracts in preventing Aβ-induced oxidative stress at mitochondrial level, the MitoTracker Red CM-H_2XRos dye was applied at the 24-h mark after the temperature upshift in the amyloidogenic *C. elegans* model [137]. For this purpose, the nematodes were growth in the same conditions as exposed for Aβ-induced toxicity test and intracellular ROS content evaluation.

As depicted in **Figure 40**, the production of $A\beta_{1-42}$ in the positive control resulted in a higher content of mitochondrial ROS compared to the negative control. This observation aligns with existing literature, which suggests that Aβ induces mitochondrial dysfunction and contributes to the generation of significant levels of ROS an to the escalation of oxidative damage [318,319]. This finding underscores the

validity of the experimental model in assessing oxidative stress in AD also at mitochondrial level.

As depicted in **Figure 40**, only the nematodes exposed to high-OL extracts presented a lower mitochondrial ROS content (∇36%) than the positive control in the amyloidogenic strain. These results are consistent with those results obtained in the RNAi experiments, which showed a strong modulatory activity of this extract through mitochondrial MnSODs. In the RNAi experiments, a mitohormetic effect was suggested. Here, the mild stress induced by the high-OL extract could potentially prime the ARE system for SOD overcompensation in the presence of amyloidogenic pathology. This heightened production of SOD-2 enzyme may significantly contribute to the amelioration of oxidative stress, as also noted by other researchers [258,259]. This effect might be attributed to the high content in secoiridoids present in the extract. These compounds have been shown to upregulate the SKN-1/NRF-2 signaling pathway and modulate mitochondrial function in *C. elegans* [244,260].

Another additional explanation can be that the high-OL extract may also act by reducing the oxidized iron pool exacerbated during AD at the mitochondrial level, as depicted FRAP assay. In this scenario, the high-OL extract may prevent iron from binding to Aβ oligomers and thereby prevent the disruption of the electron transport chain complexes in the mitochondrial membrane [316,317]. Similarly, the decrease in oxidized iron levels may contribute to a reduction in the generation of hydroxyl radicals and oxidized biomolecules, thereby aiding in the amelioration of oxidative stress [171]. This hypothesis is supported by Kondo *et al.* [320], which demonstrates that oleuropein-rich OL extract improved iron homeostasis and mitochondrial functions in hematopoietic stem cells. Regardless, a combination of both aforementioned hypotheses strongly supports the idea that the mechanistic health properties of the high-OL extract can be exerted through mitochondrial modulation in this strain.

In contrast, both low and mid-OL extracts did not affect mitochondrial ROS content in the amyloidogenic strain. Both treatments have been shown to modulate the GSH metabolism through GST-4. Notwithstanding, it should be noted that GST-4 is exclusively located in the cytosol and its overproduction may reduce the intracellular ROS content through xenobiotic detoxification, as demonstrated.

In the other hand, the role of SOD-3 in the low-OL extract treated nematodes to fight mitochondrial oxidative stress is unclear. SOD-3 is the most highly up-regulated of the MnSOD genes, but its activity is very small in *C. elegans* [309]. In fact, different studies demonstrated that SOD-3 deletion did not increase susceptibility to oxidative stress, whereas its overexpression promotes promoted a slight increase of lifespan without reducing oxidative damage in *C. elegans* [284,309,321]. In fact, beyond its antioxidant enzyme activity, it has been suggested that SOD-3 may also act as a scavenger for misfolded proteins [309].

The present results highlight the relevance of high-OL extract in countering the disruptive effects of amyloidogenic toxicity through mitochondrial oxidative stress modulation. Similarly, these findings strongly support the results obtained from the RNAi experiments and GFP-reporters, which indicated the involvement of the SKN-1/NRF-2 and MnSOD in the protective effect. However, it should be noted that the potential involvement of other antioxidant enzymes, which were not investigated in this current study, cannot be disregarded.

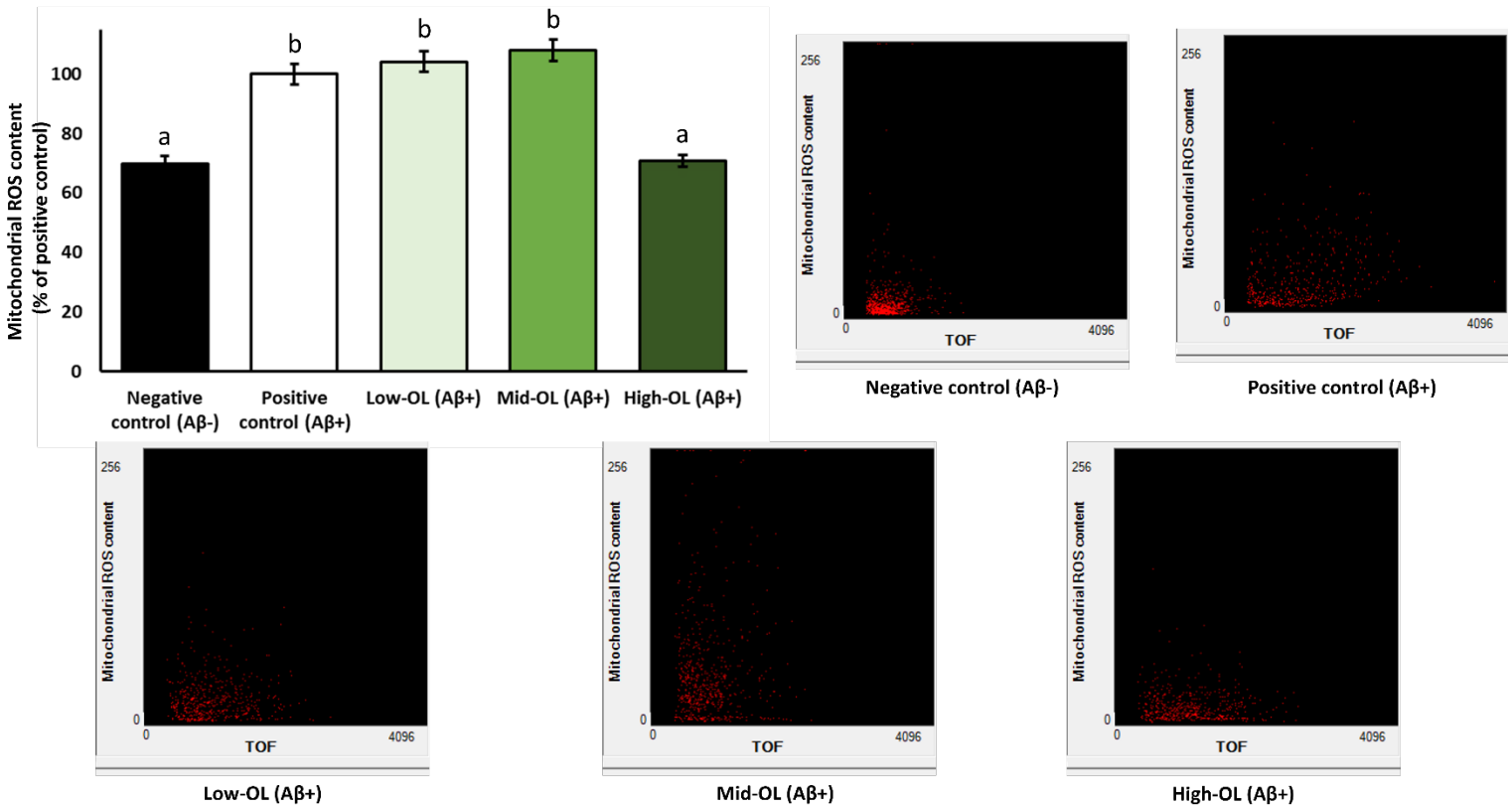

Figure 40. Mitochondrial reactive oxygen species (ROS) content of CL802 and CL4176 nematodes at 24 h after temperature up-shift and representative dot plots. Nematodes from CL802 and CL4176 treated with or without 500 µg/ml of low, mid, or high-OL extracts. Dot plot of mitochondrial ROS content *vs.* TOF (time of flight; worm size) representative panels for each experimental group of red fluorescence intensity extracted from flow cytometer software are presented. Different letters mean statistically significant differences ($p < 0.05$). Results are expressed as mean ± SEM. Abbreviatures: OL: olive leaves.

11.2.1.3. Glutathione content

GSH is a tripeptide (γ-glutamyl-cysteinyl-glycine) that constitutes a crucial intracellular thiol compound with ubiquitous presence. It serves as a primary defense mechanism against ROS and electrophiles, playing a pivotal role in antioxidant defense [322,323]. GSH synthesis occurs *de novo* within the cytosol and a small fraction (10-15%) is transported into the mitochondrial matrix through transporters like the 2-oxoglutarate and the dicarboxylate carrier, situated in the inner mitochondrial membrane [322]. The functions of GSH are significantly influenced by the sulfhydryl group of cysteine, which may act as an electron donor. In presence of ROS or oxidized molecules, GSH is rapidly oxidized to glutathione disulfide (GSSG) through GSH-Px enzymes to reduce the harmful molecules. This reaction is recycled back to GSH by the NADPH-dependent GSSG reductases. Additionally, GSH can also undergo conjugation with xenobiotics for the purpose of elimination through the action of GST enzymes [322,323].

In presence of amyloidogenic pathology, it has been observed a significant decrease in GSH levels as well as antioxidant enzymes related to GSH metabolism such as GST, GSH-Px, and GSSG reductases in the brain tissue and plasma from AD patients [324–327]. In the same way, an increase of GSSG levels were found in AD patients compared to age-matched control subjects [324–327]. In fact, this tendence seems to be similar at the mitochondrial level [325].

Hence, to examine the impact of the three OL extracts in preventing GSH depletion, the measurement of GSH levels was conducted in the amyloidogenic *C. elegans* model. For this purpose, the nematodes were growth in the same conditions as exposed previously and the MCB dye method was assessed to determinate the total GSH content at the 24-h mark after the temperature upshift. Untreated CL802 was used as negative control (Aβ-), while untreated CL4176 was used as positive control (Aβ+).

As depicted in **Figure 41**, the production of $A\beta_{1-42}$ in the positive control resulted in lower GSH content compared to the negative control. This observation aligns with existing literature, which suggests a significant decrease in GSH levels in presence of amyloidogenic pathology [324–327]. This finding underscores the validity of the experimental model in exploring the redox biology in AD *in vivo*.

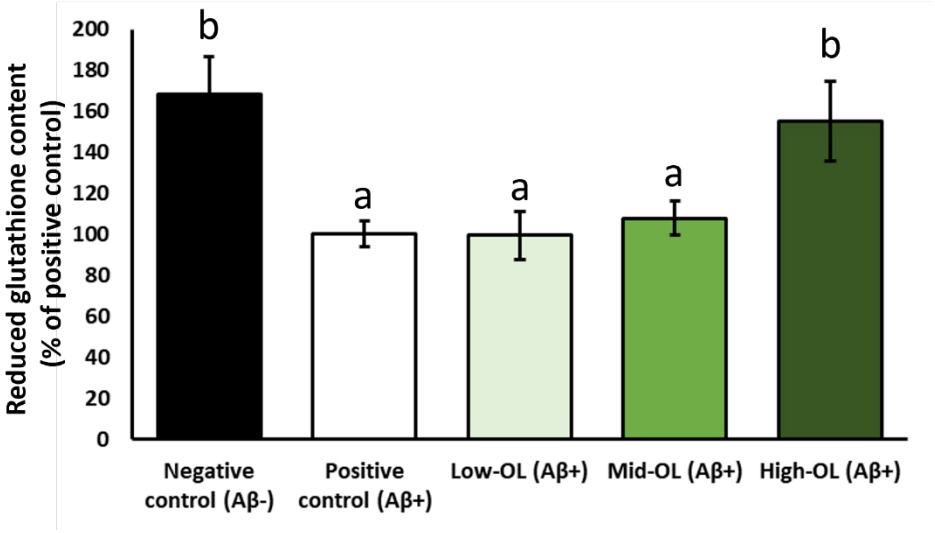

Figure 41. Reduced glutathione (GSH) content measured by monochlorobimane staining of CL802 and CL4176 nematodes at 24 h after temperature up-shift. Nematodes from CL802 and CL4176 treated with or without 500 μg/ml of low, mid, or high-OL extracts. Different letters mean statistically significant differences ($p < 0.05$). Results are expressed as mean ± SEM. Abbreviatures: OL: olive leaves.

As described **Figure 41**, the treatment with high-OL extract led to a higher GSH content (Δ36%) in the CL4176 nematodes until negative control levels, while the low and mid-OL extracts remained unchanged. This result may be attributed to the increased levels of GST-4 manifested in the GFP-reporter strain for both the low and mid-OL extracts. In this case, the treatment with 500 μg/ml of the low and mid-OL extracts led to higher GST-4 expression levels by 25% and 14%, respectively, compared to control. As mentioned, GST-4 can catalyze the conjugation of the reduced form of GSH to xenobiotic substrates for detoxification purposes [291]. Hence, it is unsurprising that with a pronounced engagement of

GST-4, there is an increased utilization of GSH [291]. Therefore, these results may suggest that the GSH content presented in the low and mid-OL extracts could be attributed to the consumption of GSH as a xenobiotic detoxification rather than the absence of an effect of the extracts, as depicted in the intracellular ROS content assay.

The above-mentioned questions might be explained through the effect of the high-OL extract. As mentioned before, the role of the high-OL extract in counteracting oxidative stress can also be attributed to its strong free radical scavenger activity, chelating oxidized iron, and preventing mitochondrial ROS production. During amyloid pathology, GSH plays a major role in chelating cytoplasmic free iron, subsequently preventing oxidized iron from undergoing uncontrolled redox reactions that could potentially cause oxidative damage [328]. Both the low and mid-OL extracts demonstrated very low FRAP values. Therefore, it is expected that there is increased utilization of GSH to counteract oxidative stress. In contrast, the high iron-reducing antioxidant capacity of the high-OL extract as well as SOD-2 involvement may reduce the consumption of GSH to bind oxidized molecules, leading to a reduction in GST-4 expression and the conservation of high levels of GSH in this strain.

Notwithstanding, a limitation of the present study is that it was only measured the total reduced GSH content and GST-4 levels, while the oxidized GSSG or GSH/GSSG ratio as well as GSSG reductases were not evaluated. Therefore, even though plausible, more research is needed to confirm this hypothesis.

11.3.1. Redox biology during tauopathy

11.3.1.1. Intracellular ROS content

AD is the best-known tauopathy with increasing prevalence. As mentioned before, oxidative stress is an early feature in AD prior to Aβ aggregation [137,305–308], but also in NFTs formation [329,330]. The aggregation and polymerization of p-tau have been related to increased toxicity and oxidative stress in both animals and humans [331]. It has been suggested that overproduction of p-tau increases intracellular ROS content through macromolecule oxidation as well as by mitochondrial dysfunction [332,333]. Similarly, NFTs have been related to a total or partial depletion of enzymatic antioxidants (SOD-1, SOD-2, GST, and GSH-Px) and non-enzymatic antioxidants (GSH levels and vitamins A, C, or E levels) in AD patients [333].

In 2012, the Baumeister Lab designed and characterized a new pan-neuronal *C. elegans* model of tauopathy. Even though ROS content was not evaluated, the authors demonstrated that the aggregation of p-tau in neurons caused locomotive alterations related to neuronal proteotoxicity, starting at day 1 of adulthood [136]. Hence, to examine the impact of the low and high-OL extracts in mitigating p-tau-induced oxidative stress, the measurement of intracellular ROS levels was conducted in the tauopathy strain of *C. elegans*. For this purpose, the H_2DCFDA dye method was employed to assess intracellular ROS levels at day 1 of adulthood, replicating the conditions observed in the work proposed by Fatouros *et al.* [136].

Surprisingly, both low and high-OL extracts failed to prevent intracellular ROS accumulation in comparison to the positive control (**Figure 42**). Given that evidence about the role of OL extract in mitigating h-tau neurotoxicity is extremely limited, the evaluation of oxidative stress modulation by this by-product in tauopathy is null. Among the 42 compounds quantified in the present research, only the role of luteolin has been investigated in countering the oxidative damage induced by p-

tau aggregation. In this study, exposure to different luteolin concentrations (1.43-28.6 μg/ml) was able to reduce zinc-induced tau protein hyperphosphorylation through the reduction of zinc-induced ROS in SH-SY5Y cells. In the present research, the content of lutein and its derivatives in the low and high-OL extract was 12 times lower and 4 times higher, respectively, than the lowest dose assayed in SH-SY5Y cells [334]. Notwithstanding, no significant preventive effect on intracellular ROS accumulation was observed in this specific strain.

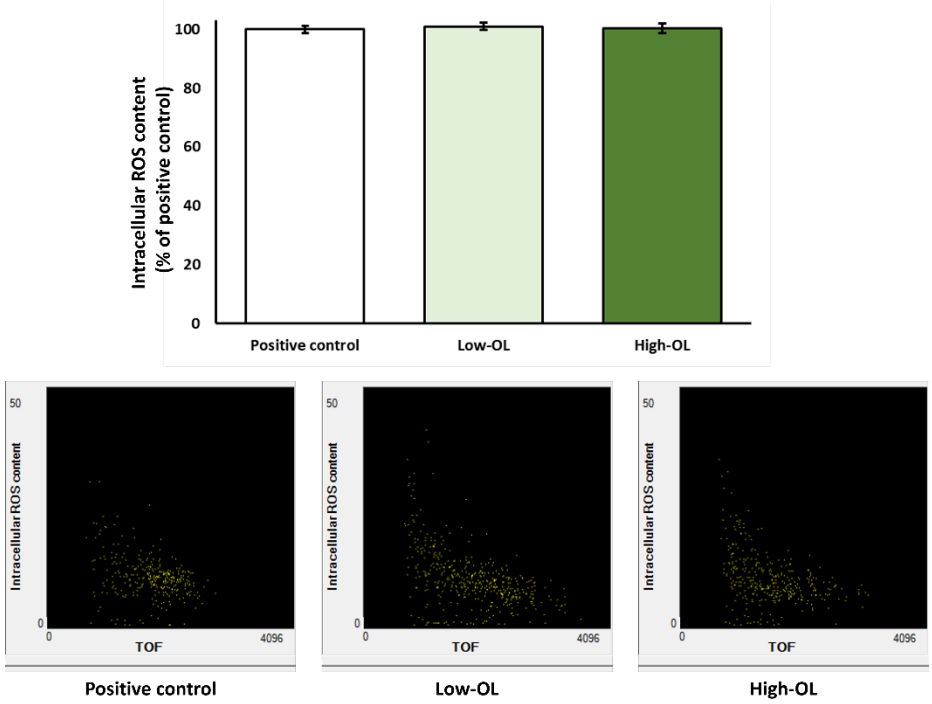

Figure 42. Intracellular reactive oxygen species (ROS) content of BR5706 and representative dot plots. Nematodes from BR5706 strain treated with or without 500 μg/ml of low or high-OL extracts. Dot plot of intracellular ROS content *vs.* TOF (time of flight; worm size) representative panels for each experimental group of yellow fluorescence intensity extracted from flow cytometer software are presented. Different letters mean statistically significant differences ($p < 0.05$). Results are expressed as mean ± SEM. Abbreviatures: OL: olive leaves.

11.3.1.2. Mitochondrial ROS content

To examine the impact of the low and high-OL extracts in mitigating p-tau-induced mitochondrial oxidative stress, the measurement of mitochondrial ROS levels was conducted in the tauopathy strain of *C. elegans*. For this purpose, the MitoTracker Red CM-H_2XRos dye was employed to assess mitochondrial ROS levels at day 1 of adulthood.

Contrarily to intracellular ROS content test, both low and high-OL extracts were able to prevent mitochondrial ROS accumulation in comparison to the positive control (**Figure 43**). However, the greatest effect was exerted by the high-OL extract (∇73%), which correlates with the highest SOD-2 involvement (Δ39%) in RNAi experiments. In fact, RNAi experiments demonstrated that DAF-16/FOXO and SKN-1/NRF-2 RNAi knock down exerted a complete abolition of the therapeutic effect of the high-OL extract, even lower than the positive control. These experiments suggested that this effect may be produced by a prolonged exposure to mild stressors which stimulates the enhancement of defense mechanisms such as SOD-2. In alignment with the results presented in this section, a great reduction of mitochondrial ROS content was observed in high-OL extract treated nematodes. The combination of the RNAi and GFP-reporter experiments as well as the results presented in this section strongly support the potential mitohormetic effect suggested by high-OL extract in this strain.

In the other hand, the nematodes exposed to low-OL extract led to a 52% lesser accumulation in mitochondrial ROS, which correlates with the SOD-2 involvement (Δ32%) in the RNAi experiments. In the same way, low-OL extract exposition was also involved as hormetic stressor in this strain through DAF-16/FOXO, SKN-1/NRF-2 and HSP-16.2 involvement. Thus, these results could indicate that the phenolic content in the present in the low-OL extract may be sufficient to induce mild-induced stress, while the individual phytochemical content may play a

role in influencing the molecular pathways involved in the observed variations in this specific *C. elegans* strain at the tested doses.

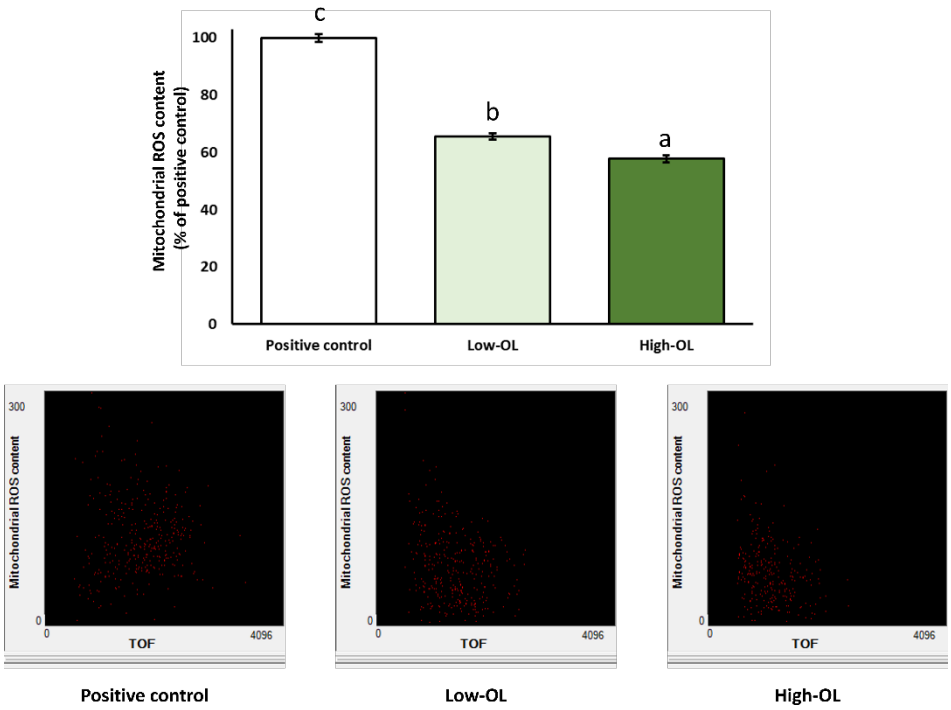

Figure 43. Mitochondrial reactive oxygen species (ROS) content of BR5706 and representative dot plots. Nematodes from BR5706 strain treated with or without 500 μg/ml of low or high-OL extracts. Dot plot of mitochondrial ROS content *vs.* TOF (time of flight; worm size) representative panels for each experimental group of red fluorescence intensity extracted from flow cytometer software are presented. Different letters mean statistically significant differences ($p < 0.05$). Results are expressed as mean ± SEM. Abbreviatures: OL: olive leaves.

An interesting aspect warrants discussion. As previously mentioned, it has been suggested that overproduction of p-tau increases intracellular ROS content through macromolecule oxidation as well as mitochondrial dysfunction [332,333]. However, this rise in mitochondrial ROS levels has not been reflected in an increase in intracellular ROS content. This disparity could potentially be attributed to the dye used for total ROS content determination. Specifically, H_2DCFDA is a cell-permeant acetylated form of fluorescein that enters the cytoplasm. Inside the cell, H_2DCFDA is acted upon by esterases, removing the acetyl groups

and forming a non-fluorescent moiety (H_2DCF) that can be oxidized by intracellular ROS to generate the fluorescent product (DCF) [335].

However, it is known that in some cell types with low esterase activity or where esterases are sequestered in inaccessible parts of the cell, detecting variations in ROS levels can be challenging because H_2DCFDA needs to be hydrolyzed to H_2DCF by cellular esterases [336]. In *C. elegans*, locomotion is regulated by acetylcholine-releasing excitatory motor neurons and GABA (γ-aminobutyric acid)-releasing inhibitory motor neurons. Acetylcholine released from cholinergic motor neurons activates acetylcholine receptors on the muscle membrane, leading to muscle excitation and contraction [135]. In the BR5706 strain, a significant impairment of presynaptic transmission has been described, resulting in low neurotransmitter production in motor neurons. This reduced neurotransmitter production is associated with moderate resistance to esterase inhibitors, likely due to the low production of cholinergic esterases [337].

Considering the information presented along with the results obtained in the assessment of mitochondrial ROS content, it is possible that H_2DCFDA might not be an optimal method to employ in this strain due to potential saturation of esterases before reaching the peak measurement of ROS, owing to its low concentration. Indeed, the raw intracellular ROS content for positive controls from both the amyloidogenic and tauopathy strains was found to be 16.5 times higher in the tauopathy strain, thereby providing support for the previously mentioned hypothesis.

11.3.1.3. Glutathione content

To examine the impact of the low and high-OL extracts in GSH content, the measurement of GSH levels was conducted in the *C. elegans* model of tauopathy. For this purpose, the nematodes were growth in the same conditions as exposed previously and the MCB dye was used to determinate the total GSH content at day 1 of adulthood. As described **Figure 44**, the treatment with low and high-OL extract led to higher GSH content in 36% and 17% in the nematodes treated, respectively. These results are in accordance with those obtained in the mitochondrial ROS content assessment, which showed a reduction in the ROS content.

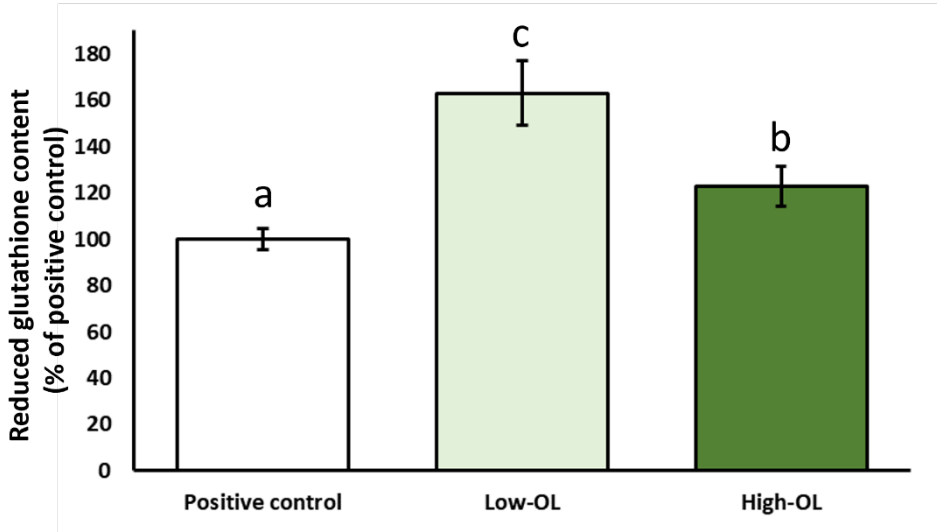

Figure 44. Reduced glutathione (GSH) content measured by monochlorobimane staining in BR5706 nematodes. Nematodes from BR5706 strain treated with or without 500 μg/ml of low or high-OL extracts Different letters mean statistically significant differences ($p < 0.05$). Results are expressed as mean ± SEM. Abbreviatures: OL: olive leaves.

Interestingly, the nematodes treated with low-OL extract exhibited the highest GSH content. In contrast to the findings in the amyloidogenic strain, the protective effect of the extract in the tauopathy strain was associated with the involvement of SOD-2 and HSP-16.2. As previously mentioned, HSP-16.2's influence on GSH levels and the

antioxidative effect of SOD-2's involvement may lead to a reduction in expended GSH [255]. These results could provide an explanation, at least partially, for the elevated GSH content observed in nematodes treated with low-OL extract in this strain.

However, it is important to note that mitochondrial GSH primarily participates in the detoxification of H_2O_2 generated by MnSOD [338–340]. Consequently, an excessive activity of SOD-2 might result in increased H_2O_2 production and greater utilization of GSH, as previously documented [338]. Therefore, the lower GSH content found in nematodes treated with high-OL extract could potentially be a consequence of involvement of SOD-2 in the reduction in mitochondrial ROS content. This hypothesis aligns with the observations in the amyloidogenic strain, where the mitochondrial ROS content decreased by 36% in response to high-OL extract treatment. Similarly, in the tauopathy strain, the reduction in mitochondrial ROS content was even more substantial at 73%. This decrease in mitochondrial ROS was accompanied by an increase in GSH content by 36% in the amyloidogenic strain and 17% in the tauopathy strain. Notably, a clear trend emerges where decreased mitochondrial ROS levels are correlated with lower GSH levels. Intriguingly, in the tauopathy strain, despite the mitochondrial ROS content being reduced by two-fold, the decrease in GSH content was 2.1 times greater than the amyloidogenic strain. This pattern is consistent across both strains and underscores the significant involvement of SOD-2 in the protective effects of high-OL extract.

These findings strongly suggest that the lower GSH content in high-OL extract-treated nematodes could be attributed to the robust engagement of SOD-2 in mediating the protective effects of high-OL extract in this strain. Notwithstanding, a limitation of the present study is that it was only measured the total reduced GSH content and GST-4 levels, while the oxidized GSSG or GSH/GSSG ratio as well as GSSG reductases were not evaluated. Therefore, even though plausible, more research is needed to confirm this hypothesis.

The modulatory effects of the three OL extracts on some of the pathological parameters of AD are summarized in **Figure 45**.

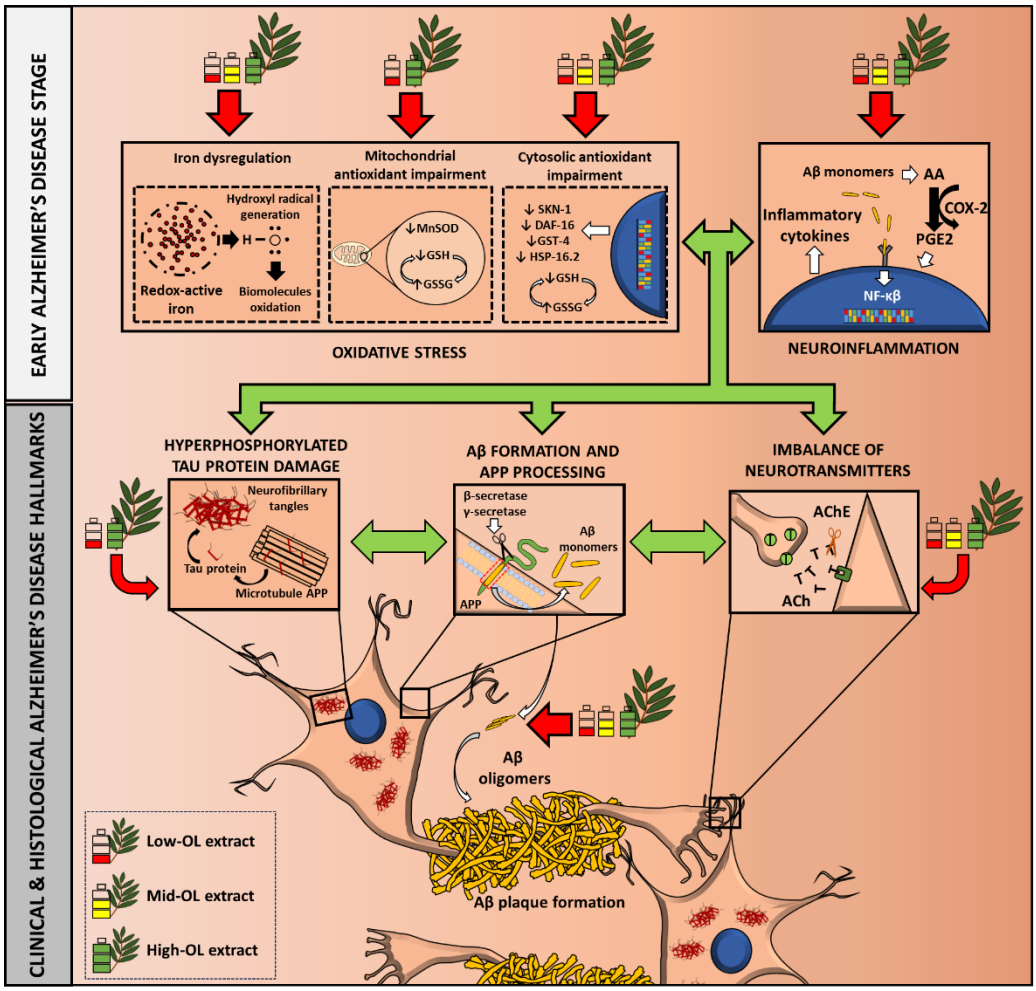

Figure 45. Modulatory effects of the three olive leaves extracts on some of the pathological markers of Alzheimer's Disease. Green arrows represent promotion of the process, whereas red arrows represent reduction in the process. Abbreviatures: AA: arachidonic acid; AChE: acetylcholinesterase; APP: amyloid precursor protein; Aβ: amyloid beta; COX-: cyclooxygenase-2; DAF: abnormal dauer formation; GST: glutathione S transferase; GSH: glutathione; GSSG: glutathione disulfide; HSP: heat shock protein; NFT: neurofibrillary tangles; MnSOD: manganese superoxide dismutase; PGE2: prostaglandin E2; SKN: skinhead; OL: olive leaves.

SECTION V: CONCLUSIONS

Conclusions

Conclusion 1: on characterization and TAC of olive leaf extracts

The results pointed out that the geographical origin considerably influenced the phytochemical profile of the olive leaf extracts, especially in relation to the content of secoiridoids, flavonoids, iridoids, hydroxycoumarins, and hydroxycinnamic acids. The antioxidant capacity was associated with the total content of phenolic compounds and flavonoids, which stood out in the samples from Spain and Italy. It was also shown that the inhibitory cholinesterase activity was influenced by several compounds present in the OL, with the Spanish, Italian, and Portuguese samples being the most interesting for this purpose. Despite the remarkable ability to inhibit COX-2 activity exerted by the different OLs, no origin-related effect was observed for this marker among the investigated countries.

Conclusion 2: on toxicity tests

The large-scale assessment of the fifty olive leaf extracts demonstrated absence of lethal toxicity in the *C. elegans* Wild type, as demonstrated by lethality, growth and embryotoxicity test. Notwithstanding, minor toxic effects in terms of lower growth of the nematodes were detected in olive leaf extracts with elevated content in apigenin, eriodyctiol, esculin, or decaffeoylverbascoside.

Conclusion 3: on Alzheimer's Disease markers *in vitro*

OL extract demonstrated significant anti-inflammatory, anti-cholinergic, and antioxidant activities. Compounds like luteolin-7-O-glucoside, isoharmnentin, and apigenin derivatives were identified as significant contributors to the AChE inhibitory activity. Among the rest of compounds, oleuropein derivatives, and hydroxytyrosol showed noteworthy potential. Regarding COX-2 inhibitory activity, the enrichment of OL in secoiridoids seemed to be a significant determinant

of the observed inhibitory effect. Oleuropein and its derivatives, along with ligstroside content, may exert an important role in the COX-2 inhibitory activity. Among the rest of compounds, luteolin 7-O-glucoside and verbascoside should be highlighted. In the same way, the diosmetin seems to be negatively associated with inhibitory effect of OL, probably attributed to the conversion of luteolin to diosmetin. Finally, authors demonstrated that both secoiridoids and flavonoids were found to contribute equally to the observed antioxidant effect. To cite, oleuropein and its derivatives, ligstroside and luteolin-7-O-glucoside content, may exert an important role in the ferric reducing antioxidant capacity. Among the rest of compounds, hydroxytyrosol, hydroxycoumarins, and verbascoside content must be highlighted. In the same way, the three olive leaf extracts have demonstrated a moderate *in vitro* inhibitory capacity of the AChE, COX-2, and iron-reducing activity, being the high-OL extract the most effective.

Conclusion 4: on Alzheimer's Disease markers *in vivo*

The low and high-OL extract showed remarkable results against Aβ and tau proteotoxicity *in vivo*. Mid-OL exerts a slight improvement of amyloidogenic toxicity but did not affect to the locomotive behavior, which could be attributed to the apigenin derivatives content. The transcription factors SKN-1/NRF-2 and its downstream SOD-2 and SOD-3 has been demonstrated to be involved in the effects of low and high-OL extracts. HSP-16.2 has been shown to participate in mid-OL extracts benefits.

Conclusion 5: on redox biology markers of Alzheimer's Disease

The three olive leaf extracts were able to modulate redox biology through hormetic stress response but in a different way. All the extract were able to promote the nucleation of DAF-16/FOXO, whereas only low and high OL extract induced SKN-1/NRF-2 nucleation. In presence of amyloidogenic pathology, all of them had great activity preventing an excess of intracellular ROS content, being the low-OL extract the most

active. The protective effects exerted by low, mid, and high-OL extract effects on GSH metabolism may involve GST-4, HSP-16.2, and SOD-2, respectively. At the mitochondrial level, only high-OL extract was able to prevent ROS content accumulation, through the involvement of SOD-2. In the hyperphosphorylated tau strain, both low and high OL extract partially prevented mitochondrial ROS content accumulation through the involvement of DAF-16/SKN-1 and its direct downstream SOD-2 and SOD-3.

General conclusion

The findings from this Doctoral Thesis support the initial hypothesis since the olive leaves, rich in bioactive compounds, were able to modulate the pathogenesis of Alzheimer's disease. Results endorse that, at least in part, the effects of the three olive leaves on AD have been exerted through the modulation of redox biology, despite additional pathways could also be involved. Future research should be carried out to delve into the molecular mechanisms underlying the effect of treatments on aging.

Overall, these results open the door for the design and testing of nutraceuticals based on olive leaf extracts aimed at preventing or mitigating various aspects related to Alzheimer's disease.

Conclusiones

Conclusión 1: sobre caracterización y capacidad antioxidante de los extractos de hoja de olivo

Los resultados señalaron que el origen geográfico influyó considerablemente en el perfil fitoquímico de las hojas de olivo, especialmente en relación con el contenido de secoiridoides, flavonoides, iridoides, hidroxicumarinas y ácidos hidroxicinámicos. La capacidad antioxidante se asoció con el contenido total de compuestos fenólicos y de flavonoides, que destacaron en las muestras de España e Italia. También se demostró que la actividad inhibidora de la colinesterasa estaba influenciada por varios compuestos presentes en el extracto de OL, siendo las muestras españolas, italianas y portuguesa las más interesantes para este propósito. A pesar de la notable capacidad para inhibir la actividad de la COX-2 ejercida por los diferentes extractos, no se observó ningún efecto relacionado con el origen de este marcador entre los países investigados.

Conclusión 2: sobre las pruebas de toxicidad

La evaluación a gran escala de los cincuenta extractos de hoja de olivo demostró la ausencia de toxicidad letal en el *C. elegans*, como lo demuestran las pruebas de letalidad, crecimiento y embriotoxicidad. No obstante, se detectaron efectos tóxicos menores en términos de menor crecimiento de los nematodos en extractos de hoja de olivo que presentaron un elevado contenido en apigenina, eriodyctiol, esculina o decaffeoilverbascósido.

Conclusión 3: sobre marcadores de la Enfermedad de Alzheimer *in vitro*

El extracto OL demostró importantes actividades antiinflamatorias, anticolinérgicas y antioxidantes. Se identificaron compuestos como luteolin-7-O-glucósido, isoharmnentina y derivados de

apigenina como contribuyentes importantes a la actividad de la AChEI. Entre el resto de los compuestos, destacan los derivados de la oleuropeína y el hidroxitirosol. En cuanto a la actividad inhibidora de la COX-2, el enriquecimiento de OL en secoiridoides parecía ser un determinante significativo del efecto inhibidor observado. La oleuropeína y sus derivados, junto con el contenido de ligstrosido, pueden ejercer un papel importante en la actividad inhibidora de la COX-2. Entre el resto de los compuestos, cabe destacar la luteolina 7-O-glucósido y el verbascósido. De la misma manera, la diosmetina parece estar asociada negativamente con el efecto inhibidor de la OL, probablemente atribuido a la conversión de luteolina en diosmetina. Tanto los secoiridoides como los flavonoides contribuyen por igual al efecto antioxidante observado. Por ejemplo, la oleuropeína y sus derivados, el contenido de ligstrosido y luteolin-7-O-glucósido, pueden ejercer un papel importante en la capacidad antioxidante reductora del hierro. Entre el resto de los compuestos destaca el contenido en hidroxitirosol, hidroxicumarinas y verbascósidos. Del mismo modo, los tres extractos de hoja de olivo han demostrado una moderada capacidad inhibidora *in vitro* de la AChE, COX-2 y la actividad reductora de hierro, siendo el extracto high OL el más eficaz.

Conclusión 4: sobre los marcadores de la enfermedad de Alzheimer *in vivo*

El extracto de low y high OL mostraron resultados notables contra la proteotoxicidad de Aβ y tau *in vivo*. Mid-OL ejerció una ligera mejora de la toxicidad amiloidogénica pero no afectó al comportamiento locomotor, lo que podría atribuirse al contenido de derivados de apigenina. Se ha demostrado que los factores de transcripción SKN-1/NRF-2 y sus dianas SOD-2 y SOD-3 están involucrados en los efectos de los extractos de low y high OL. Se ha demostrado que HSP-16.2 participa en los beneficios de los extractos de Mid-OL.

Conclusión 5: sobre la biología redox en la enfermedad de Alzheimer

Los tres extractos de hoja de olivo pudieron modular la biología redox a través de la respuesta al estrés hormético, pero de una manera diferente. Todos los extractos fueron capaces de promover la nucleación de DAF-16/FOXO, mientras que solo los extractos low y high OL indujeron la nucleación de SKN-1/NRF-2. En presencia de patología amiloidogénica, todos tuvieron una gran actividad previniendo un exceso de contenido de ROS intracelular, siendo el extracto de low OL el más activo. Los efectos protectores ejercidos por los efectos del extracto de OL bajo, medio y alto sobre el metabolismo del GSH pueden involucrar a GST-4, HSP-16.2 y SOD-2, respectivamente. A nivel mitocondrial, sólo el extracto high OL fue capaz de prevenir la acumulación de ROS mediante la participación de SOD-2. En la cepa tau hiperfosforilada, tanto el extracto low OL como el high OL previnieron parcialmente la acumulación de ROS mitocondriales mediante la participación de DAF-16/SKN-1 y sus dianas SOD-2 y SOD-3.

Conclusión general

Los hallazgos de esta Tesis Doctoral apoyan la hipótesis inicial ya que las hojas de olivo, ricas en compuestos bioactivos, fueron capaces de modular la patogénesis de la enfermedad de Alzheimer. Los resultados avalan que, al menos en parte, los efectos de las tres hojas de olivo sobre la enfermedad de Alzheimer se han ejercido mediante la modulación de la biología redox, aunque también podrían estar implicadas vías adicionales. Se deberían realizar futuras investigaciones para profundizar en los mecanismos moleculares que subyacen al efecto de los tratamientos sobre el envejecimiento.

En general, estos resultados abren la puerta al diseño y ensayo de nutracéuticos basados en extractos de hoja de olivo destinados a prevenir o mitigar diversos aspectos relacionados con la enfermedad de Alzheimer.

SECTION V: REFERENCES

1. Selim, S.; Albqmi, M.; Al-Sanea, M.M.; Alnusaire, T.S.; Almuhayawi, M.S.; AbdElgawad, H.; Al Jaouni, S.K.; Elkelish, A.; Hussein, S.; Warrad, M.; et al. Valorizing the Usage of Olive Leaves, Bioactive Compounds, Biological Activities, and Food Applications: A Comprehensive Review. *Front Nutr* **2022**, *9*, 1008349, doi:10.3389/fnut.2022.1008349.
2. Espeso, J.; Isaza, A.; Lee, J.Y.; Sörensen, P.M.; Jurado, P.; Avena-Bustillos, R. de J.; Olaizola, M.; Arboleya, J.C. Olive Leaf Waste Management. *Frontiers in Sustainable Food Systems* **2021**, *5*.
3. Agra CEAS Consulting Ltd; Arcadia; Areté; Directorate-General for Agriculture and Rural Development (European Commission) *Study on the Implementation of Conformity Checks in the Olive Oil Sector throughout the European Union*; Publications Office of the European Union: LU, 2020; ISBN 978-92-76-09264-3.
4. Zhang, C.; Xin, X.; Zhang, J.; Zhu, S.; Niu, E.; Zhou, Z.; Liu, D. Comparative Evaluation of the Phytochemical Profiles and Antioxidant Potentials of Olive Leaves from 32 Cultivars Grown in China. *Molecules* **2022**, *27*, 1292, doi:10.3390/molecules27041292.
5. Romero-Márquez, J.M.; Forbes-Hernández, T.Y.; Navarro-Hortal, M.D.; Quirantes-Piné, R.; Grosso, G.; Giampieri, F.; Lipari, V.; Sánchez-González, C.; Battino, M.; Quiles, J.L. Molecular Mechanisms of the Protective Effects of Olive Leaf Polyphenols against Alzheimer's Disease. *Int J Mol Sci* **2023**, *24*, 4353, doi:10.3390/ijms24054353.
6. Romero-Márquez, J.M.; Navarro-Hortal, M.D.; Jiménez-Trigo, V.; Vera-Ramírez, L.; Forbes-Hernández, T.J.; Esteban-Muñoz, A.; Giampieri, F.; Bullón, P.; Battino, M.; Sánchez-González, C.; et al. An Oleuropein Rich-Olive (Olea Europaea L.) Leaf Extract Reduces β-Amyloid and Tau Proteotoxicity through Regulation of Oxidative- and Heat Shock-Stress Responses in Caenorhabditis Elegans. *Food Chem Toxicol* **2022**, *162*, 112914, doi:10.1016/j.fct.2022.112914.
7. Lama-Muñoz, A.; Contreras, M. del M.; Espínola, F.; Moya, M.; Romero, I.; Castro, E. Content of Phenolic Compounds and Mannitol in Olive Leaves Extracts from Six Spanish Cultivars: Extraction with the Soxhlet Method and Pressurized Liquids. *Food Chemistry* **2020**, *320*, 126626, doi:10.1016/j.foodchem.2020.126626.
8. Alcántara, C.; Žugčić, T.; Abdelkebir, R.; García-Pérez, J.V.; Jambrak, A.R.; Lorenzo, J.M.; Collado, M.C.; Granato, D.; Barba, F.J. Effects of Ultrasound-Assisted Extraction and Solvent on the Phenolic Profile, Bacterial Growth, and Anti-Inflammatory/Antioxidant Activities of Mediterranean Olive and Fig Leaves Extracts. *Molecules* **2020**, *25*, 1718, doi:10.3390/molecules25071718.
9. Kabbash, E.M.; Ayoub, I.M.; Gad, H.A.; Abdel-Shakour, Z.T.; El-Ahmady, S.H. Quality Assessment of Leaf Extracts of 12 Olive Cultivars and Impact of Seasonal Variation Based on UV Spectroscopy and Phytochemcial

Content Using Multivariate Analyses. *Phytochem Anal* **2021**, *32*, 932–941, doi:10.1002/pca.3036.

10. Zhang, C.; Zhang, J.; Xin, X.; Zhu, S.; Niu, E.; Wu, Q.; Li, T.; Liu, D. Changes in Phytochemical Profiles and Biological Activity of Olive Leaves Treated by Two Drying Methods. *Front Nutr* **2022**, *9*, 854680, doi:10.3389/fnut.2022.854680.
11. Nicolì, F.; Negro, C.; Vergine, M.; Aprile, A.; Nutricati, E.; Sabella, E.; Miceli, A.; Luvisi, A.; De Bellis, L. Evaluation of Phytochemical and Antioxidant Properties of 15 Italian Olea Europaea L. Cultivar Leaves. *Molecules* **2019**, *24*, 1998, doi:10.3390/molecules24101998.
12. Pasković, I.; Lukić, I.; Žurga, P.; Majetić Germek, V.; Brkljača, M.; Koprivnjak, O.; Major, N.; Grozić, K.; Franić, M.; Ban, D.; et al. Temporal Variation of Phenolic and Mineral Composition in Olive Leaves Is Cultivar Dependent. *Plants (Basel)* **2020**, *9*, E1099, doi:10.3390/plants9091099.
13. Makowska-Wąs, J.; Galanty, A.; Gdula-Argasińska, J.; Tyszka-Czochara, M.; Szewczyk, A.; Nunes, R.; Carvalho, I.S.; Michalik, M.; Paśko, P. Identification of Predominant Phytochemical Compounds and Cytotoxic Activity of Wild Olive Leaves (Olea Europaea L. Ssp. Sylvestris) Harvested in South Portugal. *Chem Biodivers* **2017**, *14*, doi:10.1002/cbdv.201600331.
14. Mmopele, K.; Combrinck, S.; Hamman, J.; Willers, C.; Chen, W.; Viljoen, A. Potential Herb-Drug Pharmacokinetic Interactions between African Wild Olive Leaf Extract and Selected Antihypertensive Drugs. *Planta Med* **2018**, *84*, 886–894, doi:10.1055/a-0583-0543.
15. Yu, M.; Gouvinhas, I.; Rocha, J.; Barros, A.I.R.N.A. Phytochemical and Antioxidant Analysis of Medicinal and Food Plants towards Bioactive Food and Pharmaceutical Resources. *Sci Rep* **2021**, *11*, 10041, doi:10.1038/s41598-021-89437-4.
16. Kontogianni, V.G.; Charisiadis, P.; Margianni, E.; Lamari, F.N.; Gerothanassis, I.P.; Tzakos, A.G. Olive Leaf Extracts Are a Natural Source of Advanced Glycation End Product Inhibitors. *J Med Food* **2013**, *16*, 817–822, doi:10.1089/jmf.2013.0016.
17. Sarikurkcu, C.; Locatelli, M.; Tartaglia, A.; Ferrone, V.; Juszczak, A.M.; Ozer, M.S.; Tepe, B.; Tomczyk, M. Enzyme and Biological Activities of the Water Extracts from the Plants Aesculus Hippocastanum, Olea Europaea and Hypericum Perforatum That Are Used as Folk Remedies in Turkey. *Molecules* **2020**, *25*, E1202, doi:10.3390/molecules25051202.
18. González, E.; Gómez-Caravaca, A.M.; Giménez, B.; Cebrián, R.; Maqueda, M.; Martínez-Férez, A.; Segura-Carretero, A.; Robert, P. Evolution of the Phenolic Compounds Profile of Olive Leaf Extract Encapsulated by Spray-Drying during in Vitro Gastrointestinal Digestion. *Food Chem* **2019**, *279*, 40–48, doi:10.1016/j.foodchem.2018.11.127.
19. Romero-Márquez, J.M.; Navarro-Hortal, M.D.; Forbes-Hernández, T.Y.; Varela-López, A.; Puentes, J.G.; Pino-García, R.D.; Sánchez-González, C.;

Elio, I.; Battino, M.; García, R.; et al. Exploring the Antioxidant, Neuroprotective, and Anti-Inflammatory Potential of Olive Leaf Extracts from Spain, Portugal, Greece, and Italy. *Antioxidants* **2023**, *12*, 1538, doi:10.3390/antiox12081538.

20. Martín-Vertedor, D.; Garrido, M.; Pariente, J.A.; Espino, J.; Delgado-Adámez, J. Bioavailability of Bioactive Molecules from Olive Leaf Extracts and Its Functional Value. *Phytother Res* **2016**, *30*, 1172–1179, doi:10.1002/ptr.5625.
21. Hashmi, M.A.; Khan, A.; Hanif, M.; Farooq, U.; Perveen, S. Traditional Uses, Phytochemistry, and Pharmacology of Olea Europaea (Olive). *Evid Based Complement Alternat Med* **2015**, *2015*, 541591, doi:10.1155/2015/541591.
22. Clewell, A.E.; Béres, E.; Vértesi, A.; Glávits, R.; Hirka, G.; Endres, J.R.; Murbach, T.S.; Szakonyiné, I.P. A Comprehensive Toxicological Safety Assessment of an Extract of Olea Europaea L. Leaves (Bonolive™). *Int J Toxicol* **2016**, *35*, 208–221, doi:10.1177/1091581815619764.
23. Gallego, R.; Suárez-Montenegro, Z.J.; Ibáñez, E.; Herrero, M.; Valdés, A.; Cifuentes, A. In Vitro Neuroprotective Potential and Lipidomics Study of Olive Leaves Extracts Enriched in Triterpenoids. *Front Nutr* **2021**, *8*, 769218, doi:10.3389/fnut.2021.769218.
24. Chandler, D.; Woldu, A.; Rahmadi, A.; Shanmugam, K.; Steiner, N.; Wright, E.; Benavente-García, O.; Schulz, O.; Castillo, J.; Münch, G. Effects of Plant-Derived Polyphenols on TNF-Alpha and Nitric Oxide Production Induced by Advanced Glycation Endproducts. *Mol Nutr Food Res* **2010**, *54 Suppl 2*, S141-150, doi:10.1002/mnfr.200900504.
25. Misganaw, D.; Engidawork, E.; Nedi, T. Evaluation of the Anti-Malarial Activity of Crude Extract and Solvent Fractions of the Leaves of Olea Europaea (Oleaceae) in Mice. *BMC Complement Altern Med* **2019**, *19*, 171, doi:10.1186/s12906-019-2567-8.
26. Romero-Márquez, J.M.; Navarro-Hortal, M.D.; Jiménez-Trigo, V.; Vera-Ramírez, L.; Forbes-Hernández, T.J.; Esteban-Muñoz, A.; Giampieri, F.; Bullón, P.; Battino, M.; Sánchez-González, C.; et al. An Oleuropein Rich-Olive (Olea Europaea L.) Leaf Extract Reduces β-Amyloid and Tau Proteotoxicity through Regulation of Oxidative- and Heat Shock-Stress Responses in Caenorhabditis Elegans. *Food Chem Toxicol* **2022**, *162*, 112914, doi:10.1016/j.fct.2022.112914.
27. Anter, J.; Fernández-Bedmar, Z.; Villatoro-Pulido, M.; Demyda-Peyras, S.; Moreno-Millán, M.; Alonso-Moraga, A.; Muñoz-Serrano, A.; Luque de Castro, M.D. A Pilot Study on the DNA-Protective, Cytotoxic, and Apoptosis-Inducing Properties of Olive-Leaf Extracts. *Mutat Res* **2011**, *723*, 165–170, doi:10.1016/j.mrgentox.2011.05.005.
28. Guex, C.G.; Reginato, F.Z.; Figueredo, K.C.; da Silva, A.R.H. da; Pires, F.B.; Jesus, R. da S.; Lhamas, C.L.; Lopes, G.H.H.; Bauermann, L. de F. Safety Assessment of Ethanolic Extract of Olea Europaea L. Leaves after Acute

and Subacute Administration to Wistar Rats. *Regul Toxicol Pharmacol* **2018**, *95*, 395–399, doi:10.1016/j.yrtph.2018.04.013.
29. Filip, R.; Possemiers, S.; Heyerick, A.; Pinheiro, I.; Raszewski, G.; Davicco, M.-J.; Coxam, V. Twelve-Month Consumption of a Polyphenol Extract from Olive (Olea Europaea) in a Double Blind, Randomized Trial Increases Serum Total Osteocalcin Levels and Improves Serum Lipid Profiles in Postmenopausal Women with Osteopenia. *J Nutr Health Aging* **2015**, *19*, 77–86, doi:10.1007/s12603-014-0480-x.
30. de Bock, M.; Thorstensen, E.B.; Derraik, J.G.B.; Henderson, H.V.; Hofman, P.L.; Cutfield, W.S. Human Absorption and Metabolism of Oleuropein and Hydroxytyrosol Ingested as Olive (Olea Europaea L.) Leaf Extract. *Mol Nutr Food Res* **2013**, *57*, 2079–2085, doi:10.1002/mnfr.201200795.
31. Susalit, E.; Agus, N.; Effendi, I.; Tjandrawinata, R.R.; Nofiarny, D.; Perrinjaquet-Moccetti, T.; Verbruggen, M. Olive (Olea Europaea) Leaf Extract Effective in Patients with Stage-1 Hypertension: Comparison with Captopril. *Phytomedicine* **2011**, *18*, 251–258, doi:10.1016/j.phymed.2010.08.016.
32. Lockyer, S.; Corona, G.; Yaqoob, P.; Spencer, J.P.E.; Rowland, I. Secoiridoids Delivered as Olive Leaf Extract Induce Acute Improvements in Human Vascular Function and Reduction of an Inflammatory Cytokine: A Randomised, Double-Blind, Placebo-Controlled, Cross-over Trial. *Br J Nutr* **2015**, *114*, 75–83, doi:10.1017/S0007114515001269.
33. García-Villalba, R.; Larrosa, M.; Possemiers, S.; Tomás-Barberán, F.A.; Espín, J.C. Bioavailability of Phenolics from an Oleuropein-Rich Olive (Olea Europaea) Leaf Extract and Its Acute Effect on Plasma Antioxidant Status: Comparison between Pre- and Postmenopausal Women. *Eur J Nutr* **2014**, *53*, 1015–1027, doi:10.1007/s00394-013-0604-9.
34. Hill, E.; Goodwill, A.M.; Gorelik, A.; Szoeke, C. Diet and Biomarkers of Alzheimer's Disease: A Systematic Review and Meta-Analysis. *Neurobiol Aging* **2019**, *76*, 45–52, doi:10.1016/j.neurobiolaging.2018.12.008.
35. Zhang, X.-X.; Tian, Y.; Wang, Z.-T.; Ma, Y.-H.; Tan, L.; Yu, J.-T. The Epidemiology of Alzheimer's Disease Modifiable Risk Factors and Prevention. *J Prev Alzheimers Dis* **2021**, *8*, 313–321, doi:10.14283/jpad.2021.15.
36. Erkkinen, M.G.; Kim, M.-O.; Geschwind, M.D. Clinical Neurology and Epidemiology of the Major Neurodegenerative Diseases. *Cold Spring Harb Perspect Biol* **2018**, *10*, a033118, doi:10.1101/cshperspect.a033118.
37. Chu, L.W. Alzheimer's Disease: Early Diagnosis and Treatment. *Hong Kong Med J* **2012**, *18*, 228–237.
38. GBD 2016 Causes of Death Collaborators Global, Regional, and National Age-Sex Specific Mortality for 264 Causes of Death, 1980-2016: A Systematic Analysis for the Global Burden of Disease Study 2016. *Lancet* **2017**, *390*, 1151–1210, doi:10.1016/S0140-6736(17)32152-9.

39. Niu, H.; Álvarez-Álvarez, I.; Guillén-Grima, F.; Aguinaga-Ontoso, I. Prevalencia e incidencia de la enfermedad de Alzheimer en Europa: metaanálisis. *Neurología* **2017**, *32*, 523–532, doi:10.1016/j.nrl.2016.02.016.
40. Dorszewska, J.; Prendecki, M.; Oczkowska, A.; Dezor, M.; Kozubski, W. Molecular Basis of Familial and Sporadic Alzheimer's Disease. *Curr Alzheimer Res* **2016**, *13*, 952–963, doi:10.2174/1567205013666160314150501.
41. Bateman, R.J.; Aisen, P.S.; De Strooper, B.; Fox, N.C.; Lemere, C.A.; Ringman, J.M.; Salloway, S.; Sperling, R.A.; Windisch, M.; Xiong, C. Autosomal-Dominant Alzheimer's Disease: A Review and Proposal for the Prevention of Alzheimer's Disease. *Alzheimers Res Ther* **2011**, *3*, 1, doi:10.1186/alzrt59.
42. Ashrafian, H.; Zadeh, E.H.; Khan, R.H. Review on Alzheimer's Disease: Inhibition of Amyloid Beta and Tau Tangle Formation. *International Journal of Biological Macromolecules* **2021**, *167*, 382–394, doi:10.1016/j.ijbiomac.2020.11.192.
43. Lane, C.A.; Hardy, J.; Schott, J.M. Alzheimer's Disease. *Eur J Neurol* **2018**, *25*, 59–70, doi:10.1111/ene.13439.
44. Terry, A.V.; Buccafusco, J.J. The Cholinergic Hypothesis of Age and Alzheimer's Disease-Related Cognitive Deficits: Recent Challenges and Their Implications for Novel Drug Development. *J Pharmacol Exp Ther* **2003**, *306*, 821–827, doi:10.1124/jpet.102.041616.
45. Scheltens, P.; Strooper, B.D.; Kivipelto, M.; Holstege, H.; Chételat, G.; Teunissen, C.E.; Cummings, J.; Flier, W.M. van der Alzheimer's Disease. *The Lancet* **2021**, *397*, 1577–1590, doi:10.1016/S0140-6736(20)32205-4.
46. Crutch, S.J.; Lehmann, M.; Schott, J.M.; Rabinovici, G.D.; Rossor, M.N.; Fox, N.C. Posterior Cortical Atrophy. *Lancet Neurol* **2012**, *11*, 170–178, doi:10.1016/S1474-4422(11)70289-7.
47. Chen, Z.-R.; Huang, J.-B.; Yang, S.-L.; Hong, F.-F. Role of Cholinergic Signaling in Alzheimer's Disease. *Molecules* **2022**, *27*, 1816, doi:10.3390/molecules27061816.
48. Nuñez, M.T.; Chana-Cuevas, P. New Perspectives in Iron Chelation Therapy for the Treatment of Neurodegenerative Diseases. *Pharmaceuticals (Basel)* **2018**, *11*, 109, doi:10.3390/ph11040109.
49. Zhang, C.; Wang, Y.; Wang, D.; Zhang, J.; Zhang, F. NSAID Exposure and Risk of Alzheimer's Disease: An Updated Meta-Analysis From Cohort Studies. *Front Aging Neurosci* **2018**, *10*, 83, doi:10.3389/fnagi.2018.00083.
50. McGrattan, A.M.; McGuinness, B.; McKinley, M.C.; Kee, F.; Passmore, P.; Woodside, J.V.; McEvoy, C.T. Diet and Inflammation in Cognitive Ageing and Alzheimer's Disease. *Curr Nutr Rep* **2019**, *8*, 53–65, doi:10.1007/s13668-019-0271-4.
51. Mendiola-Precoma, J.; Berumen, L.C.; Padilla, K.; Garcia-Alcocer, G. Therapies for Prevention and Treatment of Alzheimer's Disease. *Biomed Res Int* **2016**, *2016*, 2589276, doi:10.1155/2016/2589276.

52. Caruso, G.; Torrisi, S.A.; Mogavero, M.P.; Currenti, W.; Castellano, S.; Godos, J.; Ferri, R.; Galvano, F.; Leggio, G.M.; Grosso, G.; et al. Polyphenols and Neuroprotection: Therapeutic Implications for Cognitive Decline. *Pharmacol Ther* **2022**, *232*, 108013, doi:10.1016/j.pharmthera.2021.108013.
53. Bhatia, N.K.; Srivastava, A.; Katyal, N.; Jain, N.; Khan, M.A.I.; Kundu, B.; Deep, S. Curcumin Binds to the Pre-Fibrillar Aggregates of Cu/Zn Superoxide Dismutase (SOD1) and Alters Its Amyloidogenic Pathway Resulting in Reduced Cytotoxicity. *Biochim Biophys Acta* **2015**, *1854*, 426–436, doi:10.1016/j.bbapap.2015.01.014.
54. Srivastava, A.; Arya, P.; Goel, S.; Kundu, B.; Mishra, P.; Fnu, A. Gelsolin Amyloidogenesis Is Effectively Modulated by Curcumin and Emetine Conjugated PLGA Nanoparticles. *PLoS One* **2015**, *10*, e0127011, doi:10.1371/journal.pone.0127011.
55. Arya, P.; Srivastava, A.; Vasaikar, S.V.; Mukherjee, G.; Mishra, P.; Kundu, B. Selective Interception of Gelsolin Amyloidogenic Stretch Results in Conformationally Distinct Aggregates with Reduced Toxicity. *ACS Chem Neurosci* **2014**, *5*, 982–992, doi:10.1021/cn500002v.
56. Admane, N.; Srivastava, A.; Jamal, S.; Sharma, R.; Kundu, B.; Grover, A. Molecular Insights into the Critical Role of Gallate Moiety of Green Tea Catechins in Modulating Prion Fibrillation, Cellular Internalization, and Neuronal Toxicity. *Int J Biol Macromol* **2022**, *223*, 755–765, doi:10.1016/j.ijbiomac.2022.11.049.
57. Omar, S.H.; Scott, C.J.; Hamlin, A.S.; Obied, H.K. Olive Biophenols Reduces Alzheimer's Pathology in SH-SY5Y Cells and APPswe Mice. *Int J Mol Sci* **2018**, *20*, E125, doi:10.3390/ijms20010125.
58. Gallego, R.; Suárez-Montenegro, Z.J.; Ibáñez, E.; Herrero, M.; Valdés, A.; Cifuentes, A. In Vitro Neuroprotective Potential and Lipidomics Study of Olive Leaves Extracts Enriched in Triterpenoids. *Front Nutr* **2021**, *8*, 769218, doi:10.3389/fnut.2021.769218.
59. Liang, J.; Pitsillou, E.; Man, A.Y.L.; Madzima, S.; Bresnehan, S.M.; Nakai, M.E.; Hung, A.; Karagiannis, T.C. Utilisation of the OliveNet™ Library to Investigate Phenolic Compounds Using Molecular Modelling Studies in the Context of Alzheimer's Disease. *Comput Biol Chem* **2020**, *87*, 107271, doi:10.1016/j.compbiolchem.2020.107271.
60. Omar, S.H.; Scott, C.J.; Hamlin, A.S.; Obied, H.K. Biophenols: Enzymes (β-Secretase, Cholinesterases, Histone Deacetylase and Tyrosinase) Inhibitors from Olive (Olea Europaea L.). *Fitoterapia* **2018**, *128*, 118–129, doi:10.1016/j.fitote.2018.05.011.
61. Romero-Márquez, J.M.; Navarro-Hortal, M.D.; Jiménez-Trigo, V.; Muñoz-Ollero, P.; Forbes-Hernández, T.Y.; Esteban-Muñoz, A.; Giampieri, F.; Delgado Noya, I.; Bullón, P.; Vera-Ramírez, L.; et al. An Olive-Derived Extract 20% Rich in Hydroxytyrosol Prevents β-Amyloid Aggregation and Oxidative Stress, Two Features of Alzheimer Disease, via SKN-1/NRF2 and

HSP-16.2 in Caenorhabditis Elegans. *Antioxidants (Basel)* **2022**, *11*, 629, doi:10.3390/antiox11040629.
62. Abdallah, I.M.; Al-Shami, K.M.; Yang, E.; Wang, J.; Guillaume, C.; Kaddoumi, A. Oleuropein-Rich Olive Leaf Extract Attenuates Neuroinflammation in the Alzheimer's Disease Mouse Model. *ACS Chem Neurosci* **2022**, *13*, 1002–1013, doi:10.1021/acschemneuro.2c00005.
63. Ibrahim, S.; Adeputra Nasution, I.F.; Danil, M.; Sadewo, W.; Widyawati, T.; Eyanoer, P.C.; Ritarwan, K.; Riawan, W.; Darmajaya, R. Potential Benefit of Olive Leaf Extract in Cervical Spondylotic Myelopathy Model. *Ann Med Surg (Lond)* **2022**, *73*, 103040, doi:10.1016/j.amsu.2021.103040.
64. Luccarini, I.; Ed Dami, T.; Grossi, C.; Rigacci, S.; Stefani, M.; Casamenti, F. Oleuropein Aglycone Counteracts Aβ42 Toxicity in the Rat Brain. *Neurosci Lett* **2014**, *558*, 67–72, doi:10.1016/j.neulet.2013.10.062.
65. Brogi, S.; Sirous, H.; Calderone, V.; Chemi, G. Amyloid β Fibril Disruption by Oleuropein Aglycone: Long-Time Molecular Dynamics Simulation to Gain Insight into the Mechanism of Action of This Polyphenol from Extra Virgin Olive Oil. *Food Funct* **2020**, *11*, 8122–8132, doi:10.1039/d0fo01511c.
66. Daccache, A.; Lion, C.; Sibille, N.; Gerard, M.; Slomianny, C.; Lippens, G.; Cotelle, P. Oleuropein and Derivatives from Olives as Tau Aggregation Inhibitors. *Neurochem Int* **2011**, *58*, 700–707, doi:10.1016/j.neuint.2011.02.010.
67. Senol, F.S.; Ankli, A.; Reich, E.; Orhan, I.E. HPTLC Fingerprinting and Cholinesterase Inhibitory and Metal-Chelating Capacity of Various Citrus Cultivars and Olea Europaea. *Food Technol Biotechnol* **2016**, *54*, 275–281, doi:10.17113/ftb.54.03.16.4225.
68. Suárez Montenegro, Z.J.; Álvarez-Rivera, G.; Sánchez-Martínez, J.D.; Gallego, R.; Valdés, A.; Bueno, M.; Cifuentes, A.; Ibáñez, E. Neuroprotective Effect of Terpenoids Recovered from Olive Oil By-Products. *Foods* **2021**, *10*, 1507, doi:10.3390/foods10071507.
69. Schwarz, S.; Loesche, A.; Lucas, S.D.; Sommerwerk, S.; Serbian, I.; Siewert, B.; Pianowski, E.; Csuk, R. Converting Maslinic Acid into an Effective Inhibitor of Acylcholinesterases. *Eur J Med Chem* **2015**, *103*, 438–445, doi:10.1016/j.ejmech.2015.09.007.
70. Ali, M.; Muhammad, S.; Shah, M.R.; Khan, A.; Rashid, U.; Farooq, U.; Ullah, F.; Sadiq, A.; Ayaz, M.; Ali, M.; et al. Neurologically Potent Molecules from Crataegus Oxyacantha; Isolation, Anticholinesterase Inhibition, and Molecular Docking. *Front Pharmacol* **2017**, *8*, 327, doi:10.3389/fphar.2017.00327.
71. Mamadalieva, N.Z.; Youssef, F.S.; Hussain, H.; Zengin, G.; Mollica, A.; Al Musayeib, N.M.; Ashour, M.L.; Westermann, B.; Wessjohann, L.A. Validation of the Antioxidant and Enzyme Inhibitory Potential of Selected Triterpenes Using In Vitro and In Silico Studies, and the Evaluation of Their

ADMET Properties. *Molecules* **2021**, *26*, 6331, doi:10.3390/molecules26216331.
72. Szwajgier, D.; Baranowska-Wójcik, E. Terpenes and Phenylpropanoids as Acetyl- and Butyrylcholinesterase Inhibitors: A Comparative Study. *Curr Alzheimer Res* **2019**, *16*, 963–973, doi:10.2174/1567205016666191010105115.
73. Yu, J.; Kwon, H.; Cho, E.; Jeon, J.; Kang, R.H.; Youn, K.; Jun, M.; Lee, Y.C.; Ryu, J.H.; Kim, D.H. The Effects of Pinoresinol on Cholinergic Dysfunction-Induced Memory Impairments and Synaptic Plasticity in Mice. *Food Chem Toxicol* **2019**, *125*, 376–382, doi:10.1016/j.fct.2019.01.017.
74. Gouvinhas, I.; Garcia, J.; Granato, D.; Barros, A. Seed Phytochemical Profiling of Three Olive Cultivars, Antioxidant Capacity, Enzymatic Inhibition, and Effects on Human Neuroblastoma Cells (SH-SY5Y). *Molecules* **2022**, *27*, 5057, doi:10.3390/molecules27165057.
75. Chandler, D.; Woldu, A.; Rahmadi, A.; Shanmugam, K.; Steiner, N.; Wright, E.; Benavente-García, O.; Schulz, O.; Castillo, J.; Münch, G. Effects of Plant-Derived Polyphenols on TNF-Alpha and Nitric Oxide Production Induced by Advanced Glycation Endproducts. *Mol Nutr Food Res* **2010**, *54 Suppl 2*, S141-150, doi:10.1002/mnfr.200900504.
76. Ruzzolini, J.; Chioccioli, S.; Monaco, N.; Peppicelli, S.; Andreucci, E.; Urciuoli, S.; Romani, A.; Luceri, C.; Tortora, K.; Calorini, L.; et al. Oleuropein-Rich Leaf Extract as a Broad Inhibitor of Tumour and Macrophage INOS in an Apc Mutant Rat Model. *Antioxidants (Basel)* **2021**, *10*, 1577, doi:10.3390/antiox10101577.
77. Seddik, L.; Bah, T.M.; Aoues, A.; Slimani, M.; Benderdour, M. Elucidation of Mechanisms Underlying the Protective Effects of Olive Leaf Extract against Lead-Induced Neurotoxicity in Wistar Rats. *J Toxicol Sci* **2011**, *36*, 797–809, doi:10.2131/jts.36.797.
78. Khamse, S.; Haftcheshmeh, S.M.; Sadr, S.S.; Roghani, M.; Kamalinejad, M.; Moghaddam, P.M.; Golchoobian, R.; Ebrahimi, F. The Potential Neuroprotective Roles of Olive Leaf Extract in an Epilepsy Rat Model Induced by Kainic Acid. *Res Pharm Sci* **2021**, *16*, 48–57, doi:10.4103/1735-5362.305188.
79. Boss, A.; Kao, C.H.-J.; Murray, P.M.; Marlow, G.; Barnett, M.P.G.; Ferguson, L.R. Human Intervention Study to Assess the Effects of Supplementation with Olive Leaf Extract on Peripheral Blood Mononuclear Cell Gene Expression. *Int J Mol Sci* **2016**, *17*, E2019, doi:10.3390/ijms17122019.
80. Misrani, A.; Tabassum, S.; Yang, L. Mitochondrial Dysfunction and Oxidative Stress in Alzheimer's Disease. *Frontiers in Aging Neuroscience* **2021**, *13*.
81. Butterfield, D.A.; Lauderback, C.M. Lipid Peroxidation and Protein Oxidation in Alzheimer's Disease Brain: Potential Causes and Consequences Involving Amyloid Beta-Peptide-Associated Free Radical

Oxidative Stress. *Free Radic Biol Med* **2002**, *32*, 1050–1060, doi:10.1016/s0891-5849(02)00794-3.

82. Topalović, D.; Dekanski, D.; Spremo-Potparević, B.; Pirković, A.; Borozan, S.; Bajić, V.; Stojanović, D.; Giampieri, F.; Gasparrini, M.; Živković, L. Dry Olive Leaf Extract Attenuates DNA Damage Induced by Estradiol and Diethylstilbestrol in Human Peripheral Blood Cells in Vitro. *Mutat Res Genet Toxicol Environ Mutagen* **2019**, *845*, 402993, doi:10.1016/j.mrgentox.2018.12.001.
83. Cabarkapa, A.; Zivković, L.; Zukovec, D.; Djelić, N.; Bajić, V.; Dekanski, D.; Spremo-Potparević, B. Protective Effect of Dry Olive Leaf Extract in Adrenaline Induced DNA Damage Evaluated Using in Vitro Comet Assay with Human Peripheral Leukocytes. *Toxicol In Vitro* **2014**, *28*, 451–456, doi:10.1016/j.tiv.2013.12.014.
84. Türkez, H.; Toğar, B. Olive (Olea Europaea L.) Leaf Extract Counteracts Genotoxicity and Oxidative Stress of Permethrin in Human Lymphocytes. *J Toxicol Sci* **2011**, *36*, 531–537, doi:10.2131/jts.36.531.
85. Dekanski, D.; Selaković, V.; Piperski, V.; Radulović, Z.; Korenić, A.; Radenović, L. Protective Effect of Olive Leaf Extract on Hippocampal Injury Induced by Transient Global Cerebral Ischemia and Reperfusion in Mongolian Gerbils. *Phytomedicine* **2011**, *18*, 1137–1143, doi:10.1016/j.phymed.2011.05.010.
86. Sarbishegi, M.; Charkhat Gorgich, E.A.; Khajavi, O.; Komeili, G.; Salimi, S. The Neuroprotective Effects of Hydro-Alcoholic Extract of Olive (Olea Europaea L.) Leaf on Rotenone-Induced Parkinson's Disease in Rat. *Metab Brain Dis* **2018**, *33*, 79–88, doi:10.1007/s11011-017-0131-0.
87. Asghari, A.A.; Hosseini, M.; Bafadam, S.; Rakhshandeh, H.; Farazandeh, M.; Mahmoudabady, M. Olea Europaea L. (Olive) Leaf Extract Ameliorates Learning and Memory Deficits in Streptozotocin-Induced Diabetic Rats. *Avicenna J Phytomed* **2022**, *12*, 163–174, doi:10.22038/AJP.2021.18989.
88. Wang, Y.; Wang, S.; Cui, W.; He, J.; Wang, Z.; Yang, X. Olive Leaf Extract Inhibits Lead Poisoning-Induced Brain Injury. *Neural Regen Res* **2013**, *8*, 2021–2029, doi:10.3969/j.issn.1673-5374.2013.22.001.
89. Mehraein, F.; Sarbishegi, M.; Golipoor, Z. Different Effects of Olive Leaf Extract on Antioxidant Enzyme Activities in Midbrain and Dopaminergic Neurons of Substantia Nigra in Young and Old Rats. *Histol Histopathol* **2016**, *31*, 425–431, doi:10.14670/HH-11-687.
90. Çoban, J.; Öztezcan, S.; Doğru-Abbasoğlu, S.; Bingül, I.; Yeşil-Mizrak, K.; Uysal, M. Olive Leaf Extract Decreases Age-Induced Oxidative Stress in Major Organs of Aged Rats. *Geriatr Gerontol Int* **2014**, *14*, 996–1002, doi:10.1111/ggi.12192.
91. Mikami, T.; Kim, J.; Park, J.; Lee, H.; Yaicharoen, P.; Suidasari, S.; Yokozawa, M.; Yamauchi, K. Olive Leaf Extract Prevents Obesity,

Cognitive Decline, and Depression and Improves Exercise Capacity in Mice. *Sci Rep* **2021**, *11*, 12495, doi:10.1038/s41598-021-90589-6.

92. Kendall, M.; Batterham, M.; Obied, H.; Prenzler, P.D.; Ryan, D.; Robards, K. Zero Effect of Multiple Dosage of Olive Leaf Supplements on Urinary Biomarkers of Oxidative Stress in Healthy Humans. *Nutrition* **2009**, *25*, 270–280, doi:10.1016/j.nut.2008.08.008.
93. De Cicco, P.; Maisto, M.; Tenore, G.C.; Ianaro, A. Olive Leaf Extract, from Olea Europaea L., Reduces Palmitate-Induced Inflammation via Regulation of Murine Macrophages Polarization. *Nutrients* **2020**, *12*, E3663, doi:10.3390/nu12123663.
94. Chiaino, E.; Micucci, M.; Cosconati, S.; Novellino, E.; Budriesi, R.; Chiarini, A.; Frosini, M. Olive Leaves and Hibiscus Flowers Extracts-Based Preparation Protect Brain from Oxidative Stress-Induced Injury. *Antioxidants (Basel)* **2020**, *9*, E806, doi:10.3390/antiox9090806.
95. Arslan, J.; Jamshed, H.; Qureshi, H. Early Detection and Prevention of Alzheimer's Disease: Role of Oxidative Markers and Natural Antioxidants. *Frontiers in Aging Neuroscience* **2020**, *12*.
96. Rabiei, Z.; Bigdeli, M.R.; Rasoulian, B.; Ghassempour, A.; Mirzajani, F. The Neuroprotection Effect of Pretreatment with Olive Leaf Extract on Brain Lipidomics in Rat Stroke Model. *Phytomedicine* **2012**, *19*, 940–946, doi:10.1016/j.phymed.2012.06.003.
97. N, S.; A, W.; S, H.; R, A.; R, H.; S, A.; Ba, G.; Ea, B. Interplay of Antioxidants in Alzheimer's Disease. *J Transl Sci* **2019**, *5*, doi:10.15761/JTS.1000313.
98. Osama, A.; Zhang, J.; Yao, J.; Yao, X.; Fang, J. Nrf2: A Dark Horse in Alzheimer's Disease Treatment. *Ageing Res Rev* **2020**, *64*, 101206, doi:10.1016/j.arr.2020.101206.
99. Davies, D.A.; Adlimoghaddam, A.; Albensi, B.C. Role of Nrf2 in Synaptic Plasticity and Memory in Alzheimer's Disease. *Cells* **2021**, *10*, 1884, doi:10.3390/cells10081884.
100. Stack, C.; Jainuddin, S.; Elipenahli, C.; Gerges, M.; Starkova, N.; Starkov, A.A.; Jové, M.; Portero-Otin, M.; Launay, N.; Pujol, A.; et al. Methylene Blue Upregulates Nrf2/ARE Genes and Prevents Tau-Related Neurotoxicity. *Hum Mol Genet* **2014**, *23*, 3716–3732, doi:10.1093/hmg/ddu080.
101. Al-Quraishy, S.; Othman, M.S.; Dkhil, M.A.; Abdel Moneim, A.E. Olive (Olea Europaea) Leaf Methanolic Extract Prevents HCl/Ethanol-Induced Gastritis in Rats by Attenuating Inflammation and Augmenting Antioxidant Enzyme Activities. *Biomed Pharmacother* **2017**, *91*, 338–349, doi:10.1016/j.biopha.2017.04.069.
102. Achour, I.; Arel-Dubeau, A.-M.; Renaud, J.; Legrand, M.; Attard, E.; Germain, M.; Martinoli, M.-G. Oleuropein Prevents Neuronal Death, Mitigates Mitochondrial Superoxide Production and Modulates Autophagy in a Dopaminergic Cellular Model. *Int J Mol Sci* **2016**, *17*, 1293, doi:10.3390/ijms17081293.

103. Leri, M.; Bertolini, A.; Stefani, M.; Bucciantini, M. EVOO Polyphenols Relieve Synergistically Autophagy Dysregulation in a Cellular Model of Alzheimer's Disease. *Int J Mol Sci* **2021**, *22*, 7225, doi:10.3390/ijms22137225.
104. Elmazoglu, Z.; Galván-Arzate, S.; Aschner, M.; Rangel-López, E.; Bayraktar, O.; Santamaría, A.; Karasu, Ç. Redox-Active Phytoconstituents Ameliorate Cell Damage and Inflammation in Rat Hippocampal Neurons Exposed to Hyperglycemia+Aβ1-42 Peptide. *Neurochem Int* **2021**, *145*, 104993, doi:10.1016/j.neuint.2021.104993.
105. Zare-shahabadi, A.; Masliah, E.; Johnson, G.V.W.; Rezaei, N. Autophagy in Alzheimer's Disease. *Rev Neurosci* **2015**, *26*, 385–395, doi:10.1515/revneuro-2014-0076.
106. Schnöder, L.; Hao, W.; Qin, Y.; Liu, S.; Tomic, I.; Liu, X.; Fassbender, K.; Liu, Y. Deficiency of Neuronal P38α MAPK Attenuates Amyloid Pathology in Alzheimer Disease Mouse and Cell Models through Facilitating Lysosomal Degradation of BACE1. *J Biol Chem* **2016**, *291*, 2067–2079, doi:10.1074/jbc.M115.695916.
107. Rickle, A.; Bogdanovic, N.; Volkman, I.; Winblad, B.; Ravid, R.; Cowburn, R.F. Akt Activity in Alzheimer's Disease and Other Neurodegenerative Disorders. *Neuroreport* **2004**, *15*, 955–959, doi:10.1097/00001756-200404290-00005.
108. Uddin, Md.S.; Stachowiak, A.; Mamun, A.A.; Tzvetkov, N.T.; Takeda, S.; Atanasov, A.G.; Bergantin, L.B.; Abdel-Daim, M.M.; Stankiewicz, A.M. Autophagy and Alzheimer's Disease: From Molecular Mechanisms to Therapeutic Implications. *Frontiers in Aging Neuroscience* **2018**, *10*.
109. Ma, S.; Attarwala, I.Y.; Xie, X.-Q. SQSTM1/P62: A Potential Target for Neurodegenerative Disease. *ACS Chem. Neurosci.* **2019**, *10*, 2094–2114, doi:10.1021/acschemneuro.8b00516.
110. Babić Leko, M.; Langer Horvat, L.; Španić Popovački, E.; Zubčić, K.; Hof, P.R.; Šimić, G. Metals in Alzheimer's Disease. *Biomedicines* **2023**, *11*, 1161, doi:10.3390/biomedicines11041161.
111. Bush, A.I. The Metal Theory of Alzheimer's Disease. *Journal of Alzheimer's Disease* **2013**, *33*, S277–S281, doi:10.3233/JAD-2012-129011.
112. Omar, S.H.; Kerr, P.G.; Scott, C.J.; Hamlin, A.S.; Obied, H.K. Olive (Olea Europaea L.) Biophenols: A Nutriceutical against Oxidative Stress in SH-SY5Y Cells. *Molecules* **2017**, *22*, E1858, doi:10.3390/molecules22111858.
113. Weinhouse, C.; Truong, L.; Meyer, J.N.; Allard, P. Caenorhabditis Elegans as an Emerging Model System in Environmental Epigenetics. *Environ Mol Mutagen* **2018**, *59*, 560–575, doi:10.1002/em.22203.
114. Nigon, V.M.; Félix, M.-A. History of Research on C. Elegans and Other Free-Living Nematodes as Model Organisms. *WormBook* **2017**, 1–84, doi:10.1895/wormbook.1.181.1.
115. Williams, P.L.; Dusenbery, D.B. Screening Test for Neurotoxins Using Caenorhabditis Elegans. *Prog Clin Biol Res* **1987**, *253*, 163–170.

116. Slice, L.W.; Freedman, J.H.; Rubin, C.S. Purification, Characterization, and CDNA Cloning of a Novel Metallothionein-like, Cadmium-Binding Protein from Caenorhabditis Elegans. *J Biol Chem* **1990**, *265*, 256–263.
117. Cui, Y.; McBride, S.J.; Boyd, W.A.; Alper, S.; Freedman, J.H. Toxicogenomic Analysis of Caenorhabditis Elegans Reveals Novel Genes and Pathways Involved in the Resistance to Cadmium Toxicity. *Genome Biol* **2007**, *8*, R122, doi:10.1186/gb-2007-8-6-r122.
118. Boyd, W.A.; McBride, S.J.; Freedman, J.H. Effects of Genetic Mutations and Chemical Exposures on Caenorhabditis Elegans Feeding: Evaluation of a Novel, High-Throughput Screening Assay. *PLoS One* **2007**, *2*, e1259, doi:10.1371/journal.pone.0001259.
119. Nass, R.; Hall, D.H.; Miller, D.M.; Blakely, R.D. Neurotoxin-Induced Degeneration of Dopamine Neurons in Caenorhabditis Elegans. *Proc Natl Acad Sci U S A* **2002**, *99*, 3264–3269, doi:10.1073/pnas.042497999.
120. Zhang, S.; Li, F.; Zhou, T.; Wang, G.; Li, Z. Caenorhabditis Elegans as a Useful Model for Studying Aging Mutations. *Front Endocrinol (Lausanne)* **2020**, *11*, 554994, doi:10.3389/fendo.2020.554994.
121. Chen, Y.; Scarcelli, V.; Legouis, R. Approaches for Studying Autophagy in Caenorhabditis Elegans. *Cells* **2017**, *6*, 27, doi:10.3390/cells6030027.
122. Hunt, P.R. The C. Elegans Model in Toxicity Testing. *J Appl Toxicol* **2017**, *37*, 50–59, doi:10.1002/jat.3357.
123. Tralau, T.; Riebeling, C.; Pirow, R.; Oelgeschläger, M.; Seiler, A.; Liebsch, M.; Luch, A. Wind of Change Challenges Toxicological Regulators. *Environ Health Perspect* **2012**, *120*, 1489–1494, doi:10.1289/ehp.1104782.
124. Knight, A.W.; Little, S.; Houck, K.; Dix, D.; Judson, R.; Richard, A.; McCarroll, N.; Akerman, G.; Yang, C.; Birrell, L.; et al. Evaluation of High-Throughput Genotoxicity Assays Used in Profiling the US EPA ToxCast Chemicals. *Regul Toxicol Pharmacol* **2009**, *55*, 188–199, doi:10.1016/j.yrtph.2009.07.004.
125. Bhattacharya, S.; Zhang, Q.; Carmichael, P.L.; Boekelheide, K.; Andersen, M.E. Toxicity Testing in the 21 Century: Defining New Risk Assessment Approaches Based on Perturbation of Intracellular Toxicity Pathways. *PLoS One* **2011**, *6*, e20887, doi:10.1371/journal.pone.0020887.
126. Scott, C.W.; Peters, M.F.; Dragan, Y.P. Human Induced Pluripotent Stem Cells and Their Use in Drug Discovery for Toxicity Testing. *Toxicol Lett* **2013**, *219*, 49–58, doi:10.1016/j.toxlet.2013.02.020.
127. Kim, W.; Hendricks, G.L.; Lee, K.; Mylonakis, E. An Update on the Use of C. Elegans for Preclinical Drug Discovery: Screening and Identifying Anti-Infective Drugs. *Expert Opin Drug Discov* **2017**, *12*, 625–633, doi:10.1080/17460441.2017.1319358.
128. Li, J.; Le, W. Modeling Neurodegenerative Diseases in Caenorhabditis Elegans. *Experimental Neurology* **2013**, *250*, 94–103, doi:10.1016/j.expneurol.2013.09.024.

129. Corsi, A.K.; Wightman, B.; Chalfie, M. A Transparent Window into Biology: A Primer on Caenorhabditis Elegans. *Genetics* **2015**, *200*, 387–407, doi:10.1534/genetics.115.176099.
130. Dimitriadi, M.; Hart, A.C. Neurodegenerative Disorders: Insights from the Nematode Caenorhabditis Elegans. *Neurobiol Dis* **2010**, *40*, 4–11, doi:10.1016/j.nbd.2010.05.012.
131. Lublin, A.L.; Link, C.D. Alzheimer's Disease Drug Discovery: In Vivo Screening Using Caenorhabditis Elegans as a Model for β-Amyloid Peptide-Induced Toxicity. *Drug Discov Today Technol* **2013**, *10*, e115–e119, doi:10.1016/j.ddtec.2012.02.002.
132. Alvarez, J.; Alvarez-Illera, P.; Santo-Domingo, J.; Fonteriz, R.I.; Montero, M. Modeling Alzheimer's Disease in Caenorhabditis Elegans. *Biomedicines* **2022**, *10*, 288, doi:10.3390/biomedicines10020288.
133. Chen, X.; Barclay, J.W.; Burgoyne, R.D.; Morgan, A. Using C. Elegans to Discover Therapeutic Compounds for Ageing-Associated Neurodegenerative Diseases. *Chemistry Central Journal* **2015**, *9*, 65, doi:10.1186/s13065-015-0143-y.
134. Rivas-García, L.; Quiles, J.L.; Roma-Rodrigues, C.; Raposo, L.R.; Navarro-Hortal, M.D.; Romero-Márquez, J.M.; Esteban-Muñoz, A.; Varela-López, A.; García, L.C.; Cianciosi, D.; et al. Rosa x Hybrida Extracts with Dual Actions: Antiproliferative Effects against Tumour Cells and Inhibitor of Alzheimer Disease. *Food and Chemical Toxicology* **2021**, *149*, 112018, doi:10.1016/j.fct.2021.112018.
135. Oh, K.H.; Kim, H. Aldicarb-Induced Paralysis Assay to Determine Defects in Synaptic Transmission in Caenorhabditis Elegans. *Bio Protoc* **2017**, *7*, e2400, doi:10.21769/BioProtoc.2400.
136. Fatouros, C.; Pir, G.J.; Biernat, J.; Koushika, S.P.; Mandelkow, E.; Mandelkow, E.-M.; Schmidt, E.; Baumeister, R. Inhibition of Tau Aggregation in a Novel Caenorhabditis Elegans Model of Tauopathy Mitigates Proteotoxicity. *Human Molecular Genetics* **2012**, *21*, 3587–3603, doi:10.1093/hmg/dds190.
137. Drake, J.; Link, C.D.; Butterfield, D.A. Oxidative Stress Precedes Fibrillar Deposition of Alzheimer's Disease Amyloid Beta-Peptide (1-42) in a Transgenic Caenorhabditis Elegans Model. *Neurobiol Aging* **2003**, *24*, 415–420, doi:10.1016/s0197-4580(02)00225-7.
138. Tejeda-Benitez, L.; Olivero-Verbel, J. Caenorhabditis Elegans, a Biological Model for Research in Toxicology. *Rev Environ Contam Toxicol* **2016**, *237*, 1–35, doi:10.1007/978-3-319-23573-8_1.
139. Tissenbaum, H.A. Using C. Elegans for Aging Research. *Invertebr Reprod Dev* **2015**, *59*, 59–63, doi:10.1080/07924259.2014.940470.
140. Navarro-Hortal, M.D.; Romero-Márquez, J.M.; Esteban-Muñoz, A.; Sánchez-González, C.; Rivas-García, L.; Llopis, J.; Cianciosi, D.; Giampieri, F.; Sumalla-Cano, S.; Battino, M.; et al. Strawberry (Fragaria × Ananassa Cv.

Romina) Methanolic Extract Attenuates Alzheimer's Beta Amyloid Production and Oxidative Stress by SKN-1/NRF and DAF-16/FOXO Mediated Mechanisms in C. Elegans. *Food Chem* **2022**, *372*, 131272, doi:10.1016/j.foodchem.2021.131272.

141. Ellman, G.L.; Courtney, K.D.; Andres, V.; Feather-Stone, R.M. A New and Rapid Colorimetric Determination of Acetylcholinesterase Activity. *Biochem Pharmacol* **1961**, *7*, 88–95, doi:10.1016/0006-2952(61)90145-9.
142. Huang, D.; Ou, B.; Prior, R.L. The Chemistry behind Antioxidant Capacity Assays. *J. Agric. Food Chem.* **2005**, *53*, 1841–1856, doi:10.1021/jf030723c.
143. Porta-de-la-Riva, M.; Fontrodona, L.; Villanueva, A.; Cerón, J. Basic Caenorhabditis Elegans Methods: Synchronization and Observation. *J Vis Exp* **2012**, 4019, doi:10.3791/4019.
144. Luo, S.; Jiang, X.; Jia, L.; Tan, C.; Li, M.; Yang, Q.; Du, Y.; Ding, C. In Vivo and In Vitro Antioxidant Activities of Methanol Extracts from Olive Leaves on Caenorhabditis Elegans. *Molecules* **2019**, *24*, 704, doi:10.3390/molecules24040704.
145. Navarro-Hortal, M.D.; Romero-Márquez, J.M.; Muñoz-Ollero, P.; Jiménez-Trigo, V.; Esteban-Muñoz, A.; Tutusaus, K.; Giampieri, F.; Battino, M.; Sánchez-González, C.; Rivas-García, L.; et al. Amyloid β-but Not Tau-Induced Neurotoxicity Is Suppressed by Manuka Honey via HSP-16.2 and SKN-1/Nrf2 Pathways in an in Vivo Model of Alzheimer's Disease. *Food Funct* **2022**, *13*, 11185–11199, doi:10.1039/d2fo01739c.
146. Pokorná, J.; Venskutonis, P.R.; Kraujalyte, V.; Kraujalis, P.; Dvořák, P.; Tremlová, B.; Kopřiva, V.; Ošťádalová, M. Comparison of Different Methods of Antioxidant Activity Evaluation of Green and Roast *C. Arabica* and *C. Robusta* Coffee Beans. *Acta Alimentaria* **2015**, *44*, 454–460, doi:10.1556/066.2015.44.0017.
147. Bondet, V.; Brand-Williams, W.; Berset, C. Kinetics and Mechanisms of Antioxidant Activity Using the DPPH.Free Radical Method. *LWT - Food Science and Technology* **1997**, *30*, 609–615, doi:10.1006/fstl.1997.0240.
148. Jiménez-Sánchez, C.; Olivares-Vicente, M.; Rodríguez-Pérez, C.; Herranz-López, M.; Lozano-Sánchez, J.; Segura-Carretero, A.; Fernández-Gutiérrez, A.; Encinar, J.A.; Micol, V. AMPK Modulatory Activity of Olive-Tree Leaves Phenolic Compounds: Bioassay-Guided Isolation on Adipocyte Model and in Silico Approach. *PLoS One* **2017**, *12*, e0173074, doi:10.1371/journal.pone.0173074.
149. Talhaoui, N.; Gómez-Caravaca, A.M.; León, L.; De la Rosa, R.; Segura-Carretero, A.; Fernández-Gutiérrez, A. Determination of Phenolic Compounds of 'Sikitita' Olive Leaves by HPLC-DAD-TOF-MS. Comparison with Its Parents 'Arbequina' and 'Picual' Olive Leaves. *LWT - Food Science and Technology* **2014**, *58*, 28–34, doi:10.1016/j.lwt.2014.03.014.
150. Cui, M.; Chen, B.; Xu, K.; Rigakou, A.; Diamantakos, P.; Melliou, E.; Logothetis, D.E.; Magiatis, P. Activation of Specific Bitter Taste Receptors

by Olive Oil Phenolics and Secoiridoids. *Sci Rep* **2021**, *11*, 22340, doi:10.1038/s41598-021-01752-y.
151. Ahmad-Qasem, M.H.; Cánovas, J.; Barrajón-Catalán, E.; Carreres, J.E.; Micol, V.; García-Pérez, J.V. Influence of Olive Leaf Processing on the Bioaccessibility of Bioactive Polyphenols. *J Agric Food Chem* **2014**, *62*, 6190–6198, doi:10.1021/jf501414h.
152. D'Archivio, M.; Filesi, C.; Varì, R.; Scazzocchio, B.; Masella, R. Bioavailability of the Polyphenols: Status and Controversies. *Int J Mol Sci* **2010**, *11*, 1321–1342, doi:10.3390/ijms11041321.
153. Petridis, A.; Therios, I.; Samouris, G.; Koundouras, S.; Giannakoula, A. Effect of Water Deficit on Leaf Phenolic Composition, Gas Exchange, Oxidative Damage and Antioxidant Activity of Four Greek Olive (Olea Europaea L.) Cultivars. *Plant Physiology and Biochemistry* **2012**, *60*, 1–11, doi:10.1016/j.plaphy.2012.07.014.
154. Papoti, V.T.; Papageorgiou, M.; Dervisi, K.; Alexopoulos, E.; Apostolidis, K.; Petridis, D. Screening Olive Leaves from Unexploited Traditional Greek Cultivars for Their Phenolic Antioxidant Dynamic. *Foods* **2018**, *7*, 197, doi:10.3390/foods7120197.
155. Ferreira, D.M.; de Oliveira, N.M.; Chéu, M.H.; Meireles, D.; Lopes, L.; Oliveira, M.B.; Machado, J. Updated Organic Composition and Potential Therapeutic Properties of Different Varieties of Olive Leaves from Olea Europaea. *Plants (Basel)* **2023**, *12*, 688, doi:10.3390/plants12030688.
156. Nicolì, F.; Negro, C.; Vergine, M.; Aprile, A.; Nutricati, E.; Sabella, E.; Miceli, A.; Luvisi, A.; De Bellis, L. Evaluation of Phytochemical and Antioxidant Properties of 15 Italian Olea Europaea L. Cultivar Leaves. *Molecules* **2019**, *24*, E1998, doi:10.3390/molecules24101998.
157. Lelieveld, J.; Hadjinicolaou, P.; Kostopoulou, E.; Chenoweth, J.; El Maayar, M.; Giannakopoulos, C.; Hannides, C.; Lange, M.A.; Tanarhte, M.; Tyrlis, E.; et al. Climate Change and Impacts in the Eastern Mediterranean and the Middle East. *Clim Change* **2012**, *114*, 667–687, doi:10.1007/s10584-012-0418-4.
158. Brito, C.; Dinis, L.-T.; Moutinho-Pereira, J.; Correia, C.M. Drought Stress Effects and Olive Tree Acclimation under a Changing Climate. *Plants (Basel)* **2019**, *8*, 232, doi:10.3390/plants8070232.
159. Ben Hmida, R.; Gargouri, B.; Chtourou, F.; Abichou, M.; Sevim, D.; Bouaziz, M. Study on the Effect of Climate Changes on the Composition and Quality Parameters of Virgin Olive Oil "Zalmati" Harvested at Three Consecutive Crop Seasons: Chemometric Discrimination. *ACS Omega* **2022**, *7*, 40078–40090, doi:10.1021/acsomega.2c04813.
160. Orlandi, F.; Vazquez, L.M.; Ruga, L.; Bonofiglio, T.; Fornaciari, M.; Garcia-Mozo, H.; Domínguez, E.; Romano, B.; Galan, C. Bioclimatic Requirements for Olive Flowering in Two Mediterranean Regions Located at the Same

Latitude (Andalucia, Spain and Sicily, Italy). *Ann Agric Environ Med* **2005**, *12*, 47–52.
161. Guan, P.-P.; Yu, X.; Zou, Y.-H.; Wang, P. Cyclooxygenase-2 Is Critical for the Propagation of β-Amyloid Protein and Reducing the Glycosylation of Tau in Alzheimer's Disease. *Cell Mol Immunol* **2019**, *16*, 892–894, doi:10.1038/s41423-019-0294-1.
162. Everett, J.; Collingwood, J.F.; Tjendana-Tjhin, V.; Brooks, J.; Lermyte, F.; Plascencia-Villa, G.; Hands-Portman, I.; Dobson, J.; Perry, G.; Telling, N.D. Nanoscale Synchrotron X-Ray Speciation of Iron and Calcium Compounds in Amyloid Plaque Cores from Alzheimer's Disease Subjects. *Nanoscale* **2018**, *10*, 11782–11796, doi:10.1039/C7NR06794A.
163. Ho, L.; Pieroni, C.; Winger, D.; Purohit, D.P.; Aisen, P.S.; Pasinetti, G.M. Regional Distribution of Cyclooxygenase-2 in the Hippocampal Formation in Alzheimer's Disease. *J Neurosci Res* **1999**, *57*, 295–303, doi:10.1002/(SICI)1097-4547(19990801)57:3<295::AID-JNR1>3.0.CO;2-0.
164. Ho, L.; Purohit, D.; Haroutunian, V.; Luterman, J.D.; Willis, F.; Naslund, J.; Buxbaum, J.D.; Mohs, R.C.; Aisen, P.S.; Pasinetti, G.M. Neuronal Cyclooxygenase 2 Expression in the Hippocampal Formation as a Function of the Clinical Progression of Alzheimer Disease. *Arch Neurol* **2001**, *58*, 487–492, doi:10.1001/archneur.58.3.487.
165. Pasinetti, G.M.; Aisen, P.S. Cyclooxygenase-2 Expression Is Increased in Frontal Cortex of Alzheimer's Disease Brain. *Neuroscience* **1998**, *87*, 319–324, doi:10.1016/s0306-4522(98)00218-8.
166. Xiang, Z.; Ho, L.; Yemul, S.; Zhao, Z.; Pompl, P.; Kelley, K.; Dang, A.; Qing, W.; Teplow, D.; Pasinetti, G.M. Cyclooxygenase-2 Promotes Amyloid Plaque Deposition in a Mouse Model of Alzheimer's Disease Neuropathology. *Gene Expr* **2018**, *10*, 271–278.
167. in t' Veld, B.A.; Ruitenberg, A.; Hofman, A.; Launer, L.J.; van Duijn, C.M.; Stijnen, T.; Breteler, M.M.; Stricker, B.H. Nonsteroidal Antiinflammatory Drugs and the Risk of Alzheimer's Disease. *N Engl J Med* **2001**, *345*, 1515–1521, doi:10.1056/NEJMoa010178.
168. McGeer, P.L.; Schulzer, M.; McGeer, E.G. Arthritis and Anti-Inflammatory Agents as Possible Protective Factors for Alzheimer's Disease: A Review of 17 Epidemiologic Studies. *Neurology* **1996**, *47*, 425–432, doi:10.1212/wnl.47.2.425.
169. Stewart, W.F.; Kawas, C.; Corrada, M.; Metter, E.J. Risk of Alzheimer's Disease and Duration of NSAID Use. *Neurology* **1997**, *48*, 626–632, doi:10.1212/wnl.48.3.626.
170. Steinman, M.A.; McQuaid, K.R.; Covinsky, K.E. Age and Rising Rates of Cyclooxygenase-2 Inhibitor Use. *J Gen Intern Med* **2006**, *21*, 245–250, doi:10.1111/j.1525-1497.2006.00336.x.
171. Zhao, Z. Iron and Oxidizing Species in Oxidative Stress and Alzheimer's Disease. *AGING MEDICINE* **2019**, *2*, 82–87, doi:10.1002/agm2.12074.

172. Davies, P.; Maloney, A.J. Selective Loss of Central Cholinergic Neurons in Alzheimer's Disease. *Lancet* **1976**, *2*, 1403, doi:10.1016/s0140-6736(76)91936-x.
173. Olajide, O.A.; Sarker, S.D. Alzheimer's Disease: Natural Products as Inhibitors of Neuroinflammation. *Inflammopharmacology* **2020**, *28*, 1439–1455, doi:10.1007/s10787-020-00751-1.
174. Hirschhorn, T.; Stockwell, B.R. The Development of the Concept of Ferroptosis. *Free Radical Biology and Medicine* **2019**, *133*, 130–143, doi:10.1016/j.freeradbiomed.2018.09.043.
175. Morris, G.; Berk, M.; Carvalho, A.F.; Maes, M.; Walker, A.J.; Puri, B.K. Why Should Neuroscientists Worry about Iron? The Emerging Role of Ferroptosis in the Pathophysiology of Neuroprogressive Diseases. *Behavioural Brain Research* **2018**, *341*, 154–175, doi:10.1016/j.bbr.2017.12.036.
176. Stockwell, B.R.; Friedmann Angeli, J.P.; Bayir, H.; Bush, A.I.; Conrad, M.; Dixon, S.J.; Fulda, S.; Gascón, S.; Hatzios, S.K.; Kagan, V.E.; et al. Ferroptosis: A Regulated Cell Death Nexus Linking Metabolism, Redox Biology, and Disease. *Cell* **2017**, *171*, 273–285, doi:10.1016/j.cell.2017.09.021.
177. Xun, Z.; Rivera-Sánchez, S.; Ayala-Peña, S.; Lim, J.; Budworth, H.; Skoda, E.M.; Robbins, P.D.; Niedernhofer, L.J.; Wipf, P.; McMurray, C.T. Targeting of XJB-5-131 to Mitochondria Suppresses Oxidative DNA Damage and Motor Decline in a Mouse Model of Huntington's Disease. *Cell Reports* **2012**, *2*, 1137–1142, doi:10.1016/j.celrep.2012.10.001.
178. Lee, L.C.; Liong, C.-Y.; Jemain, A.A. Partial Least Squares-Discriminant Analysis (PLS-DA) for Classification of High-Dimensional (HD) Data: A Review of Contemporary Practice Strategies and Knowledge Gaps. *Analyst* **2018**, *143*, 3526–3539, doi:10.1039/C8AN00599K.
179. Rehfeldt, S.C.H.; Silva, J.; Alves, C.; Pinteus, S.; Pedrosa, R.; Laufer, S.; Goettert, M.I. Neuroprotective Effect of Luteolin-7-O-Glucoside against 6-OHDA-Induced Damage in Undifferentiated and RA-Differentiated SH-SY5Y Cells. *Int J Mol Sci* **2022**, *23*, 2914, doi:10.3390/ijms23062914.
180. Sezen Karaoğlan, E.; Hancı, H.; Koca, M.; Kazaz, C. Some Bioactivities of Isolated Apigenin-7-O-Glucoside and Luteolin-7-O-Glucoside. *Applied Sciences* **2023**, *13*, 1503, doi:10.3390/app13031503.
181. Olennikov, D.N.; Kashchenko, N.I.; Chirikova, N.K.; Akobirshoeva, A.; Zilfikarov, I.N.; Vennos, C. Isorhamnetin and Quercetin Derivatives as Anti-Acetylcholinesterase Principles of Marigold (Calendula Officinalis) Flowers and Preparations. *Int J Mol Sci* **2017**, *18*, 1685, doi:10.3390/ijms18081685.
182. Omar, S.H.; Scott, C.J.; Hamlin, A.S.; Obied, H.K. Biophenols: Enzymes (β-Secretase, Cholinesterases, Histone Deacetylase and Tyrosinase) Inhibitors from Olive (Olea Europaea L.). *Fitoterapia* **2018**, *128*, 118–129, doi:10.1016/j.fitote.2018.05.011.

183. Orhan, I.; Kartal, M.; Tosun, F.; Sener, B. Screening of Various Phenolic Acids and Flavonoid Derivatives for Their Anticholinesterase Potential. *Z Naturforsch C J Biosci* **2007**, *62*, 829–832, doi:10.1515/znc-2007-11-1210.
184. Gao, Y.; Li, X.; Xu, R.; Guo, Y.; Yin, H.; Tan, R.; Qi, Z.; Liu, G.; Liang, J.; Ya, B. Oleuropein Improved Post Cerebral Stroke Cognitive Function by Promoting Histone Acetylation and Phosphorylation of CAMP Response Element-Binding Protein in MCAO Rats. *Dose Response* **2020**, *18*, 1559325820950102, doi:10.1177/1559325820950102.
185. Jabir, N.R.; Khan, F.R.; Tabrez, S. Cholinesterase Targeting by Polyphenols: A Therapeutic Approach for the Treatment of Alzheimer's Disease. *CNS Neurosci Ther* **2018**, *24*, 753–762, doi:10.1111/cns.12971.
186. Costanzo, P.; Oliverio, M.; Maiuolo, J.; Bonacci, S.; De Luca, G.; Masullo, M.; Arcone, R.; Procopio, A. Novel Hydroxytyrosol-Donepezil Hybrids as Potential Antioxidant and Neuroprotective Agents. *Frontiers in Chemistry* **2021**, *9*.
187. Nugroho, A.; Choi, J.S.; Hong, J.-P.; Park, H.-J. Anti-Acetylcholinesterase Activity of the Aglycones of Phenolic Glycosides Isolated from Leonurus Japonicus. *Asian Pacific Journal of Tropical Biomedicine* **2017**, *7*, 849–854, doi:10.1016/j.apjtb.2017.08.013.
188. Wang, Z.Y.; Zhang, X.D.; Whang, W.K. The Effect of Terpenoids of Dipsacus Asperoides Against Alzheimer's Disease and Development of Simultaneous Analysis by High Performance Liquid Chromatography. *Natural Product Communications* **2021**, *16*, 1934578X211044603, doi:10.1177/1934578X211044603.
189. Senol, F.S.; Ankli, A.; Reich, E.; Orhan, I.E. HPTLC Fingerprinting and Cholinesterase Inhibitory and Metal-Chelating Capacity of Various Citrus Cultivars and Olea Europaea. *Food Technol Biotechnol* **2016**, *54*, 275–281, doi:10.17113/ftb.54.03.16.4225.
190. Figueiredo-González, M.; Reboredo-Rodríguez, P.; González-Barreiro, C.; Carrasco-Pancorbo, A.; Simal-Gándara, J.; Cancho-Grande, B. Nutraceutical Potential of Phenolics from 'Brava' and 'Mansa' Extra-Virgin Olive Oils on the Inhibition of Enzymes Associated to Neurodegenerative Disorders in Comparison with Those of 'Picual' and 'Cornicabra'. *Molecules* **2018**, *23*, 722, doi:10.3390/molecules23040722.
191. Granados-Principal, S.; Quiles, J.L.; Ramirez-Tortosa, C.L.; Sanchez-Rovira, P.; Ramirez-Tortosa, M.C. Hydroxytyrosol: From Laboratory Investigations to Future Clinical Trials. *Nutr Rev* **2010**, *68*, 191–206, doi:10.1111/j.1753-4887.2010.00278.x.
192. Park, C.M.; Song, Y.-S. Luteolin and Luteolin-7-O-Glucoside Protect against Acute Liver Injury through Regulation of Inflammatory Mediators and Antioxidative Enzymes in GalN/LPS-Induced Hepatitic ICR Mice. *Nutr Res Pract* **2019**, *13*, 473–479, doi:10.4162/nrp.2019.13.6.473.

193. Grignon-Dubois, M.; Rezzonico, B. First Phytochemical Evidence of Chemotypes for the Seagrass Zostera Noltii. *Plants* **2012**, *1*, 27–38, doi:10.3390/plants1010027.
194. Castejón, M.L.; Rosillo, M.Á.; Montoya, T.; González-Benjumea, A.; Fernández-Bolaños, J.G.; Alarcón-de-la-Lastra, C. Oleuropein Down-Regulated IL-1β-Induced Inflammation and Oxidative Stress in Human Synovial Fibroblast Cell Line SW982. *Food Funct* **2017**, *8*, 1890–1898, doi:10.1039/c7fo00210f.
195. Giner, E.; Andújar, I.; Recio, M.C.; Ríos, J.L.; Cerdá-Nicolás, J.M.; Giner, R.M. Oleuropein Ameliorates Acute Colitis in Mice. *J Agric Food Chem* **2011**, *59*, 12882–12892, doi:10.1021/jf203715m.
196. Huang, W.-C.; Liou, C.-J.; Shen, S.-C.; Hu, S.; Chao, J.C.-J.; Huang, C.-H.; Wu, S.-J. Oleuropein Attenuates Inflammation and Regulates Immune Responses in a 2,4-Dinitrochlorobenzene-Induced Atopic Dermatitis Mouse Model. *Asian Pac J Allergy Immunol* **2022**, doi:10.12932/AP-200122-1309.
197. Mao, X.; Xia, B.; Zheng, M.; Zhou, Z. Assessment of the Anti-Inflammatory, Analgesic and Sedative Effects of Oleuropein from Olea Europaea L. *Cell Mol Biol (Noisy-le-grand)* **2019**, *65*, 52–55.
198. Potočnjak, I.; Škoda, M.; Pernjak-Pugel, E.; Peršić, M.P.; Domitrović, R. Oral Administration of Oleuropein Attenuates Cisplatin-Induced Acute Renal Injury in Mice through Inhibition of ERK Signaling. *Mol Nutr Food Res* **2016**, *60*, 530–541, doi:10.1002/mnfr.201500409.
199. Larussa, T.; Oliverio, M.; Suraci, E.; Greco, M.; Placida, R.; Gervasi, S.; Marasco, R.; Imeneo, M.; Paolino, D.; Tucci, L.; et al. Oleuropein Decreases Cyclooxygenase-2 and Interleukin-17 Expression and Attenuates Inflammatory Damage in Colonic Samples from Ulcerative Colitis Patients. *Nutrients* **2017**, *9*, 391, doi:10.3390/nu9040391.
200. Liang, J.; Bonvino, N.P.; Hung, A.; Karagiannis, T.C. In Silico Characterisation of Olive Phenolic Compounds as Potential Cyclooxygenase Modulators. Part 1. *J Mol Graph Model* **2020**, *101*, 107719, doi:10.1016/j.jmgm.2020.107719.
201. Liang, J.; Bonvino, N.P.; Hung, A.; Karagiannis, T.C. In Silico Characterisation of Olive Phenolic Compounds as Potential Cyclooxygenase Modulators. Part 2. *J Mol Graph Model* **2020**, *101*, 107743, doi:10.1016/j.jmgm.2020.107743.
202. Pesce, M.; Franceschelli, S.; Ferrone, A.; De Lutiis, M.A.; Patruno, A.; Grilli, A.; Felaco, M.; Speranza, L. Verbascoside Down-Regulates Some pro-Inflammatory Signal Transduction Pathways by Increasing the Activity of Tyrosine Phosphatase SHP-1 in the U937 Cell Line. *J Cell Mol Med* **2015**, *19*, 1548–1556, doi:10.1111/jcmm.12524.
203. Carrillo-Ocampo, D.; Bazaldúa-Gómez, S.; Bonilla-Barbosa, J.R.; Aburto-Amar, R.; Rodríguez-López, V. Anti-Inflammatory Activity of Iridoids and

Verbascoside Isolated from Castilleja Tenuiflora. *Molecules* **2013**, *18*, 12109–12118, doi:10.3390/molecules181012109.

204. Romero-Márquez, J.M.; Navarro-Hortal, M.D.; Jiménez-Trigo, V.; Muñoz-Ollero, P.; Forbes-Hernández, T.Y.; Esteban-Muñoz, A.; Giampieri, F.; Delgado Noya, I.; Bullón, P.; Vera-Ramírez, L.; et al. An Olive-Derived Extract 20% Rich in Hydroxytyrosol Prevents β-Amyloid Aggregation and Oxidative Stress, Two Features of Alzheimer Disease, via SKN-1/NRF2 and HSP-16.2 in Caenorhabditis Elegans. *Antioxidants (Basel)* **2022**, *11*, 629, doi:10.3390/antiox11040629.
205. Šimat, V.; Skroza, D.; Tabanelli, G.; Čagalj, M.; Pasini, F.; Gómez-Caravaca, A.M.; Fernández-Fernández, C.; Sterniša, M.; Smole Možina, S.; Ozogul, Y.; et al. Antioxidant and Antimicrobial Activity of Hydroethanolic Leaf Extracts from Six Mediterranean Olive Cultivars. *Antioxidants (Basel)* **2022**, *11*, 1656, doi:10.3390/antiox11091656.
206. Yao, Q.; Shen, Y.; Bu, L.; Yang, P.; Xu, Z.; Guo, X. Ultrasound-Assisted Aqueous Extraction of Total Flavonoids and Hydroxytyrosol from Olive Leaves Optimized by Response Surface Methodology. *Prep Biochem Biotechnol* **2019**, *49*, 837–845, doi:10.1080/10826068.2019.1630648.
207. Fuccelli, R.; Fabiani, R.; Rosignoli, P. Hydroxytyrosol Exerts Anti-Inflammatory and Anti-Oxidant Activities in a Mouse Model of Systemic Inflammation. *Molecules* **2018**, *23*, 3212, doi:10.3390/molecules23123212.
208. Ghasemi, S.; Koohi, D.E.; Emmamzadehhashemi, M.S.B.; Khamas, S.S.; Moazen, M.; Hashemi, A.K.; Amin, G.; Golfakhrabadi, F.; Yousefi, Z.; Yousefbeyk, F. Investigation of Phenolic Compounds and Antioxidant Activity of Leaves Extracts from Seventeen Cultivars of Iranian Olive (Olea Europaea L.). *J Food Sci Technol* **2018**, *55*, 4600–4607, doi:10.1007/s13197-018-3398-1.
209. Martín-García, B.; De Montijo-Prieto, S.; Jiménez-Valera, M.; Carrasco-Pancorbo, A.; Ruiz-Bravo, A.; Verardo, V.; Gómez-Caravaca, A.M. Comparative Extraction of Phenolic Compounds from Olive Leaves Using a Sonotrode and an Ultrasonic Bath and the Evaluation of Both Antioxidant and Antimicrobial Activity. *Antioxidants (Basel)* **2022**, *11*, 558, doi:10.3390/antiox11030558.
210. Bai, J.; Farias-Pereira, R.; Jang, M.; Zhang, Y.; Lee, S.M.; Kim, Y.-S.; Park, Y.; Ahn, J.B.; Kim, G.-H.; Kim, K.-H. Azelaic Acid Promotes Caenorhabditiselegans Longevity at Low Temperature Via an Increase in Fatty AcidDesaturation. *Pharm Res* **2021**, *38*, 15–26, doi:10.1007/s11095-020-02975-w.
211. Leal, L.E.; Moreira, E.S.; Correia, B.L.; Bueno, P.S.A.; Comar, J.F.; de Sá-Nakanishi, A.B.; Cuman, R.K.N.; Bracht, A.; Bersani-Amado, C.A.; Bracht, L. Comparative Study of the Antioxidant and Anti-Inflammatory Effects of the Natural Coumarins 1,2-Benzopyrone, Umbelliferone and Esculetin: In

Silico, in Vitro and in Vivo Analyses. *Naunyn Schmiedebergs Arch Pharmacol* **2023**, doi:10.1007/s00210-023-02606-2.
212. Muñiz-Mouro, A.; Oliveira, I.M.; Gullón, B.; Lú-Chau, T.A.; Moreira, M.T.; Lema, J.M.; Eibes, G. Comprehensive Investigation of the Enzymatic Oligomerization of Esculin by Laccase in Ethanol : Water Mixtures. *RSC Adv.* **2017**, *7*, 38424–38433, doi:10.1039/C7RA06972C.
213. Sánchez-Marzo, N.; Lozano-Sánchez, J.; Cádiz-Gurrea, M. de la L.; Herranz-López, M.; Micol, V.; Segura-Carretero, A. Relationships Between Chemical Structure and Antioxidant Activity of Isolated Phytocompounds from Lemon Verbena. *Antioxidants (Basel)* **2019**, *8*, 324, doi:10.3390/antiox8080324.
214. Fayez, N.; Khalil, W.; Abdel-Sattar, E.; Abdel-Fattah, A.-F.M. In Vitro and in Vivo Assessment of the Anti-Inflammatory Activity of Olive Leaf Extract in Rats. *Inflammopharmacology* **2023**, *31*, 1529–1538, doi:10.1007/s10787-023-01208-x.
215. Kimura, Y.; Sumiyoshi, M. Olive Leaf Extract and Its Main Component Oleuropein Prevent Chronic Ultraviolet B Radiation-Induced Skin Damage and Carcinogenesis in Hairless Mice, ,. *The Journal of Nutrition* **2009**, *139*, 2079–2086, doi:10.3945/jn.109.104992.
216. Hu, C.; Kitts, D.D. Luteolin and Luteolin-7-O-Glucoside from Dandelion Flower Suppress INOS and COX-2 in RAW264.7 Cells. *Mol Cell Biochem* **2004**, *265*, 107–113, doi:10.1023/b:mcbi.0000044364.73144.fe.
217. Feng, S.; Zhang, C.; Chen, T.; Zhou, L.; Huang, Y.; Yuan, M.; Li, T.; Ding, C. Oleuropein Enhances Stress Resistance and Extends Lifespan via Insulin/IGF-1 and SKN-1/Nrf2 Signaling Pathway in Caenorhabditis Elegans. *Antioxidants* **2021**, *10*, 1697, doi:10.3390/antiox10111697.
218. Xiao, Y.; Zhang, L.; Zhu, X.; Qin, Y.; Yu, C.; Jiang, N.; Li, S.; Liu, F.; Liu, Y. Luteolin Promotes Pathogen Resistance in Caenorhabditis Elegans via DAF-2/DAF-16 Insulin-like Signaling Pathway. *International Immunopharmacology* **2023**, *115*, 109679, doi:10.1016/j.intimp.2023.109679.
219. Li, J.; Wang, J.; Huang, Z.; Cui, X.; Li, C. Oxidized Quercetin Has Stronger Anti-Amyloid Activity and Anti-Aging Effect than Native Form. *Comparative Biochemistry and Physiology Part C: Toxicology & Pharmacology* **2023**, *271*, 109676, doi:10.1016/j.cbpc.2023.109676.
220. Zečić, A.; Braeckman, B.P. DAF-16/FoxO in Caenorhabditis Elegans and Its Role in Metabolic Remodeling. *Cells* **2020**, *9*, 109, doi:10.3390/cells9010109.
221. Kawasaki, I.; Jeong, M.-H.; Oh, B.-K.; Shim, Y.-H. Apigenin Inhibits Larval Growth of Caenorhabditis Elegans through DAF-16 Activation. *FEBS Lett* **2010**, *584*, 3587–3591, doi:10.1016/j.febslet.2010.07.026.
222. Milanizadeh, S.; Bigdeli, M.R.; Rasoulian, B.; Amani, D. The Effects of Olive Leaf Extract on Antioxidant Enzymes Activity and Tumor Growth in Breast Cancer. *Thrita* **2014**, *3*, doi:10.5812/thrita.12914.

223. Lee-Huang, S.; Zhang, L.; Huang, P.L.; Chang, Y.-T.; Huang, P.L. Anti-HIV Activity of Olive Leaf Extract (OLE) and Modulation of Host Cell Gene Expression by HIV-1 Infection and OLE Treatment. *Biochem Biophys Res Commun* **2003**, *307*, 1029–1037, doi:10.1016/s0006-291x(03)01292-0.
224. Yousefi, Z.; Mirsanei, Z.; Bitaraf, F.S.; Mahdavi, S.; Mirzaii, M.; Jafari, R. Dose-Dependent Effects of Oleuropein Administration on Regulatory T-Cells in Patients with Rheumatoid Arthritis: An in Vitro Approach. *Int J Immunopathol Pharmacol* **2022**, *36*, 03946320221086084, doi:10.1177/03946320221086084.
225. K, S.N.; A, S.K.; Sivarajasundari, G.T.; Ivvala, A.S. Effect of Olive Leaves Extract on Inflammatory Cyclooxygenase (COX) Levels in High Fat Diet (HFD) Induced Diabetic Animals. *Research & Reviews: A Journal of Biotechnology* **2013**, *1*.
226. Lins, P.G.; Marina Piccoli Pugine, S.; Scatolini, A.M.; de Melo, M.P. In Vitro Antioxidant Activity of Olive Leaf Extract (Olea Europaea L.) and Its Protective Effect on Oxidative Damage in Human Erythrocytes. *Heliyon* **2018**, *4*, e00805, doi:10.1016/j.heliyon.2018.e00805.
227. Scoditti, E.; Nestola, A.; Massaro, M.; Calabriso, N.; Storelli, C.; De Caterina, R.; Carluccio, M.A. Hydroxytyrosol Suppresses MMP-9 and COX-2 Activity and Expression in Activated Human Monocytes via PKCα and PKCβ1 Inhibition. *Atherosclerosis* **2014**, *232*, 17–24, doi:10.1016/j.atherosclerosis.2013.10.017.
228. Zhang, X.; Cao, J.; Zhong, L. Hydroxytyrosol Inhibits Pro-Inflammatory Cytokines, INOS, and COX-2 Expression in Human Monocytic Cells. *Naunyn Schmiedebergs Arch Pharmacol* **2009**, *379*, 581–586, doi:10.1007/s00210-009-0399-7.
229. Yonezawa, Y.; Kihara, T.; Ibi, K.; Senshu, M.; Nejishima, H.; Takeda, Y.; Imai, K.; Ogawa, H. Olive-Derived Hydroxytyrosol Shows Anti-Inflammatory Effect without Gastric Damage in Rats. *Biol Pharm Bull* **2019**, *42*, 1120–1127, doi:10.1248/bpb.b18-00979.
230. Hardy, J.A.; Higgins, G.A. Alzheimer's Disease: The Amyloid Cascade Hypothesis. *Science* **1992**, *256*, 184–185, doi:10.1126/science.1566067.
231. Barage, S.H.; Sonawane, K.D. Amyloid Cascade Hypothesis: Pathogenesis and Therapeutic Strategies in Alzheimer's Disease. *Neuropeptides* **2015**, *52*, 1–18, doi:10.1016/j.npep.2015.06.008.
232. Schenk, D.; Basi, G.S.; Pangalos, M.N. Treatment Strategies Targeting Amyloid β-Protein. *Cold Spring Harb Perspect Med* **2012**, *2*, a006387, doi:10.1101/cshperspect.a006387.
233. Rigacci, S.; Guidotti, V.; Bucciantini, M.; Nichino, D.; Relini, A.; Berti, A.; Stefani, M. Aβ(1-42) Aggregates into Non-Toxic Amyloid Assemblies in the Presence of the Natural Polyphenol Oleuropein Aglycon. *Current Alzheimer Research 8*, 841–852.

234. Diomede, L.; Rigacci, S.; Romeo, M.; Stefani, M.; Salmona, M. Oleuropein Aglycone Protects Transgenic C. Elegans Strains Expressing Aβ42 by Reducing Plaque Load and Motor Deficit. *PLOS ONE* **2013**, *8*, e58893, doi:10.1371/journal.pone.0058893.
235. Omar, S.H.; Scott, C.J.; Hamlin, A.S.; Obied, H.K. Olive Biophenols Reduces Alzheimer's Pathology in SH-SY5Y Cells and APPswe Mice. *Int J Mol Sci* **2018**, *20*, E125, doi:10.3390/ijms20010125.
236. Hamedi-Shahraki, S.; Jowshan, M.-R.; Zolghadrpour, M.-A.; Amirkhizi, F.; Asghari, S. Dietary Phytochemical Index Is Favorably Associated with Oxidative Stress Status and Cardiovascular Risk Factors in Adults with Obesity. *Sci Rep* **2023**, *13*, 7035, doi:10.1038/s41598-023-34064-4.
237. Delshad Aghdam, S.; Siassi, F.; Nasli Esfahani, E.; Qorbani, M.; Rajab, A.; Sajjadpour, Z.; Bashiri, A.; Aghayan, M.; Sotoudeh, G. Dietary Phytochemical Index Associated with Cardiovascular Risk Factor in Patients with Type 1 Diabetes Mellitus. *BMC Cardiovascular Disorders* **2021**, *21*, 293, doi:10.1186/s12872-021-02106-2.
238. Kim, C.; Park, K. Association between Phytochemical Index and Inflammation in Korean Adults. *Antioxidants (Basel)* **2022**, *11*, 348, doi:10.3390/antiox11020348.
239. Mirzababaei, A.; Taheri, A.; Rasaei, N.; Mehranfar, S.; Jamili, S.; Clark, C.C.T.; Mirzaei, K. The Relationship between Dietary Phytochemical Index and Resting Metabolic Rate Mediated by Inflammatory Factors in Overweight and Obese Women: A Cross-Sectional Study. *BMC Women's Health* **2022**, *22*, 1–11, doi:10.1186/s12905-022-01894-9.
240. Vassilaki, M.; Aakre, J.A.; Syrjanen, J.A.; Mielke, M.M.; Geda, Y.E.; Kremers, W.K.; Machulda, M.M.; Alhurani, R.E.; Staubo, S.C.; Knopman, D.S.; et al. Mediterranean Diet, Its Components and Amyloid Imaging Biomarkers. *J Alzheimers Dis* **2018**, *64*, 281–290, doi:10.3233/JAD-171121.
241. Abdallah, I.M.; Al-Shami, K.M.; Yang, E.; Wang, J.; Guillaume, C.; Kaddoumi, A. Oleuropein-Rich Olive Leaf Extract Attenuates Neuroinflammation in the Alzheimer's Disease Mouse Model. *ACS Chem Neurosci* **2022**, *13*, 1002–1013, doi:10.1021/acschemneuro.2c00005.
242. Topalović, D.Ž.; Živković, L.; Čabarkapa, A.; Djelić, N.; Bajić, V.; Dekanski, D.; Spremo-Potparević, B. Dry Olive Leaf Extract Counteracts L-Thyroxine-Induced Genotoxicity in Human Peripheral Blood Leukocytes in Vitro. *Oxid Med Cell Longev* **2015**, *2015*, 762192, doi:10.1155/2015/762192.
243. Bucciantini, M.; Leri, M.; Scuto, M.; Ontario, M.; Trovato Salinaro, A.; Calabrese, E.J.; Calabrese, V.; Stefani, M. Xenohormesis Underlyes the Anti-Aging and Healthy Properties of Olive Polyphenols. *Mechanisms of Ageing and Development* **2022**, *202*, 111620, doi:10.1016/j.mad.2022.111620.
244. Menendez, J.A.; Joven, J.; Aragonès, G.; Barrajón-Catalán, E.; Beltrán-Debón, R.; Borrás-Linares, I.; Camps, J.; Corominas-Faja, B.; Cufí, S.; Fernández-Arroyo, S.; et al. Xenohormetic and Anti-Aging Activity of

Secoiridoid Polyphenols Present in Extra Virgin Olive Oil. *Cell Cycle* **2013**, *12*, 555–578, doi:10.4161/cc.23756.

245. Di Rosa, G.; Brunetti, G.; Scuto, M.; Trovato Salinaro, A.; Calabrese, E.J.; Crea, R.; Schmitz-Linneweber, C.; Calabrese, V.; Saul, N. Healthspan Enhancement by Olive Polyphenols in C. Elegans Wild Type and Parkinson's Models. *International Journal of Molecular Sciences* **2020**, *21*, 3893, doi:10.3390/ijms21113893.
246. Gems, D.; Partridge, L. Stress-Response Hormesis and Aging: "That Which Does Not Kill Us Makes Us Stronger." *Cell Metabolism* **2008**, *7*, 200–203, doi:10.1016/j.cmet.2008.01.001.
247. Calabrese, E.J.; Baldwin, L.A. U-Shaped Dose-Responses in Biology, Toxicology, and Public Health. *Annual Review of Public Health* **2001**, *22*, 15–33, doi:10.1146/annurev.publhealth.22.1.15.
248. Zhi, D.; Wang, D.; Yang, W.; Duan, Z.; Zhu, S.; Dong, J.; Wang, N.; Wang, N.; Fei, D.; Zhang, Z.; et al. Dianxianning Improved Amyloid β-Induced Pathological Characteristics Partially through DAF-2/DAF-16 Insulin like Pathway in Transgenic C. Elegans. *Sci Rep* **2017**, *7*, 11408, doi:10.1038/s41598-017-11628-9.
249. Tullet, J.M.A.; Green, J.W.; Au, C.; Benedetto, A.; Thompson, M.A.; Clark, E.; Gilliat, A.F.; Young, A.; Schmeisser, K.; Gems, D. The SKN-1/Nrf2 Transcription Factor Can Protect against Oxidative Stress and Increase Lifespan in C. Elegans by Distinct Mechanisms. *Aging Cell* **2017**, *16*, 1191–1194, doi:10.1111/acel.12627.
250. Massaad, C.A.; Pautler, R.G.; Klann, E. Mitochondrial Superoxide: A Key Player in Alzheimer's Disease. *Aging (Albany NY)* **2009**, *1*, 758–761, doi:10.18632/aging.100088.
251. Govindan, S.; Amirthalingam, M.; Duraisamy, K.; Govindhan, T.; Sundararaj, N.; Palanisamy, S. Phytochemicals-Induced Hormesis Protects Caenorhabditis Elegans against α-Synuclein Protein Aggregation and Stress through Modulating HSF-1 and SKN-1/Nrf2 Signaling Pathways. *Biomed Pharmacother* **2018**, *102*, 812–822, doi:10.1016/j.biopha.2018.03.128.
252. Sun, T.; Wu, H.; Cong, M.; Zhan, J.; Li, F. Meta-Analytic Evidence for the Anti-Aging Effect of Hormesis on *Caenorhabditis Elegans*. *Aging* **2020**, *12*, 2723–2746, doi:10.18632/aging.102773.
253. Ai, L.; Yang, F.; Song, J.; Chen, Y.; Xiao, L.; Wang, Q.; Wang, L.; Li, H.; Lei, T.; Huang, Z. Inhibition of Abeta Proteotoxicity by Paeoniflorin in Caenorhabditis Elegans Through Regulation of Oxidative and Heat Shock Stress Responses. *Rejuvenation Res* **2018**, *21*, 304–312, doi:10.1089/rej.2017.1966.
254. Fonte, V.; Kipp, D.R.; Yerg, J.; Merin, D.; Forrestal, M.; Wagner, E.; Roberts, C.M.; Link, C.D. Suppression of in Vivo Beta-Amyloid Peptide Toxicity by Overexpression of the HSP-16.2 Small Chaperone Protein. *J Biol Chem* **2008**, *283*, 784–791, doi:10.1074/jbc.M703339200.

255. Hartwig, K.; Heidler, T.; Moch, J.; Daniel, H.; Wenzel, U. Feeding a ROS-Generator to Caenorhabditis Elegans Leads to Increased Expression of Small Heat Shock Protein HSP-16.2 and Hormesis. *Genes Nutr* **2009**, *4*, 59–67, doi:10.1007/s12263-009-0113-x.
256. Strayer, A.; Wu, Z.; Christen, Y.; Link, C.D.; Luo, Y. Expression of the Small Heat-Shock Protein Hsp16-2 in Caenorhabditis Elegans Is Suppressed by Ginkgo Biloba Extract EGb 761. *FASEB J* **2003**, *17*, 2305–2307, doi:10.1096/fj.03-0376fje.
257. Van Raamsdonk, J.M.; Hekimi, S. Deletion of the Mitochondrial Superoxide Dismutase Sod-2 Extends Lifespan in Caenorhabditis Elegans. *PLoS Genet* **2009**, *5*, e1000361, doi:10.1371/journal.pgen.1000361.
258. Massaad, C.A.; Washington, T.M.; Pautler, R.G.; Klann, E. Overexpression of SOD-2 Reduces Hippocampal Superoxide and Prevents Memory Deficits in a Mouse Model of Alzheimer's Disease. *Proc Natl Acad Sci U S A* **2009**, *106*, 13576–13581, doi:10.1073/pnas.0902714106.
259. Bitner, B.R.; Perez-Torres, C.J.; Hu, L.; Inoue, T.; Pautler, R.G. Improvements in a Mouse Model of Alzheimer's Disease through Sod2 Overexpression Are Due to Functional and Not Structural Alterations. *Magn Reson Insights* **2012**, *5*, MRI.S9352, doi:10.4137/MRI.S9352.
260. Blackwell, T.K.; Steinbaugh, M.J.; Hourihan, J.M.; Ewald, C.Y.; Isik, M. SKN-1/Nrf, Stress Responses, and Aging in Caenorhabditis Elegans. *Free Radic Biol Med* **2015**, *88*, 290–301, doi:10.1016/j.freeradbiomed.2015.06.008.
261. Burtscher, J.; Romani, M.; Bernardo, G.; Popa, T.; Ziviani, E.; Hummel, F.C.; Sorrentino, V.; Millet, G.P. Boosting Mitochondrial Health to Counteract Neurodegeneration. *Progress in Neurobiology* **2022**, *215*, 102289, doi:10.1016/j.pneurobio.2022.102289.
262. Elkhedir, A.E.; Iqbal, A.; Zogona, D.; Mohammed, H.H.; Murtaza, A.; Xu, X. Apigenin Glycosides from Green Pepper Enhance Longevity and Stress Resistance in Caenorhabditis Elegans. *Nutrition Research* **2022**, *102*, 23–34, doi:10.1016/j.nutres.2022.02.003.
263. Wang, S.; You, M.; Wang, C.; Zhang, Y.; Fan, C.; Yan, S. Heat Shock Pretreatment Induced Cadmium Resistance in the Nematode Caenorhabditis Elegans Is Depend on Transcription Factors DAF-16 and HSF-1. *Environmental Pollution* **2020**, *261*, 114081, doi:10.1016/j.envpol.2020.114081.
264. Iqbal, K.; Liu, F.; Gong, C.-X.; Grundke-Iqbal, I. Tau in Alzheimer Disease and Related Tauopathies. *Curr Alzheimer Res* **2010**, *7*, 656–664.
265. Zhen, M.; Samuel, A.D. C. Elegans Locomotion: Small Circuits, Complex Functions. *Current Opinion in Neurobiology* **2015**, *33*, 117–126, doi:10.1016/j.conb.2015.03.009.
266. Romero-Márquez, J.M.; Navarro-Hortal, M.D.; Orantes, F.J.; Esteban-Muñoz, A.; Pérez-Oleaga, C.M.; Battino, M.; Sánchez-González, C.; Rivas-García, L.; Giampieri, F.; Quiles, J.L.; et al. In Vivo Anti-Alzheimer and

Antioxidant Properties of Avocado (Persea Americana Mill.) Honey from Southern Spain. *Antioxidants* **2023**, *12*, 404, doi:10.3390/antiox12020404.
267. Tiwari, S.S.; Tambo, F.; Agarwal, R. Assessment of Lead Toxicity on Locomotion and Growth in a Nematode Caenorhabditis Elegans. *Journal of Applied and Natural Science* **2020**, *12*, 36–41, doi:10.31018/jans.v12i1.2227.
268. Sheik Mohideen, S.; Yamasaki, Y.; Omata, Y.; Tsuda, L.; Yoshiike, Y. Nontoxic Singlet Oxygen Generator as a Therapeutic Candidate for Treating Tauopathies. *Sci Rep* **2015**, *5*, 10821, doi:10.1038/srep10821.
269. Yoshiike, Y.; Yamashita, S.; Mizoroki, T.; Maeda, S.; Murayama, M.; Kimura, T.; Sahara, N.; Soeda, Y.; Takashima, A. Adaptive Responses to Alloxan-Induced Mild Oxidative Stress Ameliorate Certain Tauopathy Phenotypes. *Aging Cell* **2012**, *11*, 51–62, doi:10.1111/j.1474-9726.2011.00756.x.
270. Varela-López, A.; Vera-Ramírez, L.; Giampieri, F.; Navarro-Hortal, M.D.; Forbes-Hernández, T.Y.; Battino, M.; Quiles, J.L. The Central Role of Mitochondria in the Relationship between Dietary Lipids and Cancer Progression. *Seminars in Cancer Biology* **2021**, *73*, 86–100, doi:10.1016/j.semcancer.2021.01.001.
271. Feelisch, M.; Cortese-Krott, M.M.; Santolini, J.; Wootton, S.A.; Jackson, A.A. Systems Redox Biology in Health and Disease. *EXCLI J* **2022**, *21*, 623–646, doi:10.17179/excli2022-4793.
272. Franco, R.; Vargas, M.R. Redox Biology in Neurological Function, Dysfunction, and Aging. *Antioxid Redox Signal* **2018**, *28*, 1583–1586, doi:10.1089/ars.2018.7509.
273. Hipp, M.S.; Kasturi, P.; Hartl, F.U. The Proteostasis Network and Its Decline in Ageing. *Nat Rev Mol Cell Biol* **2019**, *20*, 421–435, doi:10.1038/s41580-019-0101-y.
274. Richter, K.; Haslbeck, M.; Buchner, J. The Heat Shock Response: Life on the Verge of Death. *Molecular Cell* **2010**, *40*, 253–266, doi:10.1016/j.molcel.2010.10.006.
275. Kumsta, C.; Chang, J.T.; Schmalz, J.; Hansen, M. Hormetic Heat Stress and HSF-1 Induce Autophagy to Improve Survival and Proteostasis in C. Elegans. *Nat Commun* **2017**, *8*, 14337, doi:10.1038/ncomms14337.
276. Guisbert, E.; Czyz, D.M.; Richter, K.; McMullen, P.D.; Morimoto, R.I. Identification of a Tissue-Selective Heat Shock Response Regulatory Network. *PLoS Genet* **2013**, *9*, e1003466, doi:10.1371/journal.pgen.1003466.
277. Schmeisser, S.; Schmeisser, K.; Weimer, S.; Groth, M.; Priebe, S.; Fazius, E.; Kuhlow, D.; Pick, D.; Einax, J.W.; Guthke, R.; et al. Mitochondrial Hormesis Links Low-Dose Arsenite Exposure to Lifespan Extension. *Aging Cell* **2013**, *12*, 508–517, doi:10.1111/acel.12076.
278. Son, H.G.; Seo, K.; Seo, M.; Park, S.; Ham, S.; An, S.W.A.; Choi, E.-S.; Lee, Y.; Baek, H.; Kim, E.; et al. Prefoldin 6 Mediates Longevity Response from

Heat Shock Factor 1 to FOXO in C. Elegans. *Genes Dev* **2018**, *32*, 1562–1575, doi:10.1101/gad.317362.118.
279. Sun, X.; Chen, W.-D.; Wang, Y.-D. DAF-16/FOXO Transcription Factor in Aging and Longevity. *Frontiers in Pharmacology* **2017**, *8*.
280. Oliveira, R.P.; Abate, J.P.; Dilks, K.; Landis, J.; Ashraf, J.; Murphy, C.T.; Blackwell, T.K. Condition-Adapted Stress and Longevity Gene Regulation by Caenorhabditis Elegans SKN-1/Nrf. *Aging Cell* **2009**, *8*, 524–541, doi:10.1111/j.1474-9726.2009.00501.x.
281. Grushko, D.; Boocholez, H.; Levine, A.; Cohen, E. Temporal Requirements of SKN-1/NRF as a Regulator of Lifespan and Proteostasis in Caenorhabditis Elegans. *PLoS One* **2021**, *16*, e0243522, doi:10.1371/journal.pone.0243522.
282. Motta, H.S.; Roos, D.; Tabarelli, G.; Rodrigues, O.E.D.; Ávila, D.; Quines, C.B. Activation of SOD-3 Is Involved in the Antioxidant Effect of a New Class of β-Aryl-Chalcogenium Azide Compounds in Caenorhabditis Elegans. *An. Acad. Bras. Ciênc.* **2020**, *92*, e20181147, doi:10.1590/0001-3765202020181147.
283. Dues, D.J.; Schaar, C.E.; Johnson, B.K.; Bowman, M.J.; Winn, M.E.; Senchuk, M.M.; Van Raamsdonk, J.M. Uncoupling of Oxidative Stress Resistance and Lifespan in Long-Lived Isp-1 Mitochondrial Mutants in Caenorhabditis Elegans. *Free Radic Biol Med* **2017**, *108*, 362–373, doi:10.1016/j.freeradbiomed.2017.04.004.
284. Cabreiro, F.; Ackerman, D.; Doonan, R.; Araiz, C.; Back, P.; Papp, D.; Braeckman, B.P.; Gems, D. Increased Life Span from Overexpression of Superoxide Dismutase in Caenorhabditis Elegans Is Not Caused by Decreased Oxidative Damage. *Free Radical Biology and Medicine* **2011**, *51*, 1575–1582, doi:10.1016/j.freeradbiomed.2011.07.020.
285. Henderson, S.T.; Bonafè, M.; Johnson, T.E. Daf-16 Protects the Nematode Caenorhabditis Elegans During Food Deprivation. *The Journals of Gerontology: Series A* **2006**, *61*, 444–460, doi:10.1093/gerona/61.5.444.
286. Jang, Y.C.; Pérez, V.I.; Song, W.; Lustgarten, M.S.; Salmon, A.B.; Mele, J.; Qi, W.; Liu, Y.; Liang, H.; Chaudhuri, A.; et al. Overexpression of Mn Superoxide Dismutase Does Not Increase Life Span in Mice. *J Gerontol A Biol Sci Med Sci* **2009**, *64A*, 1114–1125, doi:10.1093/gerona/glp100.
287. Van Raamsdonk, J.M.; Hekimi, S. Superoxide Dismutase Is Dispensable for Normal Animal Lifespan. *Proceedings of the National Academy of Sciences* **2012**, *109*, 5785–5790, doi:10.1073/pnas.1116158109.
288. Azadmanesh, J.; Borgstahl, G.E.O. A Review of the Catalytic Mechanism of Human Manganese Superoxide Dismutase. *Antioxidants (Basel)* **2018**, *7*, 25, doi:10.3390/antiox7020025.
289. Fernando, L.M.; Adeel, S.; Basar, M.A.; Allen, A.K.; Duttaroy, A. The SOD-2 Protein Is the Single Active SOD Enzyme in C. Elegans 2020, 2020.08.12.247973.

290. Fernando, L.M.; Adeel, S.; Basar, M.A.; Allen, A.K.; Duttaroy, A. In-Gel SOD Assay Reveals SOD-2 Is the Single Active, Water-Soluble SOD Enzyme in C. Elegans. *Free radical research* **2021**, *55*, 619, doi:10.1080/10715762.2021.1979228.
291. Ferguson, G.D.; Bridge, W.J. The Glutathione System and the Related Thiol Network in Caenorhabditis Elegans. *Redox Biology* **2019**, *24*, 101171, doi:10.1016/j.redox.2019.101171.
292. Raza, H. Dual Localization of Glutathione S-Transferase in the Cytosol and Mitochondria: Implications in Oxidative Stress, Toxicity and Disease. *FEBS J* **2011**, *278*, 4243–4251, doi:10.1111/j.1742-4658.2011.08358.x.
293. Kahn, N.W.; Rea, S.L.; Moyle, S.; Kell, A.; Johnson, T.E. Proteasomal Dysfunction Activates the Transcription Factor SKN-1 and Produces a Selective Oxidative-Stress Response in Caenorhabditis Elegans. *Biochemical Journal* **2007**, *409*, 205–213, doi:10.1042/BJ20070521.
294. Rathor, L.; Akhoon, B.A.; Pandey, S.; Srivastava, S.; Pandey, R. Folic Acid Supplementation at Lower Doses Increases Oxidative Stress Resistance and Longevity in Caenorhabditis Elegans. *AGE* **2015**, *37*, 113, doi:10.1007/s11357-015-9850-5.
295. Rea, S.L.; Wu, D.; Cypser, J.R.; Vaupel, J.W.; Johnson, T.E. A Stress-Sensitive Reporter Predicts Longevity in Isogenic Populations of Caenorhabditis Elegans. *Nat Genet* **2005**, *37*, 894–898, doi:10.1038/ng1608.
296. Mehlen, P.; Kretz-Remy, C.; Préville, X.; Arrigo, A.P. Human Hsp27, Drosophila Hsp27 and Human AlphaB-Crystallin Expression-Mediated Increase in Glutathione Is Essential for the Protective Activity of These Proteins against TNFalpha-Induced Cell Death. *EMBO J* **1996**, *15*, 2695–2706.
297. Detienne, G.; Van de Walle, P.; De Haes, W.; Schoofs, L.; Temmerman, L. SKN-1-Independent Transcriptional Activation of Glutathione S-Transferase 4 (GST-4) by EGF Signaling. *Worm* **2016**, *5*, e1230585, doi:10.1080/21624054.2016.1230585.
298. Jin, C.H.; So, Y.K.; Han, S.N.; Kim, J.-B. Isoegomaketone Upregulates Heme Oxygenase-1 in RAW264.7 Cells via ROS/P38 MAPK/Nrf2 Pathway. *Biomolecules & Therapeutics* **2016**, *24*, 510–516, doi:10.4062/biomolther.2015.194.
299. Oliveras-López, M.-J.; Molina, J.J.M.; Mir, M.V.; Rey, E.F.; Martín, F.; de la Serrana, H.L.-G. Extra Virgin Olive Oil (EVOO) Consumption and Antioxidant Status in Healthy Institutionalized Elderly Humans. *Archives of Gerontology and Geriatrics* **2013**, *57*, 234–242, doi:10.1016/j.archger.2013.04.002.
300. Perez-Herrera, A.; Rangel-Zuñiga, O.A.; Delgado-Lista, J.; Marin, C.; Perez-Martinez, P.; Tasset, I.; Tunez, I.; Quintana-Navarro, G.M.; Lopez-Segura, F.; Luque de Castro, M.D.; et al. The Antioxidants in Oils Heated at Frying Temperature, Whether Natural or Added, Could Protect against

Postprandial Oxidative Stress in Obese People. *Food Chemistry* **2013**, *138*, 2250–2259, doi:10.1016/j.foodchem.2012.12.023.
301. Yatin, S.M.; Yatin, M.; Aulick, T.; Ain, K.B.; Butterfield, D.A. Alzheimer's Amyloid Beta-Peptide Associated Free Radicals Increase Rat Embryonic Neuronal Polyamine Uptake and Ornithine Decarboxylase Activity: Protective Effect of Vitamin E. *Neurosci Lett* **1999**, *263*, 17–20, doi:10.1016/s0304-3940(99)00101-9.
302. Massaad, C.A. Neuronal and Vascular Oxidative Stress in Alzheimer's Disease. *Curr Neuropharmacol* **2011**, *9*, 662–673, doi:10.2174/157015911798376244.
303. Baldeiras, I.; Santana, I.; Proença, M.T.; Garrucho, M.H.; Pascoal, R.; Rodrigues, A.; Duro, D.; Oliveira, C.R. Peripheral Oxidative Damage in Mild Cognitive Impairment and Mild Alzheimer's Disease. *J Alzheimers Dis* **2008**, *15*, 117–128, doi:10.3233/jad-2008-15110.
304. Greilberger, J.; Koidl, C.; Greilberger, M.; Lamprecht, M.; Schroecksnadel, K.; Leblhuber, F.; Fuchs, D.; Oettl, K. Malondialdehyde, Carbonyl Proteins and Albumin-Disulphide as Useful Oxidative Markers in Mild Cognitive Impairment and Alzheimer's Disease. *Free Radic Res* **2008**, *42*, 633–638, doi:10.1080/10715760802255764.
305. Smith, M.A.; Rottkamp, C.A.; Nunomura, A.; Raina, A.K.; Perry, G. Oxidative Stress in Alzheimer's Disease. *Biochim Biophys Acta* **2000**, *1502*, 139–144, doi:10.1016/s0925-4439(00)00040-5.
306. Praticò, D. Alzheimer's Disease and Oxygen Radicals: New Insights. *Biochem Pharmacol* **2002**, *63*, 563–567, doi:10.1016/s0006-2952(01)00919-4.
307. Yao, Y.; Chinnici, C.; Tang, H.; Trojanowski, J.Q.; Lee, V.M.; Praticò, D. Brain Inflammation and Oxidative Stress in a Transgenic Mouse Model of Alzheimer-like Brain Amyloidosis. *Journal of Neuroinflammation* **2004**, *1*, 21, doi:10.1186/1742-2094-1-21.
308. Nunomura, A.; Castellani, R.J.; Zhu, X.; Moreira, P.I.; Perry, G.; Smith, M.A. Involvement of Oxidative Stress in Alzheimer Disease. *Journal of Neuropathology & Experimental Neurology* **2006**, *65*, 631–641, doi:10.1097/01.jnen.0000228136.58062.bf.
309. Doonan, R.; McElwee, J.J.; Matthijssens, F.; Walker, G.A.; Houthoofd, K.; Back, P.; Matscheski, A.; Vanfleteren, J.R.; Gems, D. Against the Oxidative Damage Theory of Aging: Superoxide Dismutases Protect against Oxidative Stress but Have Little or No Effect on Life Span in Caenorhabditis Elegans. *Genes Dev* **2008**, *22*, 3236–3241, doi:10.1101/gad.504808.
310. Umeno, A.; Takashima, M.; Murotomi, K.; Nakajima, Y.; Koike, T.; Matsuo, T.; Yoshida, Y. Radical-Scavenging Activity and Antioxidative Effects of Olive Leaf Components Oleuropein and Hydroxytyrosol in Comparison with Homovanillic Alcohol. *J Oleo Sci* **2015**, *64*, 793–800, doi:10.5650/jos.ess15042.

311. Rietjens, S.J.; Bast, A.; Haenen, G.R.M.M. New Insights into Controversies on the Antioxidant Potential of the Olive Oil Antioxidant Hydroxytyrosol. *J Agric Food Chem* **2007**, *55*, 7609–7614, doi:10.1021/jf0706934.
312. Youssef, P.; Chami, B.; Lim, J.; Middleton, T.; Sutherland, G.T.; Witting, P.K. Evidence Supporting Oxidative Stress in a Moderately Affected Area of the Brain in Alzheimer's Disease. *Sci Rep* **2018**, *8*, 11553, doi:10.1038/s41598-018-29770-3.
313. Parker, W.D.; Mahr, N.J.; Filley, C.M.; Parks, J.K.; Hughes, D.; Young, D.A.; Cullum, C.M. Reduced Platelet Cytochrome c Oxidase Activity in Alzheimer's Disease. *Neurology* **1994**, *44*, 1086–1090, doi:10.1212/wnl.44.6.1086.
314. Bosetti, F.; Brizzi, F.; Barogi, S.; Mancuso, M.; Siciliano, G.; Tendi, E.A.; Murri, L.; Rapoport, S.I.; Solaini, G. Cytochrome c Oxidase and Mitochondrial F1F0-ATPase (ATP Synthase) Activities in Platelets and Brain from Patients with Alzheimer's Disease. *Neurobiol Aging* **2002**, *23*, 371–376, doi:10.1016/s0197-4580(01)00314-1.
315. Smith, M.A.; Harris, P.L.R.; Sayre, L.M.; Perry, G. Iron Accumulation in Alzheimer Disease Is a Source of Redox-Generated Free Radicals. *Proc Natl Acad Sci U S A* **1997**, *94*, 9866–9868.
316. Onukwufor, J.O.; Dirksen, R.T.; Wojtovich, A.P. Iron Dysregulation in Mitochondrial Dysfunction and Alzheimer's Disease. *Antioxidants (Basel)* **2022**, *11*, 692, doi:10.3390/antiox11040692.
317. Cheng, R.; Dhorajia, V.V.; Kim, J.; Kim, Y. Mitochondrial Iron Metabolism and Neurodegenerative Diseases. *NeuroToxicology* **2022**, *88*, 88–101, doi:10.1016/j.neuro.2021.11.003.
318. Hawking, Z.L. Alzheimer's Disease: The Role of Mitochondrial Dysfunction and Potential New Therapies. *Bioscience Horizons: The International Journal of Student Research* **2016**, *9*, hzw014, doi:10.1093/biohorizons/hzw014.
319. Picone, P.; Nuzzo, D.; Caruana, L.; Scafidi, V.; Di Carlo, M. Mitochondrial Dysfunction: Different Routes to Alzheimer's Disease Therapy. *Oxidative Medicine and Cellular Longevity* **2014**, *2014*, e780179, doi:10.1155/2014/780179.
320. Kondo, S.; Ferdousi, F.; Yamauchi, K.; Suidasari, S.; Yokozawa, M.; Harrabi, M.M.; Tominaga, K.; Isoda, H. Comprehensive Transcriptome Analysis of Erythroid Differentiation Potential of Olive Leaf in Haematopoietic Stem Cells. *Journal of Cellular and Molecular Medicine* **2021**, *25*, 7229–7243, doi:10.1111/jcmm.16752.
321. Yang, W.; Li, J.; Hekimi, S. A Measurable Increase in Oxidative Damage Due to Reduction in Superoxide Detoxification Fails to Shorten the Life Span of Long-Lived Mitochondrial Mutants of Caenorhabditis Elegans. *Genetics* **2007**, *177*, 2063–2074, doi:10.1534/genetics.107.080788.

322. Ribas, V.; García-Ruiz, C.; Fernández-Checa, J.C. Glutathione and Mitochondria. *Front Pharmacol* **2014**, *5*, 151, doi:10.3389/fphar.2014.00151.
323. Marí, M.; de Gregorio, E.; de Dios, C.; Roca-Agujetas, V.; Cucarull, B.; Tutusaus, A.; Morales, A.; Colell, A. Mitochondrial Glutathione: Recent Insights and Role in Disease. *Antioxidants* **2020**, *9*, 909, doi:10.3390/antiox9100909.
324. Mandal, P.K.; Shukla, D.; Tripathi, M.; Ersland, L. Cognitive Improvement with Glutathione Supplement in Alzheimer's Disease: A Way Forward. *J Alzheimers Dis* **2019**, *68*, 531–535, doi:10.3233/JAD-181054.
325. Ansari, M.A.; Scheff, S.W. Oxidative Stress in the Progression of Alzheimer Disease in the Frontal Cortex. *J Neuropathol Exp Neurol* **2010**, *69*, 155–167, doi:10.1097/NEN.0b013e3181cb5af4.
326. Venkateshappa, C.; Harish, G.; Mahadevan, A.; Srinivas Bharath, M.M.; Shankar, S.K. Elevated Oxidative Stress and Decreased Antioxidant Function in the Human Hippocampus and Frontal Cortex with Increasing Age: Implications for Neurodegeneration in Alzheimer's Disease. *Neurochem Res* **2012**, *37*, 1601–1614, doi:10.1007/s11064-012-0755-8.
327. Rinaldi, P.; Polidori, M.C.; Metastasio, A.; Mariani, E.; Mattioli, P.; Cherubini, A.; Catani, M.; Cecchetti, R.; Senin, U.; Mecocci, P. Plasma Antioxidants Are Similarly Depleted in Mild Cognitive Impairment and in Alzheimer's Disease. *Neurobiol Aging* **2003**, *24*, 915–919, doi:10.1016/s0197-4580(03)00031-9.
328. Mandal, P.K.; Goel, A.; Bush, A.I.; Punjabi, K.; Joon, S.; Mishra, R.; Tripathi, M.; Garg, A.; Kumar, N.K.; Sharma, P.; et al. Hippocampal Glutathione Depletion with Enhanced Iron Level in Patients with Mild Cognitive Impairment and Alzheimer's Disease Compared with Healthy Elderly Participants. *Brain Commun* **2022**, *4*, fcac215, doi:10.1093/braincomms/fcac215.
329. Chen, Z.; Zhong, C. Oxidative Stress in Alzheimer's Disease. *Neurosci Bull* **2014**, *30*, 271–281, doi:10.1007/s12264-013-1423-y.
330. Stamer, K.; Vogel, R.; Thies, E.; Mandelkow, E.; Mandelkow, E.-M. Tau Blocks Traffic of Organelles, Neurofilaments, and APP Vesicles in Neurons and Enhances Oxidative Stress. *J Cell Biol* **2002**, *156*, 1051–1063, doi:10.1083/jcb.200108057.
331. Alavi Naini, S.M.; Soussi-Yanicostas, N. Tau Hyperphosphorylation and Oxidative Stress, a Critical Vicious Circle in Neurodegenerative Tauopathies? *Oxid Med Cell Longev* **2015**, *2015*, 151979, doi:10.1155/2015/151979.
332. Cente, M.; Filipcik, P.; Pevalova, M.; Novak, M. Expression of a Truncated Tau Protein Induces Oxidative Stress in a Rodent Model of Tauopathy. *Eur J Neurosci* **2006**, *24*, 1085–1090, doi:10.1111/j.1460-9568.2006.04986.x.

333. Haque, Md.M.; Murale, D.P.; Kim, Y.K.; Lee, J.-S. Crosstalk between Oxidative Stress and Tauopathy. *Int J Mol Sci* **2019**, *20*, 1959, doi:10.3390/ijms20081959.
334. Zhou, F.; Chen, S.; Xiong, J.; Li, Y.; Qu, L. Luteolin Reduces Zinc-Induced Tau Phosphorylation at Ser262/356 in an ROS-Dependent Manner in SH-SY5Y Cells. *Biol Trace Elem Res* **2012**, *149*, 273–279, doi:10.1007/s12011-012-9411-z.
335. Tetz, L.M.; Kamau, P.W.; Cheng, A.A.; Meeker, J.D.; Loch-Caruso, R. Troubleshooting the Dichlorofluorescein Assay to Avoid Artifacts in Measurement of Toxicant-Stimulated Cellular Production of Reactive Oxidant Species. *J Pharmacol Toxicol Methods* **2013**, *67*, 56–60, doi:10.1016/j.vascn.2013.01.195.
336. Eruslanov, E.; Kusmartsev, S. Identification of ROS Using Oxidized DCFDA and Flow-Cytometry. In *Advanced Protocols in Oxidative Stress II*; Armstrong, D., Ed.; Methods in Molecular Biology; Humana Press: Totowa, NJ, 2010; pp. 57–72 ISBN 978-1-60761-411-1.
337. Scimemi, A.; Beato, M. Determining the Neurotransmitter Concentration Profile at Active Synapses. *Mol Neurobiol* **2009**, *40*, 289–306, doi:10.1007/s12035-009-8087-7.
338. Montfort, C. von; Matias, N.; Fernandez, A.; Fucho, R.; Rosa, L.C. de la; Martinez-Chantar, M.L.; Mato, J.M.; Machida, K.; Tsukamoto, H.; Murphy, M.P.; et al. Mitochondrial GSH Determines the Toxic or Therapeutic Potential of Superoxide Scavenging in Steatohepatitis. *Journal of Hepatology* **2012**, *57*, 852–859, doi:10.1016/j.jhep.2012.05.024.
339. Aon, M.A.; Stanley, B.A.; Sivakumaran, V.; Kembro, J.M.; O'Rourke, B.; Paolocci, N.; Cortassa, S. Glutathione/Thioredoxin Systems Modulate Mitochondrial H2O2 Emission: An Experimental-Computational Study. *Journal of General Physiology* **2012**, *139*, 479–491, doi:10.1085/jgp.201210772.
340. Marí, M.; Morales, A.; Colell, A.; García-Ruiz, C.; Fernández-Checa, J.C. Mitochondrial Glutathione, a Key Survival Antioxidant. *Antioxid Redox Signal* **2009**, *11*, 2685–2700, doi:10.1089/ars.2009.2695.

ANNEXES

Table Annex 1. Secoiridoid contents of the fifty olive leaf extracts

	(1)	(2)	(3)	(4)	(5)	(6)	(7)	(8)	(9)	(10)	(11)	(12)	(13)	(14)
SU01	0.381	0.270	0.237	-	-	-	-	1.85	0.799	5.24	2.670	35.8	0.215	2.96
SU02	0.441	0.760	0.172	-	-	0.425	-	0.044	-	0.209	1.17	0.248	-	-
SU03	-	0.232	-	-	-	-	-	0.702	0.544	4.49	2.84	20.9	0.485	2.38
SU04	-	0.239	-	-	-	-	-	0.937	0.910	2.96	4.35	19.0	0.936	3.30
SU05	0.325	0.866	-	-	-	-	-	-	-	-	-	-	-	-
SU06	0.249	0.673	-	-	-	0.044	-	-	-	-	-	0.161	-	-
SU07	0.216	0.295	-	-	-	-	-	-	-	-	-	0.142	-	-
SU08	0.224	0.631	-	-	-	0.197	-	-	-	-	-	0.280	-	-
SU09	0.084	0.326	-	-	-	-	-	-	-	-	-	-	-	-
SU10	0.399	0.701	-	-	-	0.111	-	-	-	-	-	0.084	-	-
SU11	-	-	-	-	-	-	0.050	-	-	-	-	-	-	-
SU12	0.788	-	1.417	0.590	0.422	-	1.78	-	-	-	-	-	-	-
SU13	0.174	-	0.475	-	-	-	0.240	-	-	-	-	-	-	-
SU14	0.462	-	1.044	0.419	0.219	-	1.26	-	-	-	-	-	-	-
SU15	0.286	0.244	0.106	-	-	0.189	-	-	-	-	-	-	-	-
SU16	0.268	1.25	0.120	-	-	0.184	-	-	-	-	-	0.151	-	-
SU17	0.401	0.773	0.119	-	-	0.215	-	-	-	-	-	0.069	-	-
SU18	-	0.398	0.322	-	-	0.144	0.013	-	-	-	-	-	-	-
SU19	-	1.83	-	-	-	-	0.570	-	-	0.253	-	0.304	-	-
SU20	-	1.95	-	-	-	-	0.700	-	-	0.384	-	0.208	-	-
SU21	0.149	1.31	0.072	-	-	0.110	0.105	-	-	1.75	1.38	0.393	-	-
SU22	0.280	1.08	-	-	-	0.196	-	-	-	0.259	0.194	0.960	-	-
SU23	0.208	1.54	-	-	-	0.044	0.036	0.151		3.11	2.46	0.320	-	-
SU24	0.324	2.22	-	-	0.118	0.097	0.817	-	-	0.216	0.075	-	-	-
SU25	0.701	0.057	0.062	-	-	0.236	0.264	-	-	0.354	0.130	0.036	-	-
SU26	0.306	0.666	-	-	-	0.279	-	-	-	0.171	0.229	0.294	-	-
SU27	0.666	0.976	0.598	-	-	0.278	0.310	0.193	-	0.102	0.346	1.34	-	-
SU28	0.533	0.638	0.424	-	-	0.072	0.164	0.092	-	0.337	0.385	0.423	-	-
SU29	0.327	0.531	0.284	-	-	0.338	-	0.523	-	0.108	0.707	3.59	-	-
SU30	0.307	0.465	0.095	-	-	0.248	-	0.037	-	-	0.248	1.17	-	-

SU31	0.547	1.13	0.173	-	-	-	0.137	1.81	0.958	5.62	2.88	43.5	0.381	4.07
SU32	0.388	0.643	0.036	-	-	-	-	1.35	0.704	4.17	2.17	32.6	0.199	3.19
SU33	0.285	0.522	0.174	-	0.066	0.200	-	0.031	-	0.343	0.425	0.743	-	-
SU34	0.236	0.419	0.358	-	0.316	-	0.305	0.289	-	1.62	0.830	7.93	-	0.704
SU35	0.324	1.24	0.769	-	0.445	-	0.438	0.067	-	3.36	1.09	2.38	-	0.080
SU36	0.423	0.490	0.196	-	-	0.224	0.345	0.277	-	0.433	0.597	1.69	-	-
SU37	0.233	0.795	0.081	-	-	0.140	0.287	0.078	-	0.117	0.390	0.721	-	-
SU38	0.083	0.620	0.030	-	-	-	-	0.965	0.987	6.37	3.34	69.0	0.475	6.83
SU39	-	1.98	0.067	-	0.077	-	0.045	0.965	0.834	6.65	6.10	38.4	0.288	4.20
SU40	0.448	-	-	-	0.126	-	0.550	-	-	-	0.134	1.75	-	0.011
SU41	0.531	0.364	0.233	-	-	0.142	-	0.221	-	0.147	0.572	1.38	-	-
SU42	0.621	0.197	0.374	-	-	0.153	-	0.220	-	0.187	0.597	1.80	-	-
SU43	0.339	0.543	0.180	-	0.026	0.195	-	0.212	-	0.380	0.668	0.89	-	-
SU44	0.734	0.543	0.252	-	0.033	0.270	0.497	0.260	-	0.435	0.613	1.56	-	-
SU45	0.416	0.893	0.112	-	0.059	0.056	0.225	0.132	-	0.057	0.312	0.713	-	-
SU46	0.423	-	0.060	-	0.186	-	0.297	-	-	-	-	-	-	-
SU47	0.297	-	0.073	-	0.097	-	0.324	-	-	-	0.054	0.019	-	-
SU48	0.325	-	0.271	-	0.018	-	0.144	0.332	-	0.000	0.324	0.355	-	-
SU49	0.104	0.416	0.022	-	-	0.029	-	-	-	0.000	0.106	0.616	-	-
SU50	0.381	0.270	0.237	-	-	-	-	1.85	0.799	5.24	2.67	35.8	0.215	2.96

Results are expressed as milligram of compound per gram of dry weight. Compounds identification: (1) 1-β-D-Glucopyranosyl acyclodihydroelenolic acid isomer 1; (2) 1-β-D-Glucopyranosyl acyclodihydroelenolic acid isomer 2; (3) aldehydic form of decarboxymethyl elenolic acid; (4) decarboxylated form of hydroxy elenolic acid isomer 2; (5) hydrated product of the dialdehydic form of decarboxymethyl elenolic acid: (6) hydroxylated product of the dialdehydic form of decarboxymethyl elenolic acid isomer 1; (7) hydroxylated product of the dialdehydic form of decarboxymethyl elenolic acid isomer 2; (8) hydroxyoleuropein; (9) ligstroside; (10) oleoside; (11) oleoside methyl ester; (12) oleuropein; (13) oleuropein diglucoside (14) oleuropein isomer.

Table Annex 2. Flavonoid contents of the fifty olive leaf extracts

	(15)	(16)	(17)	(18)	(19)	(20)	(21)	(22)	(23)	(24)	(25)	(26)	(27)	(28)	(29)	(30)
SU01	-	0.081	0.388	0.422	0.333	0.829	0.104	0.057	0.313	3.07	4.24	-	-	0.157	-	-
SU02	-	0.233	0.363	0.763	0.170	0.727	0.354	-	0.148	0.458	3.35	-	-	0.088	-	-
SU03	-	-	1.03	0.131	0.173	0.986	-	0.244	0.072	6.51	6.72	-	0.016	0.038	-	-
SU04	0.011	-	0.566	0.365	0.325	0.956	-	0.238	0.156	4.33	6.72	-	0.039	0.171	-	-
SU05	-	-	0.090	0.497	0.145	0.747	0.100	0.011	0.347	0.811	6.98	-	-	0.201	-	-
SU06	-	-	0.059	0.507	0.124	0.619	0.229	0.013	0.625	0.884	8.03	-	0.144	0.136	-	-
SU07	-	-	0.132	0.458	0.110	0.670	0.120	0.038	0.514	1.09	3.36	-	0.137	0.213	-	-
SU08	-	0.066	0.099	0.727	0.424	0.508	0.252	0.069	0.805	1.13	6.91	-	-	0.173	0.014	-
SU09	-	0.059	0.116	0.468	0.108	0.641	0.246	0.027	0.611	0.875	4.25	-	-	0.177	-	-
SU10	-	0.050	0.102	0.568	0.233	0.613	0.244	-	0.362	0.760	8.23	-	-	0.190	-	-
SU11	-	0.024	-	-	0.045	-	0.104	-	0.068		0.163	-	-	-	-	-
SU12	-	0.505	-	0.298	0.210	-	0.601	-	0.225	0.018	0.978	-	-	-	-	-
SU13	-	0.216	-	0.079	0.108	-	0.340	-	0.147		0.569	-	-	-	-	-
SU14	-	0.333	-	0.364	0.142	0.037	0.507	-	0.289	0.053	1.30	-	-	-	-	-
SU15	-	0.109	0.046	0.348	0.138	0.259	0.278	0.005	0.759	0.612	2.12	-	0.024	-	-	-
SU16	-	0.079	0.133	0.382	0.115	0.450	0.237	0.073	0.898	1.43	3.46	-	0.130	0.011	-	-
SU17	-	0.068	0.077	0.401	0.130	0.349	0.247	-	0.481	0.886	2.87	-	0.053	-	-	-
SU18	-	0.111	0.086	0.357	0.163	0.263	0.242	-	0.542	0.696	2.35	-	-	-	-	-
SU19	0.041	0.060	0.481	0.293	0.175	0.648	0.059	0.082	0.202	0.831	3.82	-	-	0.047	-	-
SU20	0.053	0.066	0.492	0.261	0.149	0.607	0.047	0.072	0.205	0.852	3.89	-	-	0.051	-	-
SU21	0.077	0.134	0.413	0.443	0.310	0.698	0.182	0.025	0.198	0.758	3.30	-	-	0.081	-	-
SU22	0.065	0.054	0.296	0.309	0.162	0.680	0.178	-	0.108	0.646	3.42	-	-	0.066	-	-
SU23	0.083	0.088	0.424	0.458	0.256	0.720	0.125	0.031	0.147	0.868	3.07	-	-	0.095	-	-
SU24		0.177	0.281	0.403	0.287	0.509	0.195	0.024	0.391	0.674	2.81	-	-	0.035	-	-
SU25	0.034	0.286	0.136	0.212	0.316	0.400	0.271	-	0.193	0.349	2.98	-	-	0.014	-	-
SU26	0.271	0.110	0.310	0.336	0.457	0.783	0.187	-	0.152	0.609	4.51	-	-	0.082	-	-
SU27	0.180	0.300	0.474	0.895	0.277	0.742	0.368	0.018	0.353	0.861	7.00	-	-	0.139	-	-

SU28	0.324	0.215	0.305	0.697	0.392	0.577	0.305	-	0.345	0.614	3.17	-	-	0.094	-	-
SU29	0.199	0.179	0.488	0.845	0.239	0.887	0.312	0.056	0.226	1.15	7.29	-	-	0.183	-	-
SU30	0.199	0.146	0.407	0.601	0.438	0.695	0.233	0.035	0.183	0.837	5.95	-	-	0.146	-	-
SU31	0.118	0.046	0.385	0.333	0.804	0.677	0.031	0.080	0.222	2.788	6.12	-	0.168	0.108	-	-
SU32	0.098	0.009	0.282	0.248	0.526	0.532	0.004	0.035	0.156	2.287	4.84	-	-	0.072	-	-
SU33	0.156	0.189	0.286	0.480	0.428	0.563	0.232	-	0.144	0.635	5.10	-	-	0.086	-	-
SU34	0.110	0.131	0.088	0.141	1.06	0.293	0.126	-	0.312	0.879	1.63	-	-	-	-	-
SU35	0.200	0.128	0.197	0.228	0.650	0.413	0.118	-	0.225	0.661	1.94	-	-	-	-	0.014
SU36	0.238	0.122	0.557	0.660	0.313	0.792	0.149	0.012	0.083	1.17	7.99	-		0.201	-	-
SU37	0.045	0.078	0.310	0.579	0.317	0.784	0.158	0.046	0.203	1.13	6.99	-	0.062	0.234	-	-
SU38	0.262	-	0.179	0.156	1.10	0.368	-	0.010	0.140	1.89	2.39	-	0.065	0.015		0.081
SU39	0.123	-	0.146	0.105	1.40	0.281	-	-	0.104	1.68	1.97	-	0.049	-	-	0.011
SU40	-	0.912	0.341	0.152	1.78	0.656	0.717	0.030	0.575	1.05	3.49	0.042		-	-	-
SU41	0.224	0.202	0.401	0.629	0.834	0.605	0.207	-	0.110	0.675	6.79	-	-	0.142	-	-
SU42	0.285	0.252	0.431	0.733	1.16	0.596	0.257	-	0.120	0.657	6.99	-	-	0.143	-	-
SU43	0.298	0.188	0.311	0.528	0.607	0.528	0.180	-	0.131	0.677	5.23	-	-	0.093	-	-
SU44	0.373	0.134	0.592	0.678	0.417	0.746	0.129	0.029	0.081	1.29	7.92	-	-	0.225	-	-
SU45	0.031	0.119	0.298	0.551	0.383	0.686	0.194	0.017	0.187	0.794	5.98	-	-	0.163	-	-
SU46	-	0.684	-	-	2.96	0.106	0.570	-	0.441	0.341	0.782	-	-	-	-	-
SU47	-	0.565	0.038	-	2.97	0.158	0.396	-	0.402	0.423	0.985	-	-	-	-	-
SU48	-	1.07	0.515	0.239	3.78	0.478	0.480	0.028	0.478	1.38	2.59	0.011	-	-	-	-
SU49	-	0.062	0.206	0.480	0.087	0.692	0.281	-	0.099	0.513	3.52	-	-	0.113	-	-
SU50	-	0.401	0.583	0.213	0.463	0.774	0.399	-	0.286	0.714	3.74	-	-	-	-	-

Results are expressed as milligram of compound per gram of dry weight. Compounds identification: (15) (+)-eriodictyol; (16) apigenin; (17) apigenin-7-o-glucoside; (18) apigenin-7-o-rutinoside; (19) azelaic acid; (20) chrysoeriol-7-O-glucoside; (21) diosmetin; (22) isorhamnetin 3-O-β-d-(6-p-coumaroyl) glucoside; (23) luteolin; (24) luteolin 7-O-glucoside; (25) luteolin glucoside; (26) luteolin rutinoside isomer 1; (27) luteolin rutinoside isomer 2; (28) luteolin-7,4-O-diglucoside; (29) oxidized quercetin; (30) taxifolin.

Table Annex 3. Phenolic alcohols and acids, iridoids, hydroxycoumarin, hydroxycinnamic acid, and other compounds contents in the fifty olive leaf extracts

	(31)	(32)	(33)	(34)	(35)	(36)	(37)	(38)	(39)	(40)	(41)	(42)
SU01	0.291	0.349	0.129	0.380	0.911	1.45	0.110	0.055	1.34	0.579	-	0.177
SU02	-	-	-	0.349	1.08	1.52	0.022	0.015	0.093	1.45	-	0.718
SU03	0.594	2.54	-	0.309	0.418	0.190	0.938	0.113	0.883	1.70	0.146	0.505
SU04	0.471	1.52	-	0.411	0.995	0.819	0.115	0.052	0.545	1.33	0.415	0.928
SU05	0.101	1.96	0.052	0.325	0.487	0.597	0.198	0.045	0.120	3.10	-	0.220
SU06	0.092	1.04	-	0.285	0.487	0.647	0.221	0.035	0.088	3.05	-	0.243
SU07	0.075	0.318	-	0.210	0.424	0.444	0.018	0.002	0.131	2.63	-	0.205
SU08	0.061	0.252	0.134	0.212	0.572	0.686	0.061	0.009	0.068	2.73	0.038	0.246
SU09	0.054	0.225	0.055	0.207	0.350	0.466	0.074	0.006	0.067	2.29	0.033	0.332
SU10	0.080	0.780	0.097	0.291	0.686	0.445	0.102	0.013	0.114	2.39	0.034	0.521
SU11	-	-	0.084	0.017	0.122	0.089	0.012	-	0.043	0.090	-	-
SU12	-	0.042	0.348	0.076	1.458	0.162	0.061	0.006	0.058	0.073	0.046	-
SU13	0.035	0.032	0.133	0.022	0.281	0.087	0.028	-	0.038	0.086	0.033	-
SU14	0.035	-	0.302	0.085	0.710	0.317	0.036	-	0.143	0.161	0.041	0.074
SU15	0.065	0.215	0.083	0.151	0.524	0.909	0.082	0.012	0.155	1.42	0.041	0.286
SU16	0.063	1.05	0.091	0.256	0.501	1.65	0.045	0.010	0.063	2.03	0.041	0.659
SU17	0.048	0.522	0.092	0.246	0.574	1.37	0.043	0.005	0.070	2.04	0.037	0.704
SU18	0.050	0.313	0.071	0.173	0.151	1.36	0.064	0.009	0.062	1.75	0.040	0.143
SU19	0.077	0.257	0.049	0.234	0.239	1.20	0.071	0.025	0.154	1.32	-	1.24
SU20	0.104	0.257	0.050	0.222	0.249	1.07	0.085	0.021	0.124	1.27	-	1.28
SU21	0.053	0.198	0.107	0.330	0.495	0.938	0.078	0.029	0.168	1.25	0.034	0.622
SU22	0.050	0.138	0.056	0.192	0.541	0.660	0.082	0.037	0.114	0.981	0.033	0.508
SU23	0.058	0.313	0.092	0.354	0.585	0.755	0.138	0.055	0.180	1.20	0.030	0.703
SU24	0.050	0.147	0.144	0.310	0.450	0.857	0.041	0.014	0.072	1.13	0.031	0.633
SU25	0.098	0.040	0.062	0.087	0.615	0.196	0.077	0.025	0.129	0.244	0.029	0.040

SU26	0.093	0.123	0.076	0.169	0.436	0.577	0.178	0.064	0.145	0.670	0.032	0.455
SU27	0.224	0.087	0.122	0.324	1.050	1.38	0.103	0.067	0.156	1.36	0.035	0.327
SU28	0.136	0.072	0.105	0.257	0.757	1.57	0.184	0.104	0.135	1.22	0.039	0.133
SU29	0.055	0.078	0.073	0.298	0.804	1.51	0.152	0.078	0.098	1.62	0.030	0.555
SU30	0.046	0.061	0.056	0.222	0.558	1.12	0.123	0.086	0.103	1.30	0.031	0.496
SU31	0.360	0.459	0.147	0.334	0.685	1.04	0.181	0.149	1.58	0.567	0.037	0.266
SU32	0.322	0.501	0.109	0.190	0.449	0.853	0.175	0.129	1.49	0.461	0.031	0.125
SU33	0.077	0.054	0.075	0.228	0.765	0.742	0.090	0.071	0.121	0.840	0.038	0.043
SU34	0.179	0.091	0.256	0.181	0.449	0.532	0.158	0.112	0.465	0.187	0.034	-
SU35	0.072	0.116	0.276	0.416	0.787	1.04	0.208	0.159	0.266	0.341	-	0.126
SU36	0.062	0.098	0.058	0.243	0.881	1.02	0.115	0.072	0.097	1.10	0.034	0.201
SU37	0.072	0.199	0.088	0.267	0.633	0.738	0.158	0.060	0.538	1.22		0.251
SU38	0.235	1.15	0.059	0.217	0.647	0.952	0.309	0.207	1.38	0.460	0.029	0.336
SU39	0.153	0.599	0.087	0.224	0.459	0.753	0.182	0.150	1.27	0.327	0.029	0.122
SU40	0.274	0.085	0.105	0.109	1.24	0.071	0.539	0.026	0.264	0.388	0.040	-
SU41	0.066	0.055	0.060	0.228	0.849	1.09	0.151	0.071	0.097	1.06	-	0.396
SU42	0.056	0.058	0.073	0.227	0.944	1.12	0.148	0.091	0.083	1.21	0.030	0.418
SU43	0.070	0.055	0.082	0.221	0.740	0.847	0.141	0.109	0.091	0.868	0.033	0.099
SU44	0.089	0.113	0.064	0.258	0.994	0.892	0.168	0.111	0.119	1.06	0.036	0.288
SU45	0.054	0.162	0.085	0.261	0.667	0.816	0.110	0.044	0.577	1.14	0.030	0.194
SU46	0.247	0.059	0.104	0.016	1.19	-	0.437	0.024	0.357	0.077	0.035	-
SU47	0.388	0.050	0.103	0.028	1.10	0.037	0.793	0.034	0.241	0.130	0.034	-
SU48	0.328	0.064	0.096	0.058	1.27	0.063	0.592	0.031	0.318	0.234	0.037	-
SU49	0.035	0.680	0.038	0.271	0.438	1.14	0.005	0.001	0.075	3.14	0.033	1.23
SU50	0.255	0.178	0.049	0.149	0.673	0.130	0.766	0.032	0.247	1.05	0.038	0.099

Results are expressed as milligram of compound per gram of dry weight. Compounds identification: (31) hydroxytyrosol; (32) hydroxytyrosol glucoside; (33) 4-ethylguaiacol; (34) loganic acid; (35) 7-epiloganin; (36) lamiol; (37) esculetin; (38) esculin; (39) verbascoside; (40) decaffeoylverbascoside; (41) p-hydroxybenzoic acid; (42) lauroside B.

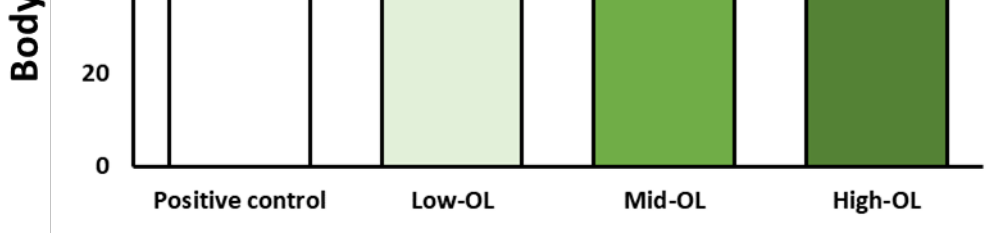

Figure Annex 1. Body length measurement of the nematodes exposed to the three olive leaf extracts in the *C. elegans* BR5706 strain. Nematodes were exposed to using 500 μg/ml of low, mid, or high-OL extract. Results are mean ± SEM. For each parameter, different lowercase letters mean statistically significant differences ($p < 0.05$).